E-ISSN 1309 - 2251

KAFKAS ÜNİVERSİTESİ VETERİNER FAKÜLTESİ DERGİSİ

Journal of the Faculty of Veterinary Medicine, Kafkas University

Published Bi-monthly

Volume: 32
Issue: 2 (March - April)
Year: 2026

E-ISSN: 1309-2251

This journal is published bi-monthly, by the Faculty of Veterinary Medicine, University of Kafkas, Kars - Turkey

This journal is indexed and abstracted in:

- Web of Science Core Collection: Science Citation Index Expanded (since 2007)
- Additional Web of Science Indexes: Essential Science Indicators - Zoological Record
- CABI - Veterinary Science Database
- China Knowledge Resource Integrated (CNKI)
- DOAJ
- EBSCO - Academic Search Premier
- Elsevier - SCOPUS
- Elsevier - EMBASE
- SOBİAD Atıf Dizini
- TÜBİTAK/ULAKBİM TR-Dizin
- Türkiye Atıf Dizini

Address for Correspondence
Kafkas Üniversitesi Veteriner Fakültesi Dergisi Editörlüğü 36040, Kars - TÜRKİYE
Phone: +90 474 2426807-2426836/5228 Fax: +90 474 2426853 E-mail: vetdergi@kafkas.edu.tr
Electronic Edition http://vetdergikafkas.org
Online Submission http://submit.vetdergikafkas.org

Kafkas Universitesi Veteriner Fakultesi Dergisi
Journal Home-Page: http://vetdergikafkas.org
E-ISSN: 1309-2251

Kafkas Univ Vet Fak Derg
Volume: 32, Issue: 2, Year: 2026

Kafkas Universitesi Veteriner Fakultesi Dergisi
Journal Home-Page: http://vetdergikafkas.org
E-ISSN: 1309-2251

Kafkas Univ Vet Fak Derg
Volume: 32, Issue: 2, Year: 2026

EDITORIAL BOARD

Kafkas Universitesi Veteriner Fakultesi Dergisi
Journal Home-Page: http://vetdergikafkas.org
E-ISSN: 1309-2251

Kafkas Univ Vet Fak Derg
Volume: 32, Issue: 2, Year: 2026

EDITORIAL BOARD

Kafkas Universitesi Veteriner Fakultesi Dergisi
Journal Home-Page: http://vetdergikafkas.org
E-ISSN: 1309-2251

Kafkas Univ Vet Fak Derg
Volume: 32, Issue: 2, Year: 2026

CONTENTS

Kafkas Universitesi Veteriner Fakultesi Dergisi
Journal Home-Page: http://vetdergikafkas.org
E-ISSN: 1309-2251

Kafkas Univ Vet Fak Derg
Volume: 32, Issue: 2, Year: 2026

CONTENTS

Kafkas Universitesi Veteriner Fakultesi Dergisi
Journal Home-Page: http://vetdergikafkas.org
E-ISSN: 1309-2251

Kafkas Univ Vet Fak Derg
32 (2): 155-164, 2026
DOI: 10.9775/kvfd.2025.35543

Review Article

The Effects of Geographic Region and Breed on the Prevalence of Foot Diseases in Dairy Cows in Türkiye: A Systematic Review and Meta-Analysis

Vildan ASLAN CANATAN [1 (*)], Uygur CANATAN [2], Ender UZABACI [3]

[1]Cukurova University, Faculty of Ceyhan Veterinary Medicine, Department of Surgery, TR-01250 Adana - TÜRKİYE
[2]Bursa Uludag University, Faculty of Veterinary Medicine, Department of Surgery, TR-16059 Bursa - TÜRKİYE
[3]Bursa Uludag University, Faculty of Veterinary Medicine, Department of Biometry, TR-16059 Bursa - TÜRKİYE

(*) **Corresponding author:**
Vildan Aslan Canatan
Phone: +90 322 613 73 11
Celluler phone: +90 506 292 01 08
Fax: +90 322 613 51 80
E-mail: vaslan@cu.edu.tr

How to cite this article?

Aslan Canatan V, Canatan U, Uzabaci E: The Effects of Geographic Region and Breed on the Prevalence of Foot Diseases in Dairy Cows in Türkiye: A Systematic Review and Meta-Analysis. *Kafkas Univ Vet Fak Derg*, 32 (2): 155-164, 2026.
DOI: 10.9775/kvfd.2025.35543

Article ID: KVFD-2025-35543
Received: 27.10.2025
Accepted: 02.03.2026
Published Online: 05.03.2026

Abstract

Foot diseases in dairy cows substantially affect animal welfare and farm profitability. This systematic review and meta-analysis estimated the pooled prevalence of foot diseases in dairy cows in Türkiye and assessed the effects of region, breed, and sample size. A comprehensive literature search was conducted for studies published between January 1999 and September 2024 in accordance with PRISMA guidelines. Eligible studies were analyzed using a random-effects meta-analysis model. Heterogeneity was assessed using Cochran's Q test and the I^2 statistic, and publication bias was evaluated through Egger's test and funnel plot analysis. Of 5,779 studies identified, 31 met the inclusion criteria. The overall pooled prevalence was 20.52% (95% CI: 16.23–25.19). By region, prevalence ranged from 6.76% to 51.59%, with Holsteins showing the highest prevalence among breeds (13.22%). A comparison of study periods revealed that the prevalence significantly increased from 16.93% (95% CI: 12.01–22.50) in 1999–2014 to 24.81% (95% CI: 17.46–32.98) in 2015–2024. These findings highlight regional and breed-related differences in the prevalence of foot diseases in dairy cows in Türkiye.

Keywords: Breed, Cow, Foot disease prevalence, Geographic region, Sample size, Türkiye

Introduction

Foot diseases and lameness in dairy cows are among the health problems that significantly affect animal welfare and rural economies all over the world [1-3], including in Türkiye [4,5]. Among the foot problems frequently encountered in cows, infectious illnesses (e.g., digital dermatitis) [6,7], and noninfectious illnesses (e.g., sole ulcer and white line disease) stand out due to the adverse conditions they create [8-10]. Foot diseases cause severe economic losses linked to early culling, decreased milk yields, and reduced reproductive performance [11-13]. Furthermore, individual treatment costs ranged from USD 51.5 to 1.517 (2019 price levels) depending on the type of lesion [14]. Additionally, a 2024 study reported an average lameness cost of USD 153.8 per case in dairy farms in Türkiye [15]. Therefore, the rapid detection and accurate diagnosis of foot lesions are important in ensuring animal welfare and minimizing economic losses [16].

Milk production and dairy farming are sustainable agricultural activities that contribute significantly to a country's economy [17]. The prevalence of foot diseases, especially in dairy farms, varies based on factors such as geographic region, herd size, and breed; it is also affected by environmental and management conditions. Different climate structures and regional differences in herds contribute to the prevalence of foot diseases [18,19]. For example, cows in humid and temperate regions may be more prone to certain foot diseases due to prolonged exposure to wet conditions, which are conducive to bacterial proliferation [20,21]. Likewise, the risk of infectious disease may increase in larger herds and foot diseases may become more common in herds due to poor management [22]. Studies conducted in different regions of Türkiye show that the prevalence of foot diseases varies from east to west, with rates ranging from 8.1% [23] to 38.77% [21]. Although there are regional studies on the prevalence

and contributing factors of foot diseases in dairy cattle in Türkiye, there is still a lack of comprehensive data. Understanding the factors affecting such diseases is critical in developing prevention strategies for dairy farms and eliminating administrative problems. This study asked the following research question: Do geographic region, breed, and sample size affect the prevalence of foot diseases in cows in Türkiye? It evaluated the prevalence of foot diseases in dairy cattle throughout Türkiye, and it calculated a combined rate. By analyzing the effects of geographic region, breed, and sample size on illness rates, this study advances the relevant literature.

Material And Methods

Research Question

Do geographic region, breed, and sample size affect the prevalence of foot diseases in cows in Türkiye?

Search Strategy and Literature Review

This study is based on the PRISMA statement and the checklist is provided in Supplementary material [24,25]. Between July and September 2024, a keyword-based search was carried out in the databases of PubMed, Web of Science, Google Scholar, Scopus, Dergipark, and the National Thesis Center using the online library platform of Cukurova University. The following search terms were employed: "cow," "foot disease," "prevalence," and "Türkiye." The complete search strategies, including Boolean operators and database-specific search strings, are provided in Supplementary material. After a detailed literature search, all relevant observational studies (e.g., cross-sectional and cohort studies), studies including the prevalence of foot illnesses, master's theses, and doctoral dissertations were considered. The findings were filtered to include only studies published in the past 26 years, from January 1999 to September 2024, in English and Turkish. The resulting studies were classified as included or excluded based on an initial review of their titles and abstracts and whether they answered the abovementioned research question.

Inclusion and Exclusion Criteria

The flow chart for the systematic review and the article selection process for the meta-analysis, which was created based on the PRISMA guidelines, is presented in *Fig. 1*. First, a total of 5.779 studies published between January 1999 and September 2024 were collected through a comprehensive literature search. Then, these studies were selected according to the following inclusion criteria: a) English and Turkish articles published in peer-reviewed journals investigating the prevalence of foot diseases in different regions of Türkiye; b) observational studies (e.g., cross-sectional and cohort studies); c) studies with data on the prevalence or rates of foot diseases in cows; d) studies specifying the geographic region, breed, and sample size; e) master's theses and doctoral dissertations providing information on the rates or prevalence of foot diseases in cows in Türkiye. The exclusion criteria were as follows: a) master's theses or doctoral dissertations without information on the rates or prevalence of foot diseases, b) studies using only male animals, and c) studies not providing details on the rates or prevalence of foot diseases. In meta-analyses involving more than one geographic region, each region was considered a separate study, and the data were evaluated by region. If more than one breed was investigated in a study, the number of cows with foot diseases was considered separately by breed.

Data Extraction

Two authors independently screened all the full-text studies to determine whether they met the inclusion and exclusion criteria. In the identified studies, only numerical data of the diseases that constitute the rates or prevalence of foot diseases were collected, and the framework of the study was created by not extracting data on the diseases. Using a standard data extraction form, the first author's name, year of publication, breed(s) of cows used in the study, geographic region, sample size, and number of cows with foot diseases were recorded. The list of the studies included in the meta-analysis and their detailed characteristics are given in *Table 1*. The data were classified by dividing them into subgroups based on animal breed (Holstein, Simmental, Brown Swiss, native, and mixed), geographic region (Marmara, Aegean, Mediterranean, Central Anatolia, Southeastern Anatolia, and Eastern Anatolia), sample size (less than 1.000 and more than 1.000), and study year (first 16 years, last 10 years, and 26 years in total). Then, the numbers of cows with foot diseases and the total sample-size values were extracted separately from these subgroups. The Black Sea region, one of the seven regions of Türkiye, was not included in the study because there was not enough information about it. Disagreements between the authors were resolved through discussion.

Data Quality Appraisal

Data quality of all the studies was assessed using 10 quality control items described by Joanna Briggs Institute prevalence critical appraisal [51]. The tool evaluated the following: sample frame, sampling methods, sample size, description of setting, sufficient coverage for data analysis, objective and reliable methods for identifying the condition, appropriate statistical analysis, and adequate response rate. The tool appraises each domain as Yes/No/Unclear/Not applicable. We assigned a value 1 to a Yes answer and a value 0 if the answer was No/Unclear/Not Applicable. A higher score denotes a higher quality study, with a maximum attainable score of 10. As the Joanna Briggs Institute tool does not define a specific cutoff for acceptable quality, a threshold of ≥5 (i.e., at least 50% of the quality domains fulfilled) was used to distinguish studies

Table 1. Information about 31 studies was included in the meta-analysis on the prevalence of foot diseases in dairy cows

Study Number	Study	Breed	Geographic Region	Sample Size	Number of Foot Diseases in Cows
1	Sağlıyan et al., 2010 [26]	Undefined	Eastern Anatolia	1352	387
2	Kulualp et al., 2021 [27]	Holstein, Simental	Aegean	1685	179
3	İstek et al., 2019 [18]	Holstein, Simental, Brown Swiss, Native, Mixed	Eastern Anatolia	422	100
4	Erol et al., 2019 [28]	Brown Swiss	Central Anatolia	200	80
5	Ormancı and Belge, 2001 [29]	Holstein, Simental, Brown Swiss, Native, Mixed	Eastern Anatolia	1800	321
6	Tutuş and Gençcelep, 2021 [23]	Simental, Brown Swiss, Native, Mixed	Eastern Anatolia	1686	128
7	Çeçen et al., 2018 [30]	Holstein	Aegean	93	33
8	Şengöz Şirin et al, 2021 [5]	Simental	Mediterranean	281	269
9	Özcan and Pamuk, 2009 [31]	Holstein, Simental, Brown Swiss, Native, Mixed	Central Anatolia	1800	195
10	Atasoy N, 2003 [32]	Holstein, Simental, Brown Swiss, Native, Mixed	Eastern Anatolia	924	210
11	Şındak et al., 2003 [33]	Undefined	Southeast Anatolia	4432	134
12	Yayla et al., 2012 [19]	Simental, Brown Swiss, Native, Mixed	Eastern Anatolia	2317	280
13	Yurdakul and Şen, 2018 [21]	Undefined	Central Anatolia	1302	514
14	Yakan S, 2018 [34]	Undefined	Eastern Anatolia	1255	222
15	Keskin and Durmuş, 2016 [35]	Undefined	Southeast Anatolia	1818	209
16	Saruhan A, 2015 [36]	Holstein, Simental, Native, Mixed	Eastern Anatolia	570	43
17	Canatan U, 2020 [37]	Undefined	Marmara	85	84
18	Daştan İ, 2009 [38]	Holstein, Simental, Brown Swiss, Native, Mixed	Aegean	1090	71
19	Aydınoğlu AG, 2009 [39]	Holstein, Simental, Native, Mixed	Mediterranean	1320	77
20	Yılmaz Tan F, 2020 [40]	Undefined	Eastern Anatolia	1303	14
21	Kavuş MT, 2022 [41]	Undefined	Eastern Anatolia	4000	292
22	Pirci B, 2011 [42]	Holstein	Central Anatolia	100	37
23	Akın İ, 2008 [43]	Holstein	Marmara	540	42
24	Yaylak et al., 2010 [22]	Holstein	Aegean	1080	305
25	İstek ve Durgun, 2004 [44]	Undefined	Eastern Anatolia	1356	184
26	Kayapınar and Han, 2021 [45]	Undefined	Eastern Anatolia	7040	547
27	Canpolat and Bulut, 2003 [46]	Undefined	Eastern Anatolia	3600	512
28	Güzel and Erden, 2000 [47]	Undefined	Aegean	505	233
29	Çeçen and Görgül, 2007 [48]	Holstein	Marmara	547	196
30	Sağlıyan and Ünsaldı, 2002 [49]	Undefined	Eastern Anatolia	1688	144
31	Ayhan HD, 2019 [50]	Undefined	Eastern- Southeast Anatolia	600	465

with moderate methodological quality from those with lower quality. This approach is consistent with previous prevalence meta-analyses using the same appraisal tool [51]. In all stages of this process, discrepancies between reviewers were resolved by consensus.

Statistical Analysis

Before the meta-analysis, publication bias was examined statistically with Egger's test [52] and graphically with the funnel plot in all subgroups. The trim-and-fill method was used to eliminate publication bias. Egger's test was not

used if the number of studies included in the meta-analysis was less than 10. Cochran's Q test evaluated the heterogeneity of the effect sizes of the studies. The Q statistics were calculated with I^2 values. If the heterogeneity was statistically significant, the random effects model was used to estimate the effect size; if the heterogeneity was not significant, the fixed effects model was employed. The effect sizes of individual studies were obtained as a result of the meta-analysis, and the combined effect sizes were shown graphically with forest plots. The heterogeneity of the subgroups was determined based on the animal breeds, geographic regions, sample sizes, and study years of the studies included in each subgroup. Then, the combined rates with 95% CI according to the sample sizes and numbers of cows with foot diseases were calculated. The chosen level of statistical significance was $P<0.05$, but $\alpha=0.10$ was taken as indicating publication bias and heterogeneity. MedCalc version 23.0.9. (free trial) was used for the meta-analysis, and the meta and metafor packages of R version 4.4.1. (R Core Team, 2021) were employed to look for publication bias.

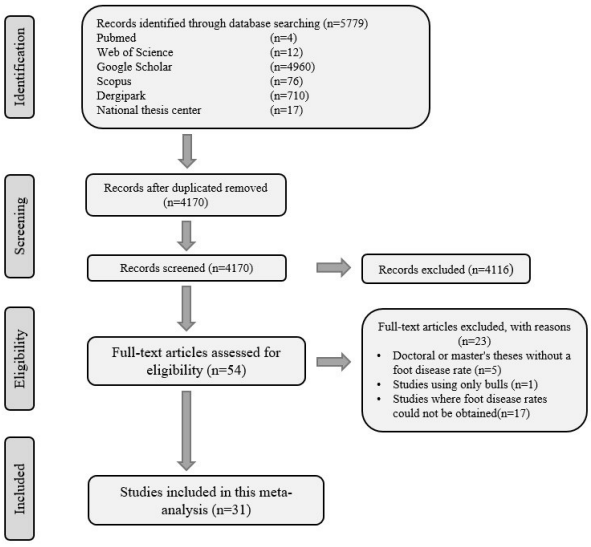

Fig 1. Flow diagram of the studies identified by the systematic review on the prevalence of foot disease in dairy cows

Results

Study Characteristics

A total of 31 articles that met the inclusion criteria were deemed suitable for meta-analysis. The selection process is shown in *Fig. 1*. Meta-analyses were performed on the subgroups based on geographic region, breed, sample size, and publication year. Among the studies, 14 articles did not specify animal breeds were not included in the meta-analysis in the breed subgroup; hence, analyses were performed on 17 articles. The list of the studies included in the meta-analysis and their detailed characteristics are presented in *Table 1*. The most common breed was the Holstein (n=13), followed by the Simmental (n=11); the other three breeds were equally common (n=9). From a geographic perspective, the eastern Anatolia region had the most studies (n=14), while the Mediterranean region had the least (n=2). Also, 11 studies with sample sizes of less than 1,000 were identified, while 20 studies with sample sizes of more than 1.000 were found. Regarding the publication years, 16 studies were published in the first 16 years (1999-2014) and 15 were published in the last 10 years (2015-2024). The quality assessment indicated that most included studies were of acceptable quality. The average score was 7.25 points (range 5-9, with higher scores denoting higher quality articles), where the best scores were associated with sampling, sample frame, methods for sampling, and sample size. A summary of the quality assessment is presented in the Supplementary Material.

Meta-Analysis Results

No evidence of publication bias was detected in the subgroups with more than 10 studies, and the trim-and-fill method was not used to determine effect sizes. Heterogeneity between the studies was statistically significant in all the subgroups according to Cochran's Q test; hence, the random effects model was used to determine effect sizes.

Breed

The meta-analysis results concerning the breeds are shown in *Table 2*. The effect sizes were calculated by considering heterogeneity. There were heterogeneous distributions in all the breeds. The rate of foot diseases was highest in Holstein cows (13.22%) and lowest in native breed cows (3.88%). The funnel and forest plots for the Holstein breed are presented in *Fig. 2*. The funnel and forest plots for the other breeds can be found in Supplementary Material.

Geographic Region

The meta-analysis findings regarding the geographic regions are shown in *Table 3*. There were heterogeneous distributions in all the regions. The prevalence rates of foot diseases were as follows: 51.59% in the Mediterranean region, 50.02% in Marmara, 30.73% in Central Anatolia, 23.45% in the Aegean, 11.82% in Eastern Anatolia, and 6.76% in Southeastern Anatolia. The funnel and forest plots for the Central Anatolia region are presented in *Fig. 3*. The funnel and forest plots for the other regions can be found in Supplementary Material.

Sample Size

The meta-analysis results concerning the two sample-size groups are shown in *Table 4*. There were heterogeneous distributions in both groups. The pooled prevalence was 41.67% in studies with sample sizes <1.000 and 11.77% in studies with sample sizes >1.000. The relevant funnel and forest plots are given in Supplementary Material.

Publication Year

Table 5 presents the findings of the meta-analysis regarding the studies' publication years. There were heterogeneous distributions in all three groups. In the group concerning the first 16 years (1999-2014), the rate of foot diseases was 16.93%; in the group pertaining to the last 10 years (2015-2024), the rate increased to 24.81%. In the group

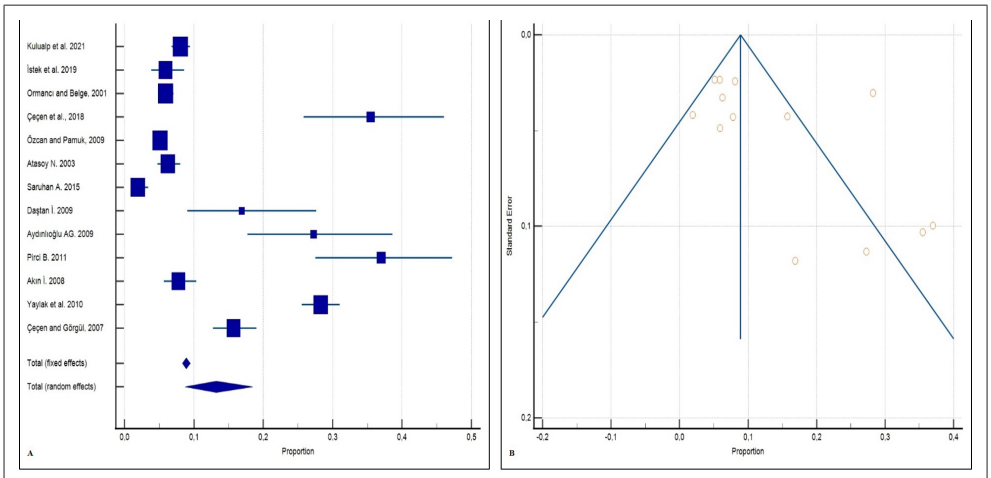

Fig 2. Forest plot (A) and funnel plot (B) of studies on the Holstein breed

Table 2. *Prevalence rates of breed, heterogeneity, and Egger test results*

Breed	Proportion (%)	95% CI	Test for Heterogeneity			Egger Test (P-value)
			Q	*P*-value	I^2 (%)	
Holstein	13.22	8.75-18.45	566.57	<0.001	97.88	0.163
Simmental	9.37	3.64-17.41	1606.64	<0.001	99.38	0.144
Brown swiss	8.17	4.26-13.21	499.44	<0.001	98.40	-
Native	3.88	2.29-5.86	146.67	<0.001	94.55	-
Mixed	5.16	3.13-7.66	181.82	<0.001	95.60	-

CI: *Confidence interval,* ***Q:*** *Cochran Q statistics,* ***I:*** *numerical expression of heterogeneity*

Table 3. *Prevalence rates of geographic region, heterogeneity, and Egger test results*

Geographic Region	Proportion (%)	95% CI	Test for Heterogeneity			Egger Test (P-value)
			Q	P-value	I^2 (%)	
Marmara	50.02	10.54-89.97	443.23	<0.001	99.55	-
Aegean	23.45	10.80-39.17	484.57	<0.001	99.17	-
Mediterranean	51.59	8.20-89.96	1153.71	<0.001	99.91	-
Central Anatolia	30.73	12.67-52.58	399.45	<0.001	99.25	-
Southeast Anatolia	6.76	3.68-10.69	165.03	<0.001	98.18	-
Eastern Anatolia	11.82	7.87-16.43	1979.49	<0.001	99.34	0.446

CI: *Confidence interval,* ***Q:*** *Cochran Q statistics,* ***I:*** *numerical expression of heterogeneity*

Table 4. *Prevalence rates of sample size, heterogeneity, and Egger test results*

Sample Size	Proportion (%)	95% CI	Test for Heterogeneity			Egger Test (P-value)
			Q	P-value	I^2 (%)	
<1000	41.67	24.45-60.01	1445.15	<0.001	99.31	0.119
>1000	11.77	8.75-15.17	2293.14	<0.001	99.17	0.258

CI: *Confidence interval,* ***Q:*** *Cochran Q statistics,* ***I:*** *numerical expression of heterogeneity*

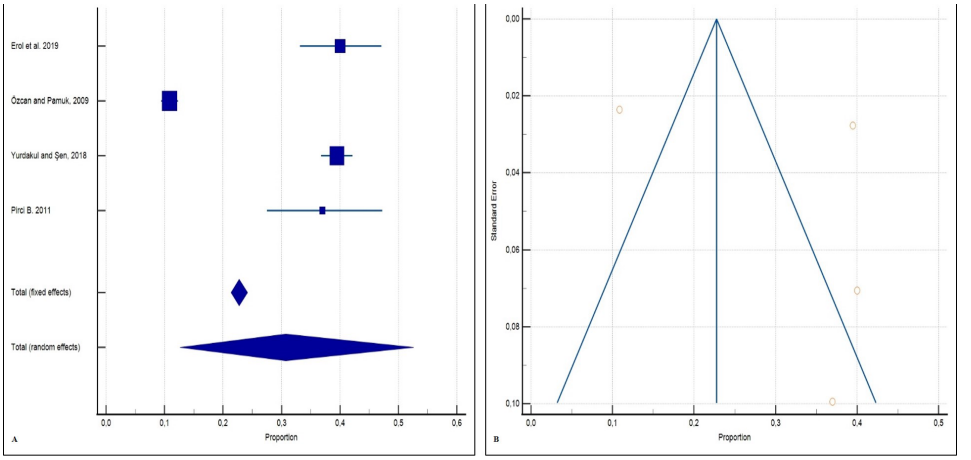

Fig 3. Forest plot (A) and funnel plot (B) of studies in the Central Anatolia region

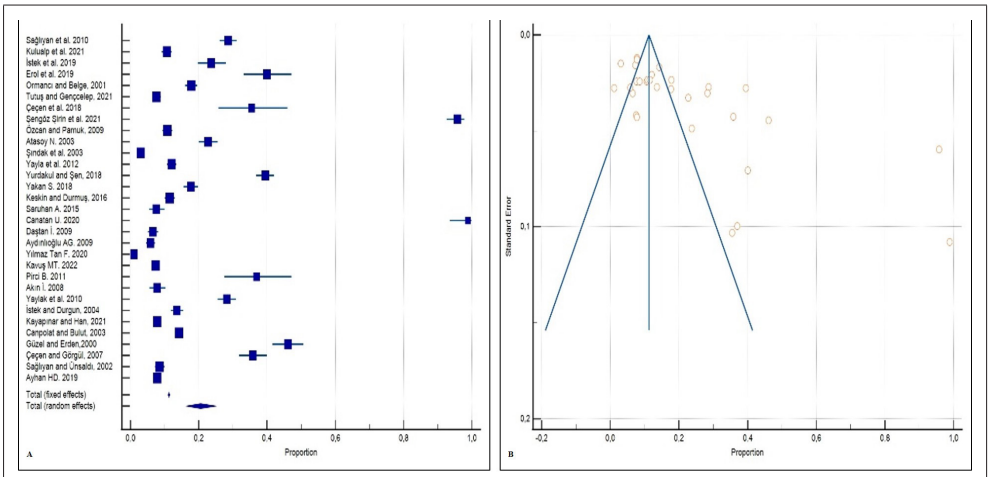

Fig 4. Forest plot (A) and funnel plot (B) of studies from the past 26 years

Table 5. *Meta-analysis results for different year intervals.*

Year	Proportion (%)	95% CI	Test for Heterogeneity			Egger Test (P-value)
			Q	P-value	I^2 (%)	
First 16 years	16.93	12.01-22.50	1801.69	<0.001	99.17	0.571
Last 10 years	24.81	17.46-32.98	2956.19	<0.001	99.53	0.225
Total 26 years	20.52	16.23-25.19	4809.29	<0.001	99.38	0.378

CI: *Confidence interval,* ***Q:*** *Cochran Q statistics,* ***I:*** *numerical expression of heterogeneity*

regarding the whole period (26 years), the foot disease rate was 20.52%. The funnel and forest plots for the studies in the latter group (whole period) are presented in *Fig. 4*. The funnel and forest plots for the other two groups can be found in Supplementary Material.

Discussion

This study examined the effects of geographic region, breed, and sample size on the prevalence of foot diseases in cows in Türkiye. It calculated a combined rate of foot disease prevalence from existing data. The prevalence of foot diseases in cows varies depending on the breed and type of disease [35,45]. Among the factors affecting the prevalence of such diseases, herd size, building type, lying space and floor type, grazing period, feeding methods, and the seasonal distribution of lameness are all important. Also, keeping regular lameness records is critical for monitoring animal health and welfare [53]. Furthermore, housing conditions have also been shown to impact prevalence; the rates of foot diseases in free-stall

systems are lower than those in tie-stall systems [54]. The present meta-analysis revealed the effects of geographic region, animal breed, and sample size on prevalence and the differences in prevalence of subgroups.

The data used in systematic reviews and meta-analyses of the prevalence of foot diseases in cows vary. These analyses combine studies conducted in different countries of the world [16] or studies from different regions of the same country [55]. Oehm et al.[56] performed meta-analysis according to the coefficients (odds ratio), standard errors, and risk factors. Afonso et al.[55] carried out meta-analysis based on the lameness incidence rates obtained from their included studies. Dutton-Regester et al.[1] conducted meta-analysis according to the sensitivity and specificity values of their selected studies. In the present meta-analysis, the percentage values of the foot disease prevalence rates were obtained based on the sample sizes and numbers of cows with foot diseases from 31 studies, and proportional meta-analyses of these data were performed. Although some primary studies used the term "incidence," it is important to distinguish between incidence and prevalence as separate epidemiological measures. Incidence refers to newly occurring cases over a defined period, whereas prevalence represents the proportion of existing cases at a given time. In the present meta-analysis, the synthesized estimates correspond to prevalence data.

According to the meta-analysis, the pooled prevalence of foot disease was 20.52% (95% CI: 16.23-25.19). A difference in pooled prevalence was observed between study periods. In the 16 studies covering the first 16 years of the study period, the pooled prevalence was 16.93% (95% CI: 12.01-22.50), whereas in the 15 studies representing the most recent 10 years, the pooled prevalence was 24.81% (95% CI: 17.46-32.98). This apparent increase in pooled prevalence should not be interpreted as a definitive rise in the true frequency of foot diseases. The higher estimates observed in more recent studies may reflect improved detection methods, increased awareness among farmers and veterinarians, changes in reporting practices, or differences in study design and sampling strategies rather than a true epidemiological increase. Compared with other studies in Europe, the foot disease rate on farms in England and Wales was 36.8% [57]. In Greece, the lameness prevalence was 18.7% [58]. In a study that reported the prevalence of lameness in four countries, the rates were as follows: 25% in Germany, 24% in France, 10% in Spain, and 7% in Switzerland [53]. In our meta-analysis, the prevalence of foot diseases in cows varied widely, from 1.07% [40] to 98.82% [37]. The latter figure comes from a study of foot diseases in slaughterhouse material collected in the Bursa region, where the presence of at least one claw lesion in almost all the feet and the scope of the study explain the high rate [37]. Overall, these findings suggest that foot diseases remain a significant health concern in dairy cattle, although prevalence estimates may vary substantially depending on study design, sampling methods, and regional management conditions.

The present meta-analysis demonstrated substantial variation in the prevalence of foot diseases across geographic regions in Türkiye. The Mediterranean region showed the highest pooled prevalence (51.59%, 95% CI: 8.20-89.96), whereas Southeastern Anatolia had the lowest prevalence (6.76%, 95% CI: 3.68-10.69). The Marmara region had the second-highest prevalence (50.02%, 95% CI: 10.05-89.97). These findings suggest notable regional differences in the burden of foot diseases. However, no eligible studies were available for the Black Sea region; therefore, analyses were limited to six regions, which represents an important limitation of this study. Additionally, the high prevalence estimates observed in the Mediterranean and Marmara regions were accompanied by wide confidence intervals, reflecting considerable statistical uncertainty. These estimates were based on a limited number of studies (e.g., n = 2 for the Mediterranean region) and may have been influenced by specific study characteristics. For example, a small-scale study conducted using slaughterhouse material in the Marmara region reported a prevalence of 98.82%, which may have disproportionately affected the pooled estimate. Therefore, these regional estimates should be interpreted with caution. Regional variations in climate, herd size, housing systems, and access to pasture may partly explain the observed differences. Previous research has shown that access to pasture improves foot health, with lower rates of foot diseases and lameness observed in cows that spend more time grazing compared to those kept in confined housing systems [59]. Moreover, elevated summer temperatures and increased heat stress have been associated with a higher risk of foot disorders [60,61]. However, in our meta-analysis, the prevalence of foot diseases in Southeastern Anatolia was the lowest despite the region's high summer average temperatures. By examining the studies conducted in this region in terms of seasonal conditions and increasing the number of studies, different explanations can be made regarding the effect of heat stress on cows.

In 6 of the 17 studies contained in the meta-analysis of animal breeds, a single breed was investigated, while in the other 11 studies, more than one breed was looked at. The most common breed was the Holstein, which was also the breed with the highest rate of foot diseases (13.22%, 95% CI: 8.75-18.45). The fact that Holstein cows dominate the industry due to their productivity and that they become less resistant to foot diseases compared to other breeds when sufficient care is not taken of them has been reported in other studies [31,62]. Foot disease rates among breeds vary according to the region where the study has

been conducted, the study methods (clinical trial, survey, etc.), and the herd's characteristics. While breeds such as Holstein [22,30,42,43], Simmental [5], and Brown Swiss [28] are used in herd-based studies, it is noticeable that the number of breeds is greater than one in prevalence studies addressing specific regions [18,29,31,32,38]. Furthermore, the rate of foot diseases in cattle is increasing, especially as intensive housing conditions have become widespread and breeds such as Holstein and Simmental have adapted to them [32,44]. In addition, changes in the genetic structure of breeds, the physical and environmental conditions to which breeds are exposed, and different care management practices all affect the prevalence of foot diseases [63].

Subgroup analyses further indicated differences in pooled prevalence according to sample size. The pooled prevalence was 11.77% (95% CI: 8.75-15.17) in studies including ≥1.000 animals and 41.67% (95% CI: 24.45-60.01) in studies with <1.000 animals. The narrower confidence interval observed in larger studies suggests greater statistical precision, whereas smaller studies demonstrated greater variability in prevalence estimates [22,64]. For example, a study involving 7.040 animals in the Malatya region reported a prevalence of 7.77% [45], whereas in a single-herd study conducted on 281 cows in the Burdur region reported a prevalence of 95.73% [5]. In our study, the rate of foot diseases was generally high in studies with sample sizes of less than 1.000 [28,42]; it is noteworthy that these studies were mostly conducted in single herds. The studies with sample sizes of more than 1,000 [33,41,46] mainly covered more than one herd; accordingly, the decrease in the rate of foot diseases was noticeable. Therefore, the observed inverse pattern between sample size and pooled prevalence likely reflects differences in study design, representativeness, and statistical precision rather than a true biological association [65].

In addition, a higher pooled prevalence was observed in studies conducted during the most recent decade (24.81%) compared with those from the earlier study period (16.93%). However, this apparent increase should be interpreted cautiously. Rather than representing a definitive rise in the true frequency of foot diseases, the difference may reflect enhanced diagnostic awareness, improved detection methods, and increased reporting practices within the Turkish dairy sector. Furthermore, the substantial methodological heterogeneity observed across studies (I^2 >99%) suggests that variations in sampling strategies, diagnostic criteria, and case definitions between study periods may have significantly influenced the pooled estimates. Without accounting for these methodological differences, a purely biological interpretation of the temporal pattern would be inappropriate. Overall, the observed trend likely reflects improvements in case detection and documentation rather than a straightforward escalation in disease occurrence.

Conclusion

Foot diseases remain an important health concern in dairy cattle in Türkiye. The pooled prevalence of 20.52% (95% CI: 16.23-25.19) obtained in this meta-analysis should not be interpreted as the true national population prevalence. Rather, this estimate represents a statistical summary of studies conducted over a 26-year period using different methodological approaches, diagnostic criteria, and sampling strategies, with substantial heterogeneity (I^2 = 99.38%). Therefore, the pooled value should be interpreted cautiously and viewed as an aggregated epidemiological indicator rather than a definitive population parameter. These findings highlight the need for standardized surveillance systems and well-designed, large-scale observational studies to better characterize the current burden of foot diseases in the national dairy herd.

Highlight Keypoints

- Geographical region, breed, and sample size are effective in the prevalence of foot diseases.
- The pooled prevalence of foot diseases in Türkiye is 20.52%.
- The Holstein breed showed the highest prevalence among breeds.
- Prevalence significantly increased after 2015.
- Prevalence ranged from 6.76% to 51.59% across geographical regions.

Declarations

Availability of Data and Materials: The datasets generated during and/or analysed during the current study are available from the corresponding author (VAC) on reasonable request.

Acknowledgements: None.

Competing Interests: The authors have no relevant financial or non-financial interests to disclose.

Declaration of Generative Artificial Intelligence (AI): The article and/or tables and figures were not written/created by AI and AI assisted technologies.

Author Contributions: All authors contributed to the study conception and design. VAC: Conceptualization, Data curation, Investigation, Methodology, Resources, Validation, Writing - original draft, Writing - review and editing, UC: Conceptualization, Data curation, Formal analysis, Investigation, Methodology, Resources, Visualization, Writing - review and editing, EU: Conceptualization, Data curation, Formal analysis, Methodology, Validation, Writing - review and editing

References

1. **Dutton-Regester KT, Barnes TS, Wright JD, Alawneh JI, Rabiee AR:** A systematic review of tests for the detection and diagnosis of foot lesions causing lameness in dairy cows. *Prev Vet Med,* 149, 53-66, 2018. DOI: 10.1016/j.prevetmed.2017.11.003

2. **Kofler J, Berger P, Egger-Danner C, Fuerst-Waltl B:** Benchmarking claw health across three dairy cow breeds in 508 dairy farms using numerical claw health indicators. *Vet J,* 308:106242, 2024. DOI: 10.1016/j.tvjl.2024.106242
3. **Sahar MW, Beaver A, Daros RR, von Keyserlingk MAG, Weary DM:** Measuring lameness prevalence: Effects of case definition and assessment frequency. *J Dairy Sci,* 105 (9): 7728-7737, 2022. DOI: 10.3168/jds.2021-21536
4. **Han MC, Sağlıyan A, Polat E:** Sığırlarda ahır zemin tiplerinin ayak hastalıkları ve tırnak deformasyonları üzerine etkilerinin araştırılması. *Harran Üniv Vet Fak Derg,* 6 (1): 19-24, 2017. DOI: 10.31196/huvfd.325680
5. **Sengöz-Şirin Ö, Önür A, Şavklıyıldız F:** Burdur yöresinde bir sağmal süt sığırı (simental) işletmesinde gözlenen ayak hastalıklarının incelenmesi. *MAE Vet Fak Derg,* 6 (1): 22-27, 2021. DOI: 10.24880/maeuvfd.884378
6. **Fürmann A, Syring C, Becker J, Sarbach A, Weber J, Ruiters MW, Steiner A:** Prevalence of painful lesions of the digits and risk factors associated with digital dermatitis, ulcers and white line disease on swiss cattle farms. *Animals,* 14 (1):153, 2024. DOI: 10.3390/ani14010153
7. **Palmer MA, O'Connell NE:** Digital dermatitis in dairy cows: A review of risk factors and potential sources of between-animal variation in susceptibility. *Animals,* 5 (3): 512-535, 2015. DOI: 10.3390/ani5030369
8. **Alrhmoun M, Gauly M, Poulopoulou I:** Seasonal prevalence and geographical distribution of claw health in dairy cows: Investigation of the causal relationship with breed. *J Dairy Sci,* 108 (1): 980-995, 2025. DOI: 10.3168/jds.2024-25204
9. **Bicalho RC, Oikonomou G:** Control and prevention of lameness associated with claw lesions in dairy cows. *Livest Sci,* 156 (1-3): 96-105, 2013. DOI: 10.1016/j.livsci.2013.06.007
10. **Shearer JK, Plummer PJ, Schleining JA:** Perspectives on the treatment of claw lesions in cattle. *Vet Med (Auckl),* 6, 273-292, 2015. DOI: 10.2147/VMRR.S62071
11. **Booth CJ, Warnick LD, Gröhn YT, Maizon DO, Guard CL, Janssen D:** Effect of lameness on culling in dairy cows. *J Dairy Sci,* 87, 4115-4122, 2004. DOI: 10.3168/jds.S0022-0302(04)73554-7
12. **Kofler J, Suntinger M, Mayerhofer M, Linke K, Maurer L, Hund A, Fiedler A, Duda J, Egger-Danner C:** Benchmarking based on regularly recorded claw health data of austrian dairy cattle for ımplementation in the cattle data network (RDV). *Animals,* 12 (7):808, 2022. DOI: 10.3390/ani12070808
13. **Shearer JK, Hutjens MF, Endres MI:** Managing the herd to minimize lameness. **In,** Beede DK (Ed): Large Dairy Herd Management. 3rd ed., 1093-1102, American Dairy Science Association, IL, 2017.
14. **Alvergnas M, Strabel T, Rzewuska K, Ewa Sell-Kubiak E:** Claw disorders in dairy cattle: Effects on production, welfare and farm economics with possible prevention methods. *Livest Sci,* 222, 54-64, 2019. DOI: 10.1016/j.livsci.2019.02.011
15. **Sarıözkan S, Küçükoflaz M:** Total financial and avoidable losses due to lameness in Turkish dairy herds. *Ankara Univ Vet Fak Derg,* 71 (3): 329-334, 2024. DOI: 10.33988/auvfd.1214635
16. **Thomsen PT, Shearer JK, Houe H:** Prevalence of lameness in dairy cows: A literature review. *Vet J,* 295:105975, 2023. DOI: 10.1016/j.tvjl.2023.105975
17. **Ergün OF, Bayram B:** Changes in the livestock sector in Turkey. *J Bahri Dagdas Anim Res,* 10 (2): 158-175, 2021.
18. **İstek Ö, Han MC, Tanrısever M:** Fırat üniversitesi hayvan hastanesine getirilen sığırlardaki tırnak deformasyonları ile ayak hastalıklarının retrospektif değerlendirilmesi. *Harran Üniv Vet Fak Derg,* 8 (1): 57-63, 2019. DOI: 10.31196/huvfd.591121
19. **Yayla S, Aksoy Ö, Kılıç E, Cihan M, Özaydın İ, Ermutlu CŞ:** Kars ve yöresinde sığırların bakım ve barındırma koşulları ile ayak hastalıkları arasındaki ilişkinin değerlendirilmesi. *Harran Üniv Vet Fak Derg,* 1 (1): 22-27, 2012.
20. **İzci C:** Sığırlarda Ayak Hastalıkları ve Topallık Kontrolü. 38-46, Selçuk Üniversitesi Basımevi, Konya, 2018.
21. **Yurdakul İ, Şen İ:** Sivas ve yöresinde sığır ayak hastalıkları prevalansının belirlenmesi. *Harran Üniv Vet Fak Derg,* 7 (1): 51-55, 2018. DOI: 10.31196/huvfd.470735
22. **Yaylak E, Akbaş Y, Kaya IA, Uzmay C:** The effects of several cow and herd level factors on lameness in Holstein cows reared in Izmir province of Turkey. *J Anim Vet Adv,* 9 (21): 2714-2722, 2010. DOI: 10.3923/javaa.2010.2714.2722
23. **Tutuş D, Gençcelep M:** Van muradiye ilçesinde ruminantlarda görülen ekstremite ve ayak hastalıklarının insidansı. *Van Vet J,* 32 (2): 82-90, 2021. DOI: 10.36483/vanvetj.957429
24. **Moher D, Liberati A, Tetzlaff J, Altman DG:** Preferred reporting items for systematic reviews and meta-analyses: The PRISMA statement. *PLoS Med,* 6 (7):e1000097, 2009. DOI: 10.1371/journal.pmed.1000097
25. **Page MJ, McKenzie JE, Bossuyt PM, Boutron I, Hoffmann TC, Mulrow CD, Shamseer L, Tetzlaff JM, Akl EA, Brennan SE, Chou R, Glanville J, Grimshaw JM, Hróbjartsson A, Lalu MM, Li T, Loder EW, Mayo-Wilson E, McDonald S, McGuinness LA, Stewart LA, Thomas J, Tricco AC, Welch VA, Whiting P, Moher D:** The PRISMA 2020 statement: An updated guideline for reporting systematic reviews. *BMJ,* 372:n71, 2021. DOI: 10.1136/bmj.n71
26. **Sağlıyan A, Gunay C, Han MC:** Prevalence of lesions associated with subclinical laminitis in dairy cattle. *Israel J Vet Med,* 65 (1): 27-33, 2010.
27. **Kulualp K, Ozturan YA, Akin I:** Assessment of animal and management based potential risk factor relation with claw health and lameness in dairy cows: A cross-sectional study. *Large Anim Rev,* 27, 323-328, 2021.
28. **Erol H, Erol M, Alkan F:** Evaluation of encountered claw lesions in dairy farm (Brown Swiss) in Konya province. *Eurasian J Vet Sci,* 35 (1): 24-28, 2019.
29. **Ormancı S, Belge A:** Van ve yöresinde süt sığırlarında ayak hastalıklarının nedenleri, dağılımı ve sağaltımı üzerine çalışmalar. *YYÜ Sağ Bil Derg,* 7 (1-2): 139-145, 2001.
30. **Ceçen G, İlhan G, Orman A:** Distribution of hoof lesions and hoof health strategies on a robotic milking farm. *Uludag Univ J Fac Vet Med,* 37 (1): 29-36, 2018. DOI: 10.30782/uluvfd.393935
31. **Özcan S, Pamuk K:** Afyonkarahisar ve çevresinde sığır ayak hastalıklarının prevalansı. *Kocatepe Vet J,* 2 (2): 15-19, 2009.
32. **Atasoy N:** Erzurum yöresinde süt sığırlarında görülen ayak hastalıklarının insidansı ve bunların sağaltımı. *YYÜ Vet Fak Derg,* 14 (1): 1-5, 2003.
33. **Şındak N, Keskin O, Selçukbiricik H, Sertkaya H:** Şanlıurfa ve yöresinde sığır ayak hastalıklarının prevalansı. *YYÜ Vet Fak Derg,* 14 (1): 14-18, 2003.
34. **Yakan S:** Ağrı ilinde sığırlarda ayak hastalıkları prevalansının belirlenmesi. *Harran Üniv Vet Fak Derg,* 7 (2): 207-212, 2018. DOI: 10.31196/huvfd.508987
35. **Keskin E, Durmuş AS:** Gaziantep ve yöresinde gözlenen sığır ayak hastalıklarının insidansı ve tedavileri üzerine gözlemler. *FÜ Sağ Bil Vet Derg,* 30 (3): 181-186, 2016.
36. **Saruhan A:** Mardin yöresinde bazı süt sığırcılığı işletmelerinde ayak hastalıklarının prevalansı. *Master's thesis,* Harran University, Institute of Health Sciences, 2015.
37. **Canatan U:** Bursa ilindeki sığırlarda ayak biyomekaniğinin morfolojik, radyolojik, patolojik ve taban yük dağılımı bulguları ile karşılaştırmalı araştırılması: randomize *eks-vivo* çalışma. *PhD thesis*, Bursa Uludag University, Institute of Health Sciences, 2020.
38. **Daştan İ:** Denizli yöresinde süt sığırlarında ayak hastalıklarının insidansı, nedenleri ve sağaltımı. *Master's thesis,* Yüzüncü Yıl University, Institute of Health Sciences, 2009.
39. **Aydınoğlu AG:** Antalya ili il merkezi ve merkez köylerinde sığırların ayak hastalıklarının insidansı. *Master's thesis,* Yüzüncü Yıl University, Institute of Health Sciences, 2009.

40. **Yılmaz Tan F:** Ardahan mezbahasına kesim için getirilen sığırlarda ayak hastalıklarının insidansı, saptanan hastalıklar üzerine radyolojik ve histopatolojik incelemeler. *Master's thesis,* Kafkas University, Institute of Health Sciences, 2020.
41. **Kavuş MT:** Elazığ ve Erzincan yöresi ayak hastalıklarının değerlendirilmesi. *Master's thesis,* Fırat University, Institute of Health Sciences, 2022.
42. **Pirci B:** Kayseri Develi Tarımsal Kalkınma Kooperatifi süt sığırı çiftliğinde bulunan sığır tırnaklarının muayenesi ve problemli tırnakların sağaltımı. *Master's thesis,* Erciyes University, Institute of Health Sciences, 2011.
43. **Akın İ:** Süt sığırlarında bazı tırnak hastalıklarının iyileşme sürecinde kan serumu ve tırnak dokusu iz element düzeyleri ile yeni oluşan tırnak dokusunun histolojik kalitesi arasındaki ilişki. *PhD Thesis,* Uludag University, Institute of Health Sciences, 2008.
44. **İstek Ö, Durgun T:** Muş ve yöresindeki sığırlarda görülen ayak hastalıklarının prevalansı üzerine araştırmalar. *Fırat Üniv Doğu Araş Derg,* 3 (1): 39-47, 2004.
45. **Kayapınar SD, Han MC:** Malatya ve yöresinde sığır ayak hastalıklarının prevalansı. *FÜ Sağ Bil Vet Derg*, 35 (1): 37-42, 2021.
46. **Canpolat İ, Bulut S:** Elazığ ve çevresinde sığırlarda görülen ayak hastalıklarının insidansı üzerine gözlemler. *FÜ Sağlık Bil Dergisi,* 17 (3): 155-160, 2003.
47. **Güzel N, Erden H:** Aydın yöresi sığırcılık işletmelerinde ayak hastalıklarının dağılımı. *Vet Cerrahi Derg,* 6 (3-4): 8-10, 2000.
48. **Çeçen G, Görgül OS:** Bursa yöresindeki bir işletmede, sağmal süt sığırı sürüsünde karşılaşılan topallıkların değerlendirilmesi. *Vet Cerrahi Derg,* 13 (1): 5-10, 2007.
49. **Sağlıyan A, Ünsaldı E:** Tunceli ve yöresindeki sığırlarda karşılaşılan ayak hastalıklarının insidansı üzerine gözlemler. *FÜ Sağlık Bil Dergisi,* 16 (1): 47-56, 2002.
50. **Ayhan HD:** Elazığ ve Adıyaman yöresinde sığırlarda ayak hastalıkları prevalansının araştırılması. *Master's thesis,* Fırat University, Institute of Health Sciences, 2019.
51. **Munn Z, Moola S, Riitano D, Lisy K:** The Development of a critical appraisal tool for use in systematic reviews: Addressing questions of prevalence. *Int J Health Policy Manag,* 3 (3): 123-128, 2014. DOI: 10.15171/ijhpm.2014.71
52. **Egger M, Smith GD, Schneider M, Minder C:** Bias in meta-analysis detected by a simple, graphical test. *BMJ,* 315, 629-634, 1997. DOI: 10.1136/bmj.315.7109.629
53. **Sjöström K, Fall N, Blanco-Penedo I, Duval JE, Krieger M, Emanuelson U:** Lameness prevalence and risk factors in organic dairy herds in four European countries. *Livest Sci,* 208, 44-50, 2018. DOI: 10.1016/j.livsci.2017.12.009
54. **Sogstad AM, Fjeldaas T, Østerås O, Forshell KP:** Prevalence of claw lesions in Norwegian dairy cattle housed in tie stalls and free stalls. *Prev Vet Med,* 70 (3-4): 191-209, 2005. DOI: 10.1016/j.prevetmed.2005.03.005
55. **Afonso JS, Bruce M, Keating P, Raboisson D, Clough H, Oikonomou G, Rushton J:** Profiling detection and classification of lameness methods in british dairy cattle research: A systematic review and meta-analysis. *Front Vet Sci,* 7:542, 2020. DOI: 10.3389/fvets.2020.00542
56. **Oehm AW, Knubben-Schweizer G, Rieger A, Stoll A, Hartnack S:** A systematic review and meta-analyses of risk factors associated with lameness in dairy cows. *BMC Vet Res,* 15:346, 2019. DOI: 10.1186/s12917-019-2095-2
57. **Barker ZE, Leach KA, Whay HR, Bell NJ, Main DCJ:** Assessment of lameness prevalence and associated risk factors in dairy herds in England and Wales. *J Dairy Sci,* 93, 932-941, 2010. DOI: 10.3168/jds.2009-2309
58. **Katsoulos PD, Christodoulopoulos G:** Prevalence of lameness and of associated claw disorders in Greek dairy cattle industry. *Livest Sci,* 122 (2-3): 354-358, 2009. DOI: 10.1016/j.livsci.2008.09.012
59. **Tillack A, Merle R, Müller KE, Hoedemaker M, Jensen KC, Bartel A, Oehm AW, Klawitter M, Stock A:** The relationship between lameness prevalence and pasture access in 659 dairy herds in Germany. *PLoS One,* 19 (6):e0305536, 2024. DOI: 10.1371/journal.pone.0305536
60. **Sanders AH, Shearer JK, De Vries A:** Seasonal incidence of lameness and risk factors associated with thin soles, white line disease, ulcers, and sole punctures in dairy cattle. *J Dairy Sci,* 92 (7): 3165-3174, 2009. DOI: 10.3168/jds.2008-1799
61. **Shearer JK, van Amstel SR, Benzaquen M, Shearer LC:** Effect of season on claw disorders (including thin soles) in a large dairy in the southeastern region of the USA. 14th International Symposium and 6th Conference on Lameness in Ruminants, 8-11 November, 110-111, Colonia, Uruguay, 2006.
62. **Baird LG, O'Connell NE, McCoy MA, Keady TWJ, Kilpatrick DJ:** Effects of breed and production system on lameness parameters in dairy cattle. *J Dairy Sci,* 92, 2174-2182, 2009. DOI: 10.3168/jds.2008-1333
63. **Heringstad B, Egger-Danner C, Charfeddine N, Pryce JE, Stock KF, Kofler J, Sogstad AM, Holzhauer M, Fiedler A, Müller K, Nielsen P, Thomas G, Gengler N, de Jong G, Ødegård C, Malchiodi F, Miglior F, Alsaaod M, Cole JB:** Invited review: Genetics and claw health: Opportunities to enhance claw health by genetic selection. *J Dairy Sci,* 101, 4801-4821, 2018. DOI: 10.3168/jds.2017-13531
64. **Akbulut Ö:** Çok değişkenli ve farklı ölçekli araştırmalarda örneklem büyüklüğünün tespiti. *J Anim Sci Prod (JASP),* 4 (2): 199-215, 2021. DOI: 10.51970/jasp.946399
65. **Chapinal N, Barrientos AK, von Keyserlingk MAG, Galo E, Weary DM:** Herd-level risk factors for lameness in freestall farms in the northeastern United States and California. *J Dairy Sci,* 96 (1): 318-328, 2013. DOI: 10.3168/jds.2012-5940

Kafkas Universitesi Veteriner Fakultesi Dergisi
Journal Home-Page: http://vetdergikafkas.org
E-ISSN: 1309-2251

Kafkas Univ Vet Fak Derg
32 (2): 165-172, 2026
DOI: 10.9775/kvfd.2025.35661

Review Article

Animal Identification in Precise Livestock Farming - A Systematic Review of Current Practices and Perspectives

Gergana BALIEVA[1(*)], Dimitar TANCHEV[1], Ivanka LAZAROVA[1], Ralitsa RANKOVA[1]

[1] Trakia University, Faculty of Veterinary Medicine, Food Quality and Safety and Veterinary Legislation Department, 6000, Stara Zagora, BULGARIA

(*) **Corresponding author:**
Gergana Balieva
Phone: +359 889005629
E-mail: gergana.balieva@trakia-uni.bg

How to cite this article?

Balieva G, Tanchev D, Lazarova I, Rankova R: Animal Identification in Precise Livestock Farming - A Systematic Review of Current Practices and Perspectives. *Kafkas Univ Vet Fak Derg*, 32 (2): 165-172, 2026.
DOI: 10.9775/kvfd.2025.35661

Article ID: KVFD-2025-35661
Received: 09.11.2025
Accepted: 23.01.2026
Published Online: 27.01.2026

Abstract

Precision Livestock Farming (PLF) operates through the implementation of modern technological approaches with regard to monitoring and managing animal health, welfare and productivity of individual animals in real-time. A crucial aspect of PLF is the individual identification of each animal, which contributes to development of personalized decisions, leading to improved health outcomes, optimized feed usage, and greater overall farm efficiency. Currently employed technologies for animal identification include means as ear tags, RFID tags and boluses, neck collars and other devices for identification. Recently, a new promising method for individual identification has emerged, implementing software technologies for animal face recognition. The present paper focuses on the comparison of the currently used methods for identification and animal face recognition on several criteria – accuracy, invasiveness, automation potential, effects on animal welfare and functional challenges. Among the methods analysed, face recognition appeared accurate for over 90%, with high automation potential, non-invasive and excellent outcomes for animal welfare. Although, there are some limitations for the large-scale implementation of this method as hardware costs, light-induced variations and needs for dataset preparation, livestock face identification has the potential to improve the precision and effectiveness of animal husbandry and management. With sustained investment in smart infrastructure for farms and on-field trials, animal face identification could be practically implemented for more efficient and intelligent livestock farming.

Keywords: Animal face recognition, Animal identification, Animal welfare, Precision livestock farming

Introduction

The identification of individual animals plays a vital role in the management of livestock farms, including operations on health monitoring, traceability of live animals and their products, reproduction management, and biosecurity measures. As global agriculture intensifies and shifts toward data-driven decision-making, the demand for accurate, efficient, and ethical identification systems continues to grow. Conventional methods such as ear tags, branding, tattooing, and injectable RFID chips, are widely used, but at the same time some of them present considerable limitations. These include potential for loss or damage [1,2], invasiveness, stress and pain to the animals [3,4], and susceptibility to human error or tampering [5]. Moreover, visual identification tools require physical proximity and often human intervention, which hinders their applicability in automated precision farming environments.

For the purpose of Precision livestock farming (PLF), identification systems must be capable of supporting automated, individualized management of large animal populations. PLF aims to enhance animal health, welfare, and productivity through the integration of real-time monitoring systems and intelligent technologies [6]. To meet these goals, researchers and technologists are exploring novel identification methods that are non-invasive, scalable, and compatible with digital infrastructure.

In the last decade less invasive and digitally applicable approaches have emerged, among which animal face recognition has gained significant attention. This method utilizes computer vision and artificial intelligence (AI) to draw on unique face features to distinguish between individuals, similar to human facial recognition systems. Recent advances in deep learning, particularly convolutional neural networks (CNNs), have enabled high-accuracy identification in various species, including cattle,

pigs, and goats [7-9]. These systems have the potential to be integrated with farm management software, surveillance cameras, and Internet of Things (IoT) networks for real-time tracking and decision support.

Furthermore, face recognition technologies promise broader functionalities such as automated monitoring of health and behavior, detection of estrus cycles, and implementation of disease outbreak control measures, all of which are among the essential components of smart farming systems [10,11]. At herd level, their application could mitigate the stress and ethical concerns associated with invasive marking techniques, which could address the growing societal demands for animal welfare and sustainable farming nowadays.

This study provides a structured comparison of different identification technology methods using unified evaluation criteria (accuracy, automation potential, welfare impact, and scalability), complemented by summary performance data and an assessment of methodological quality.

This paper critically evaluates the current state of animal face recognition technologies and their potential role in precision livestock farming. It analyses existing research, compares traditional and modern identification methods, and assesses the technological, practical, and ethical challenges of implementing face biometrics in farm environments. The objective is to determine whether face recognition can serve not only as a supplementary instrument but eventually as a reliable alternative to conventional systems of animal identification.

Material and Methods

The study was designed as a comparative systematic review with the objective to classify and compare various animal identification methods within the context of precision livestock farming, evaluating their accuracy, efficiency, impact on animal welfare, and potential for automation, with a particular focus on face recognition and whether it can fully replace or serve as a complementary method to existing practices. A structured literature search was conducted in the period January-April 2025, involving systematic searches in scientific databases such as Web of Science, Scopus, PubMed, and Google Scholar *(Fig. 1)*. The primary search strings included keywords and combination of terms as: "animal identification" AND ("ear tag" OR "RFID" OR "microchip" OR "GPS collar" OR "biometric*" OR "face recognition") "precision livestock farming" AND ("identification" OR "computer vision" OR "deep learning"). All relevant studies were subjected to selection based on predetermined criteria for inclusion - only peer-reviewed articles; published between 1995-2025; being available in English; focused on farm animal species - cattle, pigs, sheep, goats, horses, and poultry; included at least one animal identification method; reported findings on performance, accuracy or applicability. The exclusion criteria were set to removing from the study papers that were not peer-reviewed; papers from editorials, theses, conference abstracts; focus on animal species without farm relevance (like pets and wildlife); related to animal tracking or monitoring without individual identification.

All articles selected as per the criteria were checked for duplication. The compiled set after removing duplicates, was screened through titles and abstracts for relevance to the topic based on the inclusion criteria and potentially relevant articles with full text were assessed for eligibility. From each eligible study information was extracted regarding the identification method used, animal species involved, and performance indicators such as recognition accuracy, reliability, impact on animal welfare, ease of application, cost, potential for automation, integration with farm management systems, and adaptability to different environmental conditions.

The collected data were subjected to qualitative analysis in order to evaluate their methodology, transparency of performance metrics, reproducibility of methods, species diversity and field applicability. Based on this assessment, studies were categorized as of high, moderate and low methodological rigor, with the last group being excluded for further analysis. The remaining studies were used for comparative analysis encompassing traditional physical methods, electronic and biometric identification methods. Data were thematically analyzed and interpreted in light of the goals of precision livestock farming, considering not only the technical performance of each method but also its impact on animals, practical applicability, and potential for future scalability. Particular attention was given to face recognition technology and its ability to meet the requirements of modern identification systems. The results were organized to highlight the strengths and weaknesses of each technology in order to determine whether face recognition can realistically replace or enhance conventional practices in farm environments.

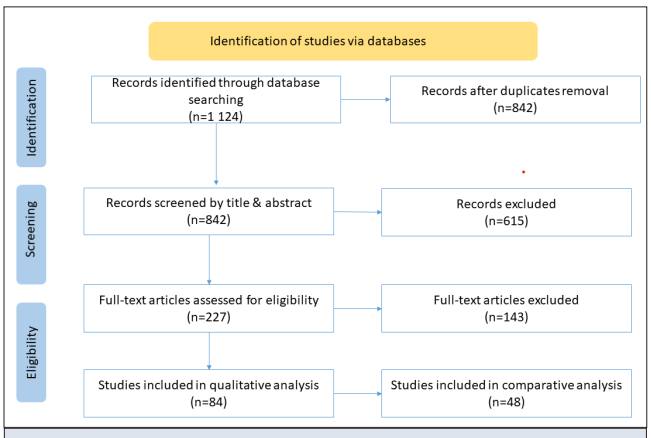

Fig 1. PRISMA flow diagram illustrating the literature search, screening, eligibility assessment, and final inclusion of studies in the systematic review

Results

Traditional Physical Approaches

The comparative review of animal identification methods that are currently available, revealed significant differences in their effectiveness, practicality, and compatibility with the goals of precision livestock farming (PLF) *(Table 1)*. Traditional approaches such as branding, tattooing, and ear tagging, although widely implemented, have several limitations in terms of animal welfare, ease of use, and the possibility of being integrated with animal holdings software. Branding, especially hot-iron branding, causes significant pain and long recovery periods, with healing taking over eight weeks in many cases. Animals subjected to this method often show clear signs of discomfort and avoidance behaviors, raising serious ethical concerns [3,4,12]. Cold branding and tattooing are somewhat less severe, but they are still invasive and not ideal for long-term tracking, especially on farms where digital monitoring is implemented [13,14].

Ear tags, particularly the visual plastic ones, are common due to being inexpensive and easy to apply. They typically display alphanumeric or barcoded information that helps track animals in a herd and are officially recognized in many countries as a main means of identification. However, these tags are easily lost, can be damaged, and often become unreadable due to dirt or wear [15,16]. If they aren't integrated with electronic components as RFID transponders, they also can't support automated tracking systems and data collection.

Electronic Identification

Electronic methods like RFID tags have addressed some of these issues. These tags allow for quicker and more accurate data collection and reduce the need for manual checking. They can be scanned automatically and synchronized with farm management systems, which reduce labour and manual error [5,17]. Even so, they are not perfect as RFID tags can be lost or damaged, and their limited reading range poses problems in crowded or complex farm environments [18]. Other tools like injectable microchips offer more security and minimal invasiveness but have their own set of challenges. They require scanners to be close to the animal, and the transponders could migrate under the skin, which may compromise identification reliability [19,20]. GPS collars are another option, providing additional data on movement and behaviour, but high costs, battery life issues, and signal interference limit their usefulness for continuous identification [21,22].

Biometric Animal Identification

More recently, biometric technologies have emerged as a promising alternative. Among them, face recognition stands out due to its non-invasive nature, high accuracy, and strong potential for full automation. Deep learning models, particularly convolutional neural networks, have shown excellent results across different animal species [30]. One study achieved over 90% accuracy in identifying individual pigs even under variable lighting and different head angles [9]. Similar outcomes were seen in cattle and goats using muzzle and facial images, often with AI-enhanced

Table 1. *Comparison of common animal identification methods with their relevance to precision livestock farming*

Identification Method	Accuracy	Invasiveness	Automation Potential	Scalability	Animal Welfare	Challenges	Reference
Hot-iron branding	High	High	Low	High	Poor	Pain, healing time, welfare concerns	Tucker et al. [4]; Schwartzkopf-Genswein et al. [3]; Hernández et al.[12]
Tattooing	High	Moderate	Low	Moderate	Moderate	Poor visibility, labor-intensive	Luetkemeier et al.[13]; Cambiaso-Daniel et al.[14]
Ear tag (visual)	Moderate	Moderate	Low (unless electronic)	High	Good	Loss, tampering, dirt interference	Caja et al.[15]; Awad [16]
RFID tags	Moderate	Low	Medium	High	Good	Read range limitations, tag loss	Rizvi et al.[5]; Harmon et al.[17]; Gao et al.[18]
Injectable microchip	High	Low to moderate	Medium	Moderate	Good	Migration, requires proximity scan	Azoulay et al.[19]; Mergl et al.[20]
Gps collars	High (location-based)	Low	High	Moderate	Good	High cost, battery/signal limitations	Hofmann et al.[21]; Waller et al.[22]
Nasal pattern recognition	High	None	Medium	Low to moderate	Excellent	Image quality sensitive, hard to capture	Choi et al.[23]
Face recognition	High(>90%)	None	High	High	Excellent	Lighting variation, dataset needs, hardware cost	Bae et al.[9]; Bello et al.[8]; Zhang et al.[24]; Choi et al. [23]; Sun et al.[25]; Ma et al.[26]; Ahmad et al., [27]; Neethirajan [28]; Li et al.[29]

detection methods like YOLO-based algorithms [8,24]. Moreover, studies on dogs have also shown that facial and nasal features remain stable over time, which is crucial for long-term identification applications [23].

Further developments in artificial intelligence have increased the extent of reliability. Advanced models such as LAD-RCNN and ViT-DL-IN21K help systems distinguish individuals with greater precision, regardless of background noise or subtle differences [25,26]. Furthermore, systems integrating face recognition with PLF technologies have already been tested in real-world farm settings, including integration into feeding and milking stations with non-contact animal monitoring. These applications allow for continuous tracking and can also provide health and behaviour data in real time, that are key components of modern, welfare-focused and data-driven farm management [27-29].

Face recognition in animals as a means of identification has several advantages, but its widespread use still faces some challenges. Most studies have been conducted in controlled environments that do not take into account many of the obstacles that may arise in real farm settings *(Table 2)*. Differences in lighting, animal movement, dirt on the face, breed diversity, and changes in appearance with age can reduce the accuracy of these systems [31,32]. One of the main disadvantages remains the high cost and initial investment, along with the need for specific technical knowledge by farm staff, which can further complicate implementation, especially for smaller animal holdings.

Alternative Biometric Identification Methods

In addition to the innovative face recognition methods that have attracted significant interest in recent years, other biometric approaches for livestock identification are also being investigated *(Table 3)*. Among them, retinal imaging is considered one of the most scientifically reliable methods for certain types of farm animals. This is due to the unique vascular structure of the retina, which remains stable throughout the animal's life and provides extremely high discrimination ability. This feature was successfully utilized through computerized techniques like U-Net-based deep learning model, as some authors reported recognition accuracy of 95.6% of cattle retinal patterns [33,34]. Confirmation of the reliability of retina as a biometric marker was achieved also by Saygılı et al.[35] through a newly developed image processing system CattNIS with 92.25% performance of matching retinal images. Extraction of retinal patterns with segmentation of retinal vessels through different deep learning algorithms further proved to be a highly precise method of animal identification in controlled farm environment [36].

Even before the introduction of modern machine learning models, the possibilities of retinal scanning as a means of identification in farm animals appeared to be a particular subject of scientific research. The studies of Allen et al.[37] and Barron et al.[38] demonstrated that the applicability of this method in both cattle and sheep, with reported accuracy levels of 98.3% in cows and 93.09% in sheep respectively, performed higher in comparison to the electronic identifiers used at the time. Despite the huge advantage of the uniqueness of retinal blood vessels, the method has a number of limitations such as necessity of a special camera for the images and close range with the animals for image acquisition, which significantly limits its scalability in large industrial farms.

A number of other non-invasive biometric methods, such as nose prints, muzzle patterns and body-shape recognition, have been investigated as reliable means of animal identification. However, these alternatives also suffer from limitations in terms of image quality, environmental factors and animal positioning. Overall,

Table 2. *Summary of reported performance* of face recognition systems in livestock species*

Species	Model/Algorithm	Dataset Size (animals/ images)	Performance Metric	Reported Accuracy or F1-Score	Reference
Cattle	CNN-based classifier	400 animals/4000 images	Accuracy	98.99%	Bello et al.[8]
Cattle	DenseNet121 Detectron2-based system	180 animals/2500 images	F1-score	0.92	Mahato et al.[31]
Pigs	Vision Transformer (ViT), YOLOv8	20 animals/1500 images	F1	0.94	Ma et al.[26]
Goats	Improved YOLOv4	30 animals/2522 images	Accuracy	96.7%	Zhang et al.[24]
Sheep	SqueezeNet-based CNN	114 animals/5371 images	Accuracy	82.39%	Min et al.[30]
Horses	Transfer learning CNN YOLOv7	- 1103 images	Accuracy	96.2%	Ahmad et al.[27]

** Summary statistics across studies: Mean reported accuracy 93.6%; Standard deviation ±4.8%; Dataset size range 1103-5371 images*

after comprehensive systematic review on the topic, Cihan et al.[39] argued that each biometric technique had its advantages and disadvantages, highlighting the need for comparative evaluations between multiple methods in terms of accuracy, practicality, and welfare considerations.

Comparative Performance Analysis of Identification Methods

Data from the reviewed studies revealed distinct differences among the explored identification technologies, based on performance indicators. Traditional physical means (branding, tattooing, ear tags) demonstrated high reliability when considered for manual identification visually, but they lacked automation capacity and negatively affected animal welfare due to their invasiveness. Reported error rates for visual ear tags in farm animals ranged from 5-20% due to tag loss or damage [40].

The performance of electronic identification systems such as RFID showed moderate to high accuracy (85-98%), which was influenced by various factors as environmental conditions and the distance between the animal and the reading device. Furthermore, when applied in large herds with big density, the reliability of the method was reported to decrease due to signal interference and tag loss [18]. Injectable transponders as microchips, on the other hand, demonstrated high identification accuracy (>95%) but their detection during reading required close proximity with the animal and showed migration events, although rarely reported [19,20].

Modern identification approaches like biometric methods, particularly face recognition, were found reliable for recognition of multiple animal species under controlled or semi-controlled conditions, with reported accuracies exceeding 90%. However, when tested under field conditions, the performance of face recognition models

Table 3. *Comparison of alternative biometric identification methods in livestock*

Biometric Method	Species	Core Technology	Dataset Size	Reported Performance	Advantages	Limitations	Reference
Retinal imaging	Cattle	Machine learning classifiers (SIFT, SURF, BRISK, FAST, HARRIS)	300 animals 2430 images	Accuracy 95.6%	Very high uniqueness and stability	Requires specialized capture device	Cihan et al.[33]
Retinal imaging	Cattle	Feature matching (CattNIS)	300 animals 2430 images	Accuracy 92.25%	High robustness	Difficult field acquisition	Saygılı et al.[35]
Retinal imaging	Cattle	U-Net segmentation	300 animals 540 images	Accuracy 97.4%	Highly accurate vascular mapping	Requires controlled setup	Cihan et al.[34]
Retinal imaging	Cattle	Dedicated retinal scanner	869 animals 1739 images	Accuracy 98.3%	Excellent permanence	High equipment cost	Allen et al.[37]
Retinal imaging	Sheep	Retinal pattern matching	64 animals 128 images	Accuracy 93.09%	Reliable biometric marker	Handling and restraint	Barron et al.[38]
Retinal vessels	Cattle	Image preprocessing and segmentation methods	234 animals 1206 images	Iidentification accuracy is not reported (segmentation performance only)	Robust biometric feature	Requires eye positioning	Cihan et al.[36]
Nose pattern	Dogs (method transferable)	CNN-based recognition	60 dogs/180 images (extended to 70 dogs/278 images)	The authors report a zero error rate in comparisons between real and fake data, which corresponds to 100% identification accuracy under controlled experimental conditions.	Highly distinctive patterns	Image capture sensitivity	Choi et al.[23]
Muzzle pattern	Cattle	SIFT feature extraction and matching	15 animals 105 images	Accuracy 93.3%	Non-invasive	Dirt/occlusion issues	Awad et al.[16]
Face recognition*	Multiple species	Deep CNN/ViT	Variable	Mean accuracy 93.6%	Fully contactless	Lighting/ pose/ sensitivity	Present review

** Summary of dataset size and mean accuracy are presented in Table 2*

change due to lighting variations, face occlusion, and age-related morphological changes. These findings highlight that while biometric systems offer superior automation and welfare outcomes, their reliability remains context-dependent.

Despite the challenges mentioned, all studies on the use of face recognition for animal identification highlight a wide range of advantages. The technology is humane, requires no physical contact with the animal, and can be integrated with automated monitoring systems, giving it strong potential for widespread adoption in the future.

Discussion

The findings of this review suggest that animal face recognition technology has a substantial potential for modernizing identification practices in precision livestock farming. While traditional and electronic identification systems have provided a stable basis for traceability and animal tracking, they continue to hold significant disadvantages with regard to animal welfare, automation capability, and long-term reliability. In contrast, face recognition emerges as a non-invasive, accurate, and potentially more scalable alternative, especially when animal husbandry holdings consider orientation toward data-driven and welfare-oriented management systems.

Electronic identification systems such as RFID and injectable microchips offer significant improvements in traceability and partial automation. RFID tags enable integration with herd management platforms and support real-time data collection [5,17], yet they still require tag placement and may be susceptible to damage or loss. Subcutaneous microchips are less prone to tampering but require proximity-based scanning and have reported issues with migration or incorrect implantation [19,20]. Additionally, GPS collars have proven valuable for environmental and movement tracking but are cost-prohibitive for many operations and remain unsuitable for identification alone [21,22].

Biometric identification, particularly face recognition, addresses several of these limitations by offering a contact-free, animal-friendly, and technologically advanced solution. Modern deep learning algorithms such as convolutional neural networks (CNNs), LAD-RCNN, and ViT-based models have demonstrated high accuracy (often exceeding 90%) across a variety of species, including cattle, pigs, goats, and poultry [26,41,42].

Beyond basic identification, face recognition systems can be integrated with smart sensors and edge devices to support real-time behavioral analysis, health monitoring, and reproductive tracking without human interference [29,43,44]. In addition, novel applications such as emotion recognition through facial expressions may open up new possibilities for welfare assessment and ethical livestock management [45].

However, face recognition techniques still could not be fully implemented due to several technical and practical challenges such as lighting variability, facial obstructions, and unpredictable animal movement, that can significantly reduce the accuracy of image-based systems [24,46]. Most current models also struggle with generalization across breeds or age groups due to morphological differences [31]. In addition, the initial infrastructure costs -including high-resolution cameras, edge processing devices, and reliable data storage- can be serious burden and challenge for small-scale farmers. The comparative review on animal identification techniques [39] comprehensively presents the perspectives of future application of such novel approaches, but simultaneously emphasizes that no single biometric modality could be considered universal across all indicators. Searching for a long-term solution for a feasable, effective, automated and non-invasive method will require probably a combination of hybrid systems with multiple biometric cues.

The successful integration of face recognition technologies into existing PLF systems also requires attention to farmer education, usability, and ethical concerns. Adoption is likely to depend on farmers' perceptions of cost-benefit balance, as well as their comfort with digital tools [47]. Stakeholder involvement, including input from veterinarians, animal welfare experts, and technologists, will be essential to ensure responsible deployment that aligns with both productivity and welfare goals [28,48].

In conclusion, the continued development of artificial intelligence, sensor technologies, and affordable edge computing is likely to reduce the barriers posed by traditional identification methods. With growing public and regulatory focus on ethical and sustainable livestock production, the demand for non-invasive, automated, and animal-friendly identification methods is expected to increase. The present systematic review demonstrates that no single animal identification method currently satisfies all technical, economic, and welfare requirements of PLF. Traditional and electronic systems remain reliable but are constrained by invasiveness, loss, and limited automation. In this context, animal face recognition is poised not only to supplement but potentially to replace conventional systems in the near future. With sustained interdisciplinary collaboration, ongoing field trials, and investment in smart farming infrastructure, face recognition can become a central tool in the transition toward more ethical, efficient, and intelligent livestock farming.

However, existing evidence indicates that face recognition systems are not yet universally robust under real farm conditions. Technical challenges, infrastructure costs,

and limited large-scale validation remain significant barriers.

In this regard, future efforts should focus on improving biometric identification performance under variable farm and environmental conditions, reducing hardware and implementation costs, and enhancing user-friendly integration with management systems that are already in operation. The focus should be directed towards development of integrative identification frameworks, possibly combining face recognition with highly reliable, although less practical approaches like retinal imaging, in order to achieve both scalability and accuracy. Using distinct benchmarks across biometric methods for comparison and creation of standardized datasets and evaluation protocols will be essential for determining their real-world suitability with regard to precision livestock farming.

Declarations

Availability of Data and Materials: Data availability is not applicable to this article as no new data were created in this study.

Acknowledgements: The authors extend their gratitude to the Faculty of Veterinary Medicine and Trakia University, Stara Zagora, for the financial support provided for this paper's publication.

Financial Support: This research was funded by the Ministry of Education and Science in Bulgaria within the framework of the Bulgarian National Recovery and Resilience Plan, Component "Innovative Bulgaria", Project No. BG-RRP-2.004-0006-C02 "Development of research and innovation at Trakia University in the service of health and sustainable well-being".

Conflict of Interest: The authors declared that there is no conflict of interest.

Declaration of Generative Artificial Intelligence (AI): The article and tables and figures were not written/created by AI and AIassisted technologies (Authors only used these technologies to improve the readability and language of the article).

Author Contributions: Each author played a significant role in the conceptualization and design of this study. The manuscript was composed by DT and GB; GB and DT prepared the diagrams and tables; IL and RR reviewed the manuscript correctly; GB arranged the references according to the journal's guidelines; the study was supervised by GB. The final manuscript was thoroughly reviewed and approved by all authors.

References

1. **Dziuk P:** Positive, accurate animal identification. *Anim Reprod Sci*, 79 (3-4): 319-323, 2003. DOI: 10.1016/s0378-4320(03)00170-2
2. **Seroussi E, Yakobso E, Garazi S, Oved Z, Halachmi I:** Short communication: Long-term survival of flag eartags on an Israeli dairy farm. *J Dairy Sci,* 94 (11): 5533-5535, 2011. DOI: 10.3168/jds.2011-4330
3. **Schwartzkopf-Genswein KS, Stookey JM, Welford R:** Behavior of cattle during hot-iron and freeze branding and the effects on subsequent handling ease. *J Anim Sci,* 75 (8): 2064-2072, 1997. DOI: 10.2527/1997.7582064x
4. **Tucker CB, Mintline EM, Banuelos J, Walker KA, Hoar B, Varga A, Drake D, Weary DM:** Pain sensitivity and healing of hot-iron cattle brands. *J Anim Sci,* 92 (12): 5674-5682, 2014. DOI: 10.2527/jas.2014-7887
5. **Rizvi R, Para P, Ganguly S:** Implantation of microchip in animals: A review. *IJPBS,* 3 (1): 19-20, 2016.
6. **Neethirajan S:** The role of sensors, big data and machine learning in modern animal farming. *Sens Biosensing Res,* 29:100367, 2020. DOI: 10.1016/j.sbsr.2020.100367
7. **Awad AI, Zawbaa HM, Mahmoud HA:** A robust cattle identification scheme using muzzle print images. **In,** 2013 Federated conference on computer science and information systems, pp. 529-534. IEEE, 2013.
8. **Bello R, Talib AZH, Mohamed ASAB:** Deep learning-based architectures for recognition of cow using cow nose image pattern. *Gazi Univ J Sci,* 33 (3): 820-833, 2020. DOI: 10.35378/gujs.605631
9. **Bae HB, Pak D, Lee S:** Dog nose-print identification using deep neural networks. *IEEE Access,* 9, 49141-49153, 2021.
10. **Shakeel PM, Aboobaider BBM, Salahuddin LB:** A deep learning-based cow behavior recognition scheme for improving cattle behavior modeling in smart farming. *Internet Things,* 19 (13):100539, 2022. DOI: 10.1016/j.iot.2022.100539
11. **Yin M, Ma R, Luo H, Li J, Zhao Q, Zhang M:** Non-contact sensing technology enables precision livestock farming in smart farms. *Comput Electron Agric,* 212:108171, 2023. DOI: 10.1016/j.compag.2023.108171
12. **Hernández A, Trindade PHE, Da Costa MJRP, Jung J, Berg C:** Limited effects of pain control treatments on behaviour and weight gain of pure and crossbred nellore heifer calves when subjected to Hot-Iron branding. *Animals*, 12 (22):3143, 2022. DOI: 10.3390/ani12223143
13. **Luetkemeier M, Allen D, Huang M, Pizzey F, Parupia I, Wilson T, Davis S:** Skin tattooing impairs sweating during passive whole body heating. *J Appl Physiol,* 129 (5): 1033-1038, 2020. DOI: 10.1152/japplphysiol.00427.2019
14. **Cambiaso-Daniel J, Luze H, Meschnark S, Fink J, Schreiver I, Rappl T, Goessler W, Kotzbeck P, Kamolz LP:** Tattoo pigment biokinetics *in vivo* in a 28-day porcine model: Elements undergo fast distribution to lymph nodes and reach steady state after 7 days. *Dermatology*, 240 (2): 304-311, 2024. DOI: 10.1159/000536126
15. **Caja G, Ghirardi JJ, Hernández-Jover M, Garin D:** Diversity of animal identification techniques: From 'fire age' to 'electronic age'. *ICAR Tech Ser,* 9, 21-39, 2004.
16. **Awad AI:** From classical methods to animal biometrics: A review on cattle identification and tracking. *Comput Electron Agric,* 123, 423-435, 2016. DOI: 10.1016/j.compag.2016.03.014
17. **Harmon ML, Downey BC, Drwencke AM, Tucker CB:** Development and application of a novel approach to scoring ear tag wounds in dairy calves. *J Dairy Sci,* 106 (7): 5043-5053, 2023. DOI: 10.3168/jds.2022-23005
18. **Gao T, Fan D, Wu H, Chen X, Song S, Sun Y, Tian J:** Research on the vision-based dairy cow ear tag recognition method. *Sensors*, 24 (7):2194, 2024. DOI: 10.3390/s24072194
19. **Azoulay F, Cauvin E, Soares A, Couturier L:** Pulmonary arterial embolism due to aberrant migration of a microchip in two dogs. *Vet Rec Case Rep,* 11 (4):e740, 2023. DOI: 10.1002/vrc2.740
20. **Mergl J, Nutt L, Pareja A:** Fluoroscopy-guided surgical removal of a microchip from the spinal canal of two cats. *J Am Anim Hosp Assoc,* 59 (4): 193-197, 2023. DOI: 10.5326/jaaha-ms-7356
21. **Hofmann W, Neal M, Woodward S, ONeill T:** GPS technology as a tool to aid pasture management on dairy farms. *J N Z Grassl,* 84, 189-196, 2022. DOI: 10.33584/jnzg.2022.84.3561
22. **Waller SJ, Morelle K, Seryodkin IV, Rybin AN, Soutyrina SV, Licoppe A, Hebblewhite M, Miquelle DG:** Resource-driven changes in wild boar movement and their consequences for the spread of African Swine Fever in the Russian Far East. *Wildl Biol,* 5:e01276, 2025. DOI: 10.1002/wlb3.01276
23. **Choi HI, Kim MY, Yoon HY, Lee S, Choi SS, Han CY, Moon HP,**

Byun C, Kwon SH: Study on the viability of canine nose pattern as a unique biometric marker. *Animals*, 11 (12):3372, 2021. DOI: 10.3390/ani11123372

24. **Zhang F, Wang S, Cui X, Wang X, Cao W, Yu H, Fu S, Pan X:** Goat-face recognition in natural environments using the improved YOLOv4 algorithm. *Agriculture*, 12 (10):1668, 2022. DOI: 10.3390/agriculture12101668
25. **Sun L, Liu G, Yang H, Jiang X, Liu J, Wang X, Yang H, Yang S:** LAD-RCNN: A powerful tool for livestock face detection and normalization. *Animals*, 13 (9):1446, 2023. DOI: 10.3390/ani13091446
26. **Ma R, Ali H, Waqar MM, Kim SC, Kim H:** Pig face open set recognition and registration using a decoupled detection system and dual-loss vision transformer. *Animals*, 15 (5):691, 2025. DOI: 10.3390/ani15050691
27. **Ahmad M, Abbas S, Fatima A, Issa G, Ghazal T, Khan M:** Deep transfer learning-based animal face identification model empowered with vision-based hybrid approach. *Appl Sci,* 13 (2):1178, 2023. DOI: 10.3390/app13021178
28. **Neethirajan S:** Happy cow or thinking pig? WUR wolf-facial coding platform for measuring emotions in farm animals. *AI*, 2 (3): 342-354, 2021. DOI: 10.3390/ai2030021
29. **Li N, Ren Z, Li D, Zeng L:** Review: automated techniques for monitoring the behaviour and welfare of broilers and laying hens: Towards the goal of precision livestock farming. *Animal*, 14 (3): 617-625, 2020. DOI: 10.1017/s1751731119002155
30. **Min H, Sun Q, Xuan C, Zhang X, Zhao M:** SqueezeNet: An improved lightweight neural network for sheep facial recognition. *Appl Sci*, 14 (4):1399, 2024. DOI: 10.3390/app14041399
31. **Mahato S, Bi H, Neethirajan S:** Dairy DigiD ~ A deep learning-based, non-invasive biometric identification system for dairy cattle using detectron2. *bioRxiv*, 12.14.628477, 2024. DOI: 10.1101/2024.12.14.628477
32. **Wang Y, Ding H, Wang L, Guo Y, Du H:** Contextualized small target detection network for small target goat face detection. *Animals*, 13 (14):2365, 2023. DOI: 10.3390/ani13142365
33. **Cihan P, Saygılı A, Akyüzlü M, Özmen NE, Ermutlu C Ş, Aydın U, Aksoy Ö:** Performance of machine learning methods for cattle identification and recognition from retinal images. *Appl Intell*, 55:536, 2025. DOI: 10.1007/s10489-025-06398-1
34. **Cihan P, Saygili A, Akyuzlu M, Özmen NE, Ermutlu CŞ, Aydın U, Aksoy Ö:** U-net-based approaches for biometric identification and recognition in cattle. *Kafkas Univ Vet Fak Derg,* 31 (3): 425-436, 2025. DOI: 10.9775/kvfd.2025.34130
35. **Saygılı A, Cihan P, Ermutlu CŞ, Aydın U, Aksoy Ö:** CattNIS: Novel identification system of cattle with retinal images based on feature matching method. *Comput Electron Agric,* 221:108963, 2024. DOI: 10.1016/j.compag.2024.108963
36. **Cihan P, Saygılı A, Akyüzlü M, Özmen NE, Ermutlu CŞ, Aydın U, Aksoy Ö:** Extraction of cattle retinal vascular patterns with different segmentation methods. *SAUCIS*, 7 (3): 378-388, 2024. DOI: 10.35377/saucis…1509150
37. **Allen A, Golden B, Taylor M, Patterson D, Henriksen D, Skuce R:** Evaluation of retinal imaging technology for the biometric identification of bovine animals in Northern Ireland. *Livest Sci,* 116 (1-3): 42-52, 2008. DOI: 10.1016/j.livsci.2007.08.018
38. **Barron UG, Corkery G, Barry B, Butler F, McDonnell K, Ward S:** Assessment of retinal recognition technology as a biometric method for sheep identification. *Comput Electron Agric,* 60 (2): 156-166, 2008. DOI: 10.1016/j.compag.2007.07.010
39. **Cihan P, Saygili A, Ozmen NE, Akyuzlu M:** Identification and recognition of animals from biometric markers using computer vision approaches: A review. *Kafkas Univ Vet Fak Derg,* 29 (6): 581-593, 2023. DOI: 10.9775/kvfd.2023.30265
40. **Karakuş F, Demir AÖ, Akkol S, Düzgün A, Karakuş M:** Readability of electronic and visual ear tags in hair goat kids. *TURJAF*, 4 (5): 407-410, 2016. DOI: 10.24925/turjaf.v4i5.407-410.675
41. **Bhole A, Udmale SS, Falzon O, Azzopardi G:** CORF3D contour maps with application to Holstein cattle recognition from RGB and thermal images. *Expert Syst Appl*, 192:116354, 2021. DOI: 10.1016/j.eswa.2021.116354
42. **Billah M, Wang X, Yu J, Jiang Y:** Real-time goat face recognition using convolutional neural network. *Comput Electron Agric*, 194:106730, 2022. DOI: 10.1016/j.compag.2022.106730
43. **Singh M, Kumar R, Tandon D, Sood P, Sharma M:** Artificial intelligence and IoT based monitoring of poultry health: A review. 2020 IEEE *International Conference on Communication, Networks and Satellite (Comnetsat)*, Batam, Indonesia, 2020, 50-54. DOI: 10.1109/Comnetsat50391.2020.9328930
44. **Pinna D, Sara G, Todde G, Atzori AS, Artizzu V, Spano LD, Caria M:** Advancements in electronic identification of animals and augmented reality technologies in digital livestock farming. *Sci Rep,* 13:18282, 2023. DOI: 10.1038/s41598-023-45772-2
45. **Neethirajan S, Kemp B:** Digital twins in livestock farming. *Animals*, 11 (4):1008, 2021. DOI: 10.3390/ani11041008
46. **Li J, Yang Y, Liu G, Ning Y, Song P:** Open-set sheep face recognition in multi-view based on Li-SheepFaceNet. *Agriculture*, 14 (7):1112, 2024. DOI: 10.3390/agriculture14071112
47. **Fragomeli R, Annunziata A, Punzo G:** Promoting the transition towards agriculture 4.0: A systematic literature review on drivers and barriers. *Sustainability*, 16 (6):2425, 2024. DOI: 10.3390/su16062425
48. **Nawroth C, Langbein J, Coulon M, Gabor V, Oestermind S, Benz-Schwarzburg J, von Borell E:** Farm animal cognition - linking behavior, welfare and ethics. *Front Vet Sci,* 6:24, 2019. DOI: 10.3389/fvets.2019.00024

Kafkas Universitesi Veteriner Fakultesi Dergisi
Journal Home-Page: http://vetdergikafkas.org
E-ISSN: 1309-2251

Kafkas Univ Vet Fak Derg
32 (2): 173-187, 2026
DOI: 10.9775/kvfd.2025.35766

Review Article

Potential Application of *Rhododendron* Flavonoids' Anti-inflammatory and Antioxidant Activities in Animal Health Support and Protection

Ziqin ZHANG [1], Sheng KANG [1], Meixue NI [1], Xiaoqing GUO [1], Hailong DONG [1], Qingxia WU [1 (*)], Zhenyu CHANG [1(*)]

[1] Xizang Agricultural and Animal Husbandry University, School of Animal Science, Tibetan Key Laboratory of Clinical Veterinary Medicine, Linzhi, Tibet, P. R. CHINA

[(*)] **Corresponding author:**
Qingxia Wu & Zhenyu Chang
Phone: +86-17689548312 (ZC), +86-18089945473 (QW)
E-mail: zychang2014@sina.com (ZC); 441594343@qq.com (QW)

How to cite this article?

Zhang Z, Kang S, Ni M, Guo X, Dong H, Wu Q, Chang Z: Potential Application of *Rhododendron* Flavonoids' Anti-inflammatory and Antioxidant Activities in Animal Health Support and Protection. *Kafkas Univ Vet Fak Derg*, 32 (2): 173-187, 2026
DOI: 10.9775/kvfd.2025.35766

Article ID: KVFD-2025-35766
Received: 25.11.2025
Accepted: 18.02.2026
Published Online: 29.03.2026

Abstract

Rhododendron plants are abundant in flavonoid compounds, whose prominent antioxidant and anti-inflammatory physiological activities have attracted considerable attention. However, the application of related research in animal health maintenance and bodily protection, along with their underlying mechanisms, remains unclear. This ambiguity has constrained their translation into practical applications as physiological protective factors within animal husbandry. This study systematically reviewed relevant literature, identifying 17 *Rhododendron* flavonoids exhibiting significant antioxidant and anti-inflammatory activity. The antioxidant effects of these flavonoids are primarily achieved through multiple pathways: direct scavenging of free radicals, inhibition of oxidative enzymes (such as NADPH oxidase and xanthine oxidase), chelation of metal ions, supply of hydrogen ions, enhancement of the antioxidant system, and regulation of endogenous antioxidant capacity via the Keap1-Nrf2/ARE and MAPKs signaling pathways. Meanwhile, their anti-inflammatory effects are mediated through four main mechanisms: inhibition of inflammatory mediator production, modulation of cytokines and their receptors, scavenging of reactive oxygen species, and regulation of cell signaling pathways (including NF-κB and AP-1). To date, flavonoids have demonstrated significant efficacy in the treatment of various human diseases, including hypertension, atherosclerosis, cardiomyopathy, myocarditis, diabetes mellitus, and cancer. However, their potential in veterinary medicine has not been fully explored. This review summarizes recent advances in the antioxidant and anti-inflammatory physiological activities of *Rhododendron* flavonoids and their underlying mechanisms. It aims to provide scientific rationale for developing flavonoid-based physiological protective agents suitable for animals, thereby advancing their scientific application in animal health management and livestock production. This aligns with current priority areas in veterinary research.

Keywords: Antioxidant, Anti-inflammatory, Animal health support and protection, Flavonoids, *Rhododendron* plants

Introduction

Rhododendron belongs to the *Rhododendron* family, which is a large genus of *Rhododendron*, with common types such as Ying shan hong, Haunted Goat Flower, Zhao shan White, Goat Tramp, and so on, about 967 species, which are widely distributed in Asia, Europe, and North America, and are mainly native to East Asia and Southeast Asia [1]. About 700 species in China, except Xinjiang, Ningxia, everywhere, but in the southwest provinces and districts, mostly [2] The flowers, leaves and stems of *Rhododendron* plants are rich in flavonoids, which are high quality herbal medicines. Flavonoids have excellent antioxidant and anti-inflammatory activities and therefore also have many pharmacological effects such as anti-cancer, treatment of cardiovascular diseases and diabetes mellitus [3].

The development of many diseases is closely related to oxidative damage in the body, and reactive oxygen species (ROS) and reactive nitrogen species (RNS) free radicals are naturally produced during normal metabolism, and they play an important role in physiological activities. However, when the concentration of ROS/RNS is too high, they produce oxidative stress, a state that leads to tissue damage and has been linked to the development of a variety of diseases, including cancer, cardiovascular disease, neurodegenerative diseases, diabetes, respiratory infections, and others [4]. The high cost of treating related diseases caused by oxidative damage places a huge economic burden on the global community. Flavonoids

possess diverse physiological activities and low toxicity. Therefore, investigating their antioxidant and anti-inflammatory mechanisms to elucidate their protective effects in alleviating oxidative stress and mitigating cellular oxidative damage holds significant value for safeguarding animal organisms from injury, maintaining health homeostasis. Clarifying the antioxidant and anti-inflammatory mechanisms of these flavonoids may also facilitate the development of physiologically protective formulations, providing theoretical support for standardised animal health management [5].

Regarding the antioxidant and anti-inflammatory activities of flavonoid compounds, existing research has predominantly focused on their pharmacological effects in humans, while studies on their physiological support applications, pharmacokinetics, and safety in animals -particularly livestock and companion animals- remain fragmented and lack systematic integration. To address this research gap, this paper first provides a comprehensive review of studies concerning the antioxidant and anti-inflammatory physiological properties of flavonoids. It systematically outlines their mechanisms of action and applications in maintaining animal health and providing physiological protection, thereby establishing a foundational reference for subsequent research into the application of *Rhododendron* flavonoids in animal health management and livestock production. Subsequently, the focus shifts to the physiological protective value of *Rhododendron* flavonoids in veterinary health management. This involves systematically reviewing relevant domestic and international research findings, thoroughly elucidating their mechanisms of action, and examining their current applications in maintaining animal health and protecting against damage. This aims to establish a robust foundation for advancing research in this field, construct a standardised reference framework, and facilitate the translational application of flavonoids (particularly represented by *Rhododendron* flavonoids) in veterinary health management and livestock production.

Flavonoid Composition

In medicinal chemistry, a compound's chemical formula not only determines its physicochemical properties, but more crucially, the presence and positioning of specific functional groups within its structure directly dictate how it interacts with biological targets. This, in turn, influences its pharmacological activity and therapeutic applications. Consequently, understanding a compound's chemical formula forms the foundation for investigating its mode of action. The research on flavonoids of *Rhododendron* plants in China was first started in 1974, when the total flavonoid glycosides isolated from *Rhododendron* plants were acid-hydrolysed by the teaching and research group of pharmacology at Lanzhou Medical College, from which 3,5,7,8,3',4'-hexahydroxyflavonoids were isolated [6]. Nowadays, flavonoids are mainly detected and analysed by ultra-high performance liquid chromatography-quadrupole time-of-flight mass spectrometry (UHPLC-TOFMS) and various chromatographic methods [7]. To date, 17 flavonoid compounds with antioxidant or anti-inflammatory activity have been studied *(Table 1)*.

Antioxidant Mechanism of Action

Antioxidant and oxidative stress are inextricably linked to the occurrence of oxidative stress, which is a state in which excessive oxidative molecules (e.g. ROS) are produced or accumulated within an organism, exceeding the antioxidant capacity of the cells or tissues, resulting in oxidative damage to biomolecules (e.g. proteins, lipids, DNA, etc.) [20], and antioxidant refers to the process of scavenging oxygen free radicals, thereby protecting cells from oxidative stress. Therefore, as illustrated in *Fig. 1*, an understanding of the factors that induce oxidative stress in cells and the subsequent application of antioxidants to mitigate these triggers enables the attainment of effective antioxidant protection. Flavonoids, as an excellent antioxidant, can address oxidative stress through several pathways, such as stabilisation or reduction of reactive oxygen species (ROS), scavenging of free radicals, and modulation of endogenous antioxidant capacity are the three main pathways.

Stabilises or Reduces ROS, Scavenges Free Radicals

The two pathways, stabilisation or reduction of ROS and scavenging of free radicals, usually occur simultaneously in the process of flavonoids exerting antioxidant effects [21]. Thus, the two pathways are described together. The antioxidant modalities of both pathways are direct scavenging of free radicals, inhibition of oxidative enzymes (NADPH oxidase, xanthine oxidase), chelation of metal ions, provision of hydrogen ions and enhancement of the antioxidant system.

Direct Scavenging of Free Radicals

Free radicals are atoms that exist in free form without pairs or free electrons, which can be produced by normal cellular metabolism [22]. Common types of free radicals include hydroxyl radicals (HO·), superoxide anion radicals (O_2^{-}·) and hydrogen peroxide radicals (HO_2·). Hydroxyl radicals (HO·) are the most active free radicals in the cell, which can react with lipids, proteins, and DNA, triggering the oxidation of unsaturated fatty acids and the formation of lipid peroxides (LPO), which can disrupt the membrane structure and lead to cell damage [23]. As illustrated in *Fig. 2-a*, quercetin, isoquercetin, rutin and other azalea plant flavonoids were able to directly scavenge HO· at concentrations up to 260 μM [24]. When

Table 1. *Flavonoid constituents of Rhododendron spp. with antioxidant and anti-inflammatory effects*

Serial Number	Phyto-Chemicals	Source Plant	Chemical Structure	Ref.
1	Quercetin	Almost all *Rhododendron* plants	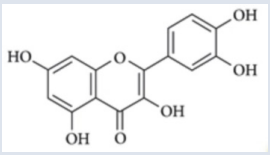	[8]
2	Rutin	*Rhododendron arboreum*	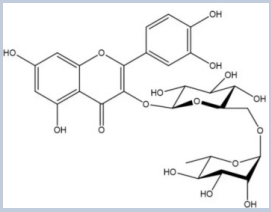	[9]
3	Catechin	*Rhododendron nivale* Hook *Rhododendron dauricum* *Rhododendron wiltonii* Hemsl	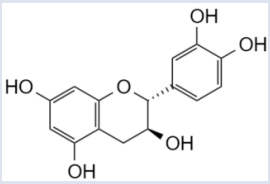	[10,11]
4	Hyperin	Almost all *Rhododendron* plants	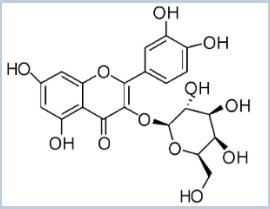	[8]
5	Farrerol	*Rhododendron primuliflorum* Bureau *Rhododendron dauricum*	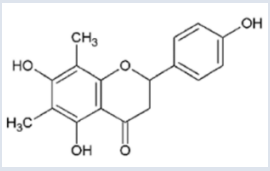	[12,13]
6	Morin-3-O-β-L-lyxoside	*Rhododendron nivale* Hook	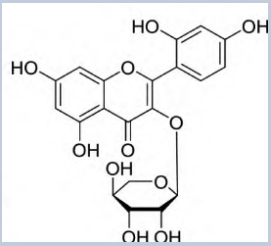	[10]
7	Epicatechin	*Rhododendron nivale* Hook	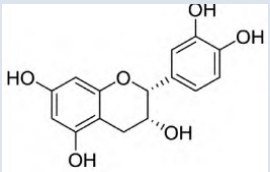	[10]
8	dihydroquercetin	*Rhododendron nivale* Hook	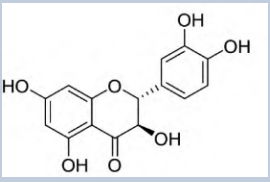	[10]

Table 1. *Continue*

Serial Number	Phyto-Chemicals	Source Plant	Chemical Structure	Ref.
9	Naringenin	*Rhododendron pachypodum* Balf	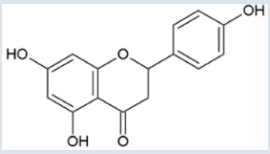	[14]
10	Kaempferol	*Rhododendron dauricum* *Rhododendron wiltonii* Hemsl	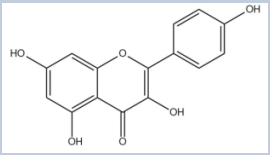	[11,13]
11	Myricetin	*Rhododendron dauricum* *Rhododendron anthopogon* D	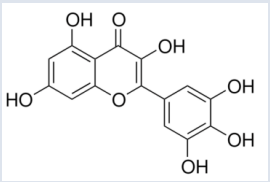	[15]
12	Luteolin	*Rhododendron anthopogonoides* Maxim	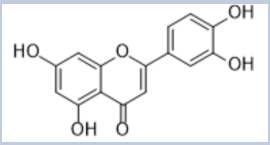	[16,17]
13	Apigenin	*Rhododendron anthopogonoides* Maxim *Rhododendron amesiae* Rehder	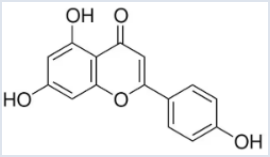	[18]
14	4-O-Methylcedrin	*Rhododendron pachypodum* Balf	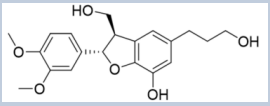	[14]
15	(2Z)-2,6 dimethyl-2,7-octadiene-1,6-diol	*Rhododendron pachypodum* Balf	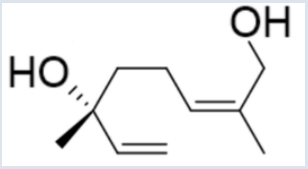	[14]
16	6,8-di-C-methyldihydrokaempferol	Rhododendron pachypodum Balf	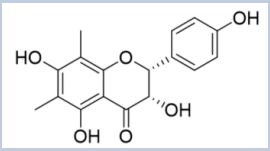	[14]
17	Isoquercitrin	*Rhododendron amesiae* Rehder	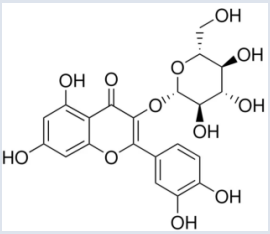	[19]

flavonoids bind to free radicals, the phenolic hydroxyl group of the flavonoid can provide an electron to the free radical, thus neutralising and deactivating it. When free radicals are scavenged, lipids, proteins, DNA and other biomolecules in the cell can exert their effects normally, reducing oxidative damage [25].

Inhibition of Oxidative Enzymes (NADPH Oxidase, Xanthine Oxidase)

Both NADPH oxidase and xanthine oxidase catalyse free radical generation. NADPH oxidase is a transmembrane enzyme complex consisting of several components such as NOX2, p22phox, p47phox, p67phox, etc., whose main function is the production of superoxide anion radicals ($O_2^{-}\cdot$). In phagocytes, such as neutrophils, NADPH oxidase is activated upon detection of pathogens, which, through the signalling pathway, leads to the production of cytokines (mainly p47phox) phosphorylation, prompting their transfer to membrane-bound NOX2 components and initiating the catalytic production of superoxide anion, the catalytic mechanism of which involves the transfer of electrons from NADPH to flavin adenine dinucleotide (FAD), then to proximal haemoglobin, rapidly to distal haemoglobin, and ultimately to molecular oxygen, to form superoxide anion [26]. Xanthine oxidase (XO), in catalysing the conversion of hypoxanthine to xanthine and further to uric acid, uses molecular oxygen as an electron acceptor to produce large amounts of uric acid and H_2O_2, of which H_2O_2 can be further decomposed to produce hydroxyl radicals (·OH), increasing the production of reactive oxygen species [27].

Both quercetin and lignans from the flavonoids of the genus *Rhododendron* showed inhibition of NADPH oxidase and xanthine oxidase. Quercetin inhibits NADPH oxidase activity and reduces ROS production, while it also inhibits xanthine oxidase activity, lowers serum uric acid levels and reduces H_2O_2 production [28]. Lignans also inhibit NADPH oxidase, reduce oxidative stress, and can reverse the elevation of xanthine oxidase activity induced by potassium oxonate, reduce serum and liver levels of uric acid and blood urea nitrogen, and reduce H_2O_2 production [29]. As illustrated in *Fig. 2-b*, populin acts on NADPH oxidase, and in silico predictions reveal a high docking score between populin and this enzyme, suggesting its potential to inhibit NADPH oxidase [30]. As illustrated in *Fig 2-c*, rutin and chrysin exert their primary inhibitory effects on xanthine oxidase; notably, rutin possesses diverse biological activities including antioxidant and anticancer properties, while chrysin inhibits xanthine oxidase activity via hydrogen bonding and van der Waals forces with the enzyme's catalytic active site, acting in a mixed competitive manner [31]. These flavonoids exert their antioxidant and protective effects by inhibiting the activity of oxidative enzymes and reducing oxidative stress and uric acid production.

Chelating Metal Ions

The mechanism of action of flavonoids chelating metal ions to achieve antioxidant action mainly includes the following aspects. The first is that flavonoids form stable complexes through the formation of ligand bonds with metal ions (Fe, Gu, etc.) through specific functional groups such as hydroxyl (-OH) and carbonyl (C=O)

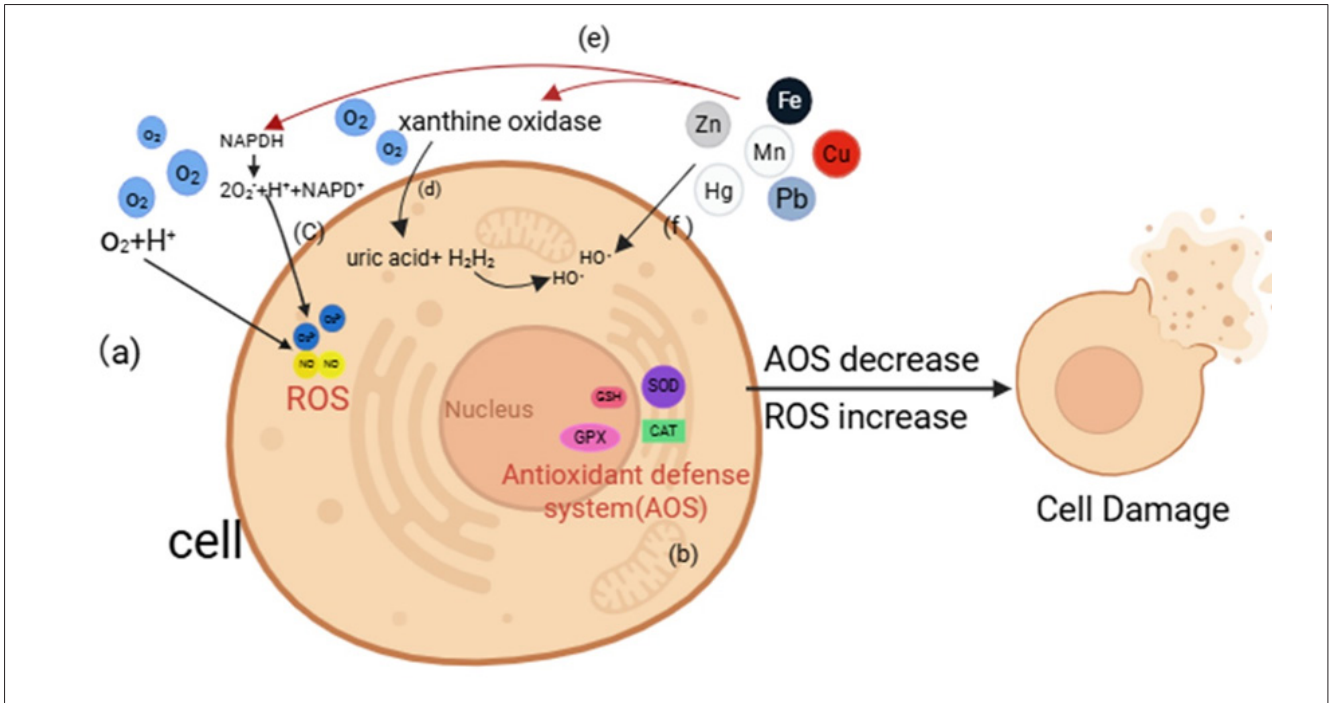

Fig 1. Several ways in which cells generate oxidative stress. (a) The reduction of oxygen to water produces ROS substances such as O_2^{2-} and NO, and the production of ROS causes oxidative damage to cells, (b) An imbalance in the antioxidant defence system increases ROS and swamps AOS, (c) Activation of NADPH oxidase leads to excessive ROS production, causing oxidative stress, (d) XOD catalyses the production of uric acid and H_2O_2 under aerobic conditions, and H_2O_2 is broken down to HO^{-}, loss of cells, (e) Metal ions catalyse the production of ROS by oxidative enzymes, (f) Metal ions such as iron and copper catalyse oxidative reactions that produce HO·, causing cell damage

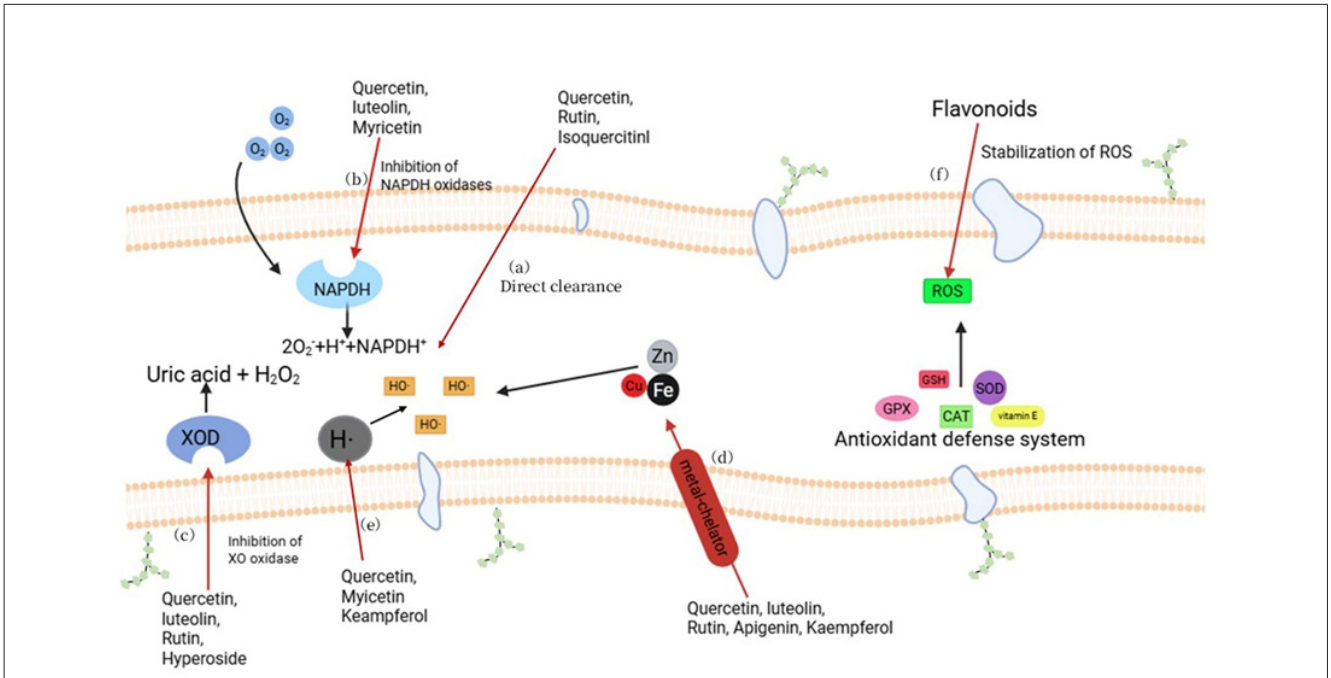

Fig 2. Azalea flavonoids as antioxidants through ROS stabilisation and free radical scavenging. (a) Quercetin, isoquercetin, and rutin directly scavenge HO·, (b) Quercetin, lignocerotin, and populin inhibit NADPH oxidase activity and reduce free radical production, (c) Quercetin, lignans, rutin, and chrysin inhibit xanthine oxidase activity and reduce free radical production, (d) Quercetin, lignans, rutin, apigenin and kaempferol chelate metal ions, reduce HO^- production and inhibit oxidase activity, (e) Quercetin, lignans, apigenin, and kaempferol provide hydrogen ions to scavenge HO-, (f) Flavonoids enhance the antioxidant capacity of the antioxidant system and stabilise ROS

groups in their molecular structure, and such complexes have stronger free radical scavenging ability than free flavonoids, in which metal ions can facilitate the transfer of electrons to enhance the capture of free radicals; finally, there may be synergistic antioxidant activity between flavonoids and metal ions in particular cases [32,33]. For example, complexes formed by flavonoids with copper ions show synergistic effects in scavenging superoxide anion $O_2^{-}\cdot$) and hydroxyl radical (OH·) [33].

As illustrated in *Fig. 2-d*, quercetin, rutin, apigenin, lignans, and kaempferol in the flavonoids of the genus *Rhododendron* can form complexes with metal ions and exhibit antioxidant activity [34].

Hydrogen Atom

Flavonoids provide hydrogen ions to scavenge free radicals in two main ways. The first is that the antioxidant activity of flavonoids interrupts the chain reaction mainly through the reaction of their phenolic hydroxyl groups with oxygen radicals to form resonance-stabilised semiquinone radicals. In this process, hydrogen atoms on the phenolic hydroxyl groups of flavonoids can combine with peroxyl radicals to form flavonoid radicals, which in turn react with other radicals, thus terminating the free radical chain reaction. The second is that intramolecular hydrogen bonding in flavonoids reduces the antioxidant activity of hydroxyl groups that act as hydrogen bond donors (e.g., 5-OH, 3-OH, and 3'-OH) while enhancing the antioxidant activity of hydroxyl groups that act as hydrogen bond acceptors (e.g., 4'-OH) [35].

As illustrated in *Fig. 2-e*, quercetin, populin and kaempferol among the flavonoids of the genus Azalea exhibit antioxidant activity by providing hydrogen atoms to scavenge free radicals [24].and the antioxidant activities of populin and kaempferol were also positively correlated with the number of phenolic hydroxyl groups on the B-ring [36].

Antioxidant Defence System

The antioxidant system is mainly composed of a number of antioxidant enzymes, non-enzymatic antioxidants, and low molecular weight antioxidants [37]. Antioxidant enzymes are the first-line defence mechanisms of the antioxidant defence system, including superoxide dismutase (SOD), catalase (CAT), glutathione peroxidase (GPx), etc. These enzymes are able to scavenge reactive oxygen species, such as superoxide radicals and hydrogen peroxide, to prevent them from causing cellular damage [37]. Non-enzymatic antioxidants, including reduced glutathione (GSH), coenzyme Q (CoQ), lipoic acid, uric acid, and various proteins (e.g. ferritin, transferrin, cuprocyanin, and albumin), which are able to directly neutralise free radicals and protect cells from oxidative damage [38]. Low molecular weight antioxidants such as vitamin C, vitamin E, polyphenols, coenzyme Q or the metabolic compound urate, which scavenge free radicals and reduce oxidative stress [37].

As illustrated in *Fig. 2-f*, flavonoids reduce oxidative stress by modulating the antioxidant enzyme system, enhancing the activity of antioxidant enzymes and the antioxidant capacity of the AsA-GSH cycle, and are also able to stimulate the ascorbic acid biosynthetic pathway and its upstream glycolytic metabolic pathway, leading to an increased accumulation of flavonoids, which act as one of the antioxidants in the non-enzymatic system, providing hydroxyl radicals to scavenge excess reactive oxygen species [39]. It can also act synergistically with vitamin E, partially regenerating in the presence of combined antioxidants, driving the regeneration process by the scavenging of semiquinone radicals in a synergistic reaction, and also by interactions with glutathione and ascorbic acid, in which oxidised flavonoids can be re-reduced by glutathione and ascorbic acid to continue to exert their antioxidant effects [40].

Modulates Endogenous Antioxidant Capacity

Azalea flavonoids regulate endogenous antioxidant capacity and enhance antioxidant capacity mainly through activation of Keap1-Nrf2/ARE and $MAPK_S$ signalling pathways [10].

Antioxidant of Keap1-Nrf2/ARE Signalling Pathway

Nuclear transcription factor E2-related factor 2 (Nrf2) is a member of the Cap'n'collar (CNC) family of regulatory proteins, and is a transcription factor with a basic leucine zip structure, which is widely found in various organs of the body, and is mainly responsible for regulating cellular redox reactions [41]. Keap1 is a Cullin3 (Cul3)-dependent substrate articulating protein of the E3 ubiquitin ligase complex that assembles with CuI3 and Rbx1 to form a functional E3 ubiquitin ligase complex (Keap1-Cul3-E3), which in turn regulates Nrf2 [42]. As illustrated in *Fig. 3-a*, under normal physiological conditions, Nrf2 binds to its endogenous inhibitor Kelch ECH-related protein 1 (Keap1), exists in an inactive state in the cytosol and is rapidly degraded via the ubiquitin proteasome pathway in order to maintain the low transcriptional activity of Nrf2 under physiological conditions [43]. As illustrated in *Fig. 3-b*, upon stimulation of cells by reactive oxygen species (ROS) or other nucleophiles, Nrf2 dissociates from Keap1, undergoes activation and translocates into the nucleus. In the nucleus, Nrf2 binds to Maf proteins to form heterodimers, which then recognize and bind to antioxidant response elements (AREs)-enhancer sequences located in the regulatory regions of Nrf2 target genes that are critical for the recruitment of transcriptionally essential factors [44]. In this way, the Nrf2-Maf heterodimer activates the expression of target genes and regulates the transcriptional activity of phase II metabolic enzymes, antioxidant enzymes or drug transporters, thus exerting antioxidant damage and counteracting the effects of oxidative stress [45].

Flavonoids, as antioxidants, can act as antioxidant damages and restore cellular homeostasis by activating the Keap1-Nrf2/ARE signalling pathway and modulating the transcriptional activity of antioxidant enzymes or drug transporters. This signalling pathway plays a key role in cellular resistance to external oxidative stress and is an important defence system against oxidative damage [46]. As illustrated in *Fig. 3-c*, quercetin and apigenin in the

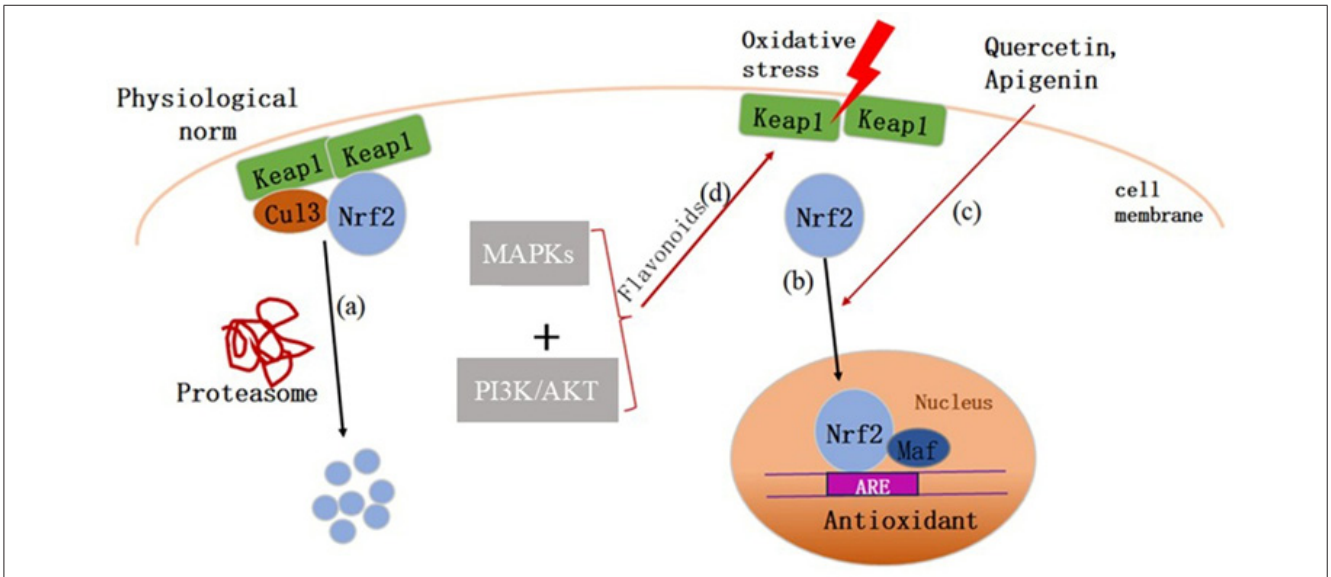

Fig 3. Flavonoids of Azalea plants are antioxidant by regulating Keap1-Nrf2 and MAPKS signalling pathways. (a) Under normal conditions, Keap1-Nrf2 signalling pathway, Nrf2 signalling molecules are degraded, (b) Suffering from oxidative stress, Nrf2 signalling molecules are released into the nucleus to bind with Maf proteins to form heterodimers and exert antioxidant effects, (c) Quercetin and apigenin promote Nrf2 translocation into the nucleus and increase the level of Nrf2 in the nucleus, (d) Flavonoids activate Nrf2 through MAPKs and PI3K/AKT signalling pathways, which in turn enhance the antioxidant response

flavonoids of genus Azalea can inhibit the degradation of Nrf2, promote the translocation of Nrf2 into the nucleus, and increase the level of Nrf2 in the nucleus as a means of up-regulating the endogenous antioxidant capacity of cells [47,48].

Antioxidant MAPK$_s$ Signalling Pathway

The mitogen-activated protein kinase (MAPK$_s$) signalling pathway consists of three major signalling pathways, JNK, ERK and p38, which play an important role in cellular responses to external stimuli (e.g. oxidative stress) [49]. It has been shown that ROS activate Nrf2 through MAPKs and phosphatidylinositol-3-kinase/protein kinase B (PI3K/AKT) cell signalling pathways in response to cellular damage caused by oxidative stress [50].

As illustrated in *Fig. 3-d*, flavonoids activate Nrf2 via MAPKs signalling pathway in conjunction with PI3K/AKT signalling pathway and thus enhance the antioxidant response.

Mechanism of Action of Anti-Inflammatory

The anti-inflammatory properties of flavonoids from the genus Azalea are achieved through four main areas: inhibition of the production of inflammatory mediators, modulation of cytokines and receptors, scavenging of oxygen free radicals and cell signalling pathways.

Inhibition of the Production of Inflammatory Mediators

Prostaglandin E2 (PGE2) and NO are the two main pro-inflammatory mediators. Arachidonic acid (AA) produces PGE2 via the cyclooxygenase pathway, which contributes to inflammation by increasing vascular permeability and vasodilation causing redness, swelling, stiffness and pain [51]. Cyclooxygenase 2 (COX-2) mainly catalyses the production of large amounts of PGE2, which is involved in the inflammatory response, and inducible NO synthase (iNOS) catalyses the production of large amounts of NO from L-arginine, resulting in cellular damage [52]. Thus, inhibition of COX-2 and iNOS expression reduces cellular inflammation and alleviates cellular damage.

As illustrated in *Fig. 4-a*, quercetin and lignans in the flavonoids of *Rhododendron* can inhibit the expression of iNOS and COX-2 at the mRNA and protein levels to reduce the production of NO and PGE2 and exert their anti-inflammatory effects [52,53].

Regulation of Cytokines and Receptors

In the inflammatory response, proliferating cells such as macrophages, neutrophils, eosinophils and epithelial cells can synthesise and release a variety of cytokines such as interleukin 1β (IL-1β)), interleukin 6 (IL-6), interleukin 8 (IL-8), and tumour necrosis factor (TNF-α), etc. Flavonoids can be used to inhibit these inflammatory cytokines by inhibiting their production and hindering

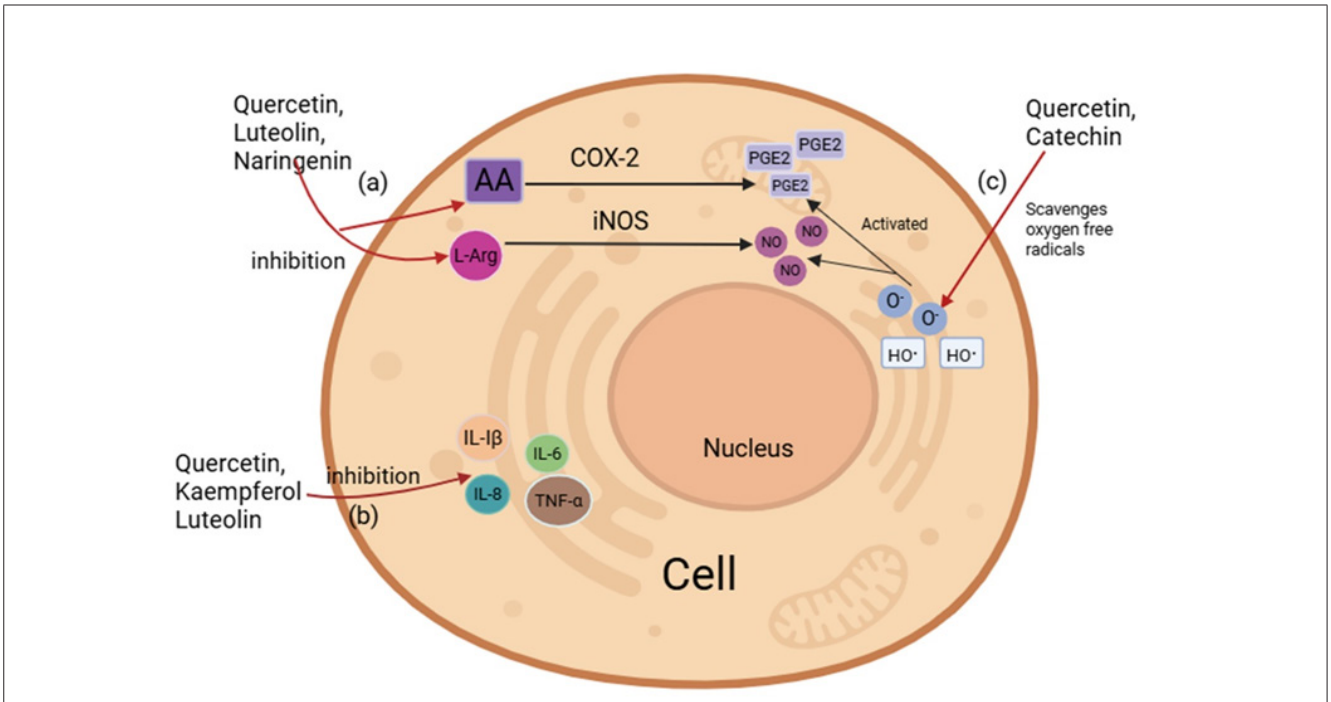

Fig 4. Azalea flavonoids are anti-inflammatory by inhibiting the production of inflammatory mediators, modulating cytokines and receptors and scavenging oxygen radicals. (a) Quercetin and lignans inhibit the expression of iNOS and COX-2 and reduce NO and PGE2 production, (b) Kaempferol, quercetin and lignans regulate cytokines and exert anti-inflammatory effects, (c) Quercetin and catechin scavenge oxygen free radicals and inhibit the activation of inflammatory mediators by oxygen free radicals

their association with the Receptor binding, play an anti-inflammatory role [54].

The flavonoids of the genus *Rhododendron*, including kaempferol, quercetin and lignans, can all have anti-inflammatory effects by modulating cytokines. Kaempferol and quercetin can rapidly scavenge DPPH and ABTS free radicals, and can effectively inhibit the secretion of IL-6, IL-1β and TNF-α [55]. A dose of quercetin (10-25 mol/L) reduces NO and TNF-α in lipopolysaccharide (LBS)-induced mouse glioma cells [56]. As illustrated in *Fig. 4-b,* mucuna pruriens has a highly significant inhibitory effect on both TNF-α and IL-6 [57].

Radical Scavenging

Oxygen free radicals are non-specific damage factors widely present in phagocytes of the body and are one of the important pathological mechanisms of inflammation. When the body is stimulated by inflammation, macrophages will produce a large number of oxygen free radicals, disrupting the dynamic balance in the body; at the same time, oxygen free radicals will also activate inflammatory factors, exacerbating the inflammatory response. Therefore, elimination of oxygen free radicals can slow down the inflammatory response [58]. The chemical structure of flavonoids, especially those with a catechol structure, tends to have a large number of phenolic hydroxyl groups, a structural advantage that gives them good free radical scavenging properties [35].

As illustrated in *Fig. 4-c,* quercetin and catechin in the flavonoids of *Rhododendron* contain o-diphenol hydroxyl structure, which can effectively scavenge oxygen free radicals [59].

Cell Signalling Pathways

NF-KB Signalling Pathway: NF-κB is a dimer consisting of five monopeptide proteins, P50 (also known as NF-κB1), p52 (also known as NF-κB2), RelA (also known as p65), RelB and c-Rel [60]. It is also a widely distributed and functional eukaryotic transcription factor. Functional NF-κB binding sequences are present in promoters and enhancers of genes, so NF-κB can bind to fixed nucleotide sequences in the promoter regions of many genes to initiate gene transcription, and control a variety of targets such as cytokines, adhesion factors, growth factors, enzymes (COX-2, iNOS), neuropeptides, and so on.It plays an important role in immune response, inflammation and cell growth regulation [61]. Flavonoids inhibit IKk (IK kinase) production and increase IkB (inhibitory factor) expression by preventing NF-κB from entering the nucleus for transcription. The anti-inflammatory effects of these compounds are exerted in three ways: by preventing NF-κB from entering the nucleus for transcription, by inhibiting IKk (IK kinase) production and by increasing IkB expression [58].

Quercetin inhibits the activation of the NF-κB signalling pathway and prevents the entry of NF-κB into the nucleus

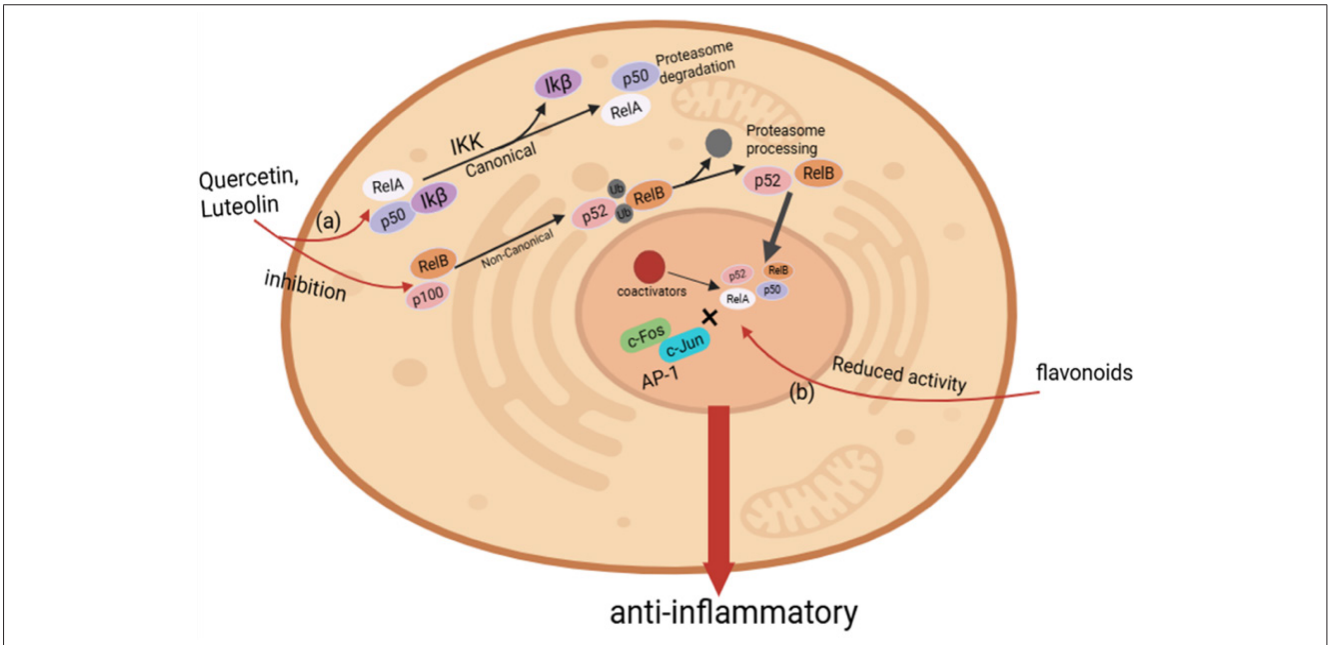

Fig 5. Flavonoids of the genus Azalea are antioxidants through the signalling pathway. NF-κB regulates the inflammatory response through both classical and non-classical pathways. The classical pathway is dependent on the activation of the IκB kinase complex (IKK), which leads to the phosphorylation of the IκB protein, which in turn triggers ubiquitination and proteasomal degradation of IκB, and after IκB degradation, the dimer of p50/RelA is released and enters the nucleus. The non-classical pathway is dependent on NF-κB-inducible kinase (NIK), activation of which leads to partial degradation of p100 into p52, which forms a dimer with RelB and enters the nucleus. (a) Quercetin and lignans inhibit the NF-κB signalling pathway and prevent its dimerisation into the nucleus, (b) Flavonoids reduce the activity of NF-κB dimer and AP-1 in the nucleus of the cell nucleus to achieve cellular anti-inflammation

for transcription, thereby reducing the inflammatory response [62]. As illustrated in *Fig. 5-a*, lignans can significantly inhibit the phosphorylation of IkKβ and IkBα in inflammatory cells, reduce the expression of P65 in the nucleus, and then better inhibit the NF-κB signalling pathway to exert anti-inflammatory activity [57].

Transcription Factor Activator Protein 1 (AP-1): AP-1 is an intracellular transcriptional activator that is a heterodimer of c-Fos and c-Jun. Often works with NF-κB to regulate the expression of inflammatory factors in mediating inflammatory responses [63]. NF-KB is mainly involved in the regulation of cytokine expression and other inflammatory mediators, whereas AP-1 is involved in the synthesis of innate immune effector molecules and cytokine responses [64]. As illustrated in *Fig. 5-b*, quercetin Significantly Reduces High Glucose-Induced NF-κB and AP-1 Activity [65].

Applications of *Rhododendron* Flavonoids

Maintain Blood Pressure Homeostasis

Flavonoids exert anti- MAPKs inflammatory and antioxidant effects by modulating the Keap1-Nrf2/ARE, NF-κB, and AP-1 signalling pathways, playing a significant role in maintaining cardiovascular homeostasis and tissue protection in animals. Research indicates that flavonoids may assist in maintaining blood pressure homeostasis, mitigate abnormal vascular lipid deposition, and safeguard myocardial structural and functional integrity, thereby demonstrating positive physiological protective effects on the cardiovascular system in animals [3].

Flavonoids exert a blood pressure-stabilising regulatory effect, with quercetin exerting a significant influence on blood pressure by reducing diastolic pressure in hypertensive animal models and systolic pressure in normotensive animal models [66]. Nitric oxide (NO), as the primary vasodilator, plays a crucial role in blood pressure regulation. In rat models, kaempferol administered orally at 10 mg kg^{-1} day^{-1} for 6 weeks significantly enhanced aortic eNOS expression, elevated serum NO levels, and reduced systolic blood pressure (approximately ↓18 mmHg) in a dose-dependent manner [67]. In spontaneously hypertensive rat models, the *Rhododendron*-derived flavonoid falarone (at doses of 10-40 mg kg^{-1} over 8 weeks) reduced systolic blood pressure in a dose-dependent manner by inhibiting angiotensin II-mediated NADPH oxidase activation. This alleviated vascular oxidative stress, restored endothelium-dependent relaxation in the aorta, and reduced intimal hypertrophy [68]. In dogs, intravenous administration of rhoifolin (5 mM/kg) and vitexin significantly reduced mean aortic pressure (by 8%), arterial and pulmonary capillary pressures, and heart rate through vasodilation and negative inotropic effects. Oral administration of Elsholtzia blanda total flavonoids (25-100 mg/kg) dose-dependently reduced myocardial infarction area (from 19.42% to 8.87%), decreased serum creatine kinase-MB (CK-MB) and malondialdehyde (MDA) levels, and inhibited lipid peroxidation in a coronary artery occlusion model [69,70]. In horses, administration of 50-75 mg horse chestnut seed extract (containing 2% aescin and flavonoids) every 12 h improved venous tone, reduced transcapillary filtration, and enhanced venous return, with clinical application in chronic venous insufficiency [71].

Lowering blood lipid levels is the optimal approach for preventing and treating atherosclerotic diseases, whilst flavonoids counteract atherosclerosis by inhibiting inflammation in adipose tissue, enhancing cholesterol reverse transport, and reducing blood lipid levels. In a high-fat diet rat model, continuous oral administration of *Rhododendron* methanolic extract (dose: 300-200 mg/kg·d) for 63 days reduced plasma total cholesterol by approximately 28%, triglycerides by approximately 32%, and low-density lipoprotein cholesterol by approximately 35%, while increasing high-density lipoprotein cholesterol by approximately 25%. Its efficacy in reducing the atherosclerosis index surpassed that of lovastatin (10 mg/kg), with no significant toxic reactions observed [72]. In a study by Shubhi Agarwal and colleagues on a high-cholesterol New Zealand rabbit model, continuous oral administration of *Rhododendron* extract reduced serum total cholesterol, triglycerides, and low-density lipoprotein cholesterol levels, increased high-density lipoprotein cholesterol, and decreased the atherosclerosis index [73].

Restriction of cardiac contraction and relaxation constitutes a common clinical manifestation of cardiomyopathy. Calcium ions represent a primary factor in cardiac contraction whilst flavonoid compounds can inhibit Ca^{2+}-sensitivity dysregulation induced by troponin I phosphorylation [74,75]. In isolated rat hearts and cardiomyocytes, total *Rhododendron* flavonoids (5-20 μg/mL) inhibited potassium-induced calcium influx and sarcoplasmic reticulum calcium release, thereby reducing intracellular Ca^{2+} levels. This mitigated hypoxia-induced injury and diminished infarct size, revealing a calcium-regulated cardioprotective mechanism [76]. In an autoimmune myocarditis rat model, green tea catechins (400 mg/kg·d administered for 4 consecutive weeks) mitigated left ventricular dysfunction, reduced inflammatory cell infiltration and myocardial fibrosis, and shifted the cytokine profile towards anti-inflammatory characteristics. This demonstrates that tea flavonoids can simultaneously alleviate inflammatory responses and adverse remodelling in experimental myocarditis [77].

Anticancer

Flavonoids, as natural radiosensitising agents and chemo-

therapeutic sensitising agents, can be integrated into comprehensive cancer management across four levels: primary prevention, synergistic radiotherapy, overcoming drug resistance, and secondary chemoprevention. They demonstrate significant potential particularly in enhancing radiotherapy sensitivity, improving the efficacy of chemotherapeutic drugs, and reversing tumour multidrug resistance [78].

Regarding radiotherapy sensitisation, multiple studies provide clear dose-response evidence. In colon cancer models, 24 h pretreatment of HT-29 and DLD-1 cells with 50 μM quercetin significantly increased sensitivity to 6 Gy X-rays by downregulating the Notch-1 signalling pathway, reducing colony survival rates by approximately 40% [79]. In mouse solid tumour studies, daily intraperitoneal administration of 25 mg/kg apigenin combined with 10 mg/kg cryptotanshinone for 14 consecutive days, alongside 2 Gy local irradiation, achieved a tumour volume suppression rate of 78% in Ehrlich tumours. This effect markedly exceeded the 44% observed in the radiotherapy-alone group, fully demonstrating the advantages of flavonoid compounds in synergising radiotherapy [80].

Flavonoids also demonstrate remarkable efficacy in enhancing chemotherapy outcomes. In a prostate cancer xenograft model, daily oral administration of 50 mg/kg quercetin concurrently with weekly docetaxel (5 mg/kg) over four weeks elevated tumour weight inhibition to 72%, substantially surpassing the 38% achieved by docetaxel monotherapy. Its mechanism of action is associated with downregulating P-glycoprotein (P-gp) expression, inhibiting the PI3K/Akt signalling pathway, and modulating androgen receptor signalling [81]. In the hormone-refractory PC-3 prostate cancer model, combining 40 mg/kg quercetin with 10 mg/kg paclitaxel (administered every 3 days for 5 consecutive cycles) prolonged tumour doubling time by 1.8-fold through inducing endoplasmic reticulum (ER) stress and reactive oxygen species (ROS) bursts, offering novel insights for enhancing chemotherapy efficacy [81]. In addition to synergising with chemotherapeutic agents, certain flavonoid compounds themselves exhibit distinct *in vivo* antitumour activity. For instance, research by Ma et al.[82] on the *in vivo* antitumour evaluation of *Rhododendron* decorum flavonoids demonstrated that in a Kunming mouse model transplanted with S180 sarcoma, oral administration of total flavonoids from *Rhododendron* grandiflorum (at doses of 50, 100, 200 mg/kg/d) via oral gavage for 10 consecutive days. The 200 mg/kg group achieved a tumour volume inhibition rate of 54.7% ($P<0.01$). Mechanistic studies revealed that this dose significantly elevated serum interleukin-2 (IL-2) and TNF-α levels while reducing VEGF levels, suggesting a synergistic anticancer effect through immune enhancement and anti-angiogenesis. No hepatotoxicity, nephrotoxicity, or abnormal body weight changes were observed during the experiment. Consequently, it is proposed that *Rhododendron* decorum flavonoids exert a dose-dependent antitumour effect in animals via a dual immune-antiangiogenic mechanism.

In the field of reversing tumour multidrug resistance (MDR), the efficacy of flavonoid compounds has also been demonstrated. In a colon cancer model resistant to 5-fluorouracil (5-FU), co-treatment with 20 μM kaempferol and 5 μM 5-FU for 48 hours produced a significant synergistic inhibitory effect on LS174-Resistant cells (combination index CI≈0.6), elevating apoptosis rates to 3.7 times that of monotherapy. primarily through inhibiting ABCB1 transporter function and inducing G_2/M phase arrest in the cell cycle [81]; In the HL-60/NB4 acute myeloid leukaemia resistance model, 40 μM kaempferol effectively restored cell sensitivity to doxorubicin by downregulating ABCB1 and ABCC1 transporter expression alongside Akt and BCL2 signalling molecules, reducing the resistance index from 8.2 to 2.1 [83].

The aforementioned studies consistently demonstrate that flavonoid compounds such as quercetin, kaempferol, and total flavonoids from *Rhododendron* anthopogon, within the dose range of 20-200 μM *(in vitro)* or 25-200 mg/kg *(in vivo),* can significantly enhance radiotherapy/chemotherapy efficacy, reverse ABC transporter-mediated resistance, or exert direct antitumour effects through diverse mechanisms. These well-defined dose-response relationships in preclinical studies provide a foundation for incorporating flavonoid compounds into clinical anticancer combination therapies or for their standalone use. chemotherapy efficacy, reverse ABC transporter-mediated resistance, or exert direct antitumour effects. This clear dose-response relationship in preclinical evidence provides substantial support for the clinical application of flavonoids in combined anticancer therapies or as monotherapy.

Animal Diabetes Mellitus

Flavonoids intervene in type 2 diabetes mellitus (T2DM) and its microvascular and macrovascular complications by lowering blood glucose, improving insulin sensitivity, and preventing complications. Regarding hypoglycaemic effects and insulin resistance improvement, high-dose quercetin (≥100 mg/kg/day via gastric lavage in db/db mice for 8 weeks) inhibits protein tyrosine phosphatase 1B (PTP1B), elevates insulin receptor substrate 2 (IRS-2) phosphorylation, and markedly reduces fasting blood glucose. administered via gastric lavage to db/db mice for 8 weeks) inhibits protein tyrosine phosphatase 1B (PTP1B), elevates insulin receptor substrate 2 phosphorylation levels, significantly reduces fasting blood glucose, and

improves oral glucose tolerance. At equivalent doses, kaempferol mitigated inflammatory insulin resistance by blocking IKKβ/NF-κB signalling, thereby downregulating inflammatory mediators such as IL-6 and TNF-α [84].

Flavonoids exert effects by promoting insulin secretion and modulating the intestinal-pancreatic axis. In a C57BL/6 high-fat diet model, 50 μmol/L quercetin or 25 μmol/L kaempferol effectively stimulated L-cell secretion of glucagon-like peptide-1 (GLP-1) in the ileum. inhibiting dipeptidyl peptidase-4 (DPP-4) activity and elevating total GLP-1 levels by 1.8-fold, thereby enhancing glucose-dependent insulin release [85]. In preventing diabetic complications, flavonoids exhibit multi-target protective effects: For retinopathy, quercetin at 50 mg/kg/d (intraperitoneal injection, STZ-induced rats, 12 weeks) suppressed retinal vascular endothelial growth factor (VEGF) and intercellular adhesion molecule-1 (ICAM-1) expression, reducing blood-retinal barrier leakage; For diabetic nephropathy, kaempferol at 75 mg/kg/day (oral administration, db/db mice for 16 weeks) reduced urinary albumin excretion and fibronectin deposition, a mechanism associated with inhibition of the TGF-β1/Smad3 signalling pathway; For cardiomyopathy and osteoporosis, quercetin alleviates myocardial oxidative stress by activating the Nrf2/HO-1 pathway and protects the bone matrix by inhibiting receptor for advanced glycation end-products (RAGE) expression [86].

Conclusion

In this paper, we review the past research progress on the mechanism and clinical application of antioxidant and anti-inflammatory activities of flavonoids from *Rhododendron* plants. We have identified 17 flavonoids in *Rhododendron* plants with significant antioxidant and anti-inflammatory activities. These compounds act through a variety of mechanisms, including direct scavenging of free radicals, inhibition of oxidative enzymes (e.g. NADPH oxidase and xanthine oxidase), chelation of metal ions, provision of hydrogen ions and enhancement of the antioxidant system to stabilise or reduce reactive oxygen species (ROS) and scavenging of free radicals, as well as modulation of the endogenous antioxidant capacity by the Keap1-Nrf2/ARE and $MAPK_S$ signalling pathways. The antioxidant is achieved by means of the Keap1-Nrf2/ARE and $MAPK_S$ signalling pathways. Its anti-inflammatory effects are achieved by inhibiting the production of inflammatory mediators, modulating cytokines and receptors, scavenging oxygen free radicals, and affecting cell signalling pathways such as NF-κB and AP-1. At present, it has become a prevailing trend to study the antioxidant and anti-inflammatory properties of flavonoids at home and abroad. *Rhododendron* is found all over the world and is rich in flavonoids, so isolating the specific composition and structure of flavonoids from *Rhododendron* will help to design and develop more effective natural antioxidant protective agents and animal health supplements [87]. An in-depth elucidation of its antioxidant and anti-inflammatory mechanisms holds promise for advancing the development of novel natural antioxidants for protecting animal organisms against oxidative damage and maintaining health homeostasis [88].

In terms of clinical applications, flavonoids have been shown to have potential therapeutic effects on cardiovascular diseases such as hypertension, atherosclerosis, cardiomyopathy and myocarditis [3]. It also shows great therapeutic potential in the fields of diabetes and anticancer [78,86]. A deeper understanding of their antioxidant and anti-inflammatory mechanisms will advance research into the application of flavonoids in animal health management, thereby fully harnessing their physiological protective and supportive efficacy.

Flavonoids and terpenoids can act synergistically to enhance each other's pharmacological activities, especially in the fight against cancer. Terpenoids modulate caspase-3 activity and flavonoid circuit affects enzyme activity [89]. Flavonoids and terpenoids collectively influence the regulation of ATP-binding cassette (ABC) transporter protein efflux function, and semi-synthetic nitrogen-containing flavonoids and terpenoids derivatives possess potential as multidrug resistance (MDR) reversal agents designed to be effective in cancer [90]. Azalea plants are rich in flavonoids and terpenoids, the study of Azalea plants can not only study flavonoids and terpenoids, but also study the synergistic effect of the two, the development of new anti-cancer drugs.

Although some progress has been made on the antioxidant and anti-inflammatory activities of flavonoids in the genus *Rhododendron*, there are still some limitations, such as the absence of systematic studies on their mechanistic mechanisms, small sample sizes, and geographical bias. Future studies need to consider a wider range of samples and different geographical regions to validate the existing findings and further systematically explore the pharmacological mechanisms of action of flavonoids [10]. Moreover, in-depth research into flavonoids holds promise for providing further scientific rationale for developing novel approaches to maintaining and safeguarding animal health, particularly demonstrating significant research and application value in antioxidant and anti-inflammatory physiological protection.

In conclusion, significant progress has been made in research concerning the antioxidant and anti-inflammatory physiological activities of flavonoids from *Rhododendron* species. This has laid a solid foundation for subsequent development of natural physiological

protective agents and their application in animal health management. Future studies should continue to explore the physiological protective and supportive potential of these compounds, overcome existing research limitations, and further expand their application scenarios in safeguarding animal organisms and maintaining health.

Declarations

Availability of Data and Materials: The data and materials used to support the findings of this study are available from the first author (Z.Z.) and the primary corresponding author (Z.C.) upon reasonable request. All relevant data have been properly curated and can be provided to facilitate reproducibility of the research results.

Acknowledgements: The authors sincerely thank Xizang Agricultural and Animal Husbandry University, School of Animal Science and Tibetan Key Laboratory of Clinical Veterinary Medicine for equipment and financial support. We also appreciate the reviewers and editors for their valuable comments that improved this manuscript.

Funding Information: This study was supported by the grants from Science and Technology Programme of Linzhi City, Tibet Autonomous Region (XDHZ-2025-07

Conflict of Interest: The authors declare no conflicts of interest.

Declaration on Generative Artificial Intelligence (AI): Generative artificial intelligence was only used for language polishing in this study; it was not involved in any other aspects of the research. All authors have reviewed the final content and take full responsibility for its authenticity and scientificity.

Author Contributions: All authors made substantial contributions to this study. Ziqin Zhang was responsible for conceptualization, methodology and original draft writing; Sheng Kang and Hailong Dong engaged in data curation and formal analysis; Meixue Ni and Xiaoqing Guo participated in investigation, resources collection and validation. As corresponding authors, Qingxia Wu was in charge of supervision, funding acquisition and manuscript review & editing; Zhenyu Chang, the primary corresponding author, undertook supervision, conceptualization, methodology and manuscript review & editing.

References

1. **Liu XJ, Su HG, Peng XR, Bi HC, Qiu MH:** An updated review of the genus *Rhododendron* since 2010: Traditional uses, phytochemistry, and pharmacology. *Phytochemistry*, 217:113899, 2024. DOI: 10.1016/j.phytochem.2023.113899
2. **Cheng J, Li M, Yuan T, Huang H, Yang G, Bai X:** A dataset on wild *Rhododendron* and geographical distribution information in China. *Biodivers Sci,* 29 (9): 1175-1180, 2021. DOI: 10.17520/biods.2021152
3. **Liu Y, Luo J, Peng L, Zhang Q, Rong X, Luo Y, Li J:** Flavonoids: Potential therapeutic agents for cardiovascular disease. *Heliyon*, 10 (12):E32563, 2024. DOI: 10.1016/j.heliyon.2024.e32563
4. **Pooja G, Shweta S, Patel P:** Oxidative stress and free radicals in disease pathogenesis: A review. *Discov Med,* 2:104, 2025. DOI: 10.1007/s44337-025-00303-y
5. **Sarkar C, Chaudhary P, Jamaddar S, Janmeda P, Mondal M, Mubarak MS, Islam MT:** Redox activity of flavonoids: Impact on human health, therapeutics, and chemical safety. *Chem Res Toxicol,* 35 (2): 140-162, 2022. DOI: 10.1021/acs.chemrestox.1c00348
6. **Pathology Teaching and Research Group, Lanzhou Medical College, Lanzhou, China:** Pharmacological study and toxicity observation of loquatoxin. *Chin Med J,* 54 (5): 279-283, 1974.
7. **Yang HX, Xu W, Huang ZH:** Chemical constituents of *Anoectochilus roxburghii* based on UPLC-Q-TOF-MS/MS. *Chin J Mod Appl Pharm,* 42 (6): 948-957, 2025. DOI: 10.13748/j.cnki.issn1007-7693.20232655
8. **Tan C, Chen X, Liu X, Hui JM, Huo XY, Gao SJ, Wang YH, Wang JR, Zhang XM, Yang Y:** Progress in the study of *Rhododendron*. *China Wild Plant Resour,* 40 (9): 29-36, 2021.
9. **Verma K, Kumar I:** A complete review on *Rhododendron arboreum*: Phytochemistry, pharmacological activities and future prospects. Int J *Pharm Pharm Res,* 19 (3): 161-176, 2020.
10. **Wang L, Zeng X, Yao HZ, Yuan T:** Studies on flavonoids from *Rhododendron tigrinum* and their antioxidant and anti-inflammatory activities. *Nat Prod Res Dev,* 36 (8): 1350-1356, 2024.
11. **Hu M, Liu YL, Xiao PG:** Chemical composition of *Rhododendron angustifolium*. *J Integr Plant Biol,* 32 (10): 777-782, 1990.
12. **Li ZL, Xue DY, Chen YZ, Shi ZX, Zhang JX:** Studies on the chemical composition of the volatile oil of *Rhododendron schoenanthus.* Nat *Prod Res Dev,* 2, 11-16, 1991. DOI: 10.16333/j.1001-6880.1991.02.003
13. **Zhao X, Che WS:** Progress of chemical composition and extraction method of Manzan Hong. *J Anhui Med Univ,* 48 (5): 580-582, 2013. DOI: 10.19405/j.cnki.issn1000-1492.2013.05.038
14. **Duan WT, Cheng Q, Bi XX, Wang Y, Cheng B, Luan J, Zhang GH, He JB:** Studies on the chemical composition of *Rhododendron* on cloud and its no production inhibiting activity. *Nat Prod Res Dev,* 36 (1): 63-71, 2023. DOI: 10.16333/j.1001-6880.2024.1.007
15. **Zhou XL, Qin CH, Mei Y, Huang S:** Studies on the chemical composition of *Rhododendron barbadensis* leaves. *Chin Herb Med,* 41 (2): 206-208, 2010.
16. **Zhou SY, Li RT:** Progress in the study of chemical composition and biological activity of *Rhododendron* plants. *Yunnan J Tradit Chin Med,* 30 (5): 51-53, 2008. DOI: 10.16254/j.cnki.53-1120/r.2008.05.036
17. **Xiao YC, Hu FZ, Du YZ, Wei LX:** Determination of seven flavonoid constituents in different parts of Tibetan medicine *Rhododendron simsii* by HPLC method. *J Pharm Anal,* 38 (8): 1325-1330, 2018. DOI: 10.16155/j.0254-1793.2018.08.06
18. **Xia X, Gong R, Zhang C:** Integrative analysis of transcriptome and metabolome reveals flavonoid biosynthesis regulation in *Rhododendron pulchrum* petals. *BMC Plant Biol,* 22 (1):401, 2022. DOI: 10.1186/s12870-022-03762-y
19. **Zhang M, Pan DR:** Progress in the study of flavonoids in *Rhododendron* plants. *Sci Across Taiwan Straits,* 28 (5): 3-4+14, 2012.
20. **Oliveira THB, Gusmao NB, Silva LAO, Coelho LCBB:** Free radicals and actinobacteria as a misexplored goldmine of antioxidant compounds. *An Acad Bras Cienc*, 93 (Suppl.-3): E20201925, 2021. DOI: 10.1590/0001-3765202120201925
21. **Shen N, Wang T, Gan Q, Liu S, Wang L, Jin B:** Plant flavonoids: Classification, distribution, biosynthesis, and antioxidant activity. *Food Chem,* 383:132531, 2022. DOI: 10.1016/j.foodchem.2022.132531
22. **Valko M, Leibfritz D, Moncol J, Cronin MTD, Mazur M, Telser J:** Free radicals and antioxidants in normal physiological functions and human disease. *Int J Biochem Cell Biol,* 39 (1): 44-84, 2007. DOI: 10.1016/j.biocel.2006.07.001
23. **Yang X, Wang H, Lu K, Ma X, Tan Z, Long B, Chen X, Li C, Zhai T, Li Y, Qu K, Xia Y, Zhang Y, Li X, Chen S, Dong H, Zeng L, Zhang YH:** Reactive aldehyde chemistry explains the missing source of hydroxyl radicals. *Nat Commun,* 15 (1):1648, 2024. DOI: 10.1038/s41467-024-45885-w
24. **Guo CM, Liu SQ, Guo YM, Yu HS, Sun MZ:** Scavenging function of hydroxyl radicals (Ho·) by flavonoids and their conformational relationships. *Nat Prod Res Dev,* 24 (12): 1724-1728, 2012. DOI: 10.16333/j.1001-6880.2012.12.007
25. **Lu L, Luan Y, Wang H, Gao Y, Wu S, Zhao X:** Flavonoid as a potent antioxidant: Quantitative structure-activity relationship analysis, mechanism study, and molecular design by synergizing molecular

simulation and machine learning. *J Phys Chem A,* 128 (30): 6216-6228, 2024. DOI: 10.1021/acs.jpca.4c03241

26. **Garcia JG, Ansorena E, Izal I, Zalba G, De Miguel C, Milagro FI:** Structure, regulation, and physiological functions of NADPH oxidase 5 (NOX5). *J Physiol Biochem,* 79 (2): 383-395, 2023. DOI: 10.1007/s13105-023-00955-3
27. **Ullah Z, Yue P, Mao G, Zhang M, Liu P, Wu X, Zhao T, Yang L:** A Comprehensive review on recent xanthine oxidase inhibitors of dietary based bioactive substances for the treatment of hyperuricemia and gout: Molecular mechanisms and perspective. *Int J Biol Macromol,* 278:134832, 2024. DOI: 10.1016/j.ijbiomac.2024.134832
28. **Balázs O, Dombi Á, Zsidó BZ, Hetényi C, Valentová K, Vida RG, Poór M:** Inhibition of xanthine oxidase-catalyzed xanthine and 6-mercaptopurine oxidation by luteolin, naringenin, myricetin, ampelopsin and their conjugated metabolites. *Biomed Pharmacother,* 167:115548, 2023. DOI: 10.1016/j.biopha.2023.115548
29. **Yan J, Zhang G, Hu Y, Ma Y:** Effect of luteolin on xanthine oxidase: Inhibition kinetics and interaction mechanism merging with docking simulation. *Food Chem,* 141 (4): 3766-3773, 2013. DOI: 10.1016/j.foodchem.2013.06.092
30. **Liu Y, Liang S, Shi D, Zhang Y, Bai C, Ye RD:** A predicted structure of NADPH oxidase 1 identifies key components of ROS generation and strategies for inhibition. *Plos One,* 18 (5):E0285206, 2023. DOI: 10.1371/journal.pone.0285206
31. **Yu Y, Xiong Y, Tong S, Li Y, Cai R, Zhang X, Gao F:** Inhibitory activity of quercetin, rutin, and hyperin against xanthine oxidase: Kinetics, fluorescence, and molecular docking. *Curr Pharm Biotechnol,* 25, 1-12, 2024. DOI: 10.2174/0113892010297269240427055003
32. **Porfirio DA, Ferreira RDQ, Malagutti AR, Valle EMA:** Electrochemical study of the increased antioxidant capacity of flavonoids through complexation with iron(II) ions. *Electrochim Acta,* 141, 33-38, 2014. DOI: 10.1016/j.electacta.2014.07.046
33. **Zhu L, Ma LL, Li XS, Lu ZK, Lv WH, Le XY:** Preparation and *in vitro* antioxidant activity of two copper(II) complexes of flavonoids. *Food Ind Sci Technol,* 40 (4): 51-55+61, 2018. DOI: 10.13386/j.issn1002-0306.2019.04.008
34. **Mira L, Fernandez MT, Santos M, Rocha R, Florencio MH, Jennings KR:** Interactions of flavonoids with iron and copper ions: A mechanism for their antioxidant activity. *Free Radic Res,* 36 (11): 1199-1208, 2002. DOI: 10.1080/1071576021000016463
35. **Zheng YZ, Deng G, Zhang YC:** Multiple free radical scavenging reactions of flavonoids. *Dyes Pigments,* 198:109877, 2022. DOI: 10.1016/j.dyepig.2021.109877
36. **Zhou W, Peng C, Wang D, Li J, Tu Z, Zhang L:** Interaction mechanism between ova and flavonoids with different hydroxyl groups on B-ring and effect on antioxidant activity. *Foods*, 11 (9): 1302, 2022. DOI: 10.3390/foods11091302
37. **Jomova K, Alomar SY, Alwasel SH, Nepovimova E, Kuca K, Valko M:** Several lines of antioxidant defense against oxidative stress: Antioxidant enzymes, nanomaterials with multiple enzyme-mimicking activities, and low-molecular-weight antioxidants. *Arch Toxicol,* 98 (5): 1323-1367, 2024. DOI: 10.1007/s00204-024-03696-4
38. **Rudenko NN, Vetoshkina DV, Marenkov TV, Borisova-Mubarakshina MM:** Antioxidants of non-enzymatic nature: Their function in higher plant cells and the ways of boosting their biosynthesis. *Antioxidants*, 12 (11):2014, 2023. DOI: 10.3390/antiox12112014
39. **Gao Y, Dong X, Wang R, Hao F, Zhang H, Zhang Y, Lin G:** Exogenous calcium alleviates oxidative stress caused by salt stress in peanut seedling roots by regulating the antioxidant enzyme system and flavonoid biosynthesis. *Antioxidants*, 13 (2):233, 2024. DOI: 10.3390/antiox13020233
40. **Sheng Yl, Liu H, Yu J:** Influence of structural and non-structural factors on the role of flavonoids in antioxidant activity. *Chin Pharm,* 24 (7): 660-663, 2013.
41. **Morgenstern C, Lastres-Becker I, Demirdöğen BC, Costa VM, Daiber A, Foresti R, Motterlini R, Kalyoncu S, Arioz BI, Genc S, Jakubowska M, Trougakos IP, Piechota-Polanczyk A, Mickael M, Santos M, Kensler TW, Cuadrado A, Copple IM:** Biomarkers of NRF2 signalling: Current status and future challenges. *Redox Biol,* 72:103134, 2024. DOI: 10.1016/j.redox.2024.103134
42. **Horie Y, Suzuki T, Inoue J, Iso T, Wells G, Moore TW, Mizushima T, Dinkova-Kostova AT, Kasai T, Kamei T, Koshiba S, Yamamoto M:** Molecular basis for the disruption of keap1-NRF2 interaction via Hinge & Latch mechanism. *Commun Biol,* 4 (1):576, 2021. DOI: 10.1038/s42003-021-02100-6
43. **Dewanjee S, Bhattacharya H, Bhattacharyya C, Chakraborty P, Fleishman J, Alexiou A, Papadakis M, Jha SK:** Nrf2/keap1/ARE regulation by plant secondary metabolites: A new horizon in brain tumor management. *Cell Commun Signal,* 22 (1):497, 2024. DOI: 10.1186/s12964-024-01878-2
44. **Ma K, Miao L, Li B, Yu W, Liu F, Liu K, Li Y, Huang C, Yang Z:** Mechanism of action of Nrf2 and its related natural regulators in rheumatoid arthritis. *J Orthop Surg Res*, 19 (1):759, 2024. DOI: 10.1186/s13018-024-05221-w
45. **Katsoka F, Motohashi H, Engel JD, Yamamoto M:** Nrf2 transcriptionally activates the mafg gene through an antioxidant response element. *J Biol Chem,* 280 (6): 4483-4490, 2005. DOI: 10.1074/jbc.m411451200
46. **Speisky H, Shahidi F, Costa De Camargo A, Fuentes J:** Revisiting the oxidation of flavonoids: Loss, conservation or enhancement of their antioxidant properties. *Antioxidants,* 11 (1):133, 2022. DOI: 10.3390/antiox11010133
47. **Dai C, Zhang Q, Shen L, Sharma G, Jiang H, Wang Z, Shen J:** Quercetin attenuates quinocetone-induced cell apoptosis in vitro by activating the P38/Nrf2/HO-1 pathway and inhibiting the ros/mitochondrial apoptotic pathway. *Antioxidants*, 11 (8):1498, 2022. DOI: 10.3390/antiox11081498
48. **Cheng YJ, Quan ZJ, Zheng N, Xie YQ, Chen J:** Apigenin alleviates high glucose-induced renal cell damage and oxidative stress by activating the keap1-Nrf2-ARE signalling pathway. *Chin Pharmacist,* 27 (6): 975-983, 2024.
49. **Liu TT, Zhang SP, Tang XY, Pan RY:** Advances in MAPK signal transduction pathway and nerve injury research. *Chin Public Health,* 32 (2): 248-254, 2015.
50. **Cheng C, Yin YY, Wu XF, Wu RR, Xu YY:** Progress in activation of Nrf2 by reactive oxygen species through MAPKs and PI3k/AKT pathways. *Chin Public Health,* 32 (6): 870-873, 2016.
51. **Kawahara K, Hohjoh H, Inazumi T, Tsuchiya S, Sugimoto Y:** Prostaglandin E2-induced inflammation: Relevance of prostaglandin E receptors. *Biochim Biophys Acta Mol Cell Biol Lipids,* 1851 (4): 414-421, 2015. DOI: 10.1016/j.bbalip.2014.07.008
52. **Jin K, Qian C, Lin J, Liu B:** Cyclooxygenase-2-prostaglandin E2 pathway: A key player in tumor-associated immune cells. *Front Oncol,* 13:1099811, 2023. DOI: 10.3389/fonc.2023.1099811
53. **Hussain MS, Gupta G, Goyal A, Thapa R, Almalki WH, Kazmi I, Alzarea SI, Fuloria S, Meenakshi DU, Jakhmova V, Pandey M, Singh SK, Dua K:** From nature to therapy: luteolin's potential as an immune system modulator in inflammatory disorders. *J Biochem Mol Toxicol,* 37 (11):E23482, 2023. DOI: 10.1002/jbt.23482
54. **Al-Khayri JM, Sahana GR, Nagella P, Joseph BV, Alessa FM, Al-Mssallem MQ:** Flavonoids as potential anti-inflammatory molecules: A review. *Molecules*, 27 (9):2901, 2022. DOI: 10.3390/molecules27092901
55. **Lee KJ, Oh YC, Cho WK, Ma JY:** Antioxidant and anti-inflammatory activity determination of one hundred kinds of pure chemical compounds using offline and online screening HPLC assay. *Evid Based Complement Alternat Med,* 2015:65457, 2015. DOI: 10.1155/2015/165457
56. **Rather MA, Khan A, Alshahrani S, Rashid H, Qadri M, Rashid S, Alsaffar RM, Kamal MA, Rehman MU:** Inflammation and Alzheimer's disease: Mechanisms and therapeutic implications by natural products. *Mediators Inflamm,* 2021:982954, 2021. DOI: 10.1155/2021/9982954

57. **Wang W, He P, Jiang XM:** Anti-inflammatory and antioxidant effects of lignans and their flavonoid glycosides. *Food Sci,* 41 (17): 208-215, 2020.

58. **Zhang P, Yang J, Gao X, Ling, Guo YR, Tian CL, Liu MC:** Progress in the study of anti-inflammatory effects of flavonoids and their mechanism of action. *Livest Vet Med,* 50 (2): 134-137, 2018.

59. **Zhao XW, Liu PY, Liu D, Sun SS, Li Z, Yu KX, Zhang ML, Shi QW:** Advances in the study of conformational relationships of flavonoids. *Chin Herb Med,* 46 (21): 3264-3271, 2015.

60. **Msweli S, Pakala SB, Syed K:** NF-KB Transcription factors: Their distribution, family expansion, structural conservation, and evolution in animals. *Int J Mol Sci,* 25 (18):9793, 2024. DOI: 10.3390/ijms25189793

61. **Geng YF, Du HB, Liu LL, Sun MY, Jiu JY, Zhang JB, Zhao CL, Tian CY:** Advances in the post-translational modification of NF-κB family member rela and its physiopathological role. *Life Sci,* 32 (5): 431-438, 2020. DOI: 10.13376/j.cbls/2020054

62. **Li L, Jiang W, Yu B, Liang H, Mao S, Hu X, Feng Y, Xu J, Chu L:** Quercetin improves cerebral ischemia/reperfusion injury by promoting microglia/macrophages M2 polarization via regulating PI3k/AKT/NF-κB signaling pathway. *Biomed Pharmacother,* 168:115653, 2023. DOI: 10.1016/j.biopha.2023.115653

63. **Han CC, Wan FS:** Advances in AP-1 research. *Chin J Cell Biol,* 39 (10): 1357-1362, 2017.

64. **Fujioka S, Niu J, Schmidt C, Sclabas GM, Peng B, Uwagawa T, Li Z, Evans DB, Abbruzzese JL, Chiao PJ:** NF-κB and AP-1 connection: Mechanism of NF-KB-dependent regulation of AP-1 activity. *Mol Cell Biol,* 24 (2): 780-794, 2004. DOI: 10.1128/mcb.24.17.7806-7819.2004

65. **Qiao Y, He H, Jonsson P, Sinha I, Zhao C, Dahlman-Wright K:** AP-1 is a key regulator of proinflammatory cytokine TNFα-mediated triple-negative breast cancer progression. *J Biol Chem,* 291 (35): 18309-18320, 2016. DOI: 10.1074/jbc.a115.702571

66. **Cao Y, Xie L, Liu K, Liang Y, Dai X, Wang X, Lu J, Zhang X, Li X, Zhang Y:** The antihypertensive potential of flavonoids from Chinese herbal medicine: A review. *Pharmacol Res,* 174:105919, 2021. DOI: 10.1016/j.phrs.2021.105919

67. **Puzserova A, Bernatova I:** Blood pressure regulation in stress: Focus on nitric oxide-dependent mechanisms. *Physiol Res*, 65 (Suppl.-3): S309-S342, 2016. DOI: 10.33549/physiolres.933442

68. **Qin Xj:** Vasorelaxant effect of farrerol on rat aorta and its protection against aortic injury in spontaneously hypertensive rats. *Msc Thesis,* Shanxi Medical University, 2015.

69. **Refaat J, Desoukey SY, Ramadan MA, Kamel MS:** Rhoifolin: A review of sources and biological activities. *Int J Pharmacogn,* 2, 102-109, 2015. DOI: 10.13040/ijpsr.0975-8232.ijp.2(3).102-09

70. **Guo X, Wang Y, Zhu Z, Li L:** The role of plant extracts in enhancing nutrition and health for dogs and cats: Safety, benefits, and applications. *Vet Sci,* 11:426, 2024. DOI: 10.3390/vetsci11090426

71. **Wakshlag JJ:** Flavonoids: Not just for cancer anymore. *Compend Contin Educ Vet,* 33, E1-4, 2011.

72. **Allyn OQ, Kusumawati E, Nugroho RA:** Antimicrobial activity of terminalia catappa brown leaf extracts against *Staphylococcus aureus* ATCC 25923 and *Pseudomonas aeruginosa* ATCC 27853. *F1000res*, 7:1406, 2018. DOI: 10.12688/f1000research.15998.1

73. **Agarwal S, Rajput A:** *Rhododendron arboreum* phytochemistry, medicinal applications and pharmacology: A review. *Int J Pharmacogn Phytochem Res,* 9 (3): 1-10, 2022.

74. **Zhang Y, Chen B, Wang M, Liu H, Chen M, Zhu J, Zhang Y, Wang X, Wu Y, Liu D, Cui G, Kitakaze M, Kim JK, Wang Y, Luo T:** A novel function of claudin-5 in maintaining the structural integrity of the heart and its implications in cardiac pathology. *Biochim Biophys Acta Mol Basis Dis,* 1870 (6):167274, 2024. DOI: 10.1016/j.bbadis.2024.167274

75. **Papadaki M, Vikhorov PG, Marston SB, Messer AE:** Uncoupling of myofilament Ca^{2+} sensitivity from troponin I phosphorylation by mutations can be reversed by epigallocatechin-3-gallate. *Cardiovasc Res,* 108 (1): 99-110, 2015. DOI: 10.1093/cvr/cvv181

76. **Zhang BN, Hou YL, Liu BJ, Liu QM, Qiao GF:** The *Rhododendron dauricum* L. flavonoids exert vasodilation and myocardial preservation. *Iran J Pharm Res,* 9 (3): 303-311, 2010.

77. **Suzuki J, Ogawa M, Futamatsu H, Kosuge H, Sagesaka YM, Isobe M:** Tea catechins improve left ventricular dysfunction, suppress myocardial inflammation and fibrosis, and alter cytokine expression in rat autoimmune myocarditis. *Eur J Heart Fail*, 9 (2): 152-159, 2007. DOI: 10.1016/j.ejheart.2006.05.007

78. **Liskova A, Samec M, Koklesova L, Brockmueller A, Zhai K, Abdellatif B, Siddeequi M, Biringer K, Kudela E, Pec M, Gadanec LK, Šudomová M, Hassan STS, Zulli A, Shakibaei M, Giordano FA, Büsselberg D, Golubnitschaja O, Kubatka P:** Flavonoids as an effective sensitizer for anti-cancer therapy: Insights into multi-faceted mechanisms and applicability towards individualized patient profiles. *Epma J,* 12 (2): 155-176, 2021. DOI: 10.1007/s13167-021-00242-5

79. **Li Y, Wang Z, Jin J, Zhu SX, He GQ, Li SH, Wang J, Cai Y:** Quercetin pretreatment enhances the radiosensitivity of colon cancer cells by targeting NOTCH-1 pathway. *Biochem Biophys Res Commun,* 523 (4): 947-953, 2020. DOI: 10.1016/j.bbrc.2020.01.048

80. **Medhat AM, Azab KS, Said MM, El Fatih NM, El Bakary NM:** Antitumor and radiosensitizing synergistic effects of apigenin and cryptotanshinone against solid Ehrlich carcinoma in female mice. *Tumor Biol,* 39 (10):101042831772848, 2017. DOI: 10.1177/1010428317728480

81. **Lu X, Yang F, Chen D, Zhao Q, Chen D, Ping H, Xing N:** Quercetin reverses docetaxel resistance in prostate cancer via androgen receptor and PI3k/AKT signaling pathways. *Int J Biol Sci,* 16 (7): 1121-1134, 2020. DOI: 10.7150/ijbs.41686

82. **Ma YZ, Cheng Q, Fan ZB, Tang XQ, Wang Y, Chen B, Luan J, Zhang GH, He JB:** Chemical constituents of *Rhododendron decorum* and their antitumor cytotoxic activities. *J Yunnan Univ (Nat Sci)*, 46 (3): 555-560, 2024. DOI: 10.7540/j.ynu.20230368

83. **Riahi-Chebbi I, Souid S, Othman H, Haoues M, Karoui H, Morel A, Srairi-Abid N, Essafi M, Essafi-Benkhadir K:** The phenolic compound kaempferol overcomes 5-fluorouracil resistance in human resistant LS174 colon cancer cells. *Sci Rep* 9 (1):195, 2019. DOI: 10.1038/s41598-018-36808-z

84. **Tiganis T:** PTP1B and TCPTP-nonredundant phosphatases in insulin signaling and glucose homeostasis. *Febs J,* 280 (2): 445-458, 2013. DOI: 10.1111/j.1742-4658.2012.08563.x

85. **Anghel SA, Badea RA, Chiritoiu G, Patriche DS, Alexandru PR, Pena F:** Novel luciferase-based glucagon-like peptide 1 reporter assay reveals naturally occurring secretagogues. *Br J Pharmacol,* 179 (19): 4738-4753, 2022. DOI: 10.1111/bph.15896

86. **Wen D, Li M:** The emerging role of flavonoids in the treatment of type 2 diabetes mellitus: Regulating the enteroendocrine system. *Explor Res Hypothesis Med,* 10 (1): 56-68, 2025. DOI: 10.14218/erhm.2024.00055

87. **Ren H, Zheng SJ, Zhang XL, Lu KK, Wu SR, Ming J:** Progress of flavonoids conformational relationships based on different antioxidant mechanisms. *Food Ind Sci Technol,* 37 (2): 384-388, 2016. DOI: 10.13386/j.issn1002-0306.2016.02.070

88. **Hussain A, Azam S, Maqsood R, Anwar R, Akash MSH, Hussain H, Wang D, Imran M, Kotwicz-Mojzych K, Khan S, Hussain S, Ayub MA:** Chemistry, biosynthesis, and theranostics of antioxidant flavonoids and polyphenolics of genus *Rhododendron*: An overview. *Naunyn-Schmiedeberg's Arch Pharmacol,* 397 (5): 1479-1505, 2024. DOI: 10.1007/s00210-024-03428-6

89. **Masood N, Dubey V, Luqman S:** Activation of caspase-3 by terpenoids and flavonoids in different types of cancer cells. *Curr Top Med Chem,* 20 (21): 1876-1887, 2020. DOI: 10.2174/1568026620666200710101859

90. **Goncalves BMF, Cardoso DSP, Ferreira MJU:** Overcoming multidrug resistance: flavonoid and terpenoid nitrogen-containing derivatives as ABC transporter modulators. *Molecules*, 25 (15):3364, 2020. DOI: 10.3390/molecules25153364

Kafkas Universitesi Veteriner Fakultesi Dergisi
Journal Home-Page: http://vetdergikafkas.org
E-ISSN: 1309-2251

Kafkas Univ Vet Fak Derg
32 (2): 189-206, 2026
DOI: 10.9775/kvfd.2026.36351

Review Article

Microplastic Contamination in Honey: A One Health-Oriented Systematic Review and Risk Assessment

Burhan BAŞARAN [1(*)], Andi Nilawati USMAN [2], Mükerrem KAYA [3], Güzin KABAN [3(*)]

[1] Department of Nutrition and Dietetics, Faculty of Health Sciences, Recep Tayyip Erdogan University, TR-53100 Rize - TÜRKİYE
[2] Department of Midwifery, Graduate School, Hasanuddin University, ID-90245 Makassar-INDONESIA
[3] Department of Food Engineering, Faculty of Agriculture, Atatürk University, TR-25240 Erzurum - TÜRKİYE

(*) **Corresponding author:**
Burhan Başaran & Güzin Kaban
Phone: +90 464 214 1059 (BB),
+90 442 231 2425 (GK),
Cellular phone: +90 543 217 1551 (BB),
+90 536 228 7895 (GK)
E-mail: burhan.basaran@erdogan.edu.tr;
gkaban@atauni.edu.tr

How to cite this article?

Başaran B, Usman AN, Kaya M, Kaban G: Microplastic Contamination in Honey: A One Health-Oriented Systematic Review and Risk Assessment. *Kafkas Univ Vet Fak Derg*, 32 (2): 189-206, 2026
DOI: 10.9775/kvfd.2026.36351

Article ID: KVFD-2026-36351
Received: 05.02.2026
Accepted: 10.04.2026
Published Online: 14.04.2026

Abstract

Microplastics have become pervasive environmental contaminants with the capacity to move across ecological and biological systems. Honey represents a unique food matrix in this context because it is produced through intensive interactions between honeybees and their surrounding environment and is consumed directly by humans with minimal processing. This review synthesizes current evidence on microplastic contamination in honey, evaluates reported concentration ranges, particle characteristics, and polymer profiles, and situates these findings within a One Health framework linking environmental pollution, bee health, and human exposure. Microplastics have been reported in honey samples from multiple geographic regions worldwide, although reported concentrations vary considerably among studies. Notably, only a limited number of investigations have translated contamination data into consumption-based exposure estimates, underscoring a significant gap in quantitative risk assessment. Experimental and field studies further indicate that microplastics can affect honeybee physiology, immunity, behavior, and colony dynamics, and that contaminated bees can transfer particles to hive products, including honey. Collectively, these findings support the use of honey as a sentinel matrix for tracing environmental microplastic pollution through biological pathways to the human diet. Addressing existing knowledge gaps through standardized methodologies and integrated exposure assessments is essential for advancing risk evaluation within a One Health perspective.

Keywords: *Apis mellifera*, Microplastic contamination, Food safety, Bee health, Human-animal-environment Nexus

Introduction

Plastics are widely used in modern society due to their durability and broad range of applications [1]. As a result of their persistence, plastics are recognized as long-lasting environmental contaminants that have been detected across diverse ecosystems [2]. Under environmental weathering, plastics undergo solar UV-induced photo-oxidation, oxidative chain scission, and surface microcracking, which embrittle the polymer matrix and make it susceptible to subsequent mechanical fragmentation, ultimately generating secondary microplastics (<5 mm) [3]. Recent studies have reported the presence that microplastics are pervasive environmental pollutants distributed across a wide range of ecosystems, including soil, glaciers, deserts, oceans, rivers, and the atmosphere, and are increasingly detected in drinking water, air, and diverse food matrices, highlighting their widespread presence in both environmental and biological compartments [4-12]. The detection of microplastics in multiple environmental components indicates that human exposure may occur via inhalation, dermal contact, and particularly through dietary intake. In this context, microplastic contamination is increasingly discussed within the context of environmental health and exposure assessment research [13].

From a human health perspective, the importance of microplastics is being increasingly debated. Evidence from human studies suggests that microplastics can be retained in the gastrointestinal tract, respiratory tract, and circulation, with their distribution likely influenced by particle size, shape, chemical composition, and surface properties [14,15]. In addition, additives used in plastic production and compounds released during polymer degradation may pose toxicological risks [16-18].

In recent years, studies have been published suggesting that microplastics may be associated with inflammation, immune system modulation, oxidative stress, endocrine effects, and cellular-level damage [19-24]. Therefore, the occurrence of microplastics in foods, their transfer through the food chain, and the resulting potential for human exposure have become major topics of scientific investigation.

Honey is consumed in many regions globally [25]. Honey is a natural product characterized by a rich biochemical composition, including simple carbohydrates, amino acids, proteins, organic acids, and a variety of phenolic and flavonoid compounds, many of which contribute to its antioxidant, antimicrobial, and anti-inflammatory properties [26,27]. Owing to this diverse composition, honey has long been associated with beneficial effects on human health and is frequently described in the literature as a functional food with preventive and supportive roles in the context of various health conditions [28,29]. Honey is a minimally processed natural product obtained directly from the environment, with its production process shaped almost entirely by the interactions between honeybees and their surrounding ecosystem [30]. This characteristic makes honey both a direct reflector of environmental contaminants and a realistic indicator of human exposure through consumption. At the same time, honey, honeybees, and the hive ecosystem have been proposed as useful bioindicators for monitoring the presence of microplastics in the environment. Indeed, a growing body of recent research has confirmed the presence of microplastics in both honey and honeybees [31-34].

The One Health perspective constitutes the theoretical foundation of this study. The One Health approach emphasizes that human, animal, and environmental health are inseparable from one another [35]. Microplastic contamination in honey represents a point of convergence among environmental exposure, animal health, and human dietary intake. Honeybees act as biological representatives of environmental exposure, honey serves as a food source for humans, and environmental conditions determine both the materials collected by bees and the level of contaminant exposure in honey. For this reason, evaluating the presence of microplastics in honey is important for understanding human health, honeybee health, and the integrated structure of ecosystems.

This study aims to systematically evaluate the levels of microplastics reported in honey and to examine variations across countries in terms of polymer types and particle characteristics. Potential human exposure through honey consumption is then assessed using the available data. In addition, the findings are integrated within a One Health framework to jointly consider environmental, animal, and human exposure dynamics. Through this approach, the study seeks to support a more comprehensive understanding of microplastic-related risks linked to honey from both scientific and public health perspectives.

Material and Methods

Methodology

A systematic literature search was conducted in the Web of Science, Scopus, and PubMed databases. No starting year restriction was applied, as research has predominantly emerge in recent years. The search included studies published up to 31 December 2025. A preliminary literature review was conducted to determine the keywords used during the database search. The final search strings combined microplastic- and polymer-related terms with product descriptors using Boolean operators. The keyword combinations were structured as follows: “microplastic AND (honey OR bee product)”, “micro-plastic AND (honey OR bee product)”, “microplastic contamination AND (honey OR bee producs)”, “microplastic morphology AND (honey OR bee product)”, “microplastic identification AND (honey OR bee product)”, “polymer AND (honey OR bee product)”, “polymer type AND (honey OR bee product)”, “polymer identification AND (honey OR bee product)”, “polymer composition AND (honey OR bee product)”, and “polymer profiling AND (honey OR bee product)”. The search strategy was designed to identify studies investigating microplastic contamination specifically in honey while excluding research focused solely on bees or hive materials. Duplicate records were removed prior to screening. These terms ensured the inclusion of all studies that investigated microplastic or nanoplastic contamination in honey while also filtering out unrelated research on bees or hive materials.

Only studies that examined the detection, quantification, or characterization of microplastics directly in honey samples were considered eligible. Studies investigating other bee-related products (e.g., pollen, propolis, beeswax, royal jelly, and bee bread) were excluded. Research focusing on bees, hive materials, foraging behavior, or environmental sampling around apiaries was excluded, as these did not align with the objective of assessing microplastic contamination in honey. The screening process was performed independently by two researchers to prevent possible errors. Review articles, conference proceedings, books, book chapters, and non-English publications were excluded. The researchers first assessed the titles and abstracts. Afterwards, they performed a full-text evaluation of potentially eligible studies. Following the selection process, a total of 13 studies were included in the systematic review. The study selection procedure is presented in detail in the PRISMA flow diagram *(Fig. 1)*.

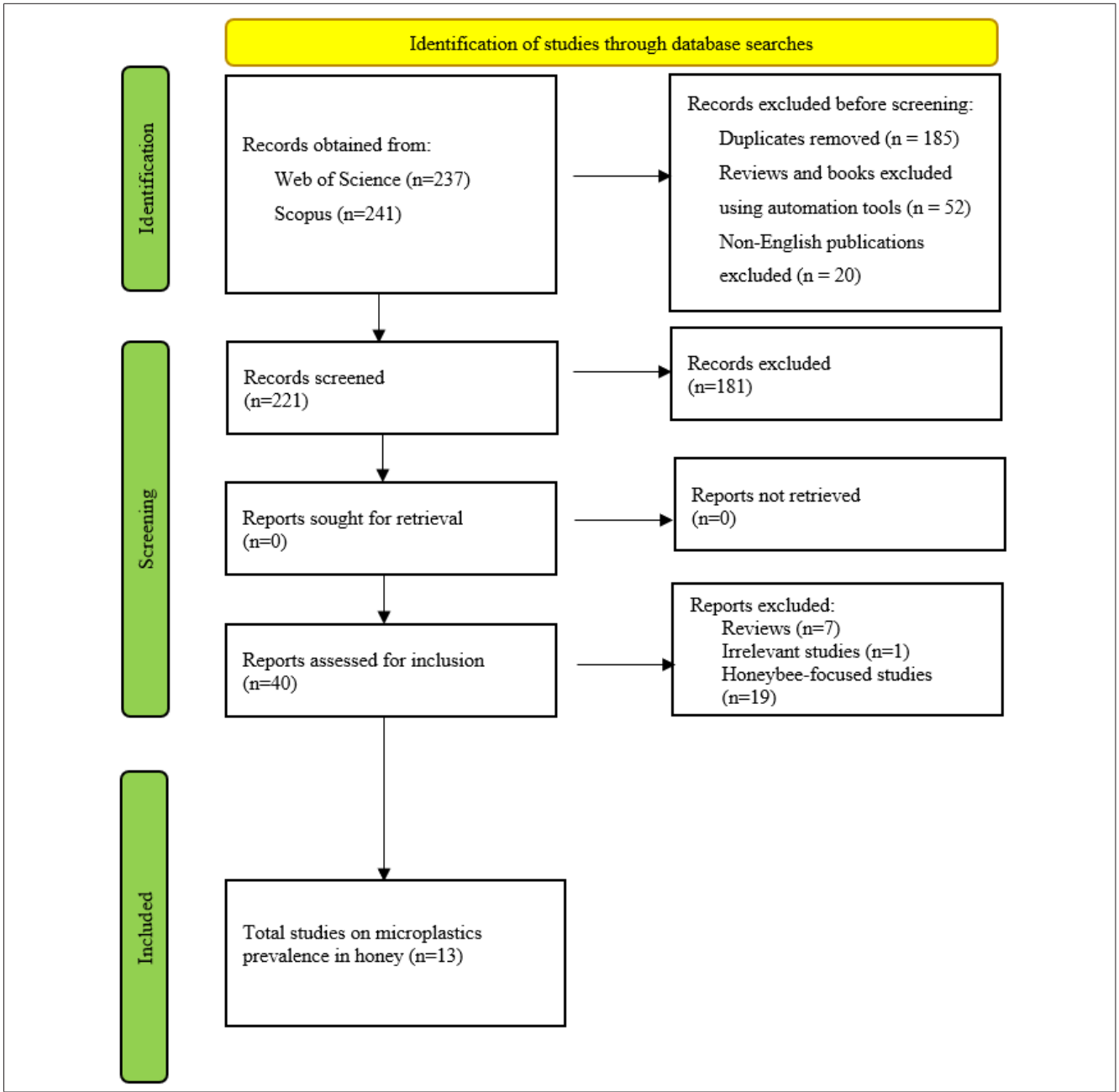

Fig 1. PRISMA flow diagram illustrating the study selection process

Results

Global Overview of Microplastic Contamination in Honey

Table 1 presents the findings of 13 studies and provides a comparative assessment of the particle levels, physical and chemical properties of microplastics detected in honey samples.

Sources and Pathways of Microplastics in Honey

Based on the findings of the systematic literature review, the reported sources of microplastic contamination in honey can be classified into several main categories. These include particles transported from the surrounding environment into the hive, beekeeping practices and in-hive materials, contamination arising during harvesting and processing stages, migration from packaging materials, and secondary contamination that may originate from analytical procedures *(Fig. 2)*.

Biological and Behavioral Effects of Microplastic Exposure in Honeybees

Experimental studies indicate that microplastic exposure represents an emerging ecotoxicological concern for honeybee health. Reported effects include alterations in physiology, immune function, gut microbiota composition,

Table 1. *Reported microplastic concentrations, size distributions, and polymer composition in honey*

Location	Samples of Number	Detection	Mean (Min.-Max.)	Physical			Chemical	Reference
				Shape	Size (µm)	Color	Polymer	
Kosovo	28	Microscopy, FT-IR	124 (20-360) MPs/kg	Fragment, fiber (dominant)	20-541 <100: 67% >100: 33%	Black (dominant), blue, transparent, green, red, brown and purple	EVA (dominant) PE, PP, PA, PET	Özçifçi et al.[30]
Türkiye	32	Microscopy, FT-IR	314 (0-1280) MPs/kg	Fiber, fragment (dominant)	133-19,950 <500: 61% 500-1000: 22% >1000: 17%	Brown (dominant), black, green, red, yellow, transparent	PE (dominant), EVA, PP, PA	Basaran et al.[32]
Ecuador	14	Microscopy, FT-IR	Craft honey: 67 (36-114) MPs/kg Industrial honey: 54 (22-76) MPs/kg	Fiber, fragment (dominant)	Fiber: 85-5174 Fragment: 5-226 Fiber: 67-3303 Fragment: 6-183	Not defined	PE (dominant), PP, PA	Diaz-Basantes et al.[36]
Malaysia	12	Microscopy, FT-IR	68.5 MPs/kg	Fragment, fiber	1000-5000	Transparent, black, red, blue, purple, brown and yellow	PE, PET	Azmi et al.[37]
Italy	10	Microscopy, FT-IR	10.4 MPs/kg	Fiber (dominant), fragment	Fiber: 190-3525 Fragment: 68-779	Transparent (dominant), black, blue, brown, gray, red	PET (dominant), PE, EVA, PA, ABS, PTFE, PCL, PVS	Schiano et al.[38]
Italy	29	Microscopy, FT-IR	62 (29-129) MPs/kg	Fragment, fiber (dominant)	Not defined	Not defined	PA, PE	Inaudi et al.[39]
Germany, France, Italy, Spain, and Mexico	19	Microscopy	Fibers: 166 (40-660) MPs/kg Fragments: 9 (0-38) MPs/kg	Fiber (dominant), fragment	10-9000	Transparent (dominant), blue	Synthetic particles	Liebezeit and Liebezeit [40]
Switzerland, Bulgaria, Italy, Spain, Latin America, Germany, and France	47	Microscopy	Fibers: 10-336 MPs/kg Fragments: 2-82 MPs/kg	Fiber (dominant), fragment	Not defined	Not defined	Synthetic particles	Liebezeit and Liebezeit [41]
Republic of Korea	6	Microscopy, FT-IR	180 (10-1020) MPs/kg	Not defined	<300	Not defined	PP (dominant), PE, PET, PS	Pham et al.[42]
Saudi Arabia	5	Microscopy, FT-IR	198 (22-660) MPs/kg	Fragment (dominant), fiber, line, sphere	1–>1000	Not defined	PE, PP, PET, PVC, PC	Ahmad et al.[43]
Brazil	8	Microscopy, FT-IR	1450 (100-2600) MPs/kg	Fiber (dominant), fragment, film	Fiber: 50-≥1000 Fragment: 50-699 Film: 50–299	Transparent (dominant), black, brown, green, red, yellow, blue	PP (dominant), PE, PET, PS	Rani-Borges et al.[44]
Switzerland	5	Microscopy, µ–Raman	Fibers: 32-728 MPs/kg Fragment: 8-8680 MPs/kg	Fiber, fragment (dominant)	Not defined	Black (dominant), white, transparent, red, blue, brown, yellow	PET, synthetic particles	Mühlschlegel et al.[45]
Colombia	24	Microscopy	Not defined	Fragment, fiber (dominant)	Not defined	Yellow, blue (dominant), white, black, purple, red, transparent, green	Not defined	Gómez-Méndez et al.[46]

Polyamide (PA), Polyethylene terephthalate (PET), Polyvinyl chloride (PVC), Polyethylene (PE), Polycarbonate (PC), Ethylene-vinyl acetate (EVA), Polystyrene (PS), Polypropylene (PP), Acrylonitrile butadiene styrene (ABS), Polytetrafluoroethylene (PTFE), Polycaprolactone (PCL), Polyvinyl siloxane (PVS), Fourier-transform infrared spectroscopy (FT-IR)

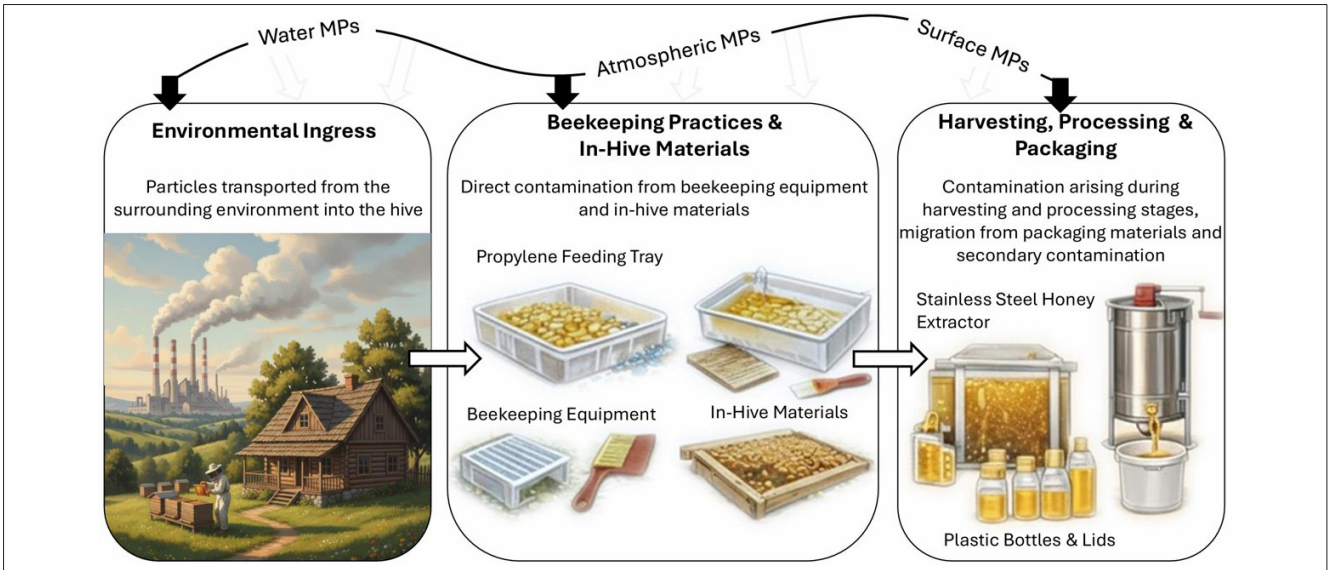

Fig 2. Sources and pathways of microplastics in honey

behavior, and neurobiology, with impacts influenced by particle type, shape, polymer composition, and dose *(Fig. 3)*.

One Health Perspective

Microplastics in honey reflect their transfer across ecosystems via bee activity, creating a pathway for human exposure; thus, their assessment should be considered within a One Health perspective linking environmental, animal, and human health *(Fig. 4)*.

Discussion

Studies reporting microplastic levels in honey can be descriptively grouped into three categories: low, moderate, and high contamination. These categories do not represent standardized thresholds, but were used only as a narrative aid in summarising the distribution of reported values.

In studies reporting low levels of contamination, mean microplastic concentrations were reported in the range of 10-70 MPs/kg [36-39]. In this group, minimum and maximum values remained within relatively narrow ranges. Although mean microplastic concentrations were not explicitly reported, the studies by Liebezeit and Liebezeit [40,41] can also be considered to reflect low-level contamination when minimum and maximum values are taken into account *(Table 1)*.

In studies reporting moderate microplastic intensities, mean concentrations generally fall within the range of 100-200 MPs/kg. In these datasets, minimum values were again reported at low levels, whereas maximum values reached the range of 500-1000 MPs/kg [30,42,43] *(Table 1)*. This pattern suggests that contamination in this group is not evenly distributed across samples. Rather, moderate mean values appear alongside a wider internal

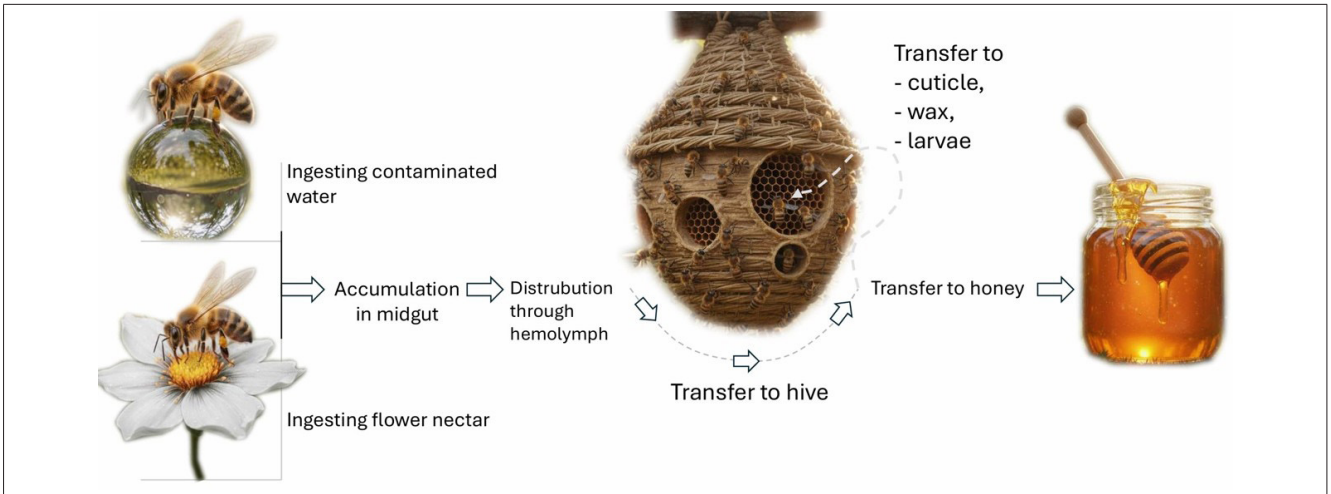

Fig 3. Microplastics pahtways in honeybees

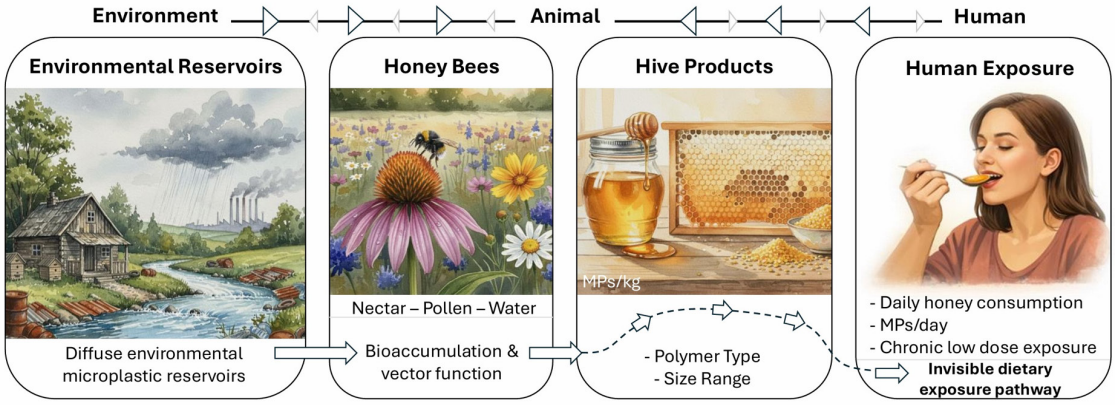

Fig 4. From environment to table: A One Health perspective on microplastic transfer via honey bees

spread, indicating greater variability than in the low-contamination group.

The third group includes studies reporting the highest mean microplastic concentrations. For example, Basaran et al.[32] reported a mean concentration of 314 MPs/kg. Within this study, minimum values decreased to 0 MPs/kg, while maximum values reached 1280 MPs/kg, indicating a wide concentration range. Another study in this group is the dataset reported by Rani-Borges et al.[44], which documented a mean concentration of 1450 MPs/kg. This value represents the highest mean concentration among all studies included in the table. The corresponding maximum values, reaching up to 2600 MPs/kg, further characterize this dataset as representing a high level of contamination *(Table 1)*.

When studies reporting wide maximum ranges are examined in more detail, the dataset reported by Mühlschlegel et al.[45] shows the widest reported range. This study reported fragment-shaped microplastics in the range of 8-8680 MPs/kg, representing the widest maximum range across all datasets and demonstrating that very high particle loads can occur in individual samples. In contrast, for fiber-shaped microplastics, the same study reported a narrower range of 32-728 MPs/kg, indicating that morphology-dependent differences can be observed even within a single dataset. Gómez-Méndez et al.[46], on the other hand, did not report quantitative information on microplastic abundance in their study *(Table 1)*.

Overall, comparative evaluation shows that even in studies reporting low mean concentrations, maximum values may extend over broad ranges; studies with moderate mean concentrations are associated with higher upper limits; and datasets reporting high mean concentrations are characterized by maximum particle numbers reaching the order of thousands. Overall, reported microplastic concentrations in honey show substantial variability across studies and within individual datasets. The consistent detection of microplastics were detected in all included studies, although reported concentrations varied considerably.

When the physical characteristics of microplastics detected in honey samples are examined, available data indicate that similar morphological categories have been reported across all studies. Fiber and fragment forms were reported in the majority of studies and appeared to constitute the primary structural classes of microplastics detected in honey [30,32,36-41,43-46] *(Table 1)*. This consistency indicates a high level of agreement in morphological classification despite differences in study periods, geographic regions, and analytical methodologies.

Although the dominant morphology varied among studies, fibers and fragments were the two most frequently reported forms of microplastics in honey. In some datasets, fibers were reported as the dominant morphology [38,40,44], whereas other studies reported a higher abundance of fragment-shaped microplastics [30,43]. This variation indicates that the relative distribution of particle morphologies differs across studies; however, fibers and fragments remain the two most consistently reported structural forms of microplastics in honey. Only two studies reported additional microplastic forms (line, sphere, film) beyond fibers and fragments [43,44] *(Table 1)*.

Particle size distributions varied markedly among studies. However, direct comparison remains limited because the included studies differed in their analytical conditions, including size detection ranges and particle recovery approaches. In the Kosovo study, for example, 67% of the detected microplastics were reported to be smaller than 100 µm, indicating that small-sized particles may predominate in some datasets [30]. Other studies reported size ranges extending from 1 µm to values exceeding 1000 µm, demonstrating that microplastics may occur across multiple size classes even within a single dataset [32,43]. More detailed morphometric analyses revealed fiber lengths ranging from 190 to 3525 µm and fragment sizes between 68 and 779 µm [38]. In addition, some datasets reported

particle sizes reaching up to 19.950 µm; however, because this exceeds the commonly accepted <5 mm size criterion for microplastics, such values should be interpreted with caution [32]. The fragment size ranges reported by Mühlschlegel et al.[45] exhibit the widest reported range among the included studies *(Table 1)*.

With respect to color distribution, black and transparent particles were among the most frequently reported color categories across the included studies [30,38,44,45]. In addition, blue, red, green, yellow, and brown particles were reported in different studies [34,46] *(Table 1)*. The diversity observed in color distribution is consistent with the overall morphological heterogeneity of microplastics detected in honey.

Taken together, these findings indicate that fiber and fragment morphologies represent the most consistently reported forms across the included studies, while particle size ranges span a broad spectrum and color categories exhibit considerable diversity. From a physical perspective, microplastics detected in honey therefore display both shared structural features and a high degree of heterogeneity.

Polymer composition is one of the parameters showing the appears to vary considerably among studies. In particular, polyethylene (PE), polypropylene (PP), and polyethylene terephthalate (PET) are the principal polymers reported in the majority of studies [30,32,36-39,43,44]. These three polymers constitute a recurring compositional pattern in honey samples, although their reported abundances may vary depending on the analytical methods used. However, some studies have reported a broader range of polymers beyond these core types. Ethylene–vinyl acetate (EVA) was reported as the predominant polymer in specific studies [30,32]. Other polymers (polyamide (PA), polystyrene (PS), polyvinyl chloride (PVC), polycarbonate (PC), acrylonitrile butadiene styrene (ABS), polytetrafluoroethylene (PTFE), polycaprolactone (PCL), and polyvinyl siloxane (PVS)) were observed in isolated datasets, indicating variability in polymer composition across studies [38,43,44]. The fact that these polymers do not recur in every dataset indicates that the composition of analyzed samples may vary substantially between studies. In earlier investigations, polymer identification was more limited. Mühlschlegel et al.[45] reported PET and other synthetic particles, whereas Liebezeit and Liebezeit [40,41] employed the broader term "synthetic particles" without detailed classification. This reflects the progression from visual inspection toward advanced techniques, such as FT-IR and Raman spectroscopy, which allow more precise polymer identification *(Table 1)*.

Overall, the distribution of polymers detected in honey exhibits a two-layered structure. The first layer comprises PE, PP, and PET, which recur across all studies and constitute the core polymer composition of honey samples. The second layer consists of polymers such as EVA, PA, and other polymer classes that appear in specific studies and contribute greater compositional diversity. The coexistence of these two layers demonstrates that polymer composition in honey includes both common and variable components.

As shown in *Table 1*, microplastics have been reported in honey samples from multiple countries, indicating that this is not a location-specific finding. However, microplastic concentrations, physical characteristics, and polymer compositions show pronounced variability between countries. These differences should not be attributed solely to environmental conditions but should also be considered in relation to analytical methods, sampling strategies, beekeeping practices, and local socio-economic contexts.

In Europe, mean microplastic concentrations reported from Italy ranged between 10 and 62 MPs/kg [38,39]. These results indicate that even in countries with advanced environmental management systems and strong regulatory frameworks, microplastics are not entirely absent. By contrast, an average concentration of 180 MPs/kg reported in South Korea [42], a country with similarly high environmental governance capacity, suggests that high population density, intensive industrial activity, and the spatial overlap between urban expansion and beekeeping areas may contribute to elevated levels. The mean concentration reported from Türkiye (314 MPs/kg) [32] is notably higher than the low values observed in European examples. In Türkiye, the widespread practice of beekeeping across both rural and peri-urban settings, together with its broad ecological diversity and rich floral resources, may increase the extent of environmental contact, providing a contextual background for this variability. In Saudi Arabia, the reported mean concentration of 198 MPs/kg [43] does not fully align with the common assumption that arid climates and sparse vegetation would limit environmental exposure. This finding suggests that materials used along the production chain may also influence microplastic levels. Data from developing countries such as Colombia and Malaysia [37,46] fall within low to intermediate ranges, supporting the view that microplastic levels are not directly correlated with national development status. In contrast, the mean value of 1450 MPs/kg reported from Brazil [44] represents one of the most distinctive results in the dataset. This exceptionally high value evokes a complex environmental context shaped by intensive agricultural activity, extensive tropical biomes, and diverse production conditions. Its magnitude suggests that country-specific sampling locations, beekeeping practices, or methodological factors may also play a decisive role.

The most extreme value is the maximum concentration of 8680 MPs/kg reported in Switzerland [45]. Observing such a high maximum value in a country characterized by strong environmental indicators and strict regulations underscores the high spatial variability of microplastic occurrence under local environmental conditions. This finding represents an exceptional case, illustrating that national-level environmental quality alone is insufficient to explain maximum microplastic values in honey and that local sampling contexts are critical determinants.

The evaluation of inter-country differences represents a central scientific rationale of this study. Microplastic contamination does not occur uniformly across regions. Factors such as population density, industrial production, agricultural practices, waste management capacity, climatic conditions, and beekeeping traditions vary substantially between countries, and these differences are directly reflected in honey samples. Accordingly, comparing microplastic levels in honey across countries provides valuable insight into both the spatial distribution of environmental contamination and potential human exposure. Moreover, variations in honey production chains, including equipment use, packaging practices, and storage conditions, may further influence microplastic diversity. Systematic integration of these environmental and methodological determinants is essential for developing a standardized and globally comparable assessment framework.

The studies summarised in *Table 1* employed different analytical approaches for the detection and characterisation of microplastics in honey, and these methodological differences should be taken into account when interpreting the reported findings. Most studies used microscopy combined with FT-IR (Kosovo, Türkiye, Ecuador, Malaysia, two studies from Italy, Republic of Korea, Saudi Arabia, and Brazil), whereas three studies relied on microscopy alone (Germany/France/Italy/Spain/Mexico; Switzerland/Bulgaria/Italy/Spain/Latin America/Germany/France; and Colombia), and one Swiss study used microscopy together with μ-Raman. This distribution shows that the current evidence base is dominated by microscopy-supported spectroscopic confirmation rather than by visual identification alone.

These differences are important because the analytical technique directly influences the level of particle characterisation that can be achieved. Studies using microscopy alone generally provided limited chemical detail, often reporting particles broadly as "synthetic particles" or leaving polymer identity undefined. By contrast, studies combining microscopy with FT-IR or μ-Raman were able to identify specific polymers such as PE, PP, PET, PA, EVA, PS, PVC, and PC, thereby offering a more detailed chemical profile of contamination. A similar pattern is also visible in the reporting of particle properties: spectroscopy-supported studies tended to provide more specific information on polymer composition, while microscopy-only studies were more restricted to visual categories such as shape, colour, and approximate size.

From an interpretive standpoint, this methodological heterogeneity limits strict cross-study comparability. Reported differences in microplastic occurrence may reflect not only geographical or environmental variation, but also differences in analytical sensitivity, particle confirmation, and reporting detail. For this reason, the findings in *Table 1* should be read comparatively but cautiously. At the same time, the fact that microplastics were detected across studies using different analytical approaches strengthens the broader conclusion that honey is a relevant matrix for investigating environmental microplastic contamination and potential exposure pathways.

Literature findings indicate that microplastics in honey originate mainly from environmental exposure, beekeeping materials, processing stages, packaging, and potential analytical contamination *(Fig. 2)*.

From an environmental perspective, honeybees represent the initial biological interface in the transfer of microplastics into honey [47]. Microplastics that are widely documented in air, water, and soil can enter the matrices encountered by bees through plant surfaces, nectar, pollen, and water sources [40,41,48,49]. Through the ingestion of contaminated nectar and water, or the inadvertent collection of particles resembling pollen in size and morphology, microplastics may adhere to the bee cuticle or enter the digestive tract and subsequently be introduced into hive products [50]. In a field study conducted by Alma et al.[51], colonies fed with a sucrose solution containing polyester microfibers showed the presence of these fibers on the cuticle and within the digestive tract of adult worker bees, as well as in larvae, wax, and honey samples, experimentally demonstrating that environmentally derived or feed-associated particles can be directly transferred into the honey matrix. Similarly, recent studies emphasize that a substantial proportion of microplastics reported in honey and other bee products may be linked to an indirect exposure chain originating from environmental particles accumulated in soil, water, and plant tissues [34,47,52]. The geographic distribution of environmental load is also relevant: Diaz-Basantes et al.[36] reported higher microplastic counts in honey samples collected from urban and industrial areas compared with rural regions, suggesting that the observed contamination was primarily environmentally driven.

Beekeeping practices and in-hive materials constitute a second major source of microplastic contamination in honey. Artificial feeding, synthetic textile fibers from

protective clothing, and plastic hive components -including frames and feeders- may introduce microplastics through mechanical degradation or fiber shedding [32,51,53,54]. Mühlschlegel et al.[45] attributed the low-level microplastic contamination detected in commercial honey samples particularly to synthetic textile-derived fibers associated with beekeepers' clothing, interpreting this pathway as one of the main potential sources. A striking example in this context is the use of microfiber sheets applied to control the small hive beetle *(Aethina tumida)*. Buteler et al.[55] demonstrated that non-woven microfiber covers placed inside hives were chewed by bees, leading to fiber fragmentation, and that after three months of application, the abundance of blue microfibers on the cuticle and within the digestive tract of bees, as well as in honey samples, increased significantly compared with control hives. This finding indicates that such widely used pest management practices can become a direct source of microplastic contamination in honey.

Harvesting and processing stages also represent potential points of contamination. Inappropriate plastic containers, buckets, filters, uncapping tools, and centrifuges used during honey extraction, transport, and storage may release microplastic particles under surface abrasion and mechanical stress, allowing direct contact with honey [30,34,36]. Fuente-Ballesteros et al.[47] noted that direct contact with "inappropriate plastic cups, containers, honey extraction machines, and uncapping devices" represents an additional contamination pathway for hive products, including honey. This observation indicates that, beyond environmental exposure, human-controlled stages of the production chain also play a role in shaping the microplastic load of honey.

Packaging materials and storage conditions represent another major source of microplastic contamination in honey, particularly when considering the final product reaching consumers. Indeed, many researchers have emphasized that packaging materials may act as a secondary source of microplastic contamination for foods, including honey, and have highlighted the need for further studies specifically addressing migration processes under realistic storage conditions [42,56-58]. Katsara et al.[59] further stressed that plastic packaging used for honey and other foods can undergo abrasion under environmental conditions, transferring microplastics and associated chemical additives into food, and therefore should be considered an independent contamination source for honey. The absence of such migration in studies using glass packaging supports the notion that packaging-related contributions are primarily associated with plastic-based systems.

Finally, contamination arising from analytical procedures represents a critical methodological limitation that must be carefully considered when interpreting findings on microplastic detection in honey. Numerous studies have emphasized that microplastic quantification in food matrices is highly susceptible to laboratory-derived contamination due to the widespread use of plastic consumables, synthetic filter materials, textile fibers from laboratory clothing, and background airborne particles [60-62]. This concern is further reinforced by the fact that recovery rates have not been reported in a substantial proportion of existing studies. The lack of recovery calculations creates a critical gap in assessing laboratory-derived contamination as well as the sensitivity, accuracy, and validity of analytical methods. Consequently, particularly for studies reporting low microplastic levels, uncertainty regarding whether the observed load originates from the actual matrix or from analytical processes becomes increasingly important.

Overall, microplastic contamination in honey appears to arise from a multilayered network of sources, including particles transported into hives through environmental exposure of bees, plastic- and textile-based materials used in apicultural practices, plastic equipment employed during harvesting and processing stages, plastic packaging systems utilized at the consumer level, and background contamination introduced during analytical procedures. The existing literature demonstrates that each of these sources can independently contribute to increasing the microplastic burden of honey, indicating that contamination represents a complex process that cannot be explained by a single factor.

When evaluating the existing literature on the presence of microplastics in honey, it is observed that the vast majority of primary studies report their findings in terms of concentrations measured in the honey matrix, whereas studies that quantitatively calculate the daily microplastic intake attributable to honey consumption remain limited. Of the 13 primary studies reviewed, only four numerically reported human exposure based on honey consumption [30,32,42,43]. This indicates that, in most studies, microplastic exposure specific to honey has been confined solely to contamination levels, while consumption-based human exposure has not yet been addressed systematically in the literature, revealing a clear methodological gap in this area.

A comparative evaluation of studies that report daily intake values demonstrates considerable variability across countries. The value of 2.5×10^{-3} MPs/day calculated by Ahmad et al.[43] (Saudi Arabia) reflects an approach in which microplastic intake from honey consumption is reported at very low levels, whereas the 9.0×10^{-2} and 3.7×10^{-1} MPs/day values reported by Pham et al.[42] and Özçifçi et al.[30] (Republic of Korea and Kosovo, respectively) correspond to studies in which exposure is considered measurable but relatively limited. In contrast,

the 1.05 MPs/day reported by Başaran et al.[32] (Türkiye) provides an example in which the daily intake calculated from honey consumption is evaluated at a higher level. In particular, the fact that the microplastic levels reported in honey vary markedly across countries suggests that this difference is closely related to environmental conditions, production and processing practices, as well as variations in honey consumption amounts across societies. This contextual diversity causes honey consumption–based microplastic exposure calculations to yield different results from study to study and makes it difficult to consolidate the reported daily intake values under a single representative level. Although direct evidence showing that honey-derived microplastic exposure alone is sufficient to produce these effects remains limited, the documented presence of microplastics in human biological samples and tissues suggests that dietary intake may contribute to the overall body burden of microplastics. In this context, honey consumption can reasonably be considered one potential component of cumulative dietary exposure, even if a direct causal link has not yet been established.

Interpreting calculated daily microplastic intake levels in terms of potential human health implications requires a multidimensional framework that extends beyond particle number alone. In addition to particle number, the size, shape, polymer type, and the additives or environmental contaminants carried by microplastics stand out as key factors determining the direction of interactions with biological systems and the nature of potential effects. In this context, an increasing number of studies in recent years have demonstrated that microplastics can access biological environments in the human body, and the reporting of microplastics in human blood, urine, and feces [63-65], as well as in certain tissue samples [66], has brought the possibility of systemic uptake via multiple exposure routes, including diet, to the forefront.

Reports documenting microplastics in the skin, lungs, liver, spleen, kidneys, colon, blood, saliva, placenta, and breast milk suggest that these particles may enter systemic circulation following different exposure pathways and potentially distribute to various tissues [67-69]. In this regard, understanding the absorption, distribution, metabolism, and excretion (ADME) characteristics of microplastics is considered a fundamental requirement for interpreting possible toxicological outcomes [20]. Data from different populations show that the presence of microplastics has been reported in feces, colon, lungs, bronchoalveolar lavage fluid, sputum, blood, placenta, and breast milk together with polymer types and size ranges; in particular, it is emphasized that fractions below 10 μm can interact more easily with cell membranes and have the potential to be transported to different tissues via circulation [70-74]. One of the notable findings for human health is that microplastics have also been detected in biological structures associated with the cardiovascular system [75]. Human studies demonstrating the presence of microplastics and nanoplastics in atheroma plaques have strengthened debates suggesting that these particles may not only be indicators of environmental exposure but also potentially represent a biological burden that can be linked to clinical outcomes [76,77].

The most frequently reported mechanistic framework associated with microplastic exposure is the triggering of oxidative stress and inflammatory responses and linking this to cellular damage processes. Experimental studies suggest that exposure to microplastics can activate pathways such as Toll-like receptors, NF-κB signaling, and the NLRP3 inflammasome, leading to increased production of reactive oxygen species and progression of inflammatory cascades [78-83]. In parallel, it has been reported that different PS micro- and nanoparticles can increase the production of reactive oxygen species, trigger endoplasmic reticulum stress, and are associated with apoptosis and autophagic cell death in many cell types, including human lung and intestinal cell models [84-86]. It also indicates that microplastic exposure can lead to impairment of intestinal barrier integrity, microbiota dysbiosis, and changes in bile acid and amino acid metabolism [87-90].

In the context of dietary exposure, the digestive system represents the primary site where microplastics first interact with the human body. Available data show that microplastics can accumulate in the intestine and that this accumulation is associated with intestinal barrier dysfunction, changes in microbiota composition, and deviations in bile acid metabolism [83,91,92]. From a systemic perspective, microplastic exposure has been linked to gastrointestinal inflammation, endocrine disruption, dysregulation of lipid and energy metabolism, as well as non-alcoholic fatty liver disease and hepatocarcinogenesis. It is stated that most of these effects develop through multiple mechanisms such as oxidative stress, chronic inflammation, immunosuppression, and disruption of hormonal regulation [93-95]. In addition, it is emphasized that toxicity is sensitive to particle size and that mixture exposures can further amplify biological effects [75]. Effects of microplastic exposure via the respiratory route have also been reported to extend beyond local tissues, potentially impacting inter-system interaction [77,96]. From the perspective of reproductive and developmental health, the reporting of microplastics in the placenta and breast milk provides important evidence strengthening the possibility of exposure in early life periods [67,97,98].

Overall, while the current literature accepts that the presence of microplastics in human biological systems has been clearly demonstrated, it also shows that there

remains a significant gap between evidence of "presence" and clinical-level "causality" in interpreting health effects. Although detection of microplastics in various tissues suggests that systemic access is possible, reaching definitive health outcomes requires the generation of multilayered evidence that jointly considers exposure level, particle characteristics, and mixture effects. Accordingly, mechanistic toxicology data should be interpreted in conjunction with human biomonitoring findings within a cautious, holistic framework.

Experimental data suggest that microplastics pose a growing ecotoxicological risk to honeybees, affecting physiology, immunity, gut microbiota, behavior, and neurobiology depending on particle characteristics and döşe *(Fig. 3)*. Several laboratory studies indicate that PS and PE microplastics affect honeybee physiology. In a 14-day laboratory exposure study, Wang et al.[99] used 50 mg/L of PS microplastics, but it was not stated whether this corresponded to an environmentally realistic level. Environmental reference is needed for ecosystem risk assessment. However, despite the absence of marked survival effects, PS microplastics exposure led to a reduction in gut bacterial diversity and induced pronounced alterations in the bee gut microbiome, accompanied by changes in the expression of genes associated with oxidative stress, detoxification pathways, and immune responses. In contrast, Balzani et al.[50] observed that oral exposure to PE microplastics at 50 mg/L increased honeybee mortality, whereas lower doses had no significant effects. The results indicated that exposure to PE at 50 mg/L resulted in a significant increase in mortality, whereas no significant effects on survival were observed at the lower concentrations. Deng et al.[100] exposed honeybees to spherical PS microplastics under two complementary designs. First, mixed-size PS (0.5:5:50 µm = 1:1:1) was tested at 0.1, 1, 10, and 100 mg/L for 14 days. In this concentration-response experiment, survival was significantly reduced in *Apis mellifera* at 1 mg/L ($P<0.05$), 10 mg/L ($P<0.01$), and 100 mg/L ($P<0.01$), and in *Apis cerana* at 10 and 100 mg/L ($P<0.05$). Based on the survival curves, the final survival proportions at day 14 were approximately 62% in controls, 50% at 0.1 mg/L, 48% at 1 mg/L, 45% at 10 mg/L, and 38% at 100 mg/L for *Apis mellifera*, and approximately 62% in controls, 50% at 0.1 mg/L, 55% at 1 mg/L, 45% at 10 mg/L, and 42% at 100 mg/L for *Apis cerana*. Second, a size-response experiment was performed in *Apis mellifera* using 0.5, 5, and 50 µm PS at 10 and 100 mg/L for 21 days. In this experiment, cumulative mortality was significantly higher particularly in the 0.5 µm PS group at 100 mg/L compared with the control ($P<0.05$); visually, survival at the end of the experiment was approximately 5% in the 0.5 µm/100 mg/L group versus about 28% in the control group. The study further showed that 0.5 µm PS caused more pronounced midgut damage and stronger tissue translocation than larger particles. In addition, combined exposure to 5 µm PS (10 mg/L) and Israeli acute paralysis virus (IAPV) reduced survival to approximately 20% in *Apis mellifera* and 27% in *Apis cerana* by day 7, compared with roughly 33% and 38%, respectively, in the virus-only groups, while viral titers increased by more than fourfold on days 6 and 7 in *Apis mellifera* and by more than fourfold, twofold, and sixfold on days 5, 6, and 7 in *Apis cerana*. Buteler et al.[101] investigated the effects of acute exposure to polyester microplastic fibers on the foraging behaviour of *Apis mellifera carnica*. In the acute oral toxicity assay, honeybees fed with 100 mg MPs/L in 50% sucrose solution showed no increase in short-term mortality compared with the control group, with mortality remaining 0% at 24 h and 3.33% at 48 h in both groups. In the behavioural assays, control and MP-containing dishes were presented simultaneously, and bees showed no significant preference or avoidance when MPs were offered in sucrose solution or water (blue fibers: sugar solution, $t=0.7$, $P=0.49$, $n=12$; water, $t=0.21$, $P=0.83$, $n=18$; yellow fibers: sugar solution, $t=1.13$, $P=0.27$, $n=12$; water, $t=0.04$, $P=0.96$, $n=18$). Likewise, proportional consumption did not differ significantly among sucrose solutions containing 0, 10, and 100 mg MPs/L (GLMM, $\chi^2=0.54$, $df=2$, $p=0.76$, $n=180$), although MP-free solutions were consumed more rapidly ($\chi^2=8.31$, $df=2$, $p=0.01$, $n=20$). These results indicate that acute microfiber ingestion did not cause immediate mortality, but honeybees did not avoid microplastic-contaminated food or water, suggesting that repeated exposure may still contribute to longer-term risk. Wang et al.[102] investigated, under controlled laboratory conditions, the effects of PS nano- and microplastics on *Apis mellifera*, focusing on body weight, intestinal development, particle accumulation, gut microbiota, and susceptibility to bacterial infection. Using PS particles of 100 nm, 1 µm, and 10 µm, the study showed that the smallest particles, particularly 100-nm PS, caused the most pronounced adverse effects, including intestinal dysplasia, reduced body weight, accumulation in the rectum, and increased susceptibility to *Hafnia alvei*, leading to a fivefold higher mortality rate. With respect to the gut microbiota, no significant difference in alpha diversity was found in either the Chao1, Shannon, or Simpson indices ($P>0.05$). However, compositional changes were still evident: the initial relative abundance of *Lactobacillus* and *Bifidobacterium* was 72% and 12.33%, respectively, whereas in the PS-100 nm group *Lactobacillus* declined to 54.3% on day 10 and *Bifidobacterium* declined to 6.35% on day 15. These microbiota changes were accompanied by altered expression of genes related to immune regulation, detoxification, and energy metabolism. However, these findings were obtained using selected PS particles under

laboratory exposure conditions and should therefore be interpreted as evidence of potential biological effects rather than as a direct representation of the full diversity of microplastics present in natural environments. These different results demonstrate the determining effect of particle shape on toxicity and suggest that microplastics with different shapes lead to varying biological interactions.

Recent studies also demonstrate that microplastics impact honeybee cognition and behavior. Pasquini et al.[103] investigated the effects of short-term oral exposure to spherical microplastics on cognitive functions in *Apis mellifera*. Bees were exposed for 48 hours to PS, polymethyl methacrylate (PMMA), and their combination at concentrations of 0.5, 5, and 50 mg/L. Exposure to PS at 50 mg/L resulted in reduced sucrose responsiveness, indicating impaired ability to detect and respond to nectar sources. While PMMA alone did not produce significant effects, combined exposure led to pronounced reductions in sucrose responsiveness at 5 and 50 mg/L, suggesting potential synergistic interactions. Furthermore, all treatments negatively affected learning and memory, with PS inducing the most marked cognitive impairment. This is critically important in that it shows microplastics have biological accessibility in the nervous system and that behavioral impairments are neurologically based. Behavioral effects constitute some of the most critical outcomes in terms of bee ecology. Ferrante et al. [104] evaluated the effects of PS, PMMA, and their combination on the survival and immune responses of *Apis mellifera*. Bees were orally exposed to three concentrations (0.5, 5, and 50 mg/L). Exposure to both materials resulted in reduced food consumption and increased mortality at medium and high concentrations compared with controls. In addition, alterations in cuticular chemical profiles were observed, particularly for PMMA. Despite these changes, exposed workers were not discriminated against by guard bees and were allowed to re-enter the colony, suggesting that contaminated individuals may act as vectors for the spread of particulate matter within the hive. Overall, the findings indicate that microplastic exposure can impair individual health and pose potential risks to colony integrity.

The accumulation of microplastics in the bee body and their transport to the hive are noteworthy in terms of both ecology and food safety. Alma et al.[51] experimentally investigated whether honeybees ingest microplastics through feeding and how these particles are subsequently transferred to different matrices within the colony, including adult bees, larvae, honey, and beeswax. Colonies were fed a sucrose solution containing polyester microfibers at an environmentally relevant concentration (50 mg/L) based on levels reported in drinking water. After one month of exposure, microfibers were detected in the bristles and digestive tracts of adult worker bees and were shown to be redistributed to other hive components. The results demonstrated that microfibers accumulated predominantly in beeswax, whereas lower amounts were detected in honey and in the digestive systems of bees. Mitton et al.[105] examined the effects of microplastics alone and in combination with glyphosate on honeybee larvae. While exposure to MPs alone did not significantly affect larval survival or body weight, combined exposure to microplasticsand glyphosate resulted in reduced survivorship and lower larval weight. At the molecular level, the combined treatment suppressed immune-related gene expression and increased catalase activity, indicating enhanced oxidative stress. These findings suggest that microplastics may exert synergistic adverse effects on honeybee larval development when co-occurring with other environmental pollutants. Al Naggar et al.[54] state that immune weakening, behavioral impairments, nutritional inefficiency, and larval developmental disorders may weaken colony health in the long term and increase the risk of colony collapse.

These findings provide strong field-based evidence that plastic particles present in the environment can be transferred directly to hive products through honeybee behavior, confirming a structural link between bee exposure and microplastic contamination in honey. They further indicate that microplastic exposure under natural ecological conditions frequently co-occurs with other chemical and biological stressors, and that such combined exposures may amplify toxic effects. Although most available studies have been conducted at the individual level, they raise the possibility that microplastics may also affect colony-level processes; however, this remains to be confirmed by direct colony-scale evidence. This integrated assessment demonstrates that microplastics represent more than a superficial environmental contaminant for honeybees; rather, they act as a complex biological stressor capable of exerting multifaceted effects on immune function, neurophysiology, behavior, and colony organization. Their transfer into hive products, especially honey, underscores the relevance of microplastics for both ecosystem integrity and food safety research.

According to the World Health Organization (WHO) and the World Organisation for Animal Health (WOAH; formerly the World Organisation for Animal Health/ OIE), One Health is an integrated and unifying approach that recognizes the interdependence of human, animal, plant, and ecosystem health and promotes coordinated action across sectors and disciplines [106,107]. In the context of microplastics, this approach is particularly relevant for understanding the transfer of plastic particles across ecological and biological systems and their potential

impacts on health at multiple levels. Honey constitutes a food matrix in which environmental microplastics are concentrated through bee foraging activity. This provides a biologically mediated route for human exposure. Consequently, the assessment of microplastics in honey should be regarded not solely as a matter of food safety, but also as a component of a comprehensive One Health framework encompassing environmental, animal, and human health *(Fig. 4)*.

It is evident that bees interact with a variety of substances, including pollen, nectar, water, and airborne particulate matter. These substances are present in a variety of geographic areas, and it is therefore suggested that bees function as biological sentinels, reflecting environmental microplastic loads. Due to these characteristics, they function as biological receivers that passively reflect the presence of microplastics in the environment. From a One Health perspective, the environmental microplastic load is not only a source of exposure for bees but also an interface that functions in the transfer of this load into biotic systems. Bees' feeding and foraging behaviors make it possible for microplastics to be transported from natural ecosystems to biological material and ultimately into the food chain. Environmental microplastics can enter the food chain via biological vectors without direct detection [108].

Honey can be defined as the biochemical product of the interaction between bees and their environment. The physiological and behavioural changes reported in bees due to microplastic exposure are analogous to the ecosystem-level disruptions that have been observed. This finding indicates that microplastics are not merely environmental pollutants but can produce functional outcomes by interacting with biological systems. In this context, the presence of microplastics in honey reflects not merely environmental pollution itself, but the outcome of an environment–animal interaction through which bees collect and transfer microplastic particles from the surrounding environment into the hive and, ultimately, into honey [47]. This unique position of honey indicates that microplastic pollution should be monitored not only through environmental measurements but also through biological products.

Within the One Health framework, physiological and behavioural changes in animals may serve as early warning indicators of environmental disturbances that could also have indirect implications for human health [109]. Physiological and behavioral changes reported in bees due to microplastic exposure reflect the biological counterparts of ecosystem-level disruptions. This reveals that microplastics are not merely environmental pollutants but can produce functional outcomes by interacting with biological systems. The observed effects on bee health suggest the presence of a risk line that may indirectly impact human health through the consumption of bee products, such as honey.

Within the One Health framework, honey consumption represents a pathway through which environmentally derived microplastics may contribute incrementally to human exposure. Although exposure to microplastic is frequently characterised as low-level and chronic, it possesses the capacity to generate a cumulative health burden due to the uninterrupted nature of this exposure. From a One Health perspective, honey-derived microplastic exposure should be evaluated not as an isolated risk on its own but as a component of an individual's total environmental and dietary exposure. This approach demonstrates that, despite honey's status as a "natural" product, it is not entirely independent from contemporary environmental contamination. This underscores the necessity for novel assessment frameworks to be developed in order to ascertain its impact on human health.

The One Health approach provides a useful framework for interpreting microplastic pollution in honey beyond contamination measurements alone. By considering environmental microplastic load, biological effects on bee health, and human exposure through honey together, it highlights the interconnected nature of this issue across ecosystem, animal, and human health. This holistic standpoint indicates that the presence of microplastics in honey should be regarded as a matter of One Health concern, with implications for both food safety and environmental sustainability, as well as ecosystem health.

Knowledge Gaps and Future Directions

Although the number of studies addressing the presence of microplastics in honey and exposure associated with bee products is increasing, significant knowledge gaps that limit a holistic evaluation within the One Health approach continue to persist. Chief among these gaps is the fact that studies converting microplastic concentrations reported in honey into human-consumption–based exposure calculations remain quite limited. The vast majority of existing studies report microplastic contamination levels, but these data are rarely evaluated in terms of defined consumption scenarios, such as average versus high consumers, different age groups, or body weight-adjusted exposure metrics such as Estimated Daily Intake (EDI; particles/day or particles/kg bw/day). As a result, microplastic contamination data reported for honey are still rarely translated into probabilistic exposure modelling or cumulative dietary exposure assessment. At the same time, formal risk characterization remains constrained because harmonized health-based benchmark values for microplastics have not yet been established, and current

datasets are still considered insufficient for a robust risk assessment [110,111]. Another fundamental shortcoming is methodological incompatibility. Differences in sample preparation, lower size cut-offs, particle size thresholds, identification techniques, and quality control practices significantly restrict comparability across studies. In particular, the lack of harmonized size cut-offs, the limited detection of nanoplastics (<1 μm), inconsistent polymer confirmation techniques, and the absence of standardized QA/QC frameworks further increase uncertainty. The failure to report recovery rates, procedural blanks, and blank-correction practices in many studies creates additional difficulty in interpreting results, especially those reporting low-level contamination [10,112,113].

From a biological standpoint, causal links between environmental microplastic load, effects on bee health, and human exposure through honey consumption have not yet been sufficiently elucidated. Although the potential of bees as bioindicators of environmental pollution is increasingly recognized, long-term and multi-center studies that address environmental measurements, biological effects, and dietary exposure within the same framework are still limited. Future research should focus on harmonizing analytical methods, establishing standard exposure metrics, and developing consumption-based exposure models that account for age group, body weight, and consumption scenario. It should also promote interdisciplinary study designs integrating analytical chemistry, ecotoxicology, food safety, exposure science, and epidemiology in order to assess the environment-bee-honey-human pathway more comprehensively. Such efforts would support a more robust evaluation of microplastic pollution in honey within a One Health framework.

Conclusion

This study reveals that the presence of microplastics in honey is not an isolated finding but one that has been consistently reported across different geographies. However, the reported particle levels do not cluster around a single typical value, and wide maximum ranges accompanying low averages indicate that microplastic contamination in honey varies in a spatially and production-context-sensitive manner. This positions honey as a biotic reflection of the environmental microplastic load. Morphological and chemical profiles have been demonstrated to support the structural basis of this variability. The uniform reporting of fibre and fragment forms across all studies suggests the presence of a specific morphology for microplastics in honey. The presence of a wide size range and recurring PE, PP, and PET polymers indicates that contamination carries both shared and context-specific components. Cross-country comparisons suggest that microplastic levels cannot be explained solely by environmental quality or economic development and that local production practices, sampling points, and exposure pressures are determinative. It is evident that there is a discernible absence of literature addressing the subject of human exposure. Only a limited portion of studies reporting microplastics in honey have calculated consumption-based daily intake, and most studies have left the evaluation at the concentration level. However, the health implications of microplastics in humans and experimental animals suggest that microplastics can interact with biological systems, emphasising the necessity for a comprehensive One Health approach to address this issue. Consequently, honey serves as a compelling exemplar, illustrating the manner in which contemporary environmental contamination impacts the perception of a "natural product". Microplastic pollution in honey is not merely a measured number; it is a risk signal circulating along the environment-bee-food-human line and produced in a multilayered manner. Consequently, research focusing on honey and microplastic contamination emerges as a strategic research domain, necessitating concurrent deliberations on food safety and ecosystem health.

Declarations

Availability of Data and Materials: Data and materials for this research are available upon request.

Acknowledgements: The authors declare no acknowledgements.

Competing Interests: The authors have no conflicts of interest to declare.

Declaration of Generative Artificial Intelligence (AI): The article and tables and figures were not written/created by AI and AI assisted technologies.

Authors Contributions: BB: Investigation, Methodology, Formal analysis, Writing - Original Draft, Review & Editing. ANU: Visualization, Review & Editing. MK: Review & Editing. GK: Concept Design, Visualization, Writing, review and editing. All authors approved the final version of the manuscript and accept responsibility for the scientific integrity of the work in accordance with the journal's Ethical Principles and Authorship Policy.

References

1. **Kargar M, Hamidian AH, Basaran B:** A review on microplastics in bivalves: Analysis, quantification, and effects. *Environ Monit Assess,* 198 (1):70, 2026. DOI: 10.1007/s10661-025-14931-5
2. **Talbot R, Chang H:** Microplastics in freshwater: A global review of factors affecting spatial and temporal variations. *Environ Pollut*, 292, 118393, 2022. DOI: 10.1016/J.ENVPOL.2021.118393
3. **Kadac-Czapska K, Knez E, Gierszewska M, Olewnik-Kruszkowska E, Grembecka M:** Microplastics derived from food packaging waste-their origin and health risks. *Materials,* 16 (2):674, 2023. DOI: 10.3390/ma16020674
4. **Allen S, Allen D, Phoenix VR, Le Roux G, Durántez Jiménez P, Simonneau A, Galop D:** Atmospheric transport and deposition of microplastics in a remote mountain catchment. *Nature Geosci,* 12 (5):

339-344, 2019. DOI:10.1038/s41561-019-0335-5

5. **Abd Rahim NN, Peng PWY, Shahrir NF, Wan Mahiyuddin WR, Sayed Mohamed Zain SM, Ismail R:** Characteristics, distribution, and sources of atmospheric microplastics in Southeast Asia: A scoping review. *Atmosphere,* 16 (5):515, 2025. DOI: 10.3390/atmos16050515
6. **Özçifçi Z, Basaran B, Akçay HT:** Microplastic contamination and risk assessment in table salts: Turkey. *Food Chem Toxicol,* 175:113698, 2023. DOI: 10.1016/j.jfca.2025.107831
7. **Altunışık A, Tatli H, Doğan N, Sezen G, Parmaksiz A:** Microplastics in the euphrates: Assessing contamination in water, sediment, and commercial fish species. *Environ Pollut,* 383:126863, 2025. DOI: 10.1016/j.envpol.2025.126863
8. **Rosso B, Scoto F, Hallanger IG, Larose C, Gallet JC, Spolaor A, Bravo B, Barbante C, Gamnaro A, Corami F:** Characteristics and quantification of small microplastics (< 100 µm) in seasonal svalbard snow on glaciers and lands. *J Hazard Mater,* 467:133723, 2024. DOI: 10.1016/j.jhazmat.2024.133723
9. **Li H, Liu H, Lin Q, Chen T, Peng R:** The hidden threat of microplastics in desert environments: environmental ımpact, challenges, and response measures. *Sustainability,* 17 (5):1897, 2025. DOI: 10.3390/su17051897
10. **Gürmeriç HE, Basaran B:** Microplastics in dairy products: Occurrence, characterization, contamination sources, detection methods, and future challenges. *Appl Sci,* 15 (17):9411, 2025. DOI: 10.3390/app15179411
11. **Naqash N, Yadav KK, Shaik AS, Alam MW, Djajadi D, Sunarto DA, Marjani M, Sujak S, Rochman F, Rachmawati D, Riajaya DD, Kadarwati FT, Rahayu F, Wani AK:** Microplastic pollution in terrestrial systems: Sources and implications for soil functioning and plant performance. *Water Air Soil Pollut,* 236 (3):172, 2025. DOI: 10.1007/s11270-025-07818-1
12. **Şirin M, Mutlu T, Eryaşar AR, Gedik, K:** Assessing microplastic contamination and health risks in infant formula: A case study from Turkey. *Food Cont,* 182:111872, 2025. DOI: 10.1016/j.foodcont.2025.111872
13. **Ghosh S, Sinha JK, Ghosh S, Vashisth K, Han S, Bhaskar R:** Microplastics as an emerging threat to the global environment and human health. *Sustainability,* 15 (14):10821, 2023. DOI: 10.3390/su151410821
14. **Saha SC, Saha G:** Effect of microplastics deposition on human lung airways: A review with computational benefits and challenges. *Heliyon,* 10 (2):e24355, 2024. DOI: 10.1016/j.heliyon.2024.e24355
15. **Zhu L, Kang Y, Ma M, Wu Z, Zhang L, Hu R, Xu Q, Zhu J, Gu X, An L:** Tissue accumulation of microplastics and potential health risks in human. *Sci Total Environ,* 915:170004, 2024. DOI: 10.1016/j.scitotenv.2024.170004
16. **Khalid N, Aqeel M, Noman A, Khan SM, Akhter N:** Interactions and effects of microplastics with heavy metals in aquatic and terrestrial environments. *Environ Pollut,* 290:118104, 2021. DOI: 10.1016/j.envpol.2021.118104
17. **Li S, Keenan JI, Shaw IC, Frizelle FA:** Could microplastics be a driver for early onset colorectal cancer? *Cancers,* 15 (13):3323, 2023. DOI: 10.3390/cancers15133323
18. **Dueñas-Moreno J, Mora A, Kumar M, Meng XZ, Mahlknecht J:** Worldwide risk assessment of phthalates and bisphenol A in humans: The need for updating guidelines. *Environ Int,* 181:108294, 2023. DOI: 10.1016/j.envint.2023.108294
19. **Hwang J, Choi D, Han S, Choi J, Hong J:** An assessment of the toxicity of polypropylene microplastics in human derived cells. *Sci Total Environ,* 684, 657-669, 2019. DOI: 10.1016/j.scitotenv.2019.05.071
20. **Wu P, Lin S, Cao G, Wu J, Jin H, Wang C, Wong HM, Yang Z, Cai Z:** Absorption, distribution, metabolism, excretion and toxicity of microplastics in the human body and health implications. *J Hazard Mater,* 437:129361, 2022. DOI: 10.1016/j.jhazmat.2022.129361
21. **Gautam R, Jo J, Acharya M, Maharjan A, Lee D, K C PB, Kim C, Kim K, Kim H, Heo Y:** Evaluation of potential toxicity of polyethylene microplastics on human derived cell lines. *Sci Total Environ,* 838:156089, 2022. DOI: 10.1016/j.scitotenv.2022.156089
22. **Park JH, Hong S, Kim OH, Kim CH, Kim J, Kim JW, Hong S, Lee HJ:** Polypropylene microplastics promote metastatic features in human breast cancer. *Sci Rep,* 13 (1):6252, 2023. DOI: 10.1038/s41598-023-33393-8
23. **Yang Q, Peng Y, Wu X, Cao X, Zhang P, Liang Z, Zhang J, Zhang Y, Gao P, Fu Y, Liu P, Cao Z, Ding T:** Microplastics in human skeletal tissues: Presence, distribution and health implications. *Environ Int,* 196:109316, 2025. DOI: 10.1016/j.envint.2025.109316
24. **Nihart AJ, Garcia MA, El Hayek E, Liu R, Olewine M, Kingston JD, Castillo EF, Gullapalli RR, Howard T, Bleske B, Scott J, Gonzalez-Estrella J, Gross JM, Spilde M, Adolphi NL, Gallego DF, Jarrell HS, Dvorscak G, Zuluaga-Ruiz ME, West AB, Campen MJ:** Bioaccumulation of microplastics in decedent human brains. *Nat Med,* 31 (4): 1114-1119, 2025. DOI: 10.1038/s41591-024-03453-1
25. **Usman AN, Yulianty R, Ariyandy A, Basaran B, Tamar M, Fendi F:** Pure honey candy wrapped in nori *(Phorphyra* spp.): Innovative low-temperature processing to enhance antioxidant activity and immunomodulatory effects. *J Funct Foods,* 136:107129, 2026. DOI: 10.1016/j.jff.2025.107129
26. **Wang H, Li L, Lin X, Bai W, Xiao G, Liu G:** Composition, functional properties and safety of honey: A review. *J Sci Food Agric,* 103 (14): 6767-6779, 2023. DOI: 10.1002/jsfa.12720
27. **Santos-Buelga C, González-Paramás AM:** Chemical composition of honey. **In,** Bee Products-Chemical and Biological Properties. 47-104. Cham: Springer Nature Switzerland, 2025.
28. **Ayoub WS, Ritu, Zahoor I, Dar AH, Farooq S, Mir TA, Ganaie TA, Srivastava S, Pandey KV, Altaf A:** Exploiting the polyphenolic potential of honey in the prevention of chronic diseases. *Food Chem Advan,* 3:100373, 2023. DOI: 10.1016/j.focha.2023.100373
29. **Tlak Gajger I, Dar SA, Ahmed MMM, Aly MM, Vlainić J:** Antioxidant capacity and therapeutic applications of honey: Health benefits, antimicrobial activity and food processing roles. *Antioxidants,* 14 (8):959, 2025. DOI: 10.3390/antiox14080959
30. **Özçifçi Z, Dizman S, Basaran B, Aliu H, Akçay HT:** Occurrence and evaluation of microplastics in honeys: Dietary intake and risk assessment. *J Food Compos Anal,* 145:107831, 2025. DOI: 10.1016/j.jfca.2025.107831
31. **Edo C, Fernández-Alba AR, Vejsnæs F, van der Steen JJ, Fernández-Piñas F, Rosal R:** Honeybees as active samplers for microplastics. *Sci Total Environ,* 767:144481, 2021. DOI: 10.1016/j.scitotenv.2020.144481
32. **Başaran B, Özçifçi Z, Kanbur ED, Akçay HT, Gül S, Bektaş Y, Aytan Ü:** Microplastics in honey from Türkiye: Occurrence, characteristic, human exposure, and risk assessment. *J Food Compos Anal,* 135:106646, 2024. DOI: 10.1016/j.jfca.2024.106646
33. **Altunışık A, Barcelo D, Gallitelli L:** Pollination under attack: First insights from Türkiye plain reveal microplastics in bees from both urban and rural areas. *Ecol Indic,* 178:114077, 2025. DOI: 10.1016/j.ecolind.2025.114077
34. **Shavali Gilani P, Moradian M, Tajdar-Oranj B, Basaran B, Peivasteh-Roudsari L, Javanmardi F, Khodaei SM, Mirza Alizadeh A:** Microplastics comprehensive review: İmpact on honey bee, occurrence in honey and health risk evaluation. *J Appl Ecol,* 62: 1772-1794, 2025. DOI: 10.1111/1365-2664.70030
35. **Roy S, Malla S, Dekari D, Choudhury TG:** One Health approach: Human, environment, and animal health. **In,** Management of Fish Diseases. 281-297, Singapore: Springer Nature Singapore, 2025.
36. **Diaz-Basantes MF, Conesa JA, Fullana A:** Microplastics in honey, beer, milk and refreshments in Ecuador as emerging contaminants. *Sustainability,* 12:5514, 2020. DOI: 10.3390/su12145514
37. **Azmi WA, Ibrahim YS, Rosazan MN, Mamat MII, Anuar ST:** Detection of microplastics in honey of stingless bee (Heterotrigona itama) and honey bee (Apis mellifera) from Malaysia. *SSRN Electron J,* 4632805, 2023. DOI:10.2139/ssrn.4632805
38. **Schiano ME, D'Auria LJ, D'Auria R, Seccia S, Rofrano G, Signorelli D, Sansone D, Caprio E, Albrizio S, Cocca M:** Microplastic

contamination in the agri-food chain: The case of honeybees and beehive products. *Sci Total Environ,* 948:174698, 2024. DOI: 10.1016/j.scitotenv.2024.174698

39. **Inaudi P, Sicurella GM, Rivoira L, Favilli L, Bracco P, Bertinetti S, Abollino O, Bruzzoniti MC, Isaja V, Giacomino A:** Pollution profiling in Italian honeys: Elements and microplastics as comprehensive indicators of environmental contamination and food safety. *Sci Total Environ,* 993:179981, 2025. DOI: 10.1016/j.scitotenv.2025.179981
40. **Liebezeit G, Liebezeit E:** Non-pollen particulates in honey and sugar. *Food Addit Contam Part A,* 30 (12): 2136-2140, 2013. DOI: 10.1080/19440049.2013.843025
41. **Liebezeit G, Liebezeit E:** Origin of synthetic particles in honeys. *Pol J Food Nutr Sci,* 65 (2): 143-147, 2015. DOI: 10.1515/pjfns-2015-0025
42. **Pham DT, Kim J, Lee SH, Kim J, Kim D, Hong S, Jung J, Kwon JH:** Analysis of microplastics in various foods and assessment of aggregate human exposure via food consumption in Korea. *Environ Pollut,* 322:121153, 2023. DOI: 10.1016/j.envpol.2023.121153
43. **Ahmad M, Ahmad J, Usama M, Al-Swadi HA, Mousa MA, Rafique MI, Al-Wabel MI, Al-Farraj ASF:** Microplastic contamination in commercial food and drink products and associated risk of potential human intake in Riyadh, Saudi Arabia. *Environ Monit Assess,* 197 (3):246, 2025. DOI: 10.1007/s10661-025-13680-9
44. **Rani-Borges B, Arena MVN, Gomes IN, de Carvalho Lins LHF, Cestaro LDSC, Pompêo M, Ando RA, Alves-dos-Santos I, Toppa RH, Martines MR, Queiroz LG:** More than just sweet: Current insights into microplastics in honey products and a case study of *Melipona quadrifasciata* honey. *Environ Sci Process Impacts,* 26, 1-12, 2024. DOI: 10.1039/D4EM00262H
45. **Mühlschlegel P, Hauk A, Walter U, Sieber R:** Lack of evidence for microplastic contamination in honey. *Food Addit Contam Part A,* 34 (11): 1982-1989, 2017. DOI: 10.1080/19440049.2017.1347281
46. **Gómez-Méndez LD, Robles-Camargo JE, Vera-Bravo R, Moncaleano-Niño AM, Devia Castillo CA, Ospina-Torres R, Escobar-Cortes Y, Camacho-Erazo M, Amarillo-Suárez AR:** Characterization of microplastics in bees and their products in urban and rural areas of the Sabana de Bogotá, Colombia. *Microplastics,* 3 (4): 589-598, 2024. DOI: 10.3390/microplastics3040036
47. **Fuente-Ballesteros A, Ciulu M, Haque SM, Syrgabek Y, Basaran B:** Honeybees as active bioindicators of plastic pollution: Environmental exposure, analytical strategies, and monitoring perspectives. *Sci Total Environ,* 1003:180722, 2025. DOI: 10.1016/j.scitotenv.2025.180722
48. **Martín-Gómez B, Valverde S, Bernal J, Ares AM:** Development and validation of a new analytical method for the determination of plasticizers in bee pollen. *Microchem J,* 205:111404, 2024. DOI: 10.1016/j.microc.2024.111404
49. **Rodrigues KFS, Carvalho BRR, Contrera FAL, Smith WS:** Bees and microplastic studies: A systematic review. *Neotrop Entomol,* 54 (1): 1-14, 2025. DOI: 10.1007/s13744-025-01268-4
50. **Balzani P, Galeotti G, Scheggi S, Masoni A, Santini G, Baracchi D:** Acute and chronic ingestion of polyethylene (PE) microplastics has mild effects on honey bee health and cognition. *Environ Pollut,* 305:119318, 2022. DOI: 10.1016/j.envpol.2022.119318
51. **Alma AM, de Groot GS, Buteler M:** Microplastics incorporated by honeybees from food are transferred to honey, wax and larvae. *Environ Pollut,* 320:121078, 2023. DOI: 10.1016/j.envpol.2023.121078
52. **Negri I, Mavris C, Di Prisco G, Caprio E, Pellecchia M:** Honey bees *(Apis mellifera* L.) as active samplers of airborne particulate matter. *PLoS One,* 10 (7):e0132491, 2015. DOI: 10.1371/journal.pone.0132491
53. **Al Naggar Y, Brinkmann M, Sayes CM, Al-Kahtani SN, Dar SA, El-Seedi HR, Grünewald B, Giesy JP:** Are honey bees at risk from microplastics? *Toxics,* 9 (5):109, 2021. DOI: 10.3390/toxics9050109
54. **Al Naggar Y, Ali H, Mohamed H, Kholy SE, El-Seedi HR, Mohamed A, Sevin S, Ghramh HA, Wang K:** Exploring the risk of microplastics to pollinators: Focusing on honey bees. *Environ Sci Pollut Res,* 31 (34): 46898-46909, 2024. DOI: 10.1007/s11356-024-34184-y
55. **Buteler M, Villalobos E, Alma AM, Silva L, Tomba JP:** Management practice for small hive beetle as a source of microplastic contamination in honey and honeybee colonies. *Environ Pollut,* 334:122151, 2023. DOI: 10.1016/j.envpol.2023.122151
56. **Peñalver R, Arroyo-Manzanares N, Campillo N, Viñas P:** Targeted and untargeted gas chromatography-mass spectrometry analysis of honey samples for determination of migrants from plastic packages. *Food Chem,* 334:127547, 2021. DOI: 10.1016/j.foodchem.2020.127547
57. **Kaseke T, Lujic T, Cirkovic Velickovic T:** Nano-and Microplastics migration from plastic food packaging into dairy products: Impact on nutrient digestion, absorption, and metabolism. *Foods,* 12 (16):3043, 2023. DOI: 10.3390/foods12163043
58. **Katsara K, Kenanakis G, Alissandrakis E, Papadakis VM:** Honey quality and microplastic migration from food packaging: A potential threat for consumer health? *Microplastics,* 1 (3): 406-427, 2022. DOI: 10.3390/microplastics1030030
59. **Katsara K, Viskadourakis Z, Alissandrakis E, Kenanakis G, Papadakis VM:** Microplastic migration from plastic packaging into honey. *Microplastics,* 4 (4):90, 2025. DOI: 10.3390/microplastics4040090
60. **Aminah IS, Ikejima K:** Potential sources of microplastic contamination in laboratory analysis and a protocol for minimising contamination. *Environ Monit Assess,* 195 (7):808, 2023. DOI: 10.1007/s10661-023-11410-7
61. **Canga EM, Gowen A, Xu JL:** Assessing the inconsistency of microplastic measurements in foods and beverages. *Compr Rev Food Sci Food Saf,* 23 (2):e13315, 2024. DOI: 10.1111/1541-4337.13315
62. **Katsara K, Viskadourakis Z, Alissandrakis E, Kountourakis N, Kenanakis G, Papadakis VM:** Microplastics' detection in honey: Development of protocols in a simulation. *Appl Sci,* 14 (11):4720, 2024. DOI: 10.3390/app14114720
63. **Pironti C, Notarstefano V, Ricciardi M, Motta O, Giorgini E, Montano L:** First evidence of microplastics in human urine, a preliminary study of intake in the human body. *Toxics,* 11 (1):40, 2022. DOI: 10.3390/toxics11010040
64. **Leonard SV, Liddle CR, Atherall CA, Chapman E, Watkins M, Calaminus SD, Rotchell JM:** Microplastics in human blood: Polymer types, concentrations and characterisation using μFTIR. *Environ Int,* 188:108751, 2024. DOI: 10.1016/j.envint.2024.108751
65. **Zhang N, Li YB, He HR, Zhang JF, Ma GS:** You are what you eat: Microplastics in the feces of young men living in Beijing. *Sci Total Environ,* 767:144345, 2021. DOI: 10.1016/j.scitotenv.2020.144345
66. **Roslan NS, Lee YY, Ibrahim YS, Anuar ST, Yusof KMKK, Lai LA, Brentnall T:** Detection of microplastics in human tissues and organs: A scoping review. *J Glob Health,* 14:04179, 2024. DOI: 10.7189/jogh.14.04179
67. **Yang Z, Wang M, Feng Z:** Human microplastics exposure and potential health risks to target organs by different routes: A review. *Curr Pollut Rep,* 9, 468-485, 2023. DOI: 10.1007/s40726-023-00273-8
68. **Enyoh CE, Devi A, Kadono H, Wang Q, Rabin MH:** The plastic within: Microplastics invading human organs and bodily fluids systems. *Environments,* 10 (11):194, 2023. DOI: 10.3390/environments10110194
69. **La Porta E, Exacoustos O, Lugani F, Angeletti A, Chiarenza DS, Bigatti C, Spinelli S, Kajana X, Garbarino A, Bruschi M, Candiano G, Caridi G, Mancianti N, Calatroni M, Verzola D, Esposito P, Viazzi F, Verrina E, Ghiggeri GM:** Microplastics and kidneys: An update on the evidence for deposition of plastic microparticles in human organs, tissues and fluids and renal toxicity concern. *Int J Mol Sci,* 24 (18):14391, 2023. DOI: 10.3390/ijms241814391
70. **Abbasi S, Turner A:** Human exposure to microplastics: A study in Iran. *J Hazard Mater,* 403:123799, 2021. DOI: 10.1016/j.jhazmat.2020.123799
71. **Baeza-Martínez C, Olmos S, González-Pleiter M, López-Castellanos J, García-Pachón E, Masiá-Canuto M, Bayo J:** First evidence of

microplastics isolated in European citizens' lower airway. *J Hazard Mater,* 438:129439, 2022. DOI: 10.1016/j.jhazmat.2022.129439

72. **Ragusa A, Svelato A, Santacroce C, Catalano P, Notarstefano V, Carnevali O, Giorgini E: Plasticenta:** First evidence of microplastics in human placenta. *Environ Int,* 146:106274, 2021. DOI: 10.1016/j.envint.2020.106274
73. **Ragusa A, Notarstefano V, Svelato A, Belloni A, Gioacchini G, Blondeel C, Zucchelli E, De Luca C, D'Avino S, Gulotta A, Carnevali O, Giorgini E:** Raman microspectroscopy detection and characterisation of microplastics in human breastmilk. *Polymers,* 14 (13):2700, 2022. DOI: 10.3390/polym14132700
74. **Huang S, Huang X, Bi R, Guo Q, Yu X, Zeng Q, Huang Z, Liu T, Wu H, Chen Y, Xu J, Wu Y, Guo P:** Detection and analysis of microplastics in human sputum. *Environ Sci Technol,* 56 (4): 2476-2486, 2022. DOI: 10.1021/acs.est.1c03859
75. **Zhu X, Wang C, Duan X, Liang B, Xu EG, Huang Z:** Micro- and nanoplastics: A new cardiovascular risk factor? *Environ Int,* 171:107662, 2023. DOI: 10.1016/j.envint.2022.107662
76. **Marfella R, Prattichizzo F, Sardu C, Fulgenzi G, Graciotti L, Spadoni T, Paolisso G:** Microplastics and nanoplastics in atheromas and cardiovascular events. *N Engl J Med,* 390 (10): 900-910, 2024. DOI: 10.1056/NEJMoa2309822
77. **Zhi Wang Z, Li N, Ding Y, Li N, Su M, Zhang C, Li Y, Wang Q, Sha C, Xia B, Cheng J, Jiang G:** Microplastics and human health: Exposure pathways, toxicity mechanisms, and future research challenges. *J Environ Chem Eng,* 13:118807, 2025. DOI: 10.1016/j.jece.2025.118807
78. **Hu M, Palić D:** Micro- and nano-plastics activation of oxidative and inflammatory adverse outcome pathways. *Redox Biol,* 37:101620, 2020. DOI: 10.1016/j.redox.2020.101620
79. **Xie X, Deng T, Duan J, Xie J, Yuan J, Chen M:** Exposure to polystyrene microplastics causes reproductive toxicity through oxidative stress and activation of the p38 MAPK signaling pathway. *Ecotoxicol Environ Saf,* 190:110133, 2020. DOI: 10.1016/j.ecoenv.2019.110133
80. **Hou J, Lei Z, Cui L, Hou Y, Yang L, An R, Wang Q, Li S, Zhang H, Zhang L:** Polystyrene microplastics lead to pyroptosis and apoptosis of ovarian granulosa cells via NLRP3/Caspase-1 signaling pathway in rats. *Ecotoxicol Environ Saf,* 212:112012, 2021. DOI: 10.1016/j.ecoenv.2021.112012
81. **Meng X, Yin K, Zhang Y, Wang D, Lu H, Hou L, Zhao H, Xing M:** Polystyrene microplastics induced oxidative stress, inflammation and necroptosis via NF-κB and RIP1/RIP3/MLKL pathway in chicken kidney. *Toxicology,* 478:153296, 2022. DOI: 10.1016/j.tox.2022.153296
82. **Wang X, Jia Z, Zhou X, Su L, Wang M, Wang T, Zhang H:** Nanoplastic-induced vascular endothelial injury and coagulation dysfunction in mice. *Sci Total Environ,* 865:161271, 2023. DOI: 10.1016/j.scitotenv.2022.161271
83. **Zhao B, Rehati P, Yang Z, Cai Z, Guo C, Li Y:** The potential toxicity of microplastics on human health. *Sci Total Environ,* 912:168946, 2024. DOI: 10.1016/j.scitotenv.2023.168946
84. **Chiu HW, Xia T, Lee YH, Chen CW, Tsai JC, Wang YJ:** Cationic polystyrene nanospheres induce autophagic cell death through the induction of endoplasmic reticulum stress. *Nanoscale,* 7 (2): 736-746, 2015. DOI: 10.1039/C4NR05509H
85. **Wang S, Wu H, Shi X, Wang Y, Xu S:** Polystyrene microplastics with different sizes induce apoptosis and necroptosis in liver through the PTEN/PI3K/AKT/autophagy axis. *Sci Total Environ,* 899:165461, 2023. DOI: 10.1016/j.scitotenv.2023.165461
86. **Wang Y, Zhang A, Liang T, Chen L, Feng S, Zhao Z, Jing Z, Lv J, Xie J, Zhou B:** Polystyrene microplastics induce nephrotoxicity through DDIT4-mediated autophagy and apoptosis. *Ecotoxicol Environ Saf,* 294:118066, 2025. DOI: 10.1016/j.ecoenv.2025.118066
87. **Luo T, Zhang Y, Wang C, Wang X, Zhou J, Shen M, Jin Y:** Maternal exposure to different sizes of polystyrene microplastics during gestation causes metabolic disorders in their offspring. *Environ Pollut,* 255:113122, 2019. DOI: 10.1016/j.envpol.2019.113122
88. **Hirt N, Body-Malapel M:** Immunotoxicity and intestinal effects of nano- and microplastics: A review of the literature. *Part Fibre Toxicol,* 17 (1):57, 2020. DOI: 10.1186/s12989-020-00387-7
89. **Yee MS, Hii LW, Looi CK, Lim WM, Wong SF, Kok YY, Tan BK, Wong CY, Leong CO:** Impact of microplastics and nanoplastics on human health. *Nanomaterials,* 11 (2):496, 2021. DOI: 10.3390/nano11020496
90. **Wei G, Zhang K, Shen FJ, Xie RR, Wang FW, Guo HQ, Liu L:** Low-dose polystyrene microplastics exposure increases susceptibility to obesity-induced MASLD via disrupting intestinal barrier integrity and gut microbiota homeostasis. *Ecotoxicol Environ Saf,* 299:118310, 2025. DOI: 10.1016/j.ecoenv.2025.118310
91. **Chen X, Zhuang J, Chen Q, Xu L, Yue X, Qiao D:** Polyvinyl chloride microplastics induced gut barrier dysfunction, microbiota dysbiosis and metabolism disorder in adult mice. *Ecotoxicol Environ Saf,* 241:113809, 2022. DOI: 10.1016/j.ecoenv.2022.113809
92. **Xie S, Zhang R, Li Z, Liu C, Chen Y, Yu Q:** Microplastics perturb colonic epithelial homeostasis associated with intestinal over-proliferation, exacerbating the severity of colitis. *Environ Res,* 217:114861, 2023. DOI: 10.1016/j.envres.2022.114861
93. **Li X, Li Y, Liu B, Sui G, Liu S, Song G:** A digestive system microphysiological platform for assessment of internal-exposure risks and metabolic disease mechanisms induced by multi-size nano-plastics. *J Hazard Mater,* 485:136865, 2025. DOI: 10.1016/j.jhazmat.2024.136865
94. **Liang B, Huang Y, Zhong Y, Li Z, Ye R, Wang B, Zhang B, Meng H, Lin X, Du J, Hu M, Wu Q, Sui H, Yang X, Huang Z:** Brain single-nucleus transcriptomics highlights that polystyrene nanoplastics potentially induce Parkinson's disease-like neurodegeneration by causing energy metabolism disorders in mice. *J Hazard Mater,* 430:128459, 2022. DOI: 10.1016/j.jhazmat.2022.128459
95. **Tian S, Li R, Li J, Zou J:** Polystyrene nanoplastics promote colitis-associated cancer by disrupting lipid metabolism and inducing DNA damage. *Environ Int,* 195:109258, 2025. DOI: 10.1016/j.envint.2025.109258
96. **Dong CD, Chen CW, Chen YC, Chen HH, Lee JS, Lin CH:** Polystyrene microplastic particles: *In vitro* pulmonary toxicity assessment. *J Hazard Mater,* 385:121575, 2020. DOI: 10.1016/j.jhazmat.2019.121575
97. **Fournier SB, D'Errico JN, Adler DS, Kollontzi S, Goedken MJ, Fabris L, Yurkow EJ, Stapleton PA:** Nanopolystyrene translocation and fetal deposition after acute lung exposure during late-stage pregnancy. *Part Fibre Toxicol,* 17 (1):55, 2020. DOI: 10.1186/s12989-020-00385-9
98. **Tang KHD, Li R, Li Z, Wang D:** Health risk of human exposure to microplastics: A review. *Environ Chem Lett,* 22 (3): 1155-1183, 2024. DOI: 10.1007/s10311-024-01727-1
99. **Wang K, Li J, Zhao L, Mu X, Wang C, Wang M, Xue X, Qi S, Wu L:** Gut microbiota protects honey bees (*Apis mellifera* L.) against polystyrene microplastics exposure risks. *J Hazard Mater,* 402:123828, 2021. DOI: 10.1016/j.jhazmat.2020.123828
100. **Deng Y, Jiang X, Zhao H, Yang S, Gao J, Wu Y, Diao Q, Hou C:** Microplastic polystyrene ingestion promotes the susceptibility of honeybee to viral infection. *Environ Sci Technol,* 55 (17): 11680-11692, 2021. DOI: 10.1021/acs.est.1c01619
101. **Buteler M, Alma AM, Stadler T, Gingold AC, Manattini MC, Lozada M:** Acute toxicity of microplastic fibers to honeybees and effects on foraging behavior. *Sci Total Environ,* 822:153320, 2022. DOI: 10.1016/j.scitotenv.2022.153320
102. **Wang K, Zhu L, Rao L, Zhao L, Wang Y, Wu X, Zheng H, Liao X:** Nano- and micro-polystyrene plastics disturb gut microbiota and intestinal immune system in honeybee. *Sci Total Environ,* 842:156819, 2022. DOI: 10.1016/j.scitotenv.2022.156819
103. **Pasquini E, Ferrante F, Passaponti L, Pavone FS, Costantini I, Baracchi D:** Microplastics reach the brain and interfere with honey bee cognition. *Sci Total Environ,* 912:169362, 2024. DOI: 10.1016/j.scitotenv.2023.169362

104. **Ferrante F, Pasquini E, Cappa F, Bellocchio L, Baracchi D:** Unravelling the microplastic menace: Different polymers additively increase bee vulnerability. *Environ Pollut,* 352:124087, 2024. DOI: 10.1016/j.envpol.2024.124087

105. **Mitton GA, Corona M, Alburaki M, Iglesias AE, Ramos F, Fuentes G, Vazquez MM, Mitton MF, Chan P, Ruffinengo RS, Maggi MD:** Synergistic effects between microplastics and glyphosate on honey bee larvae. *Environ Toxicol Pharmacol,* 111:104550, 2024. DOI: 10.1016/j.etap.2024.104550

106. **WHO:** Tripartite and UNEP support OHHLEP's definition of "One Health". World Health Organization. https://www.who.int/news/item/01-12-2021-tripartite-and-unep-support-ohhlep-s-definition-of-one-health. *Accessed:* 30 March 2026.

107. **OIE/WOAH:** One Health Joint Plan of Action (2022–2026). World Organisation for Animal Health. https://www.who.int/publications/i/item/9789240059139. *Accessed:* 30 March 2026.

108. **Cverenkárová K, Valachovičová M, Mackuľak T, Žemlička L, Bírošová L:** Microplastics in the food chain. *Life,* 11 (12):1349, 2021. DOI: 10.3390/life11121349

109. **Singh S, Sharma P, Pal N, Sarma DK, Tiwari R, Kumar M:** Holistic one health surveillance framework: synergizing environmental, animal, and human determinants for enhanced infectious disease management. *ACS Infect Dis,* 10 (3): 808-826, 2024. DOI: 10.1021/acsinfecdis.3c00625

110. **EFSA CONTAM Panel:** Presence of microplastics and nanoplastics in food, with particular focus on seafood. *EFSA J, 14* (6):4501, 2016. DOI: 10.2903/j.efsa.2016.4501

111. **European Food Safety Authority:** A coordinated approach to assess the human health risks of micro- and nanoplastics in food (EFSA Scientific Colloquium 25, Briefing Notes). European Food Safety Authority. https://www.efsa.europa.eu/sites/default/files/2021-05/briefing-notes.pdf. *Accessed:* 15 January 2026.

112. **Heo SJ, Moon N, Kim, JH:** A systematic review and quality assessment of estimated daily intake of microplastics through food. *Rev Environ Health, 40* (2): 371-392, 2025. DOI: 10.1515/reveh-2024-0111

113. **Pekmezci H, Sipahi S, Başaran B:** Health risk Assessment of dietary chemical exposures: A comprehensive review. *Foods,* 14 (23):4133, 2025. DOI: 10.3390/foods14234133

Kafkas Universitesi Veteriner Fakultesi Dergisi
Journal Home-Page: http://vetdergikafkas.org
E-ISSN: 1309-2251

Kafkas Univ Vet Fak Derg
32 (2): 207-218, 2026
DOI: 10.9775/kvfd.2025.35390

Research Article

Evaluation of 305-Day Lactation Milk Yield Predictions from Pre-Peak Partial Milk Yields Using Some Data Mining Algorithms

Özcan ŞAHİN [1 (*)], Rabia ALBAYRAK DELİALİOĞLU [2], Gizem ÇİNİ [1], İbrahim AYTEKİN [1], Yasin ALTAY [3,4]

[1] Selcuk University, Faculty of Agriculture, Animal Science Department, TR-42250 Konya - TÜRKİYE
[2] Ankara University, Faculty of Agriculture, Animal Science Department, Biometry and Genetics Unit, TR-06100 Ankara - TÜRKİYE
[3] Eskisehir Osmangazi University, Faculty of Agriculture, Animal Science Department, Biometry and Genetics Unit, TR-26040 Eskişehir - TÜRKİYE
[4] Eskisehir Osmangazi University, Agricultural Studies Practices and Research Center, TR-26040 Eskişehir - TÜRKİYE

[(*)] **Corresponding author:**
Özcan Şahin
Phone: +90 332 223 2815
Cellular phone: +90 532 675 4184
Fax: +90 332 241 0108
E-mail: osahin006@gmail.com

How to cite this article?

Şahin Ö, Albayrak Delialioğlu R, Çini G, Aytekin İ, Altay Y: Evaluation of 305-Day Lactation Milk Yield Predictions from Pre-Peak Partial Milk Yields Using Some Data Mining Algorithms. *Kafkas Univ Vet Fak Derg*, 32 (2): 207-218, 2026
DOI: 10.9775/kvfd.2025.35390

Article ID: KVFD-2025-35390
Received: 30.09.2025
Accepted: 23.02.2026
Published Online: 24.02.2026

Abstract

A total of 75,640 test-day milk yield records of 248 Holstein cows in the first (124 heads), second (75 heads), and third lactation (49 heads) were used as material in the study. All data used in this study were obtained from the database of the Afikim herd management software used on a private dairy farm. To predict 305-day adjusted milk yields (MY305) using some partial milk yield parameters, ALM (Automatic Linear Modeling), C&RT (Classification and Regression Tree), CHAID (Chi-square Automatic Interaction Detector), RF (Random Forest), MARS (Multiple Adaptive Regression Splines), Bagging MARS (Bootstrap Aggregating Multiple Adaptive Regression Splines), and BRNN (Bayesian Regularized Neural Network) data mining algorithms were used with group five-fold cross-validation. When all algorithms are compared in terms of 15 different prediction performance measures, the most successful algorithms are MARS (R^2_{Adj} = 0.844, RRMSE = 6.530 and MAPE = 5.182), Bagging MARS (R^2_{Adj} = 0.840, RRMSE = 6.547 and MAPE = 5.103), while C&RT (R^2_{Adj} = 0.828, RRMSE = 7.028 and MAPE = 5.542) is the most efficient tree-based algorithm. When the model evaluation criteria, including systematic bias and limits of agreement (LoA) among prediction performance measures, were examined together, the prediction success of the data mining algorithms was determined as MARS, Bagging MARS, C&RT, ALM, BRNN, CHAID, and RF, respectively. As a result, it can be stated that 75-day partial milk yield totals before peak milk yield is an important time period and an indirect selection criterion in determining 305-day milk yield. Additionally, it can help producers evaluate the impact of past milk yields on future cow productivity and predict overall herd performance, thereby facilitating timely and informed decision-making.

Keywords: Bagging MARS, BRNN, C&RT, CHAID, Data mining, MARS, Milk yield, Partial milk record, Random forest

Introduction

Most of the total milk production in the world (about 80%) is obtained from cattle. Although the share of cattle in total milk production varies depending on regions and production conditions, it also constitutes a large part of the income sources of enterprises. In Türkiye, most of the milk production is obtained from cattle and approximately 92% of the milk produced is obtained from cattle. The remaining approximately 8% is made up of sheep, goat and buffalo milk [1]. Milk production is the process that starts after calving and continues until the animal is dry. This physiological period is defined as the lactation length and is accepted as 305 days on average in dairy cattle [2]. The curve showing the increasing and decreasing changes in milk yield during this period, which is shaped by the effects of genetic and environmental factors, is called the "lactation curve" [2,3].

With good herd management, there is a rapid increase in milk yield after birth and milk yield reaches its maximum level (peak) within 4-6 weeks. The peak period continues for a certain period of time and then milk production gradually decreases at a lower rate than the postpartum increase. But, peak yield and day to peak can vary

depending on the genetic and herd management factors [3,4]. The success of the enterprises in increasing their milk yields is primarily to keep records and to make optimization in terms of the factors in question thanks to these records. Using the records accurately and in the easiest way facilitates herd management. Keeping these records daily defines the actual lactation milk yield. However, different lactation milk yield prediction methods have been developed so far in order to predict the actual lactation milk yield in terms of time and convenience. In addition, both 305-day milk yields and actual lactation milk yields have been estimated by using partial lactation milk records [5,6]. Another importance of estimating lactation milk yields from partial lactation milk yields is that the animals that will not be used for breeding in the herd are not kept waiting until the first lactation milk yields are determined and the necessary labor force is disabled by eliminating the care and feeding costs to be applied to them. In addition, it is also possible to eliminate the risks of health protection measures (vaccination and disease etc.) of these animals. In other words, estimating the lactation yields of animals based on partial milk yield records enables indirect selection, which can shorten the generation interval by approximately one year. With this application in herd management, selection efficiency is increased. In brief, because milk yield is a quantitative trait, it is easily affected by environmental factors. Therefore, unlike past production approaches, modern dairy producers tend to identify and intervene in the factors affecting milk yield as quickly as possible. This necessitates analyzing and interpreting shorter timeframes and optimizing production processes to ensure sustainability in a competitive market.

Today, alongside the advancement of artificial intelligence technologies, digital tools and systems such as Smaxtech technology [7] that incorporate these algorithms have increasingly found their place in animal husbandry. Therefore, it is important to develop alternative calculation methods to the classical methods used in the calculation of lactation milk yields. Numerous prediction models have taken their place in the literature in terms of determining the traits that have been emphasized until today and evaluating them in animal breeding [2,5,6,8]. Classical regression methods and traditional lactation curve models require certain preconditions, such as linearity, exogeneity, heteroskedasticity, and autocorrelation. However, data mining algorithm applications can model nonlinear and complex interactions in the data structure without any preconditions. In recent years, studies on data mining have been carried out in many livestock breeding areas because they have some advantages due to practical, accurate, successful, and appropriate fit criteria as well as the ability to use larger data sets; prediction of end-of-fattening body weight [9], determination of mastitis with thermal camera [10], body weight prediction in goats [11], body weight prediction in sheep [12], prediction of body measurements in camels [13], prediction of body weight from some body measurements of cattle during growth and development [14], prediction of body weight by biometric measurements [15], prediction of milk yield [16], and honey yield and quality [17,18] were used. Although classical statistical methods are still widely used across various fields, they may fall short when it comes to analyzing large and complex datasets, especially with the rapid advancement of technology. In this context, data mining algorithms have gained prominence, as they are capable of effectively analyzing datasets that traditional statistical methods cannot handle [14,19].

This study aimed to evaluate of 305-day adjusted milk yields (MY_{305}) predictions using the total and mean of pre-peak 15, 30, 45, 60, and 75-day partial milk yields in different Lactation Number (LN) 248 Holstein cows via some data mining algorithms such as Automatic Linear Modeling (ALM), Classification and Regression Tree (C&RT), Chi-squared Automatic Interaction Detector (CHAID), Random Forest (RF), Multiple Adaptive Regression Splines (MARS), Bootstrap Aggregating Multiple Adaptive Regression Splines (Bagging MARS) and Bayesian regularized neural network (BRNN).

Material And Methods

Experimental Animals

The animal material of the study consisted of a total of 75,640 test-day milk yield records of 248 Holstein cows (mean LMY305=8,765 /. and mean days to peak milk yield=68 days) in the first (124 heads), second (75 heads), and third lactation (49 heads) of a private dairy farm in the Ilgın district of Konya province. All data used in the study were obtained from the database of the Afikim herd management software (AfiFarm v. 3.0) used at the farm. The farm used an 8x2 herringbone milking system and milking was done twice a day. In order to standardize milk yields to a 305-day lactation basis for cows with days in milk shorter or longer than 305 days, the correction factors recommended by Akman and Eliçin [20] were applied.

Prediction Methods

In this study, three regression tree-based algorithms (C&RT, CHAID, and RF) and four different data mining algorithms (ALM, MARS, Bagging MARS, and BRNN) were employed.

ALM Algorithm

The ALM algorithm, implemented as an Automated Linear Modeling procedure, is used in multiple regression analysis and data mining to determine the most suitable linear

model by automatically selecting a subset of predictors when a large number of independent variables are available. By automating variable selection and model optimization, the ALM algorithm facilitates the model-building process and can improve predictive performance [21].

C&RT Algorithm

C&RT algorithm, developed by Breiman et al.[22], is one of the most widely used decision tree algorithms. This algorithm utilizes a binary tree structure, where each node results in only two branches. The C&RT algorithm builds a classification model when the dependent variable is categorical and a regression model when the dependent variable is continuous. It generally uses the Gini index as the branching criterion [23]. The Gini index measures how effectively a node in a decision tree separates individuals into different classes. This metric ranges from 0 to 1, where 0 indicates perfect separation, representing a completely homogeneous (pure) group, and 1 represents complete heterogeneity. The lower the Gini index, the more homogeneous the node is [22,24,25].

CHAID Algorithm

Chi-squared Automatic Interaction Detector (CHAID) algorithm, introduced to the literature by Kass [26], is a tree-based method that constructs decision trees by employing the chi-square statistic to achieve optimal splits. The split decisions are made based on Bonferroni-adjusted p-values. One of the key characteristics of the CHAID algorithm is its ability to handle categorical and ordinal variables, as well as variables with missing data. Furthermore, as a non-parametric method that does not rely on linear assumptions, CHAID is particularly effective in multidimensional datasets [26], Unlike C&RT, this algorithm allows for more than two branches to emerge from a single node [27,28].

RF Algorithm

RF algorithm, developed by Breiman [29], is widely used for both classification and regression problems. It combines the predictions of multiple decision trees to obtain a single aggregated result. The fundamental difference between the RF algorithm and a single decision tree algorithm lies in the randomization of the processes involved in bootstrap sampling and in selecting a random subset of predictors at each split [30].

MARS Algorithm

The MARS algorithm, developed by Friedman [31], is a non-parametric regression method that identifies the relationship between dependent and independent variables. Through a stepwise process, it generates basis functions by considering candidate knots and potential interaction terms [15]. These basis functions are typically defined as piecewise linear functions and are chosen in such a way as to minimize the error variance at each step. Moreover, MARS is capable of modeling interactions among predictors by including interaction terms in the model [32,33].

Bagging MARS Algorithm

The Bagging MARS algorithm is a method that combines Multivariate Adaptive Regression Splines (MARS) with the Bootstrap Aggregating (Bagging) technique. The primary objective of this method is to improve the accuracy of the final model by modeling nonlinear relationships in regression analysis, while also addressing the issue of overfitting. Bagging MARS generates multiple MARS models, each trained on different bootstrap samples, and aggregates their predictions. This approach, particularly effective with high-dimensional and complex data, reduces overfitting while simultaneously enhancing the model's generalization ability, thus leading to more reliable results [34,35].

BRNN Algorithm

The Bayesian Regularized Neural Network (BRNN) algorithm is a method used to model complex relationships within data, combining artificial neural networks (ANNs) with Bayesian regularization techniques. This approach regulates the learning process by assigning prior probability distributions to the network weights, thereby providing better generalization in both regression and classification tasks. Additionally, it reduces overfitting and delivers effective results, especially with noisy datasets. Compared to other methods, BRNN has proven highly reliable in improving neural network performance, particularly with complex and nonlinear datasets [36].

Prediction Performance Evaluation Criteria of Data Mining Algorithms

The prediction performance criteria of the algorithms used in the study are presented in *Table 1*.

In evaluating the predictive performance of the algorithms, smaller values are expected for Akaike's Information Criterion (AIC), corrected Akaike's Information Criterion (AICC), mean error (ME), mean absolute percentage error (MAPE), mean relative approximation error (MRAE), mean absolute deviation (MAD), global relative approximation error (RAE), standard deviation ratio (SDratio), root mean square error (RMSE), and relative root mean square error (RRMSE). In contrast, the coefficient of determination (R^2) and the adjusted coefficient of determination (Adj. R^2) should take values close to 1 [37-39]. Also, Bland-Altman analysis was used to determine the systematic bias and limits of agreement (LoA) between the predictions of data mining algorithms and the 305-day adjusted milk yield.

Table 1. *Performance criteria and formulae of the algorithms*

Performance Criteria	Experission
Root mean square error	$RMSE = \sqrt{\frac{1}{n}\sum_{i=1}^{n}(y_i - y_{ip})^2}$
Relative root mean square error	$RRMSE = \frac{\sqrt{\frac{1}{n}\sum_{i=1}^{n}(y_i - y_{ip})^2}}{\overline{y}} x100$
Standard deviation ratio	$SD_{ratio} = \frac{\sqrt{\frac{1}{n}\sum_{i=1}^{n}(y_i - \overline{y_i})^2}}{\sqrt{\frac{1}{n}\sum_{i=1}^{n}(y_{ip} - \overline{y_{ip}})^2}}$
Coefficient of variation	$CV(\%) = \frac{\sqrt{\frac{1}{n}\sum_{i=1}^{n}(\varepsilon_i - \overline{\varepsilon})^2}}{\overline{Y}} * 100$
Pearson's correlation coefficients	$PC = \frac{cov(y_i, y_{ip})}{S_{y_i} S_{y_{ip}}}$
Performance index	$P = \frac{\sqrt{\frac{1}{n}\sum_{i=1}^{n}(y_i - y_{ip})^2}}{(1+r)\frac{1}{n}\sum_{i=1}^{n} y_i} * 100$
Mean error	$ME = \frac{1}{n}\sum_{i=1}^{n} y_i - y_{ip} \vee$
Relative approximation error	$RAE = \sqrt{\frac{\sum_{i=1}^{n}(y_i - y_{ip})^2}{\sum_{i=1}^{n} y_i^2}}$
Mean relative approximation error	$MRAE = \sqrt{\frac{1}{n}\frac{\sum_{i=1}^{n}(y_i - \hat{y}_i)^2}{\sum_{i=1}^{n} y_i^2}}$
Mean absolute percentage error	$MAPE = \frac{1}{n}\sum_{i=1}^{n}\left\lvert\frac{y_i - y_{ip}}{y_i}\right\rvert x100$
Mean absolute deviation	$MAD = \frac{1}{n}\sum_{i=1}^{n}\lvert y_i - y_{ip}\rvert$
Coefficient of determination	$R^2 = 1 - \frac{\sum_{i=1}^{n}(y_i - y_{ip})^2}{\sum_{i=1}^{n}(y_{ip} - \overline{y_{ip}})^2}$
Adjusted coefficient of determination	$AdjR^2 = 1 - \frac{\sum_{i=1}^{n}(y_i - y_{ip})^2/(n-1)}{\sum_{i=1}^{n}(y_{ip} - \overline{y_{ip}})^2/(n-p-1)}$
Akaike's information Criterion	$AIC = n.\in\left[\frac{1}{n}\sum_{i=1}^{n}(y_i - y_{ip})^2\right] + 2k$
Corrected Akaike's information criterion	if n/k>40, or $AIC_c = AIC + \frac{2k(k+1)}{n-k-1}$

Statistical Analysis

In the study, a total of seven different data mining algorithms were used, three of which were regression tree-based. Differences among the means of the lactation number (LN) levels for the traits considered in the study were tested using one-way ANOVA. Additionally, the Tukey HSD test was used to identify which LN levels differed significantly. Also, the differences between the 305-day adjusted milk yield and the predictions of each data mining algorithm were compared using a paired t-test. All analyses followed a group 5-fold cross-validation procedure using an individual animal-based strategy rather than an observation-based one. The ALM, C&RT and CHAID algorithms were performed using IBM SPSS Statistics (v23) [40]. In the C&RT and CHAID regression tree algorithms, the minimum parent node size was set to 10 and the minimum child node size to 5. In the RF algorithm, the number of trees (ntree) and mtry were set to 100 and 5, respectively, using the 'randomForest (v4.7.1.1)' package in R [41,42]. For the MARS and Bagging MARS algorithms, the 'caret (v6.0.94)', 'earth (v5.3.4)', and 'mda (v0.5-5)' R packages were used, while the 'brnn (v0.9.0)' package was used to predict MY305 using the BRNN algorithm with three neurons and a tangent hyperbolic activation function [43-45]. Finally, the R package 'ehaGoF (v0.1.1)' was used to calculate the goodness-of-fit criteria [46]. Furthermore, a Bland-Altman analysis was conducted at 95% confidence intervals to evaluate the statistical agreement between data mining algorithms and 305-day adjusted milk yield predictions.

Results

In the present study, some descriptive statistics of partial total ($PART_{15}$, $PART_{30}$, $PART_{45}$, $PART_{60}$, $PART_{75}$) and mean traits of Holstein cows in the first (124 heads), second (75 heads), and third lactation (49 heads) before peak milk yield are presented in *Table 2*.

According to *Table 2*, it is evident that as the number of lactation increases, both total milk yield and partial period milk yields rise significantly (P<0.01). It is an anticipated trend in dairy production that, with increasing LN, the milk yield potential of cows improves until adulthood. Average milk yields follow the same trend, reaching their highest levels particularly in the third lactation. This increase can be attributed to the improvement of cows' physiological capacity with age and the enhanced efficiency of mammary tissue function. Furthermore, the lower coefficient of variation (CV) observed in the third lactation indicates that milk yields are more homogeneous at this stage. Therefore, cows in their third lactation not only achieve higher but also more stable milk production.

C&RT Algorithm

The regression tree diagram of the C&RT algorithm with group 5-fold cross-validation and MY_{305} prediction is given in *Fig. 1*.

Table 2. Descriptive statistics of partial total and average milk yields of Holstein cows in different lactations

Variables	LN	N	Min	Max	$\overline{X} \pm S_{\overline{x}}$	S_x	CV	P-value
MY_{305}	1	124	5345.00	11260.00	7552.00 ± 100.00^{C}	1118.00	14.81	<0.000**
	2	75	5917.00	11577.00	9115.00 ± 138.00^{B}	1199.00	13.15	
	3	49	7891.00	12360.00	9627.00 ± 146.00^{A}	1021.00	10.61	
$PART_{15}$	1	124	165.90	557.40	313.76 ± 5.75^{C}	64.02	20.40	<0.000**
	2	75	172.40	586.70	423.27 ± 9.58^{B}	83.00	19.61	
	3	49	291.10	611.00	462.20 ± 10.30^{A}	72.20	15.61	
$PARTM_{15}$	1	124	11.06	37.16	20.92 ± 0.38^{C}	4.27	20.40	<0.000**
	2	75	11.49	39.11	28.22 ± 0.64^{B}	5.53	19.61	
	3	49	19.41	40.73	30.81 ± 0.69^{A}	4.81	15.61	
$PART_{30}$	1	124	396.90	1186.00	686.20 ± 11.70^{C}	129.90	18.92	<0.000**
	2	75	451.20	1299.30	948.80 ± 19.10^{B}	165.00	17.39	
	3	49	667.50	1370.30	1037.40 ± 21.50^{A}	150.70	14.53	
$PARTM_{30}$	1	124	13.23	39.53	22.87 ± 0.39^{C}	4.33	18.92	<0.000**
	2	75	15.04	43.31	31.63 ± 0.64^{B}	5.50	17.39	
	3	49	22.25	45.68	34.58 ± 0.72^{A}	5.02	14.53	
$PART_{45}$	1	124	661.90	1803.00	1092.30 ± 17.20^{C}	192.10	17.58	<0.000**
	2	75	770.50	2039.50	1502.00 ± 27.50^{B}	238.50	15.88	
	3	49	1114.80	2172.30	1643.00 ± 32.40^{A}	226.70	13.80	
$PARTM_{45}$	1	124	14.71	40.07	24.27 ± 0.38^{C}	4.27	17.58	<0.000**
	2	75	17.12	45.32	33.38 ± 0.61^{B}	5.30	15.88	
	3	49	24.77	48.27	36.51 ± 0.72^{A}	5.04	13.80	
$PART_{60}$	1	124	946.40	2457.00	1514.70 ± 22.60^{C}	251.70	16.62	<0.000**
	2	75	1096.20	2680.00	2049.50 ± 35.50^{B}	307.50	15.00	
	3	49	1627.20	2894.80	2243.90 ± 41.40^{A}	289.70	12.91	
$PARTM_{60}$	1	124	15.77	40.95	25.25 ± 0.38^{C}	4.20	16.62	<0.000**
	2	75	18.27	44.67	34.16 ± 0.59^{B}	5.13	15.00	
	3	49	27.12	48.25	37.40 ± 0.69^{A}	4.83	12.91	
$PART_{75}$	1	124	1257.00	3091.60	1935.70 ± 27.50^{C}	305.90	15.80	<0.000**
	2	75	1438.10	3311.20	2583.40 ± 43.20^{B}	374.30	14.49	
	3	49	2185.10	3588.90	2830.90 ± 48.50^{A}	339.40	11.99	
$PARTM_{75}$	1	124	16.76	41.22	25.81 ± 0.37^{C}	4.08	15.80	<0.000**
	2	75	19.18	44.15	34.45 ± 0.58^{B}	4.99	14.49	
	3	49	29.14	47.85	37.75 ± 0.65^{A}	4.53	11.99	

***(P<0.01; A, B, C; LN: Lactation Number; MY_{305}: 305-day milk yield; PART: Partial milk total; PARTM: Partial milk mean*

The C&RT algorithm generated a total of 24 homogeneous subsets and 5 main branches for the MY_{305} prediction. The most important independent variables are the partial sum $PART_{75}$, $PART_{15}$, $PART_{60}$ and $PART_{45}$, respectively. In the prediction model, partial milk yield means and $PART_{30}$ variables were eliminated by the algorithm because they were not effective in MY_{305} prediction. When the regression tree diagram is carefully analyzed, it is determined that the most important independent variable in MY_{305} prediction is $PART_{75}$. Because 7 of the 12 branches in the tree diagram belong to the $PART_{75}$ feature. In other words, the independent variable $PART_{75}$ contributes more to the MY_{305} prediction than other variables.

The root node (Node 0) is branched into less (Node 1) and more (Node 2) than 2367.75 *l* of $PART_{75}$ feature. It was estimated that if the total milk yield ($PART_{75}$) of lactating animals in the first 75 days was less than 2367.75 *l*, 7436.818 *l*, and if it was more than 2367.75 *l*, the animals

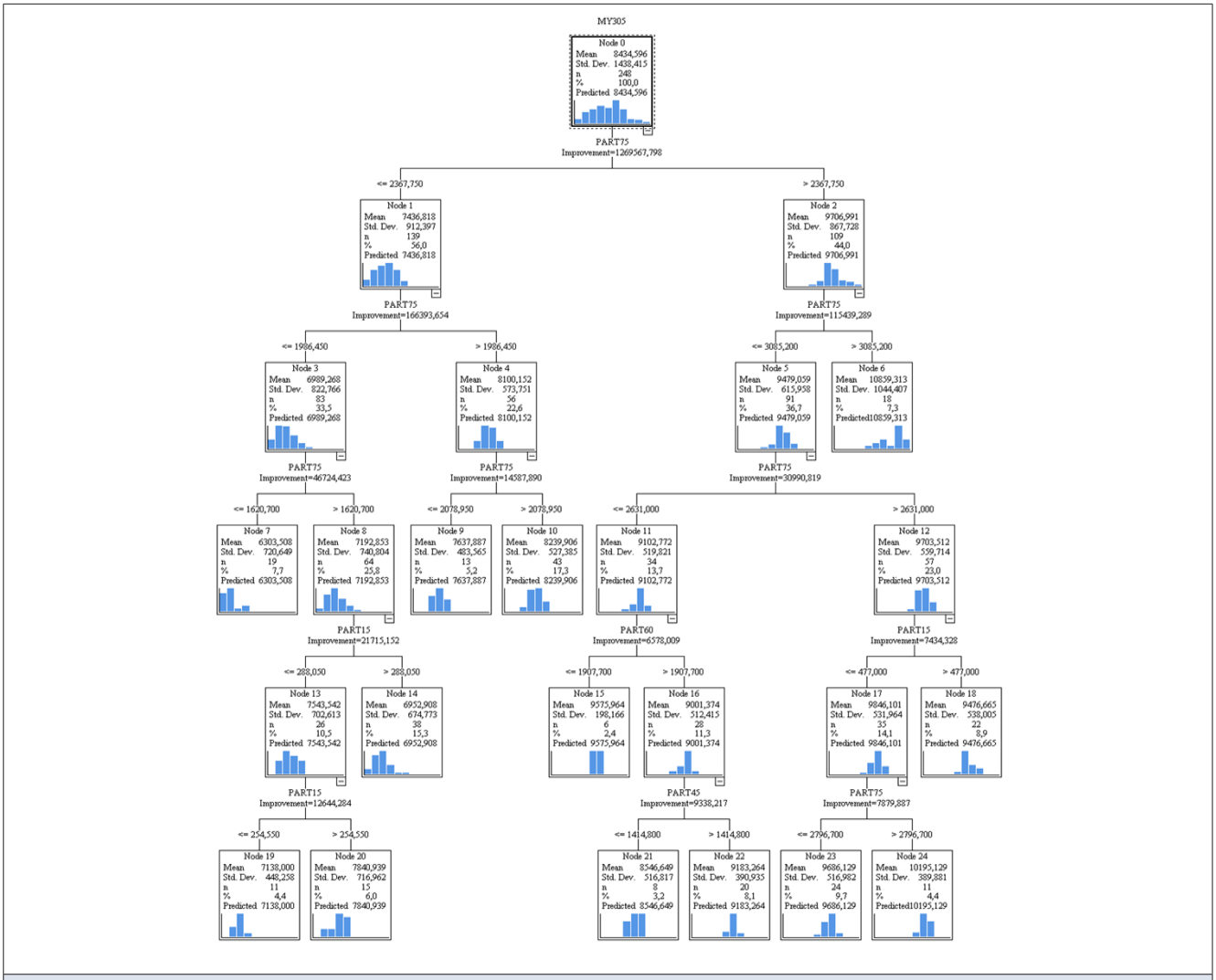

Fig 1. Classification tree diagrams constructed by C&RT for MY_{305} (Group cross-validation 5 parent 10 child node 5)

would reach a milk yield of 9706.991 *l*. In the regression diagram, the highest MY_{305} prediction occurred at node 24. If the total milk yield in the first 15 days of lactation ($PART_{15}$) was lower than 477 *l* and the total milk yield in the first 75 days ($PART_{75}$) was higher than 2796.70 *l*, it was predicted to reach 10195.129 *l* milk yield after 305 days (Node 24). The lowest MY_{305} was estimated as 6303.508 *l* when total milk yield in the first 75 days ($PART_{75}$) was lower than 1620.70 *l* (Node 7).

MARS Algorithm

MY_{305}, the parameter results of the model obtained using the MARS algorithm are given in *Table 3*.

In the MY_{305} MARS algorithm prediction equation, $PART_{75}$, LN_3, $PART_{15}$, $PARTM_{15}$, $PARTM_{15}$, $PARTM_{75}$, $PARTM_{45}$, $PART_{60}$ and $PARTM_{60}$ independent variables and 12 basis functions were used. The MARS algorithm does not use a single variable as the main variable but uses binary and triple interactions. In the MARS prediction equation, the basis functions BF_5, BF_7, BF_8, BF_{10} and

Table 3. *MARS algorithm prediction equation of MY_{305}*

Functions	Terms	Coefficients
BF_1	Intercept	8930.00
BF_2	max(0, $PART_{75}$ - 2536) x LN_3	-1.180
BF_3	max(0, 546 - $PART_{15}$) x max(0, $PARTM_{15}$ - 31.3)	-5.650
BF_4	max(0, 546 - $PART_{15}$) x max(0, 25.9 - $PARTM_{75}$)	-4.270
BF_5	max(0, 25.1 - $PARTM_{45}$) x max(0, 2536 - $PART_{75}$)	+0.425
BF_6	max(0, $PART_{60}$ - 1219) x max(0, $PARTM_{60}$ - 31.8)	-0.314
BF_7	max(0, $PART_{60}$ - 1219) x max(0, 31.8 - $PARTM_{60}$)	+1.250
BF_8	max(0, $PART_{60}$ -1219) x max(0, $PART_{75}$ - 2404)	+0.00646
BF_9	max(0, $PART_{60}$ - 1219) x max(0, 2404 - $PART_{75}$)	-0.0262
BF_{10}	max(0, 546 - $PART_{15}$) x max(0, 31.3 - $PARTM_{15}$) x max(0, 1522 - $PART_{60}$)	+0.00127
BF_{11}	max(0, 25.1- $PARTM_{45}$) x max(0, $PART_{60}$ - 1327) x max(0, 2536 - $PART_{75}$)	+0.00757
BF_{12}	max(0, 25.1- $PARTM_{45}$) x max(0, 2536 - $PART_{75}$) x max(0, $PARTM_{75}$ - 22.8)	-0.493

BF_{11} contributed positively to MY_{305}, while the remaining basis functions had a negative effect. For the MARS algorithm to work, the basis functions must take values within the range of the specified constraints. Otherwise, it does not affect the dependent variable (MY_{305}) and can be considered as a zero contribution. As can be seen from *Table 3*, the MARS algorithm, in the BF1 function (Intercept), predicted the MY_{305} milk yield to be 8930 *l* if other functions were not working. In BF_2, it was predicted that the MY_{305} milk yield would decrease if the total milk yield of animals in their third lactation was less than 2536 *l* in the first 75 days. A total milk yields greater than 2536 *l* in the first 75 days of animals in their third lactation can be considered an indirect selection criterion for the MY_{305} trait. Since the regression coefficient in BF_3 is negative (-5.650), regardless of the number of lactation, it is desired that the total milk yield of animals in the first 15 days be greater than 546 *l*, while the average milk yield in the first 15 days is expected to be greater than 31.3 *l*. The cutoff points determined for total and average milk yields in the first 15 days for dairy cows can be used as practical information in herd management and feeding. In short, the MARS algorithm prediction equation of MY_{305} (*Table 3*) was given that the product of the coefficient and the related variables indicates the contribution of that term to the estimated milk yield. To avoid the complexity of the MARS algorithm model and to make it more understandable, the MY_{305} estimate is made in *Table 4* using the independent variables of a random dairy cow in the dataset. The independent variables of the randomly selected 3rd lactation (LN_3) dairy cattle were $PART_{15}$=442.70 *l*, $PART_{30}$=979.60 *l*, $PART_{45}$=1514.70 *l*, $PART_{60}$=2086.50 *l*, $PART_{75}$=2696.50 *l* and $PARTM_{15}$=29.51 *l*, $PARTM_{30}$=32.65 *l*, $PARTM_{45}$=33.66 *l*, $PARTM_{60}$=34.78 *l*, and $PARTM_{75}$=35.95 *l*, respectively. Accordingly, the MARS algorithm MY_{305} prediction calculation process details are given in *Table 4*.

While the MY_{305} of the dairy cattle randomly selected from the data set was 9799.92 *l* in reality, it was estimated as 9568.05 liters as a result of the MARS algorithm. In making this prediction, it was found that the MARS algorithm made predictions using only BF_1, BF_2, BF_6 and BF_8 basis functions.

Variable Importance Results of Data Mining Algorithms

Table 5 shows the sensitivity analysis results for each

Table 4. *MARS algorithm prediction of MY_{305} of a random dairy cattle selected from dataset*

Functions	Algorithm Terms and Calculations	Coefficients	Contribution to MY_{305}
BF_1*	Intercept	**8930.00**	**8930.00**
BF_2*	(0, $PART_{75}$ - 2536) * LN_3 (0, 2696.50 - 2536) * 1 = 160.50*1 = **160.50**	**- 1.180**	- 1.180*160.50= - **189.39**
BF_3	(0, 546 - $PART_{15}$) * (0, $PARTM_{15}$ - 31.3) (0, 546 - 442.70) * (**0**, 25.84 – 29.51) = 103.30*0 = 0	- 5.650	- 5.650*0=0
BF_4	(0, 546 - $PART_{15}$) * (0, 25.9 - $PARTM_{75}$) (0, 546 - 442.70) * (**0**, 25.9 – 35.95) = 103.30*0 = 0	- 4.270	- 4.270*0=0
BF_5	(0, 25.1 - $PARTM_{45}$) * (0, 2536 - $PART_{75}$) (**0**, 25.1 – 33.66) * (**0**, 2536 - 2696.50) = 0*0 = 0	+ 0.425	+ 0.425*0=0
BF_6*	(0, $PART_{60}$ - 1219) * (0, $PARTM_{60}$ - 31.8) (0, 2086.50 - 1219) * (0, 34.78 - 31.8) = 867.50*2.98 = **2585.15**	**- 0.314**	- 0.314*2585.15 = - **811.74**
BF_7	(0, $PART_{60}$ - 1219) * (0, 31.8 - $PARTM_{60}$) (0, 2086.50 - 1219) * (**0**, 31.8 – 34.78) = 867.50*0 = 0	+ 1.250	+ 1.250*0 = 0
BF_8*	(0, $PART_{60}$ -1219) * (0, $PART_{75}$ - 2404) (0, 2086.50 - 1219) * (0, 2696.50 - 2404) = 867.50*292.50 = **253743.75**	**+ 0.00646**	+ 0.00646*253743.75= + **1639.18**
BF_9	(0, $PART_{60}$ - 1219) * (0, 2404 - $PART_{75}$) (0, 2086.50 - 1219) * (**0**, 2404 - 2696.50) = 867.50 * 0 = 0	- 0.0262	- 0.0262*0 = 0
BF_{10}	(0, 546 - $PART_{15}$) * (0, 31.3 - $PARTM_{15}$) * (0, 1522 - $PART_{60}$) (0, 546 - 442.70) * (0, 31.3 - 29.51) * (**0**, 1522 - 2086.50) = 103.30*1.79*0 = 0	+ 0.00127	+ 0.00127*0 = 0
BF_{11}	(0, 25.1- $PARTM_{45}$) * (0, $PART_{60}$ - 1327) * (0, 2536 - $PART_{75}$) (**0**, 25.1- 33.66) * (0, 2086.50 - 1327) * (**0**, 2536 – 2696.50) = 0*759.50*0 = 0	+ 0.00757	+ 0.00757*0 = 0
BF_{12}	(0, 25.1- $PARTM_{45}$) * (0, 2536 - $PART_{75}$) * (0, $PARTM_{75}$ - 22.8) (**0**, 25.1- 33.66) * (**0**, 2536 - 2696.50) * (0, 35.95 - 22.8) = 0*0*13.15 = 0	- 0.493	- 0.493*0 = 0
	Prediction	**= 8930.00 - 189.39 - 811.74 + 1639.18 = 9568.05**	

** The basic functions and operations used in MY_{305} prediction calculation were given in bold*

data mining algorithm in order to predict the variable importance values of the independent variables of MY_{305}.

In MY_{305}, $PART_{75}$ independent variable had the highest relative importance value in ALM (61.90%) algorithm, followed by MARS (41.49%) and BRNN (12.34%) algorithms. In $PARTM_{30}$ independent variable, Bagging had the highest relative importance value with MARS (28.87%), while RF (14.21%) algorithm had the highest relative importance value in $PARTM_{75}$. In addition, the highest and lowest percentages of the independent variables included in the model of ALM, RF, MARS, Bagging MARS and BRNN algorithms used in the current study were 61.90-5.30%, 14.21-5.21%, 41.49-3.19%, 28.87-0.01% and 12.34-6.79%, respectively. ALM ($PART_{15}$, $PARTM_{15}$, $PART_{30}$, $PARTM_{30}$, $PART_{45}$, $PARTM_{60}$ and $PARTM_{75}$), MARS ($PART_{30}$, $PARTM_{30}$, $PART_{45}$ and $PARTM_{45}$), and BRNN algorithm (LN) independent variables were included in the model, while all independent variables were included in the model in RF and Bagging MARS algorithms.

Table 5. *Variable importance of data mining algorithms*

Variables	ALM	RF	MARS	Bagging MARS	BRNN
$PART_{15}$	0.00%	10.35%	3.19%	3.86%	6.79%
$PARTM_{15}$	0.00%	7.62%	4.63%	0.26%	6.79%
$PART_{30}$	0.00%	5.21%	0.00%	8.66%	9.13%
$PARTM_{30}$	0.00%	6.24%	0.00%	28.87%	9.13%
$PART_{45}$	0.00%	6.82%	0.00%	13.98%	10.31%
$PARTM_{45}$	0.00%	6.87%	0.00%	0.31%	10.31%
$PART_{60}$	32.80%	10.91%	32.34%	19.19%	11.43%
$PARTM_{60}$	0.00%	11.50%	9.46%	0.32%	11.43%
$PART_{75}$	61.90%	14.16%	41.49%	24.22%	12.34%
$PARTM_{75}$	0.00%	14.21%	4.24%	0.32%	12.34%
LN	5.30%	6.13%	4.65%	0.01%	0.00%

Prediction Performances of Data Mining Algorithms

The performance criteria values of data mining algorithms are presented in *Table 6*.

The difference between the 305-day adjusted milk yield and the predictions of the data mining algorithms was found to be statistically nonsignificant (P>0.05). According to *Table 6*, we found that MARS, Bagging MARS, C&RT, ALM, BRNN, CHAID, and RF were the data mining algorithms with the best prediction performance when we combined the model evaluation criteria, which include systematic bias and limits of agreement (LoA) among prediction performance indicators. When all algorithms are compared, the results obtained from the MARS algorithm of the algorithm with the best criteria in terms

Table 6. *Predictive performance of data mining algorithms*

Model Performance Criteria	ALM	C&RT	CHAID	RF	MARS	Bagging MARS	BRNN
RMSE	593.408	592.790	675.514	734.114	550.754	552.227	595.225
RRMSE	7.035	7.028	8.009	8.704	6.530	6.547	7.057
SDR	0.413	0.413	0.471	0.511	0.384	0.385	0.415
CV	7.050	7.040	8.030	8.720	6.540	6.560	7.070
r	0.911	0.911	0.882	0.860	0.923	0.923	0.910
PI	3.682	3.678	4.255	4.680	3.395	3.404	3.695
Bias (ME)	-1.782	-0.001	0.000	4.150	0.000	2.832	-1.645
RAE	0.005	0.005	0.006	0.007	0.004	0.004	0.005
MRAE	0.004	0.004	0.005	0.005	0.004	0.004	0.004
MAPE	5.680	5.542	6.530	6.924	5.182	5.103	5.730
MAD	469.352	453.917	537.991	570.093	427.008	421.737	472.576
R^2	0.829	0.829	0.779	0.738	0.853	0.852	0.828
R^2_{adj}	0.828	0.828	0.777	0.738	0.844	0.840	0.828
AIC	3171.398	3170.881	3235.675	3272.937	3158.399	3167.724	3168.914
AIC_c	3171.447	3170.930	3235.724	3272.937	3160.202	3170.711	3168.914
LoA	±1163.08	±1161.87	±1324.01	±1438.86	±1079.48	±1082.36	±1166.64
P-value	0.962	0.999	1.000	0.929	1.000	0.936	0.965

RMSE; Root mean square error, RRMSE; Relative root mean square error, SDR; Standard deviation ratio, CV; Coefficient of variation, r; Pearson's correlation coefficients, PI; Performance index, ME; Mean error; RAE, Relative approximation error, MRAE; Mean relative approximation error, MAPE; Mean absolute percentage error; MAD; Mean absolute deviation, R^2; Coefficient of determination, R^2_{adj}; Adjusted coefficient of determination, AICc; Akaike's information criterion, CAI_C; Corrected Akaike's information criterion, LoA; Lower-Upper limits of agreement

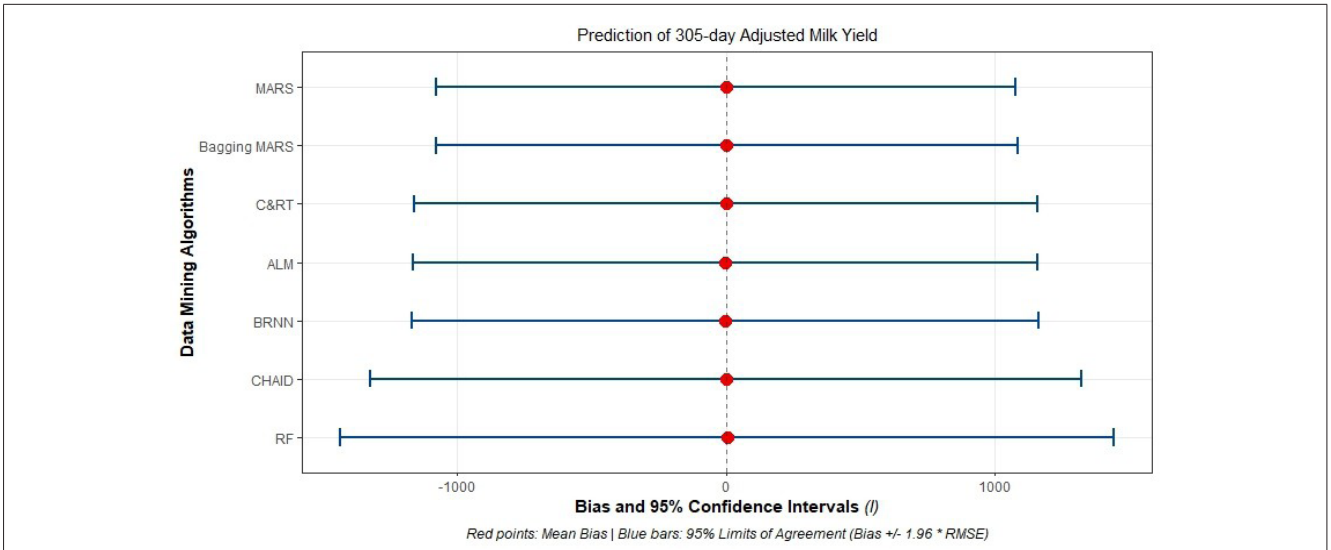

Fig 2. Bland-Altman statistical limits of agreement (LoA) for 305-day adjusted milk yield prediction by data mining algorithms

of performance criteria; high Pearson correlation coefficient (0.92), R^2 (85.3%), R^2_{adj} (84.4%), low MAPE (5.18%), SD ratio (0.38), RMSE (550.75), RAE (0. 004), CV (6.54%) and AIC (3158.39), while the Bagging MARS algorithm with the second best performance criteria was found as high Pearson correlation coefficient (0.92), R^2 (85.2%), R^2_{adj} (84.00%), low MAPE (5.10%), SD ratio (0.38), RMSE (552.22), RAE (0.004), CV (6.56%) and AIC (3167.72). In addition, the best performing tree algorithm is the C&RT algorithm with performance criteria of 0.91, 82.9%, 82.8%, 5.54%, 0.41, 592.79, 0.005, 7.04% and 3170.88 in the same order. These algorithms were followed by ALM, BRNN, CHAID and RF algorithms in terms of performance criteria.

The Bland-Altman statistical (LoA) for 305-day adjusted milk yield estimation using data mining algorithms are given in *Fig. 2*.

In predicting adjusted milk yield over 305 days, the MARS, CHAID, and C&RT algorithms were found to provide unbiased predictions as they were quite close to the zero point. The Bagging MARS and RF algorithms exhibited low positive bias, while the ALM and BRNN algorithms showed negative bias. When data mining algorithms were evaluated based on their prediction precision, the 95% confidence interval was found to be as follows: MARS, Bagging MARS, C&RT, ALM, BRNN, CHAID, and RF.

Discussion

Traditional methods for predicting milk yield are widely used in the literature [5,6]. Nowadays, studies are being focused on different algorithms other than traditional milk yield methods, but they are still limited. Studies evaluating the efficacy of novel methodologies in animal husbandry are currently insufficient. Traditional lactation curve models are defined by mathematical functions such as constant, exponential or gamma. These models are successful in plotting the average curve at the population level. However, they lack flexibility in capturing individual variations at the onset of lactation, abrupt peak deviations, and irregularities due to environmental factors. High variance and stochastic variations at the onset of lactation, which classical regression models cannot explain, can be predicted with a lower margin of error (RMSE) using machine learning algorithms [47]. However, these innovative approaches, which can replace complex traditional models, may play a crucial role in preventing anomalies in animal care and feeding management. For instance, continuous monitoring of milk yield at the individual or herd level not only provides detailed insights into health and nutritional requirements but also establishes a robust data foundation that supports decisions regarding culling or selection. Researchers are working intensively on algorithms with high predictive power that will help breeders make early and rapid decisions in herd management.

Salehi et al.[48] employed conventional artificial neural networks (ANNs) to classify monthly milk yield records into two categories such as high yield (≥9000 kg) and low yield (<9000 kg). The study compared two distinct classifier models one trained on records spanning the entire yield range, and another trained exclusively on records concentrated around the 9000 kg threshold. The results demonstrated that the classifier trained on threshold-specific records achieved markedly higher accuracy (99.7%) compared with the general classifier (92.3%). Grzesiak et al.[49], in the study of MY305 prediction using partial lactation records, examined the artificial neural networks (ANN) and multiple linear regression (MLR) model for cows in their 1st, 2nd or 3rd lactation and lactation

duration not less than 200 days. They found that $R^2 = 0.87$ for MLR and $R^2 = 0.85$ for the test set, and the partial regression coefficients were significant at $P \leq 0.01$. The mean prediction error (MEP) for 305-day lactation yield was determined as MLR (7.4%) and ANN (6.9%), and the mean milk yield for 305-day lactation predicted by ANN was 13.12 *l* lower than the mean actual yield of 49 control cows, while the mean difference in MLR was -91.33 *l*. The same researchers reported that the predictions made by neural network or multiple regression model were not different from the values predicted by the current traditional evaluation system ($P>0.05$). Sharma et al.[50] used an artificial neural network (ANN) to predict first lactation 305-day milk yield using partial lactation records of Karan Fries crossbred dairy cattle and reported that the best training algorithm was the 'Levenberg-Marquardt algorithm with Bayesian adjustment', which achieved more than 92% prediction accuracy, which was comparatively higher than the traditional MLR model. Eyduran et al.[11] evaluated the relationship between 305-day milk yield and various environmental factors (calving season, calving year, number of births, calving interval, and dry period) of 645 head Brown Swiss cattle from 1884 lactation records using the Regression Tree method. They found that year of calving was statistically the most effective factor on 305-day milk yield of Brown Swiss cattle, followed by parity and calving interval in the regression tree diagram ($P<0.01$). As a result, they reported that among the cows, those with more than 352 calving intervals had higher yields with an average of 3629.345 *l* and cows with more than 2 parities had higher yields than cows with 1 and 2 parities. Akıllı and Atıl [51] in their study titled evaluation of normalization techniques on artificial neural networks for prediction of 305-day milk yield in Holstein Friesen cows, comparatively tested eight normalization techniques and five different back propagation algorithms. They reported that the Bayesian Regularization algorithm and the Decimal Scaling normalization technique had the best performance ($R^2_{Adj} = 0.8181$, RMSE = 0.0068, MAPE = 160.42 for the test set; $R^2_{Adj} = 0.8141$, RMSE = 0.0067, MAPE = 114.12 for the validation set). Usman et al. [52] compared the performance of three different artificial neural network algorithms for the prediction of 305-day milk yield in the first lactation of 1092 head of Vrindavani crossbred cattle and used two different input sets in the analysis to predict milk yield. For the first input set, the R^2 values of Bayesian Regularization (BR), Levenberg Marquardt (LM) and Scaled Conjugate Gradient (SCG) algorithms were found to be 79.89%, 73.65% and 74.65% respectively, while the lowest RMSE values were 16.89, 20.52 and 20.45 respectively. For the second input set-2, the R^2 values of BR, LM and SCG algorithms were found to be 82.67%, 74.22% and 76.69% respectively, while the lowest RMSE values were reported as 14.45%, 17.45% and 16.56% respectively. As a result, they emphasized that BR algorithm can be used to predict 305-day milk yield in the first lactation in crossbred cattle since it shows higher accuracy than LM and SCG algorithms. Genç and Mendeş [21] reported that the most influential factors affecting 305-day milk yield were breed, lactation period, province, and parity. They found that the Automated Linear Model (ALM) achieved an accuracy rate of 64.2%. Furthermore, they emphasized that the ALM approach was particularly effective in identifying the determinants of the outcome variable, especially when dealing with large and complex datasets containing numerous predictors. Boğa [53] used MARS and Bagging MARS algorithms to create a lactation model for 305-day milk yield in dairy cattle. The prediction performance values for the Mars algorithm were r (0.988), R^2 (96.8%), Adj- R^2 (96.8%), low MAPE (1.374%), SD ratio (0.178), RMSE (10.204) and AIC (143. 073), while Bagging MARS algorithm had r (0.762), R^2 (43.6%), Adj- R^2 (43.5%), low MAPE (4.515%), SD ratio (0.751), RMSE (7.364) and AIC (735.927). The researcher reported that the MARS algorithm gave better results in modeling milk yield for 305-day lactation. Liseune et al.[54] suggested a model to predict the entire lactation curve of dairy cows by leveraging historical lactation milk yield information observed in the preceding cycle by using deep learning. They concluded that the ANN model, in addition to herd statistics, can predict the entire lactation curve of a cow in the next cycle by using the cow's past milk yield sequence and reproductive and health events from the previous cycle. This advantage of these algorithms also highlights their current applicability in herd management programs. Boğa et al.[16] investigated seasonal milk yield predictions using MARS algorithm in 157 head Holstein cross breeds. The three threshold values determined in the model were number of days milked (159 days), age (39.6 months), and peak yield (37.1 kg). They also determined that the number of days milked, average seven-day milk yield and lactation number are the most important variables in determining the prediction equation, and the most appropriate value for the prediction equation of the dependent variables is the winter milk yield variable.

In conclusion, in the studies conducted, the differences in the results of calculating or estimating real milk yields in both data mining and traditional methods vary depending on the size of the data used and the methods. However, in model comparisons, the criteria for the goodness of fit of RMSE, RRMSE, RAE, CV, MRAE, MAPE, SDR, and MAD should generally be very close to 0 and the closeness of r, R^2, and Adj- R^2 values to 1 should be taken into account. In this respect, comparisons should be made and the most appropriate algorithm and model should be selected. Furthermore, the bias and precision of algorithm predictions must also be considered. Among

the algorithms considered in the study, it can be said that the MARS and Bagging MARS algorithms were more preferable than the others. MARS and Bagging MARS algorithms can be integrated into existing herd management systems to overcome their complexities. Some herd management systems already have simple regression-based predictions in their software. Integrating these models into decision support tools within herd management software used in farms can support early decision-making mechanisms in herd management programs such as maintenance and feeding, thereby increasing dairy farm profitability. To the best of our knowledge, there are only a limited number of studies in the literature that employ algorithms based on partial lactation records, and this study represents the first to use such algorithms with partial lactation data. These findings may help producers assess the impact of historical milk yields on future cow productivity and predict overall herd performance, thereby facilitating timely and informed decision-making. Briefly, by using these algorithms in herd management, early culling of cows from the herd could facilitate the rapid integration of genetically superior individuals, thereby supporting increased productivity and offering the potential to enhance the herd's average performance. Furthermore, this practice accelerates genetic progress, too.

Declarations

Availability of Data and Materials: The datasets and analyzed during the current study available from the corresponding author (ÖŞ) on reasonable request.

Ethical Statement: As this study was conducted within the scope of non-experimental agricultural practices, ethical committee approval was not required. Also, no animals were used in laboratory procedures, and therefore, no violation of animal rights is involved.

Funding Support: No funding was received for this study.

Conflict of Interest: The authors declare that they have no conflicts of interest. All authors have given their consent that this work is valid and represent their views of the study and have given their consent for this work to be published.

Declaration of Generative Artificial Intelligence (AI): The authors declare that the article, tables and figures were not written/created by AI and AI-assisted Technologies.

Authors Contribution: ÖŞ, YA and IA contributed to the conceptualization, design and writing of the study. RAD contributed to the writing of the methodology part of the study and the evaluation of the statistical analysis results. GÇ contributed to the collection of literature and the correction of the study. All authors have written, read and agreed to the published version of the manuscript.

References

1. **FAO:** FAOSTAT. http://www.fao.org/faostat/en/#data/QL; *Accessed:* 01.11.2024.
2. **Gök Y, Şahin M, Yavuz E:** Comparatıve analysıs of indıvıdual lactatıon curve models in some cattle breeds. *KSU J Agric Nat,* 24 (5): 1118-1125, 2021. DOI: 10.18016/ksutarimdoga.vi.845660
3. **Orhan H, Kaygısız A:** Comparison of different lactation curve models for Holstein cattle. *Anim Prod,* 43 (1): 94-99, 2002.
4. **Boztepe S, Aytekin İ, Zülkadir U:** Dairy Cattle. Selçuk University Press, Konya, Türkiye, 2015.
5. **Keskin İ, Boztepe S:** Prediction of 305 days milk yield using partial milk yield in Holstein cattle. *JOTAF,* 8 (1): 1-7, 2011.
6. **Altay Y:** Prediction of (Actual) 305 days milk yield using different lactation milk yield prediction methods and partial milk yield in Holstein cattle. **In**, 4th *International Conference on Agriculture Animal Science and Rural Development,* June 12-14, 47-55, Ankara, Türkiye, 2020.
7. **Girdauskaitė A, Arlauskaitė S, Rutkauskas A, Džermeikaitė K, Krištolaitytė J, Televičius M, Malašauskienė D, Anskienė L, Japertas S, Antanaitis R:** In-line monitoring of milk lactose for evaluating metabolic and physiological status in early-lactation dairy cows. *Life,* 15 (8): 1204, 2025. DOI: 10.3390/life15081204
8. **Kellogg DW, Urquhart NS, Ortega AJ:** Estimating Holstein lactation curves with a gamma curve. *J Dairy Sci,* 60 (8): 1308-1315, 1977. DOI: 10.3168/jds.S0022-0302(77)84028-9
9. **Coşkun G, Şahin Ö, Altay Y, Aytekin İ:** Final fattening live weight prediction in Anatolian Merinos lambs from some body characteristics at the initial of fattening by using some data mining algorithms. *BSJ Agri,* 6 (1): 47-53, 2023. DOI: 10.47115/bsagriculture.1181444
10. **Coşkun G, Aytekin İ:** Early detection of mastitis by using infrared thermography in Holstein-Friesian dairy cows via classification and regression tree (CART) analysis. *Selcuk J Agr Food Sci,* 35 (2): 115-124, 2021. DOI: 10.15316/SJAFS.2021.237
11. **Eyduran E, Zaborski D, Waheed A, Celik S, Karadas K, Grzesiak W:** Comparison of the predictive capabilities of several data mining algorithms and multiple linear regression in the prediction of body weight by means of body measurements in the indigenous Beetal goat of Pakistan. *Pak J Zool,* 49, 257-265, 2017. DOI: 10.17582/journal.pjz/2017.49.1.257.265
12. **Ali M, Eyduran E, Tariq MM, Tirink C, Abbas F, Bajwa MA, Jan S:** Comparison of artificial neural network and decision tree algorithms used for predicting live weight at post weaning period from some biometrical characteristics in Harnai sheep. *Pak J Zool,* 47 (6): 1579-1585, 2015.
13. **Tırınk C, Eyduran E, Faraz A, Waheed A, Tauqir NA, Nabeel MS, Sheikh IS:** Use of multivariate adaptive regression splines for prediction of body weight from body measurements in Marecha *(Camelus dromedaries)* camels in Pakistan. *Trop Anim Health Prod,* 53: 339, 2021. DOI: 10.1007/s11250-021-02788-y
14. **Coşkun G, Şahin Ö, Ozkan İA, Aytekin İ:** Comparison of data mining algorithms used in predictive of live weight from body measurements in Holstein cattle at different growth and development periods. *Agric Eng,* 375, 37-46, 2022. DOI: 10.33724/zm.1092837
15. **Tırınk C:** Comparison of bayesian regularized neural network, random forest regression, support vector regression and multivariate adaptive regression splines algorithms to predict body weight from biometrical measurements in Thalli sheep. *Kafkas Univ Vet Fak Derg,* 28 (3): 411-419, 2022. DOI: 10.9775/kvfd.2022.27164
16. **Boğa DÇ, Boğa M, Bulut M:** Forecasting seasonal milk production using MARS algorithm for multiple continuous responses in Holstein dairy cattles. *BSJ Agri,* 7 (2): 25-26, 2024. DOI: 10.47115/bsagriculture.1383832
17. **Kibar M:** A cheaply non-destructive technique to estimate honey quality: thermal imaging and machine learning. *Uludağ Bee J,* 24, 79-92, 2024. DOI: 10.31467/uluaricilik.1429971
18. **Kibar M, Altay Y, Aytekin İ:** Exploring the integration of thermal imaging technology with the data mining algorithms for precise prediction of honey and beeswax yield. *Anim Sci J,* 95:e70015, 2024. DOI: 10.1111/asj.70015
19. **Şahin Ö:** Evaluation of some factors on birth and weaning weights in

Awassi sheep by using GLM and CART analysis. *Trop Anim Health Prod,* 54:400, 2022. DOI: 10.1007/s11250-022-03405-2

20. **Akman N, Eliçin A:** Record Keeping and Evaluation in Dairy Cattle Farming. Ministry of Agriculture, Forestry and Rural Affairs, General Directorate of Agricultural Enterprises, Advanced Techniques in Livestock Seminar, pp 304-327, Tahirova-Gönen. Ankara University, Faculty of Agriculture, Offset Unit, Ankara, Türkiye, 1984.
21. **Genç S, Mendeş M :** Linear modeling analysis using for determining the factors affecting 305-day milk yield. *Arq Bras Med Vet Zootec*, 73, 949-954, 2021. DOI: 10.1590/1678-4162-12346
22. **Breiman L, Friedman JH, Olshen RA, Stone CJ:** Classification and Regression Trees. Chapman and Hall/CRC. 1984.
23. **Altay Y:** Phenotypic characterization of hair and honamli goats using classification tree algorithms and multivariate adaptive regression spline (MARS). *Kafkas Univ Vet Fak Derg,* 28 (3): 401-410, 2022. DOI: 10.9775/kvfd.2022.27163
24. **Loh WY, Shih YS:** Split selection methods for classification trees. *Statistica Sinica,* 7, 815-840. 1997.
25. **Hastie T, Tibshirani R, Friedman J:** The Elements of Statistical Learning: Data Mining, Inference, and Prediction. 2nd ed. Springer, 2009.
26. **Kass GV:** An exploratory technique for investigating large quantities of categorical data. *J R Stat Soc Ser C-Appl Stat,* 29 (2): 119-127, 1980. DOI: 10.2307/2986296
27. **Loh WY:** Fifty years of classification and regression trees. *Inter Stat Rev,* 82 (3): 329-348, 2014. DOI: 10.1111/insr.12016
28. **Olfaz M, Tirink C, Önder H:** Use of CART and CHAID algorithms in Karayaka sheep breeding. *Kafkas Univ Vet Fak Derg,* 25 (1): 105-110, 2019. DOI: 10.9775/kvfd.2018.20388
29. **Breiman L:** Random forests. *Mach Learn,* 45, 5-32, 2001. DOI: 10.1023/A:1010933404324
30. **Cutler DR, Edwards Jr TC, Beard KH, Cutler A, Hess KT, Gibson J, Lawler JJ:** Random forests for classification in ecology. *Ecology,* 88 (11): 2783-2792, 2007. DOI: 10.1890/07-0539.1
31. **Friedman J:** Multivariate adaptive regression splines. *Ann Stat,* 19 (1): 1-67, 1991. DOI: 10.1214/aos/1176347963
32. **Zhang W, Goh AT, Zhang Y:** Multivariate adaptive regression splines application for multivariate geotechnical problems with big data. *Geotech Geol Eng,* 34, 193-204, 2016. DOI: 10.1007/s10706-015-9938-9
33. **Jekabsons G:** VariReg: A Software Tool for Regression Modeling Using Various Modeling Methods. Riga Technical University, Latvia, 2010.
34. **Akın M, Eyduran SP, Eyduran E:** MARS Algorithm in Solving Regression and Classification Type Problems in Agricultural Sciences with R Software. Ankara Nobel Yayın. 2020.
35. **Arleina O, Otok B:** Bootstrap aggregating multivariate adaptive regression splines (Bagging MARS) for poor households classification in region of Jombang. *SSRN Electronic J,* 2014:1-6, 2014. DOI: 10.2139/ssrn.2489898
36. **Burden F, Winkler D:** Bayesian regularization of neural networks. Artificial neural networks: Methods and applications. Humana Press, Totowa, NJ. 23-42. 2009.
37. **Zhang W, Goh ATC:** Multivariate adaptive regression splines and neural network models for prediction of pile drivability. *Geosci Front,* 7 (1): 45-52, 2016. DOI: 10.1016/j.gsf.2014.10.003
38. **Zaborski D, Ali M, Eyduran E, Grzesiak W, Tariq MM, Abbas F, Waheed A, Tirink C:** Prediction of selected reproductive traits of indigenous Harnai sheep under the farm management system via various data mining algorithms. *Pak J Zool,* 51 (2): 421-431, 2019. DOI: 10.17582/journal.pjz/2019.51.2.421.431
39. **Altay Y:** Prediction of the live weight at breeding age from morphological measurements taken at weaning in indigenous Honamli kids using data mining algorithms. *Trop Anim Health Prod,* 54 (3):172, 2022. DOI: 10.1007/s11250-022-03174-y
40. **IBM Corp:** IBM SPSS statistics for Windows, version 23.0. Armonk, NY: IBM Corp. 2015.
41. **Liaw A, Wiener M:** Classification and regression by random forest. *R News,* 2 (3): 18-22, 2002.
42. **R Core Team:** R: A language and environment for statistical computing. R Foundation for Statistical Computing, Vienna, Austria. https://www.R-project.org/; *Accessed:* 15.03.2025.
43. **Kuhn M:** caret: Classification and regression training. Version 6.0-93 [R package]. https://CRAN.R-project.org/package=caret; *Accessed:* 20.12.2024.
44. **Milborrow S:** "earth: Multivariate adaptive regression splines". Version 5.3.4 [R package]. https://CRAN.R-project.org/package=earth; *Accessed:* 05.01.2025.
45. **Hastie T, Tibshirani R:** "mda: Mixture and flexible discriminant analysis". Version 0.5-5 [R package]. https://CRAN.R-project.org/package=mda; *Accessed:* 10.12.2024.
46. **Eyduran E:** ehaGoF: Calculates goodness of fit statistics. Version 0.1.1 [R package]. https://CRAN.R-project.org/package=ehaGoF; *Accessed:* 12.01.2025.
47. **Guevara L, Castro-Espinoza F, Fernandes AM, Benaouda M, Muñoz-Benítez AL, del Razo-Rodríguez OE, Peláez-Acero A, Angeles-Hernandez JC:** Application of machine learning algorithms to describe the characteristics of dairy sheep lactation curves. *Animals,* 13 (17):2772, 2023. DOI: 10.3390/ani13172772
48. **Salehi F, Lacroix R, Wade KM:** Improving dairy yield predictions through combined record classifiers and specialized artificial neural networks. *Comput Electron Agric,* 20 (3): 199-213, 1998. DOI: 10.1016/S0168-1699(98)00018-0
49. **Grzesiak W, Lacroix R, Wójcik J, Blaszczyk P:** A comparison of neural network and multiple regression predictions for 305-day lactation yield using partial lactation records. *Can J Anim Sci,* 83 (2): 307-310, 2003. DOI: 10.4141/A02-00
50. **Sharma AK, Sharma RK, Kasana HS:** Prediction of first lactation 305-day milk yield in Karan Fries dairy cattle using ANN modeling. *Appl Soft Comput,* 7 (3): 1112-1120, 2007. DOI: 10.1016/j.asoc.2006.07.002
51. **Akıllı A, Atıl H:** Evaluation of normalization techniques on neural networks for the prediction of 305-day milk yield. *Turk J Agr Eng Res,* 1 (2): 354-367, 2020. DOI: 10.46592/turkager.2020.v01i02.011
52. **Usman SM, Singh NP, Dutt T, Tiwari R, Kumar A:** Comparative study of artificial neural network algorithms performance for prediction of FL305DMY in crossbred cattle. *J Entomol Zool Stud,* 8 (5): 516-520, 2020.
53. **Boğa DÇ:** Creating a lactation model for 305-day milk yield with different resampling techniques (Bagging Mars) in Mars modeling. *The Black Sea J Sci,* 14 (2): 522-539, 2024. DOI: 10.31466/kfbd.1383458
54. **Liseune A, Salamone M, Van den Poel, D, Van Ranst, B, Hostens M:** Predicting the milk yield curve of dairy cows in the subsequent lactation period using deep learning. *Comput Electron Agric,* 180:105904, 2021. DOI: 10.1016/j.compag.2020.105904

Kafkas Universitesi Veteriner Fakultesi Dergisi
Journal Home-Page: http://vetdergikafkas.org
E-ISSN: 1309-2251

Kafkas Univ Vet Fak Derg
32 (2): 219-228, 2026
DOI: 10.9775/kvfd.2025.35519

Research Article

Bone Marrow Mesenchymal Stem Cell Therapy for Cyclophosphamide-Induced Premature Ovarian Failure in Rats

Rania A. LOTFY [1 (*)], Faten A. M. ABO-AZIZA [2(*)], Nehal ABD EL FATTAH [1]

[1] Zoology Department, Faculty of Women for Arts, Science, and Education, Ain Shams University, 11757, Cairo, EGYPT
[2] Department of Parasitology and Animal Diseases, Veterinary Research Institute, National Research Centre, Cairo, EGYPT

(*) **Corresponding author:**
Faten A. M. Abo-Aziza & Rania A. Lotfy
Phone: +20 1005233692
E-mail: faten.aboaziza@gmail.com (FAMA), rania.ata@women.asu.edu.eg (RAL)
How to cite this article?
Lotfy RA, Abo-Aziza FAM, Abd el fattah N: Bone Marrow Mesenchymal Stem Cell Therapy for Cyclophosphamide-Induced Premature Ovarian Failure in Rats. *Kafkas Univ Vet Fak Derg*, 32 (2): 219-228, 2026
DOI: 10.9775/kvfd.2025.35519

Article ID: KVFD-2025-35519
Received: 21.10.2025
Accepted: 24.02.2026
Published Online: 24.02.2026

Abstract

Premature ovarian failure (POF), often induced by cyclophosphamide (CP), leads to hormonal imbalance. Current treatments are ineffective at restoring fertility, creating a need for novel therapies. This study aimed to investigate the therapeutic potential of bone marrow-derived mesenchymal stem cells (BM-MSCs) in restoring ovarian function in a rat model of CP-induced POF. Thirty female rats were divided into control, POF (induced by CP injections), and treated group received a single intravenous injection of BM-MSCs (POF+BM-MSCs). After four weeks, hormonal levels, ovarian oxidative stress markers, and histopathological changes were analyzed. CP induction successfully created a POF model, evidenced by significantly decreased E2 ($P<0.001$); increased FSH, LH ($P<0.01$), elevated oxidative stress, thyroid dysfunction ($P<0.01$), and severe follicular degeneration. BM-MSC transplantation effectively reversed these effects, normalizing hormone profiles, reducing oxidative stress, restoring thyroid function, and improving ovarian follicular architecture. However, BM-MSC treatment did not significantly improve the CP-induced uterine damage. It was concluded that BM-MSC therapy demonstrates a strong protective effect against CP-induced POF. Despite its pronounced efficacy within the ovary, the therapeutic benefits were incompletely extended to the uterus under the employed treatment protocol. This suggests that further investigation into optimized delivery methodologies to ensure a comprehensive, whole-reproductive-tract reparative outcome.

Keywords: Bone marrow mesenchymal stem cells, Cyclophosphamide, Ovarian toxicity, Oxidative stress marker, Premature ovarian failure

Introduction

Premature ovarian failure (POF) is a diverse condition characterized by the termination of ovarian activity, along with increased levels of the follicle-stimulating hormone (FSH) and lower levels of estradiol (E2) [1,2]. Ovarian toxicity reduces follicle stores, causes menstrual irregularities, and leads to ovarian dysfunction and subsequent infertility. Furthermore, decreased ovarian estrogen secretion increases the incidence of other diseases, including Alzheimer's, cardiovascular diseases, autoimmune diseases, metabolic syndrome, and gynecological malignancies [3]. The World Health Organization (WHO) classifies POF as hypogonadotropic hypogonadism [4]. Various factors contribute to POF, such as genetic predispositions, autoimmune disorders, or prior anti-cancer treatments (including surgery, radiotherapy, or chemotherapy) [5]. Moreover, long-term exposure to gonadotoxic chemotherapy is increasingly recognized as a significant cause, particularly given the rising incidence of cancer among primates [6]. Approximately 60-80% of chemotherapy patients may experience POF [7].

Cyclophosphamide (CP) is a widely used drug in clinical practice, especially for cancer treatment also exhibits significant reproductive toxicity. CP accelerates the maturation of ovarian follicles, leading to a depletion of the follicular reserve and ultimately resulting in ovarian failure or even POF [8,9]. Gonadotropin and steroid hormones are crucial regulators of folliculogenesis in all mammals. Disrupted endocrine system regulation impairs follicular growth, and follicular storage, contributing to ovarian abnormalities, such as POF. Various researches suggested that fewer primordial and early antral follicles may result in decreased amounts of anti-mullerian hormone (AMH) in the blood. Along with FSH and E2, AMH is a good predictor of POF and represents follicular storage [10]. Following elderly, this tissue atrophies due to ovarian failure and decline in E2. Estradiol promotes the development of free and bound ribosomes, mitochondria, Golgi, and primary lysosomes in glandular cells and likely

in uterine stromal cells. Biochemically, these organelles are essential for protein matrix production, energy provision, and the synthesis of varied enzymes. The form and activity of a functional endometrium reflect the pattern of ovarian hormone secretion. Normally, the glandular cells are typically cuboidal or columnar; therefore, a decrease in E2 leads to the flattening of this epithelium [11]. Oxidative stress has been proposed as a key factor in apoptosis within the reproductive system [12]. Elevated levels of reactive oxygen species (ROS) inhibit follicle development in antral follicles, while antioxidants such as N-acetyl cysteine, can restore ROS and protect ovaries from damage caused by free oxygen radicals [13]. Although the production of ROS over extended periods may have cumulative effects, increasing the risk of ovarian diseases [14]. Despite being the most common treatment for POF, hormone replacement therapy (HRT) has not been shown to restore ovarian function or fertility and carries potential risks of endometrial and breast cancer [11]. Furthermore, multiple attempts at ovarian stimulation are typically unsuccessful. Consequently, a POF diagnosis often leads to significant physical and emotional distress for animals, highlighting the urgent need for novel and effective treatments [15].

Transplanting stem cells has become a viable strategy for restoring compromised ovarian function. Therefore, this study aimed to investigate the therapeutic potential of bone marrow-derived mesenchymal stem cells (BM-MSCs) in restoring ovarian function in a rat model of CP-induced POF.

Material and Methods

Ethical Approval

All ethical considerations for the studies on animals were considered carefully and the experimental protocol was approved by the Ethics Committee for research on laboratory animals at Ain Shams University (Ethics Code # ASU-SCI-ZOOL/2023/5/4).

Culture and Isolation of BM-MSCs

Adult male albino rats with average weight of 100-200 g were used for the isolation of BM-MSCs. The tibiae and femurs were flushed with Dulbecco's modified Eagle's medium (DMEM; Gibco, USA) supplemented with 10% fetal bovine serum (Gibco, USA) in order to extract bone marrow. Using density gradient Ficoll/Paque (Sigma Aldrich, USA), nucleated cells were separated and subsequently suspended in a full culture medium that contained 1% penicillin-streptomycin (Gibco, USA). The cells were kept in a humidified environment with 5% CO_2 at 37°C. The cultures were washed with phosphate buffer saline (PBS; Lonza, Switzerland) when they reached 80% confluence, and the cells were separated using 0.25% trypsin and 1 mM EDTA (Gibco, USA) for five minutes at 37°C. Following centrifugation, the cells were resuspended in media supplemented with serum. Flow cytometry analysis was employed to immunophenotype the BM-MSCs by detecting the expression of positive indicators include CD90 and CD73, whereas negative markers include the lack of CD45 and CD34 [16].

Experimental Design

A total of 30 healthy adult female Wistar albino rats, weighing between 180 and 190 g, were used in this study. The rats were obtained from the Animal House of the National Research Centre, Egypt. They were housed in a stainless-steel cage and maintained in the animal facility for one week prior to study commencement under a 12/12-h light/dark cycle. Water and a standard diet were given *ad-libitum*. Following a week, the rats were divided into two groups at random: the POF group (n=20) and the normal control group (n=10). Rats were given an intraperitoneal injection of 200 mg/kg CP (Endoxan, Germany) on day 1 and then 8 mg/kg/day for the next 14 days to induce POF [17]. After 14 days, the POF group was randomly divided into two subgroups (n=10/each): POF and POF+BM-MSCs in order to evaluate the impact of BM-MSCs on CP-induced POF. BM-MSCs were adiminstered to the rats via a single intravenous injection into the tail vein (3x106 cells in a 200 µL), and the rats were observed for 4 weeks. The control group did not receive any treatment. Blood samples were drawn from the orbital plexus after the animals were anesthetized with pentobarbital sodium at the end of the experiment. Serum was separated for the subsequent hormonal analysis. The ovaries were excised for biochemical and histopathological analysis and the uterus was removed for histopathological analysis.

Hormonal Assay

The following hormones were measured in rat serum using enzyme-linked immunosorbent assay (ELISA) kits; Follicle-stimulating hormone (FSH, SunLong Biotech Co., Ltd, China, Cat. No: SL0286Ra), luteinizing hormone (LH, SunLong Biotech Co., Ltd, China, Cat. No: SL1093_1Ra), prolactin (PRL, SunLong Biotech Co., Ltd, China, Cat. No: SL0598Ra), progesterone (P4, ALPCO, USA, Cat. No: 55-PROMS-E01), estradiol (E2, SunLong Biotech Co., Ltd, China, Cat. No: SL0268Ra), and anti-Müllerian hormone (AMH, SunLong Biotech Co., Ltd, China, Cat. No: SL0504Ra) were measured in the serum of rats using enzyme-linked immunosorbent assay (ELISA) kits. Thyroid -stimulating hormone (TSH, ALPCO, USA, Cat. No: 55-TSHRT-E01), free triiodothyronine (FT3, ALPCO, USA, Cat. No: MBS260625), and free thyroxine (FT4, ALPCO, USA, Cat. No: SL0295Ra) were similarly determined.

Biochemical Assay

Ovarian tissues were prepared for biochemical analysis

to determine the concentrations of antioxidant enzymes and oxidative stress markers. Briefly, the excised ovaries were washed with ice-cold phosphate-buffered saline (PBS) and mechanically homogenized in 10 volumes (1:10 weight/volume) of ice-cold PBS. The resulting homogenates were centrifuged at 16.000 × g for 10 min at 4°C, and the supernatants were collected for further analysis. Total protein concentration in the ovarian homogenates was determined using the Bradford assay according to the manufacturer's instructions, with bovine serum albumin (BSA) used as the standard. The levels of superoxide dismutase (SOD), glutathione peroxidase (GPx), and catalase (CAT) were estimated using specific ELISA kits ((RayBiotech, GA, MyBiosource, USA; Cat. No: MBS036924, MBS732529 and MBS701908 respectively), with activities expressed as Units per milligram of protein (U/mg protein). Malondialdehyde (MDA) levels, serving as an indicator of lipid peroxidation, were assessed using a colorimetric assay kit (Elabscience, USA, Cat. No: E-BC-Ko25-S) and normalized to the protein content, expressed as nanomoles per milligram of protein (nmol/mg protein).

Histopathological Examinations

The collected ovarian and uterine tissue samples from rats in the various groups were preserved by fixation in 10% formalin saline for 24 h. The samples were then washed in distilled water, dehydrated through a series of graded ethanol solutions, cleared in xylene and embedded in paraffin wax at 56°C in a hot air oven for 24 h. Paraffin wax tissue blocks were prepared and sectioned at 4 µm using a sledge microtome. For regular light microscopy examination, the acquired tissue sections were deparaffinized, and stained with hematoxylin and eosin stain (H&E) [18].

Statistical Analysis

The mean ± standard deviation (S.D.) is used to display all values. The Statistical Processor System Support (SPSS) program (version 18.0; SPSS Inc., Chicago, IL, USA) was used to conduct statistical analysis. One-way analysis of variance (ANOVA) and the Tukey's honestly significant difference (HSD) post hoc test were used to evaluate the data.

Results

Flow cytometric analysis was performed to identify specific cell surface markers of BM-MSCs. The findings are consistent with the anticipated immunophenotype of BM-MSCs *(Fig. 1)*, revealing the cells to be negative for hematopoietic (CD34, CD45) markers and strongly positive for mesenchymal stromal cell markers (CD73, CD90).

The present study demonstrated a significant reduction in serum levels of E2 (52.27±2.94 pg/mL), P4 (8.26±1.80 ng/mL), and AMH (0.97±0.07 ng/mL) in rats within

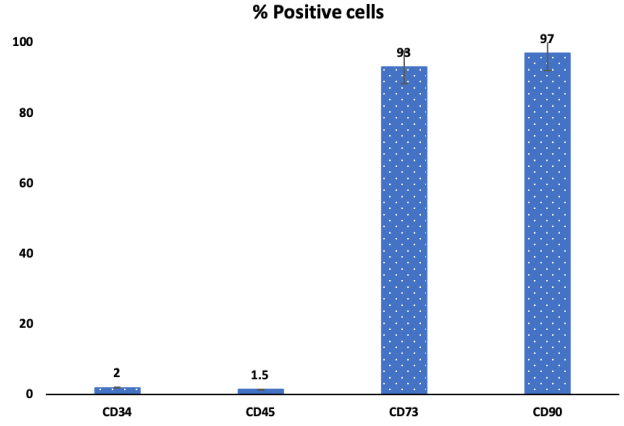

Fig 1. The percentage of positive cells, indicating the proportion of the BM-MSCs population expressing each marker. The x-axis lists the different CD markers analyzed: CD34, CD45, CD73, and CD90.The error bars represent the standard error of the mean, indicating the variability within the measurements. The error bars are relatively small for CD73 and CD90, suggesting consistent expression of these markers across the analyzed samples

the POF group (P<0.001). Conversely, a significant elevation (P<0.001) in serum levels of FSH (6.94±0.50 IU/L), LH (5.37±0.73 IU/L), and PRL (0.98±0.22 ng/mL) were observed in the POF group comparing to the control group *(Fig. 2)*. In contrast, treatment with BM-MSCs transplantation resulted in a significant increase in serum E2 (79.06±5.76 pg/mL, P<0.001), P4 (13.07±1.23 ng/mL, P<0.01), and AMH (1.98±0.11 ng/mL, P<0.001). Concurrently, serum levels of FSH (3.97±0.74 IU/L, P<0.01), LH (3.57±0.30 IU/L, P<0.01), and PRL (0.72±0.07 ng/mL, P<0.05) were significantly reduced compared to the POF group. However, no significant differences were observed in these parameters when comparing rats in the control group and the POF+BM-MSCs group *(Fig. 2)*.

Rats in the POF group exhibited a significant reduction in serum levels of FT3 (1.50±0.33 pg/mL, P<0.001) and FT4 (0.80±0.04 pg/mL, P<0.01). Conversely, serum level of TSH was significantly elevated (3.67±0.51 µIU/mL, P<0.01) compared to control group *(Fig. 3)*. In contrast, treatment with BM-MSCs transplantation resulted in a significant increase (P<0.01) of FT3 (2.42±0.37 pg/mL) and FT4 (1.62±0.48 pg/mL). Concurrently, TSH was significantly decreased (2.74 µIu/mL) in contrast with the POF group (P<0.05). However, no significant notable variations were observed in these parameters in POF+BM-MSCs group comparing to the control group *(Fig. 3)*.

In rats within the POF group, significant reduction (P<0.001) was observed in the concentrations of SOD (74.48±3.62 U/gm tisssue), GPx (35.22±4.46 u/gm protein), and CAT (134.70±2.78 u/gm protein). Conversely, MDA levels were significantly elevated (2.81±0.35 nmol/gm protein, P<0.01) compared to the control group *(Fig. 4)*. In contrast, treatment with BM-MSCs transplantation led to

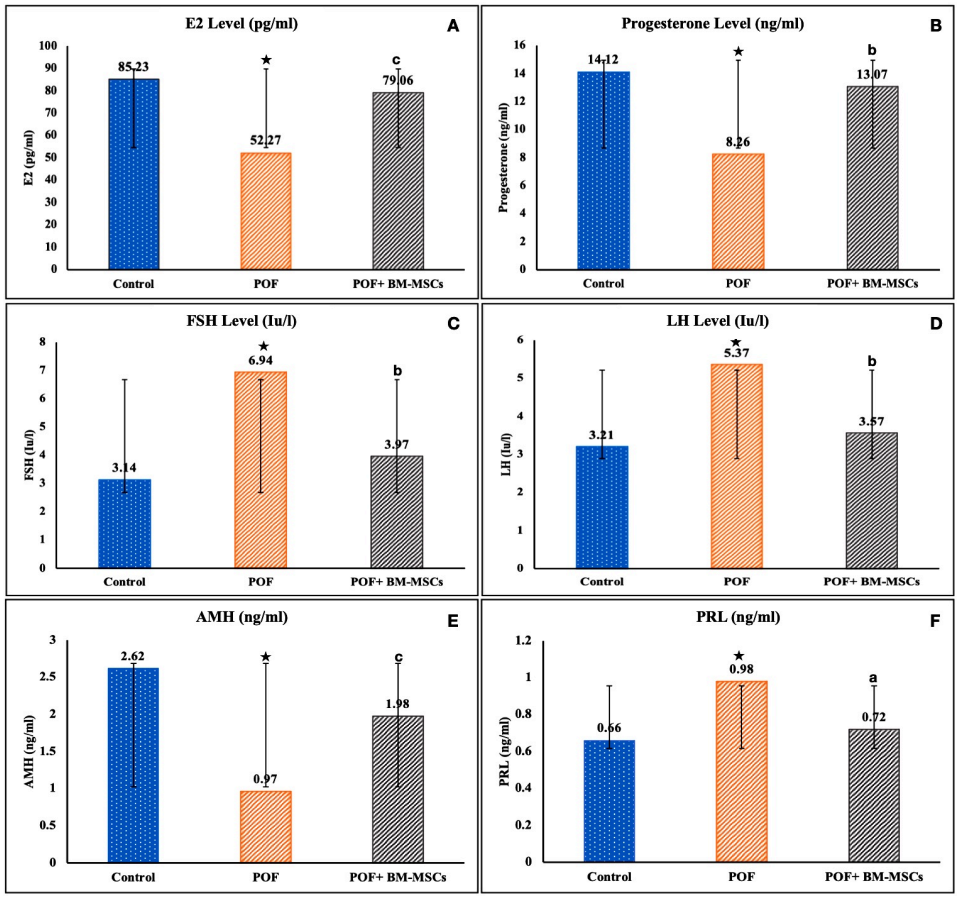

Fig 2. Effect of CP administration and subsequent treatment with BM-MSCs transplantation on serum E2, P4, FSH, LH, AMH and PRL levels in female albino rats. * is significantly different than control at P<0.001. a, b, c are significantly different than POF at P<0.05, P<0.01 and P<0.001 respectively. POF: premature ovarian failure, BM-MSCs: bone marrow mesenchymal stem cells

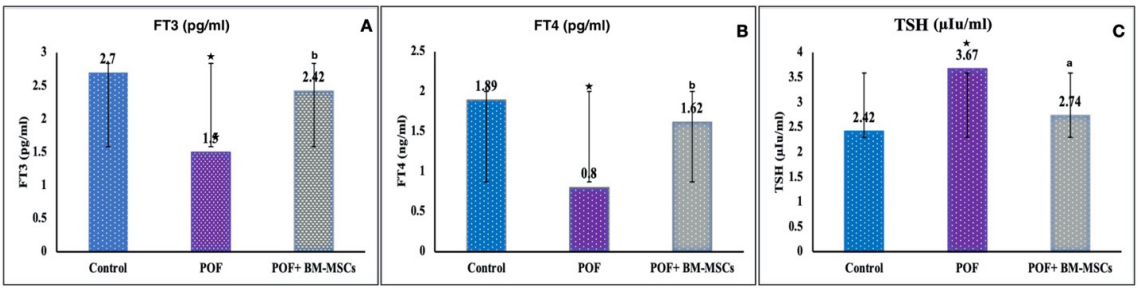

Fig 3. Effect of CP administration and subsequent treatment with BM-MSCs transplantation on serum FT3, FT4 and TSH levels in female albino rats. * and ** are significantly different than control at P<0.01 and P<0.001 respectively. a, b are significantly different than POF at P<0.05 and P<0.01 respectively. POF: premature ovarian failure, BM-MSCs: bone marrow mesenchymal stem cells

a significant increase of SOD (93.46±4.25 U/gm protein, P<0.001), GPx (47.07±3.06 u/gm protein, P<0.05), and CAT (183.48±2.67 u/gm protein, P<0.001). Concurrently, MDA levels were significantly decreased with (1.98±0.31 nmol/gm protein) compared to the POF group (P<0.01).

In the histological examination, control ovary exhibited various stages of follicular maturation and graafian follicles accompanied by corpus luteum and interstitial stromal cells consistent with normal histological structures *(Fig. 5-A,B)*. Conversely, the ovaries of POF rats displayed degeneration and nuclear pyknosis within the theca interna cell layer of the mature follicles in the ovarian tissue. The stromal cells situated between the follicles were increased, potentially due to impaired ovulation, and multiple corpus luteum were observed *(Fig. 5-C,D)*. However, treatment with BM-MSCs resulted in the restoration of normal histological structures, characterized by the presence of Graafian follicles, corpus lutea and various stages of follicular maturation *(Fig. 5-E,F)*. It was found that CP administration resulted in a notable reduction in the number of ovarian follicles *(Fig. 5-C,D)*.

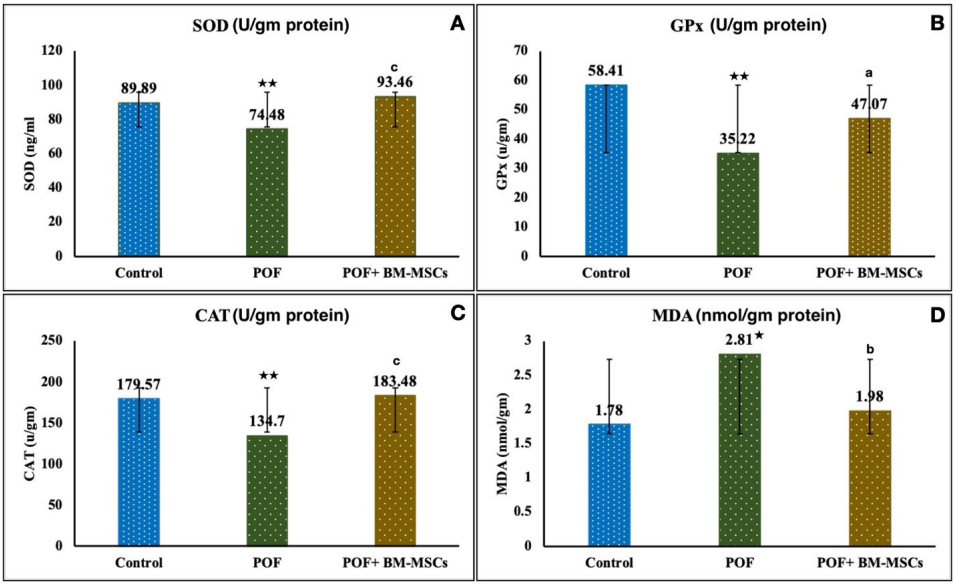

Fig 4. Effect of CP administration and subsequent treatment with BM-MSCs transplantation on SOD, GPx, CAT and MDA levels in ovarian tissue of female albino rats. * and ** are significantly different than control at P<0.01 and P<0.001 respectively. a, b are significantly different than POF at P<0.05, P<0.01, and P<0.001 respectively. POF: premature ovarian failure, BM-MSCs: bone marrow mesenchymal stem cells

Regarding the uterine structure, the histological structure of the mucosa was normal in control rats including the lining epithelium and the underlying lamina propria containing glandular structure, as well as the submucosa, muscularis and serosa *(Fig. 6-A,B)*. In contrast, the uteri of POF rats displayed a flattened mucosal epithelium with atrophy of the glandular structures in the underlying lamina propria with degeneration of the uterine glandular lining epithelial cells within the lamina propria mucosal layer *(Fig. 6-C,D)*. Following treatment with BM-MSCs, degeneration was observed in the uterine glandular lining epithelial cells within the lamina propria and mucosa, and atrophy was noted the in uterine glands within lamina propria *(Fig. 6-E-F)*. Moreover, CP administration led to flattened mucosal epithelium with atrophy of the glandular structure in the underlying lamina propria and degeneration in the uterine glandular lining epithelial cells within the lamina propria mucosal layer *(Fig. 6-C,D)*. However, BM-MSCs transplantation did not exhibit a significant effect on uterine tissue.

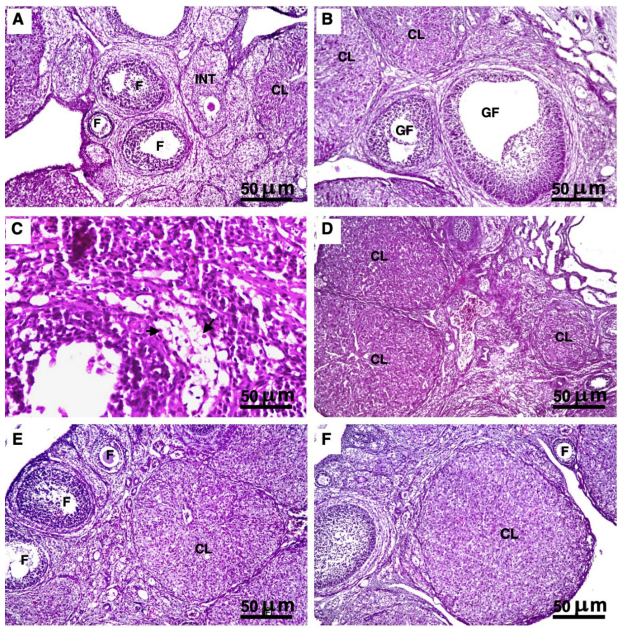

Fig 5. Histological examination of ovaries of different groups. (A) Photomicrograph of control ovary showing different stage of follicles (F) with corpus luteum (CL) and interstitial stromal cells (INT) in normal histological structure (H&E, ×16). (B) The graafian follicles (GF) and corpus luteum (CL) in normal histological structure (H&E, ×16). (C, D) Photomicrograph of ovary of POF rats showing degeneration and nuclear pyknosis in the theca interna cell layer of the mature follicles in ovarian tissue (arrows) and multiple corpus luteum (CL) with stromal cells in between the follicles are increased due to weak ovulation (H&E, ×16). (E, F) Photomicrograph of ovary of BM-MSCs treated rats showing normal histological structure of the graafian follicles (GF) and corpus luteum (CL) and different stages of follicular maturation (F) (H&E, ×16)

Discussion

Stem cells, with their remarkable ability to self-renew and differentiate into various specialized cell types, hold immense potential in regenerative medicine. They offer hope for treating a wide array of diseases and injuries. Several studies were exploring stem cells use to repair damaged tissues, grow replacement organs, and develop new drug therapies [19].

In this study BM-MSCs were isolated to test the possibility that they could increase fertility and restore ovarian function. Flow cytometric analysis was performed to identify specific cell surface markers of BM-MSCs. The findings are consistent with the anticipated immunophenotype of BM-MSCs. This specific pattern

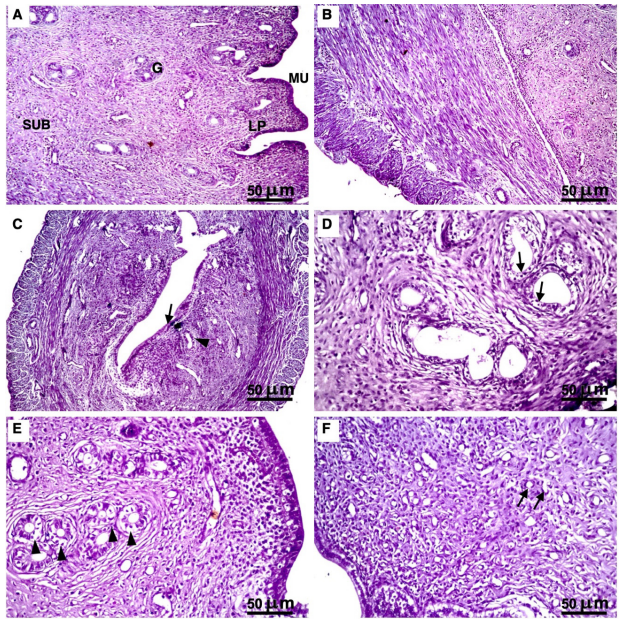

Fig 6. Histological examination of uterus of different groups. (A, B) Photomicrograph of uterus of control group showing normal mucosal (MU) histology, including lining epithelium and underlying lamina propria (LP) with glandular structure (G) and submucosa (SUB) (H&E, ×16). (C) Photomicrograph of uterus of POF rats showing flattened mucosal epithelium (FMU) with atrophy of uterine glands (arrow head) (H&E, ×16) and (D) showing degeneration (arrow) in uterine glandular lining epithelial cells in lamina propria mucosal layer (H&E × 40). (E) Photomicrograph of uterus of BM-MSCs treated rats showing degeneration (arrow head) in uterine glandular lining epithelial cells in lamina propria and mucosa (H&E × 40) and (F) showing atrophy (arrow) in uterine gland in lamina propria (H&E × 40)

of marker expression serves as a crucial criterion for the definition and characterization of BM-MSC populations isolated using flow cytometry as reported previously by Abo-Aziza et al.[20].

The reduction in the levels of E2, P4 and AMH and the elevation of FSH, LH, and PRL in serum the POF group were align with previous studies [21] that reported increased serum FSH and LH following CP administration. Hence, CP-induced POF is characterized by severe follicular depletion and a subsequent loss of regular cyclicity, often resulting in persistent diestrus. This hormonal profile reflects a significant ovarian toxic effect, evidenced by the substantial decrease in serum P4, E2, and AMH, coupled with a notable decline in the number of follicles, ultimately leading to POF. Furthermore, several studies have shown that chemotherapeutic drugs can induce POF across various species, including mice, rats, rabbits, and humans [22,23]. A potential mechanism for the observed reduction in serum E2 and P4 levels involves alkylating agents. Cyclophosphamide (CP), recognized as one of the most ovotoxic chemotherapy drugs, creates DNA crosslinks, subsequently inducing DNA breaks and ultimately triggering apoptosis [24]. CP causes ovarian toxicity due to a compromised antioxidant defense system and an overabundance of free radicals, leading to apoptosis in granulosa cells (GCs) within the follicles and was associated with the significant decreased in E2 and P4 [9]. This process may involve alteration in endogenous antioxidant enzymes within healthy ovarian tissues, as indicated in the present study. Another contributing factor could be the strong toxic effects CP exerts on the gonads, with its medical applications resulting in POF. CP use contributes significantly to iatrogenic consequences and can result in diseases including amenorrhea, infertility, menstrual abnormalities, and diminished libido. POF hinders follicular stage development and may lead to interstitial fibrosis, necrosis, and endocrine alterations that can increase blood levels of LH and FSH while decreasing levels of E2 and P4 [25,26].

Female ovarian granulosa cells generate AMH, one of the transforming growth factors β-super family. Serum AMH levels fluctuate according to developmental stage, starting during puberty and falling off throughout aging. AMH has shown considerable value as an indication of ovarian reserve function. As ovarian reserve function declines with age, changes in AMH levels manifest earlier than changes in FSH, E2, and antral follicle count. Moreover, pregnancy, hormonal contraceptives, or the menstrual cycle have no effect on its concentration [27], establishing it as the most accurate biomarker of ovarian aging. Additionally, a significant elevation in serum FSH and LH was observed following CP administration. This increase may be attributed to the substantial decrease in E2 levels, which disrupts the negative feedback mechanism, leading to the stimulation of GnRH from the hypothalamus and consequently a significant rise in FSH and LH secretion from the anterior pituitary [28,29]. In contrast, treatment with BM-MSCs transplantation resulted in a significant increase in serum E2, P4, and AMH. Concurrently, the significant elevation of FSH and LH in the POF group followed by their significant reduction after BM-MSC treatment reflects a stable shift in the endocrine profile rather than transient fluctuations. The trigger of POF is multifaceted and can be attributed to various factors, including genetic defects, autoimmune reactions, chemotherapy, radiotherapy, and surgery. Stem cells, as a multipotent cell type with the capacity for self-renewal and multilineage differentiation, have been identified as a promising tool in tissue engineering for regenerative medicine [30,31]. Their potential as a treatment provides a fresh approach to protecting or repairing impaired ovarian function in primates undergoing radiation or chemotherapy. The following are some theories as to how stem cells in POF restore the impaired ovarian function: The process by which stem cells migrate into damaged ovarian tissue and differentiate into cells that resemble ovarian tissue, especially granulosa cells, which are vital

parts of the ovarian microenvironment and are essential for controlling ovarian physiology, including luteal regression and ovulation [32]. The homing and residence of stem cells within ovarian tissue, where they contribute to improving damaged ovarian niches among paracrine effect by secreting various growth factors, cytokines, angiogenic factors, and extracellular matrix proteins [33]. Moreover, the effective alleviation of chemotherapy-induced inflammatory reactions in ovarian tissue through the secretion of anti-inflammatory substances following stem cell transplantation [34]. Moreover, MSCs may lower GC apoptosis by affecting G-protein coupled receptor protein signalling and MAPK pathways, both of which are essential for follicle and oocyte formation [35]. These mechanisms support the therapeutic benefit of stem cell therapy for improving ovarian function in individuals with POF. Elevated FSH levels can accelerate follicle recruitment and deplete the follicular pool. Deceased E2 and FSH levels could result from increased apoptosis in the POF group. Stem cell transplantation increased E2 secretion and prevented granulosa cell death, subsequently, leading to downregulation of FSH and LH secretion from the pituitary gland and the consequent inhibition of follicular recruitment [36].

Chemotherapy stands as one of the most effective systemic therapies for cancers. In cancer patients, thyroid function is considered susceptible to chemotherapy due to the active hypothalamic-pituitary axis and the systemic nature of the treatment. The impact of chemotherapy on thyroid function was thought to be a side effect that mostly showed up as hypothyroidism. Thyroid hypofunction was thought to be connected with the suppression of hepatic thyroglobulin secretion and an increase in antithyroid antibodies, specifically anti-thyroid peroxidase (TPO) and antithyroglobulin, induced by chemotherapy [37]. It is hypothesized that endocrine cells with compromised mitochondria exhibit elevated oxidative stress and/or decreased adenosine triphosphate synthesis, along with distention and vacuolization of the endoplasmic reticulum cisternae within thyroid follicles, may result in the inability to synthesize and/or secrete hormones during cyclophosphamide chemotherapy [37]. In contrast, treatment with BM-MSCs transplantation resulted in a significant increase of FT3 and FT4. Concurrently, TSH was significantly decreased in contrast with the POF group. However, no significant notable variations were observed in these parameters in POF+BM-MSCs group comparing to the control group.

In rats within the POF group, significant reduction was observed in the concentrations of SOD, GPx, and CAT. Conversely, MDA levels were significantly elevated. The toxicity of CP exacerbated lipid peroxidation in ovarian tissue. MDA, a by-product of lipid peroxidation, acts as oxidative stress indicator. Furthermore, Cyclophosphamide-induced ovarian damage resulted in decreased concentrations of SOD, GPx, and CAT. Oxidative stress inhibited both nuclear and cytoplasmic maturation of oocytes, and triggering apoptosis led to ovarian failure [38]. In contrast, treatment with BM-MSCs transplantation led to a significant increase of SOD, GPx, and CAT. Concurrently, MDA levels were significantly decreased with compared to the POF group. Stem cells transplantation presents an ideal potential treatment for repairing cytotoxic effect of CP and serves also a powerful tool in restoring fertility and the potential of pregnancy, consequences that could be linked to stem cells' paracrine, homing, and differentiation [39,40]. Control ovary exhibited various stages of follicular maturation and graafian follicles, accompanied by corpus luteum and interstitial stromal cells consistent with normal histological structures. Conversely, the ovaries of POF rats displayed degeneration and nuclear pyknosis within the theca interna cell layer of the mature follicles in the ovarian tissue. The stromal cells situated between the follicles were increased, potentially due to impaired ovulation, and multiple corpus luteum were observed. However, treatment with BM-MSCs resulted in the restoration of normal histological structures, characterized by the presence of Graafian follicles, corpus lutea and various stages of follicular maturation.

Regarding the uterine structure in this study, the histological structure of the mucosa was normal in control rats including the lining epithelium and the underlying lamina propria containing glandular structure, as well as the submucosa, muscularis and serosa. In contrast, the uteri of POF rats displayed a flattened mucosal epithelium with atrophy of the glandular structures in the underlying lamina propria with degeneration of the uterine glandular lining epithelial cells within the lamina propria mucosal layer. Following treatment with BM-MSCs, degeneration was observed in the uterine glandular lining epithelial cells within the lamina propria and mucosa, and atrophy was noted the in uterine glands within lamina propria.

This study demonstrated a significant decrease of the count of Graafian follicles and other follicles in female rats within the POF group, while the corpus luteum count was significantly increased. These results are consistent with the observation of Zhang et al.[41] that CP increases ovarian follicle maturation, decreases follicular reserve, and ultimately causes ovarian failure or even POF. A potential explanation for these observations lies in the critical role of ovarian granulosa cells (GCs) are the primary stroma cells within the ovary, surrounding the oocyte and playing a key role in folliculogenesis [42]. Given their capacity to secrete growth factors and provide hormonal support, GCs are essential for oocyte growth and survival. The main cause

of POF and follicular atresia is increased GC apoptosis that carried out by chemotherapy [43]. In this study, it was found that CP administration resulted in a notable reduction in the number of ovarian follicles. This decrease in ovarian follicles may be due to the reduction in serum E2 which is necessary for early folliculogenesis. Decreased E2 level inhibits follicular progression, thereby disrupting folliculogenesis. FSH receptors are predominantly expressed on GCs. Elevated FSH level can accelerate the depletion of the follicular pool; thus, increased FSH acts as both a cause and a marker diminished ovary reserve [44]. This study also revealed a significant decrease in serum AMH. AMH has been used as a predictor of the quality of oocytes remaining within the ovaries (ovarian reserve) and has been shown to correlate with antral follicle counts and outcomes of ovarian stimulation. Consequently, AMH was previously considered to be an ideal marker of ovarian reserve due to its exclusively production by GSc. According to research on animals, AMH influences the recruitment of primordial follicles and how developing follicles react to FSH [45].

Furthermore, the oocyte has both isoforms of thyroid hormone receptor mRNA, indicating that thyroid hormone may have a direct effect on the oocyte. Rat preantral follicle growth and ovulated oocyte counts are both stimulated by thyroid hormone. T3 stimulated granulosa cell proliferation and suppressed apoptosis by activating the PI3K/Akt signaling pathway [46]. Hence, the decreased serum T3 observed in this study may have contributed to the reduction in ovarian follicles and increased granulosa cell apoptosis. In contrast, following treatment with BM-MSCs, normal histological structure of the Graafian follicles and corpora lutea, along with various stages of follicular maturation, were observed. These findings are consistent with the study of Jalalie et al.[47], who reported that transplantation of MSCS reduced degenerative changes and increased follicular quantitative parameters in ovarian follicles compared to the CP group. These beneficial effects may be attributed to stem cells' migration into damaged ovarian tissue and subsequent differentiation into cells that resemble ovarian tissue, especially granulosa cells [34].

In this study CP administration led to flattened mucosal epithelium with atrophy of the glandular structure in the underlying lamina propria and degeneration in the uterine glandular lining epithelial cells within the lamina propria mucosal layer. These results coincide with the observation of Chen et al.[48], who reported that CP administration caused damage to the ovary, potentially leading to primary ovarian insufficiency. These results may be due to CP-induced significant decrease in E2 and FSH, resulting in defects in folliculogenesis and subsequent atrophy in the uterus. However, BM-MSCs transplantation did not exhibit a significant effect on uterine tissue in this study. The lack of significant uterine tissue improvement after BM-MSC transplantation in this study could stem from the therapeutic regimen's duration and delivery route. A single systemic dose might have been insufficient for the uterus, potentially requiring repeated administrations or a longer observation period for noticeable effects. Furthermore, systemic delivery might have resulted in limited MSC homing to the uterus compared to the ovaries, where damage signals were stronger. A more direct delivery route targeting the uterus could be necessary to achieve a therapeutic concentration of BM-MSCs in that specific tissue. The uterine microenvironment might also necessitate a more sustained or different stimulus from BM-MSCs than the ovaries.

In conclusion, the present study offers novel insights into the significant clinical potential of BM-MSCs therapy in premature ovarian failure by ameliorating the disrupted endocrine secretion system, mitigating ovarian toxicity through the improvement of tissue oxidative stress marker levels, modulating thyroid hormones and TSH, and alleviating histological damage in ovarian tissue. Furthermore, future studies investigating the therapeutic potential of BM-MSCs for POF-related uterine issues might consider exploring different dosages, repeated administrations, alternative routes of injection (potentially local), and longer follow-up periods to better understand their effects on this tissue.

Declarations

Availability of Data and Materials: The data that support the findings of this study are available from the corresponding authors, upon reasonable request.

Funding Support: This research did not receive any specific grant from funding agencies in the public, commercial, or not-for-profit sectors.

Competing Interests: The authors declare no competing interests.

Declaration of Generative Artificial Intelligence (AI): The authors declare that the article, tables and figures were not written/created by AI and AI-assisted technologies.

Authors' Contributions: R.A.L., F.A.M.A. and N.A. conceptualization and design the study. R.A.L. and N.A. contributed to data curation, formal analysis, investigation and methodology. F.A.M.A. contributed to the isolation and characterization of BM-MSCs. R.A.L. and N.A. wrote original draft. F.A.M.A. revised the final manuscript and prepare it for publication. All authors agreed writing – review and editing.

References

1. **Cooper AR, Baker VL, Sterling EW, Ryan ME, Woodruff TK, Nelson LM:** The time is now for a new approach to primary ovarian insufficiency. *Fertil Steril,* 95, 1890-1897, 2011. DOI: 10.1016/j.fertnstert.2010.01.016
2. **Flatt SB, Baillargeon A, McClintock C, Pudwell J, Velez MP:** Premature ovarian insufficiency in female adolescent and young adult survivors of non-gynecological cancers: A population-based cohort

study. *Reprod Health,* 20 (1):4, 2023. DOI: 10.1186/s12978-022-01559-8

3. **Podfigurna-Stopa A, Czyzyk A, Grymowicz M, Smolarczyk R, Katulski K, Czajkowski K, Meczekalski B:** Premature ovarian insufficiency: The context of long-term effects. *J Endocrinol Invest,* 39, 983-990, 2016. DOI: 10.1007/s40618-016-0467-z
4. **Zhu SF, Hu HB, Xu HY, Fu XF, Peng DX, Su WY:** Human umbilical cord mesenchymal stem cell transplantation restores damaged ovaries. *J Cell Mol Med,* 19, 2108-2117, 2015. DOI: 10.1111/jcmm.12571
5. **Elfayomy AK, Almasry SM, El-Tarhouny SA, Eldomiaty MA:** Human umbilical cord blood-mesenchymal stem cells transplantation renovates the ovarian surface epithelium in a rat model of premature ovarian failure: Possible direct and indirect effects. *Tissue Cell,* 48, 70-382, 2016. DOI: 10.1016/j.tice.2016.05.001
6. **Karavani G, Rottenstreich A, Schachter-Safrai N, Cohen A, Weintraub M, Imbar T, Revel A:** Chemotherapy-based gonadotoxicity risk evaluation as a predictor of reproductive outcomes in post-pubertal patients following ovarian tissue cryopreservation. *BMC Womens Health,* 21 (1):201, 2021. DOI: 10.1186/s12905-021-01343-z
7. **Ayuandari S, Dewanto A, Oktasari R, Rahmawati NR, Alma NA, Hamurajib KC, Mulatsih S:** Anti-Mullerian hormone and puberty development in girls and adolescents who underwent cancer treatment. *Arch Gynecol Obstet,* 305, 1581-1586, 2022. DOI: 10.1007/s00404-021-06364-5
8. **Qin X, Zhao Y, Zhang T, Yin C, Qiao J, Guo W, Lu B:** TrkB agonist antibody ameliorates fertility deficits in aged and cyclophosphamide induced premature ovarian failure model mice. *Nat Commun,* 13:914, 2022. DOI: 10.1038/s41467-022-28611-2
9. **Zheng S, Ma M, Chen Y, Li M:** Effects of quercetin on ovarian function and regulation of the ovarian PI3K/Akt/FoxO3a signalling pathway and oxidative stress in a rat model of cyclophosphamide-induced premature ovarian failure. *Basic Clin Pharmacol Toxicol,* 130, 240-253, 2022. DOI: 10.1111/bcpt.13696
10. **Sükür YE, Kıvançlı LB, Ozmen B:** Ovarian aging and premature ovarian failure. *J Turk Ger Gynecol Assoc,* 15, 190-196, 2014. DOI: 10.5152/jtgga.2014.0022
11. **Chen H, Liu C, Zhu S, Li S, Zhang Q, Song L, Liang X:** The therapeutic effect of stem cells on chemotherapy-induced premature ovarian failure. *Curr Mol Med,* 21 (5): 376-384, 2021. DOI: 10.2174/1566524020666200905113907
12. **Yan F, Zhao Q, Li Y, Zheng Z, Kong X, Shu C, Liu Y, Shi Y:** The role of oxidative stress in ovarian aging: A review. *J Ovarian Res,* 15 (1):100, 2022. DOI: 10.1186/s13048-022-01032-x
13. **Wang W, Craig ZR, Basavarajappa MS, Hafner KS, Flaws JA:** Mono-(2-ethylhexyl) phthalate induces oxidative stress and inhibits growth of mouse ovarian antral follicle. *J Biol Reprod,* 87:152, 2012. DOI: 10.1095/biolreprod.112.102467
14. **Behrman HR, Kodaman PH, Preston SL, Gao S:** Oxidative stress and the ovary. *J Soc Gynecol Invest,* 8, S40-S42, 2001.
15. **Chen L, Guo S, Wei C, Li H, Wang H, Xu Y:** Effect of stem cell transplantation of premature ovarian failure in animal models and patients: A meta-analysis and case report. *Exp Ther Med,* 5, 4105-4118, 2018. DOI: 10.3892/etm.2018.5970
16. **Haasters F, Prall WC, Anz D, Bourquin C, Pautke C, Endres S, Mutschler W, Docheva D, Schieker M:** Morphological and immunocytochemical characteristics indicate the yield of early progenitors and represent a quality control for human mesenchymal stem cell culturing. *J Anat,* 214, 759-767, 2009. DOI: 10.1111/j.1469-7580.2009.01065.x
17. **Melekoglu R, Ciftci O, Eraslan S, Cetin A, Basak N:** Beneficial effects of curcumin and capsaicin on cyclophosphamide-induced premature ovarian failure in a rat model. *J Ovarian Res,* 11:33, 2018. DOI: 10.1186/s13048-018-0409-9
18. **Banchroft JD, Stevens A, Turner DR:** Theory and Practice of Histological Techniques. Fourth ed., Churchil Living stone, New York, London, San Francisco, Tokyo, 1996.
19. **Abo-Aziza FAM, Zaki AA, Adel RM, Fotouh A:** Amelioration of aflatoxin acute hepatitis rat model by bone marrow mesenchymal stem cells and their hepatogenic differentiation. *Vet World,* 15 (5): 1347-1364, 2022. DOI: 10.14202/vetworld.2022.1347-1364
20. **Abo-Aziza FAM, Zaki AA, Alajaji IA, Albarrak SM:** Bone marrow mesenchymal stem cell co-adjuvant therapy with albendazole for managing *Toxocara vitulorum* - Rat model. *Vet World,* 14 (2): 347-363, 2021. DOI: 10.14202/vetworld.2021.347-363
21. **Yoo C, Yun MR, Ahn JH, Jung KH, Kim HJ, Kim JE, Park JY, Park KO, Yoon DH, Kim SB:** Chemotherapy-induced amenorrhea, menopause-specific quality of life, and endocrine profiles in premenopausal women with breast cancer who received adjuvant anthracycline-based chemotherapy: A prospective cohort study. *J Cancer Chemother Pharmacol,* 72, 565-575, 2013. DOI: 10.1007/s00280-013-2227-5
22. **Edessy M, Hosni HN, Shady Y, Waf Y, Bakr S, Kamel M:** Autologous stem cells therapy, the first baby of idiopathic premature ovarian failure. *Acta Med Int,* 3, 19-23, 2016. DOI: 10.5530/ami.2016.1.7
23. **Zhang T, Yan D, Yang Y, Ma A, Li L, Wang Z, Pan Q, Sun Z:** The comparison of animal models for premature ovarian failure established by several different source of inducers. *Regul Toxicol Pharmacol,* 81, 223-232, 2016. DOI: 10.1016/j.yrtph.2016.09.002
24. **Lopes F, Smith R, Anderson RA, Spears N:** Docetaxel induces moderate ovarian toxicity in mice, primarily affecting granulosa cells of early growing follicles. *Mol Hum Reprod,* 20, 948-959, 2014. DOI: 10.1093/molehr/gau057
25. **Huang C, Song K, Ma W:** Immunomodulatory mechanism of Bushen Huoxue Recipe alleviates cyclophosphamide-induced diminished ovarian reserve in mouse model. *J Ethnopharmacol,* 208, 44-56, 2017. DOI: 10.1016/j.jep.2017.06.022
26. **Yang DM, Zhang JQ, Fei YF:** *Lycium barbarum* polysaccharide attenuates chemotherapy-induced ovarian injury by reducing oxidative stress. *J Obstet Gynaecol Res,* 43, 1621-1628, 2017. DOI: 10.1111/jog.13416
27. **Sefrioui O, Madkour A, Aboulmaouahib S, Kaarouch I, Louanjli N:** Women with extreme low AMH values could have *in vitro* fertilization success. *J Gynecol Endocrinol,* 35, 170-173, 2019. DOI: 10.1080/09513590.2018.1505850
28. **Huang B, Ding C, Zou Q, Wang W, Li H:** Cyclophosphamide regulates N6-methyladenosine and m6A RNA enzyme levels in human granulosa cells and in ovaries of a premature ovarian aging mouse model. *Front Endocrinol (Lausanne),* 10:415, 2019. DOI: 10.3389/fendo.2019.00415
29. **Zheng Q, Fu X, Jiang J, Zhang N, Zou L, Wang W, Ding M, Chen H:** Umbilical cord mesenchymal stem cell transplantation prevents chemotherapy induced ovarian failure via the NGF/TrkA pathway in rats. *J Biomed Res Int,* 2019:6539294, 2019. DOI: 10.1155/2019/6539294
30. **Jiang X, Zhang HMT:** Effectiveness of autologous stem cell therapy for the treatment of lower extremity ulcers: A systematic review and metaanalysis. *J Med (Baltimore),* 95:e2716, 2016. DOI: 10.1097/MD.0000000000002716
31. **Dai F, Wang R, Deng Z, Yang D, Wang L, Wu M, Hu W, Cheng Y:** Comparison of the different animal modeling and therapy methods of premature ovarian failure in animal model. *Stem Cell Res Ther,* 14:135, 2023. DOI: 10.1186/s13287-023-03333-4
32. **Huang Y, Zhu M, Liu Z, Hu R, Li F, Song Y, Geng Y, Ma W, Song K, Zhang M:** Bone marrow mesenchymal stem cells in premature ovarian failure: Mechanisms and prospects. *Front Immunol,* 13:997808, 2022. DOI: 10.3389/fimmu.2022.997808
33. **Spees JL, Lee RH, Gregory CA:** Mechanisms of mesenchymal stem/stromal cell function. *J Stem Cell Res Ther,* 7:125, 2016. DOI: 10.1186/s13287-016-0363-7
34. **Zhang Q, Xu M, Yao X, Li T, Wang Q, Lai D:** Human amniotic epithelial cells inhibit granulosa cell apoptosis induced by chemotherapy and restore the fertility. *J Stem Cell Res Ther,* 6:152, 2015. DOI: 10.1186/s13287-015-0148-4
35. **Jozkowiak M, Hutchings G, Jankowski M, Kulcenty K, Mozdziak P, Kempisty B, Spaczynski RZ, Piotrowska-Kempisty H:** The stemness

of human ovarian granulosa cells and the role of resveratrol in the differentiation of MSCs - A review based on cellular and molecular knowledge. *Cells,* 9:1418, 2020. DOI: 10.3390/cells9061418

36. **Liu R, Zhang X, Fan Z, Wang Y, Yao G, Wan X, Liu Z, Yang B, Yu L:** Human amniotic mesenchymal stem cells improve the follicular microenvironment to recover ovarian function in premature ovarian failure mice. *J Stem Cell Res Ther,* 10:299, 2019. DOI: 10.1186/s13287-019-1315-9
37. **Majkowska-Mlynarczyk A, Kinalski M, Zaczek-Kucharska E:** The thyroid gland function assessment in women after mastectomy and chemotherapy during breast cancer therapy. *Endokrynol Pol,* 58, 397-402, 2017.
38. **Yang L, Chen Y, Liu Y, Xing Y, Miao C, Zhao Y, Chang X, Zhang Q:** The role of oxidative stress and natural antioxidants in ovarian aging. *Front Pharmacol,* 14 (11):617843, 2021. DOI: 10.3389/fphar.2020.617843
39. **Zhang C:** The roles of different stem cells in premature ovarian failure. *J Curr Stem Cell Res Ther,* 15, 473-481, 2020. DOI: 10.2174/1574888X14666190314123006
40. **Liu X, Li J, Wang W, Ren X, Hu JF:** Therapeutic restoration of female reproductive and endocrine dysfunction using stem cells. *Life Sci,* 1 (322):121658, 2023. DOI: 10.1016/j.lfs.2023.121658
41. **Zhang BF, Hu Y, Liu X, Cheng Z, Lei Y, Liu Y, Zhao X, Mu M, Yu L, Cheng ML:** The role of AKT and FOXO3 in preventing ovarian toxicity induced by cyclophosphamide. *PLoS One,* 13:e0201136, 2018. DOI: 10.1371/journal.pone.0201136
42. **Iorio R, Castellucci A, Ventriglia G, Teoli F, Cellini V, Macchiarelli G, Cecconi S:** Ovarian toxicity: From environmental exposure to chemotherapy. *Curr Pharm Des,* 20, 5388-5397, 2014. DOI: 10.2174/1381612820666140205145319
43. **Umer A, Khan N, Greene DL, Habiba UE, Shamim S, Khayam AU:** The therapeutic potential of human umbilical cord derived mesenchymal stem cells for the treatment of premature ovarian failure. *Stem Cell Rev Rep,* 19, 651-666, 2023. DOI: 10.1007/s12015-022-10493-y
44. **Broekmans FJ, Knauff EA, te Velde ER, Macklon NS, Fauser B:** Female reproductive ageing: Current knowledge and future trends. *Trends Endocrinol Metab,* 18, 58-65, 2007. DOI: 10.1016/j.tem.2007.01.004
45. **Campbell BK, Clinton M, Webb R:** The role of anti-Müllerian hormone (AMH) during follicle development in a monovulatory species (sheep). *J Endocrinol,* 153, 4533-4543, 2012. DOI: 10.1210/en.2012-1158
46. **Zhang C, Guo L, Zhu B, Feng Y, Yu S, An N, Wang X:** Effects of 3, 5, 3'-triiodothyronine (t3) and follicle stimulating hormone on apoptosis and proliferation of rat ovarian granulosa cells. *Chin J Physiol,* 56, 298-305, 2013. DOI: 10.4077/CJP.2013.BAB186
47. **Jalalie L, Rezaee MA, Rezaie MJ, Jalili A, Raoofi A, Rustamzade A:** Human umbilical cord mesenchymal stem cells improve morphometric and histopathologic changes of cyclophosphamide-injured ovarian follicles in mouse model of premature ovarian failure. *Acta Histochem,* 123:151658, 2020. DOI: 10.1016/j.acthis.2020.151658
48. **Chen Y, Zhao Y, Miao C, Yang L, Wang R, Chen B, Zhang Q:** Quercetin alleviates cyclophosphamide-induced premature ovarian insufficiency in mice by reducing mitochondrial oxidative stress and pyroptosis in granulosa cells. *J Ovarian Res,* 15:138, 2022. DOI: 10.1186/s13048-022-01080-3

Kafkas Universitesi Veteriner Fakultesi Dergisi
Journal Home-Page: http://vetdergikafkas.org
E-ISSN: 1309-2251

Kafkas Univ Vet Fak Derg
32 (2): 229-237, 2026
DOI: 10.9775/kvfd.2025.35569

Research Article

Abundance and Diversity of The Faecal Resistome and Microbiome in Broilers

Özkan ASLANTAŞ [1(*)], Suzan ŞAHİN DOĞAN [2]

[1] Hatay Mustafa Kemal University, Faculty of Veterinary Medicine, Department of Microbiology, TR-31060 Hatay - TÜRKİYE
[2] Karamanoğlu Mehmetbey University, Kamil Özdağ Faculty of Science, Department of Biology, TR-70100 Karaman - TÜRKİYE

[(*)] **Corresponding author:**
Özkan Aslantaş
Phone: +90 326 245 85 45/11523
Cellular phone: +90 533 641 22 36
Fax: +90 326 245 57 04
E-mail: ozkanaslantas@yahoo.com, aslantas@mku.edu.tr

How to cite this article?

Aslantaş Ö, Şahin Doğan S: Abundance and Diversity of The Faecal Resistome and Microbiome in Broilers. *Kafkas Univ Vet Fak Derg*, 32 (2): 229-237, 2026
DOI: 10.9775/kvfd.2025.35569

Article ID: KVFD-2025-35569
Received: 03.11.2025
Accepted: 16.04.2026
Published Online: 26.04.2026

Abstract

Antimicrobial resistance (AMR) is a growing problem, posing a threat to human and animal health. The use of antimicrobials in livestock selects for AMR that can subsequently be transferred to humans. This flow of AMR between reservoirs demands continuous surveillance in livestock and in humans. Although there are numerous studies to determine the fecal carriage of antibiotic-resistant bacteria in broiler flocks, there is a lack of comprehensive metagenomic research targeting the resistome in broilers in Türkiye. The aim of this study was to investigate the microbial composition and the profiles of antimicrobial resistance genes (ARGs, resistome) in three selected broiler farms in Hatay, using a shotgun metagenomics approach. The microbiota of broilers from Flock A and C was dominated by Bacillota (formerly Firmicutes) (46.83% and 43.87%, respectively), whereas Flock B exhibited a high relative abundance of Pseudomonadota (formerly *Proteobacteria*) (82.5%). At the genus level, *Brachybacterium, Escherichia*, and *Ligilactobacillus* were significantly more abundant in Flocks A, B, and C, respectively. It was also noticed that the most abundant KEGG pathways belonged to metabolism and genetic information processing. Furthermore, xenobiotics biodegradation and metabolism pathways were more abundant in Flock B than in Flocks A and C. Similarly, a higher ARG diversity was observed in Flock B. A total of 137 ARGs were identified, comprising different resistance mechanisms. The *MLS23S* gene, conferring macrolide resistance through a 23S rRNA gene mutation, was the predominant ARG in all flocks. These findings provide a baseline characterization of the broiler gut resistome, highlighting the importance of metagenomic surveillance in poultry production despite the unavailability of farm-level antimicrobial usage records.

Keywords: Broilers, Metagenomics, Microbiome, Bacillota, Pseudomonadota, *Ligilactobacillus*, Resistome

Introduction

According to World Health Organization (WHO), antimicrobial resistance (AMR) is a growing health concern worldwide, promoting international cooperation due to depth, breadth and complexity [1]. The emergence of resistance to antibiotics in bacteria is mainly associated with target mutations and horizontal transfer of resistance genes [2]. The poultry sector employs a variety of antimicrobials to maintain flock health and enhance production efficiency. These antimicrobials serve different functions and are categorized into therapeutic, prophylactic, and growth promotion uses [3]. Therefore, the widespread and intensive use of antibiotics in poultry farming has significantly contributed to the selection and emergence of antibiotic-resistant bacteria (ARB) and antibiotic-resistant genes (ARGs) [4].

Several national surveillance programs have been implemented to monitor the occurrence of AMR in different reservoirs using indicator bacteria (e.g. *Escherichia coli, Enterococcus* spp.) and to follow its trends over time [5-7]. There is currently no national program in the field of veterinary medicine in Türkiye for the determination of AMR. However, previous studies have reported have showed high levels resistance against critically important antimicrobials, especially in broiler flocks [8-11] and chicken meats [12,13]. Although these studies are important in demonstrating the emergence and spread of resistance, they target a limited number of species present in the gut microbiota and their associated resistance genes, thus representing only a limited portion of the resistome. Shotgun metagenomics has the potential to overcome the drawbacks of these approaches by directly identifying and characterizing the microbiome

and resistome [14]. This technique provides a substantial overview of the abundance, diversity, and structure of the acquired broiler resistomes. Understanding circulating resistomes is thus important to provide critical insights for developing robust, tailored strategies to mitigate AMR risks and safeguard both public and environmental health [15]. For instance, the presence of mobile genetic elements (MGEs) such as the *mcr-1* gene in broiler gut microbiota can lead to the transmission of colistin resistance to human pathogens through the food chain or environmental runoff, posing a significant threat to public health.

In this study, it was aimed to perform comprehensive analysis of broiler's gut microbiomes and resistomes using shotgun sequencing.

Material and Methods

Ethical Approval

This study was approved by Hatay Mustafa Kemal University Animal Experiments Local Ethics Committee (Decision number: 2025/07-11)

Animals, Sample Collection and Processing

Three commercial broiler flocks, labeled flock A, flock B and flock C and located about 50 km from each other in Hatay, Türkiye, were selected for this study, between 10 and 20 September 2025 to minimize seasonal influences. On each farm, 25 undisturbed, fecal droppings were collected in different areas covering the whole house (a minimum of 3 g faeces per sample). All samples were collected aseptically in plastic containers and stored at 4°C and transported to the laboratory within 1-2 h after sampling. Upon laboratory arrival, individual fecal samples were homogenized by stirring thoroughly with a sterile wooden spatula for a few minutes. To obtain a representative profile of the entire house, a composite sample was created for each flock by pooling equal weights (approximately 2 g) of the 25 homogenized individual samples. These composite pools (one per flock) were then used for downstream DNA extraction.

DNA Extraction and Sequencing

DNA was extracted from 200 mg of each homogenized sample using the QIAamp Fast DNA Stool Mini Kit (Qiagen) based on the manufacturer's instructions. A bead beating step was applied at the beginning of the DNA extraction process. The concentration and quality of DNA were checked using NanoDrop spectrophotometer. To evaluate the flock-level microbial and resistance profiles, three metagenomic libraries (one per flock) were constructed from the homogenized composite DNA pools using the Nextera XT DNA library kit (Illumina). This pooling approach allowed for a comprehensive surveillance of the diverse genetic material present across the entire broiler house within a single sequencing run per farm. Fragment size was evaluated by an automated capillary electrophoresis system (Fragment Analyzer, Agilent Technologies, Santa Clara,CA, USA). The constructed libraries were subjected to high-throughput sequencing on the NovaSeq 6000 platform (Illumina), using 2 × 150-bp paired-end sequencing.

Bioinformatic Analysis

The quality of the reads was checked by FastQC tool [16]. After removal of low-quality reads and Illumina adapters by using Trimmomatic [17], the paired end sequences were aligned against the host reference genome (*Gallus gallus*) using the Bowtie2 tool [18]. After alignment, the mapped sequences, that is, reads derived from the host were removed. The integrated pipeline SqueezeMeta v1.4.0 was applied for further processing and annotation of the trimmed and host-removed reads from each sample [19]. Clean reads were assembled by MEGAHIT (v1.2.9) using default parameters and the Open Reading Frames (ORFs) were detected by Prodigal v2.6.3 (Li et al. 2016). Cleaned sequences were analyzed for antimicrobial resistance genes (ARGs) using the AMR++ pipeline v3 as well as for taxonomic assignment using Kraken2 [20]. For resistome profiling, clean reads were aligned against the MEGARes v3.0 database. A gene was identified as present only if it met a gene fraction coverage cutoff of 0.80 (80%), ensuring that the majority of the reference gene sequence was represented in our data. Furthermore, an identity threshold of 90% and a minimum alignment length of 75 bp were maintained to ensure the specificity of the ARG detection. Transcripts per million (TPM) normalization adjusts raw read counts so that the total expression across all genes is constant among samples, allowing each TPM value to represent the relative expression level of a gene within a sample. Statistical analyses and data visualizations were conducted using RStudio (R version 4.5.1) and the STAMP software [21]. For each sample, the Chao1, Shannon, and Simpson indices were calculated using the R package vegan, based on taxonomic units at the genus level. To find the correlation between the relative abundances of ARGs and bacterial genera, Spearman's rank correlation coefficients were calculated using the rcorr() function in the Hmisc package [22].

A correlation network was constructed based on strong and statistically significant associations, defined by a Spearman's rho (ρ) >0.8 and a P-value <0.01. Network graphs were created using the igraph and ggraph packages in R [23,24], applying the Fruchterman-Reingold force-directed layout for optimal visualization of the nodes and edges. Venn diagrams were plotted using ggvenn package [25] for the number of shared and unique anti-microbial resistance genes in the flocks.

Results

Microbial Composition and Diversity

A total of 223,331,799 paired-end reads were generated after host removal and quality trimming. The sequencing depth per flock ranged from 74 million to 80 million reads, with an average of 77 million reads per sample. In addition, a total of 1,239,781 contigs were assembled during the metagenomic analysis, with a total assembly length of 1.15 Gbp and an N50 value of 1366 bp. At the taxonomic level, 84 phyla, 96 classes, 161 orders, 268 families, 879 genera and 1663 species were identified. The taxonomic distribution of the broiler gut microbiota at the phylum level was dominated by Bacillota (formerly Firmicutes) and Pseudomonadota (formerly Proteobacteria). Specifically, Bacillota accounted for 46.83% and 43.87% of the total sequences in Flocks A and C, respectively, while Pseudomonadota was the most prevalent phylum in Flock B (82.5%) *(Fig. 1)*. There were significant differences in the absolute abundances among the flocks *(Table 1)*. Notably, relative abundance of Pseudomonadota (82.5%) in flock B was significantly greater than that of other flocks *(Fig. 2)*. Whereas Bacillota (46.83%) and Actinomycetota (39.02%) in flock A and, Bacillota (43.87%) and Bacteroidota (28.51%) in flock C were noted as the dominant phyla. At the genus level, *Ligilactobacillus*, *Escherichia*, and *Brachybacterium* were identified as the most abundant taxa. The relative abundance of *Ligilactobacillus* was significantly higher in Flock C compared to the other groups. At the species level, *Escherichia coli* was significantly more abundant in Flock B, whereas *Ligilactobacillus salivarius* was more prevalent in Flock A *(Fig. 2-a)*

It was calculated several alpha-diversity indexes for each flock. The range of microbial diversity was much higher in Flock A and B than Flock C *(Table 2)*.

The ARG Diversity of Flocks

The relative abundance of AMR to the corresponding class of antimicrobial's level for each flock was presented in *Fig. 3*. Shannon, Richness, and Simpson indexes were also calculated to assess ARG diversity. It was found that ARG diversity was relatively higher in Flock B *(Table 2)*. Both within and among poultry farms, the relative abundances of AMR per drug were more varied *(Fig 4)*. As seen in *Fig. 3*, macrolide AMR was more abundant in all flocks, but the relative abundance of tetracycline, aminoglycoside and beta-lactam drug classes differed in flocks. For example, relative abundance of beta-lactam resistance genes was higher in flock B, was much lower in other flocks. Aminoglycoside and tetracycline AMR genes were the most abundant in flock C, but flock A and

Table 1. *Relative abundance (%) of the dominant bacterial phyla and their associated major genera across the three sampled broiler flocks (Flock A, B, and C)*

Phylum	Genus	Flock A (%)	Flock B (%)	Flock C (%)
Bacillota	*Ligilactobacillus*	12	0.2	23
	Streptococcus	7	0.1	0.1
	Lactobacillus	12	0.4	6
	Faecalibacterium	2	0.5	1.7
	Staphylococcus	0.9	2.7	0.6
Bacteroidota	*Bacteroides*	0.2	0.1	6
	Alistipes	0.6	0.7	3
	Parabacteroides	0.2	0.3	1.9
Actinomycetota	*Corynebacterium*	16	1.8	0.06
	Brachybacterium	17	4	0.5
	Brevibacterium	3.9	1.4	0.05
	Dietzia	4	0.01	0.005
Fusobacteriota	*Fusobacterium*	0.009	0.05	9
Lentisphaerota	*Candidatus Spyradenecus*	0.0002	8	6
Pseudomonadota	*Escherichia*	10	83	9
Others (<1%)		12	5	31

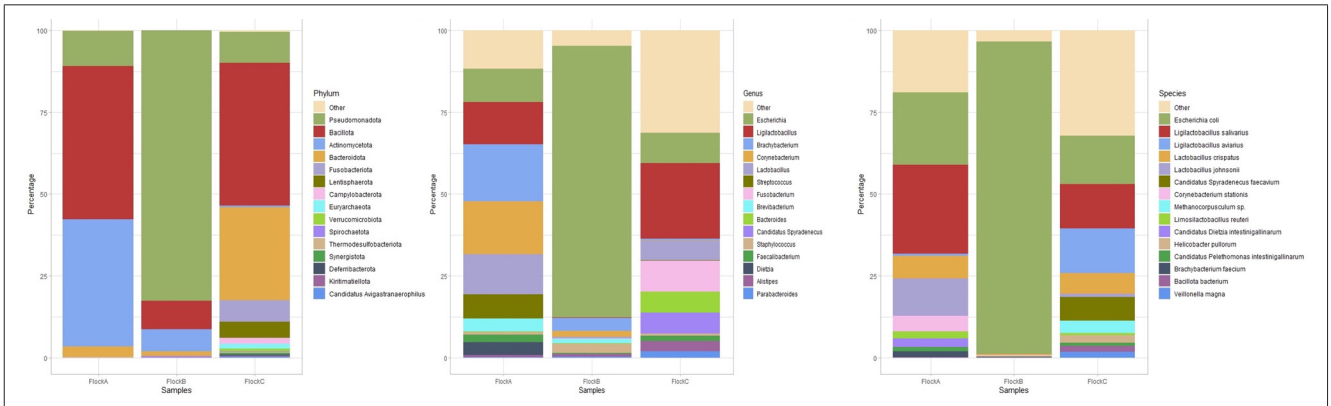

Fig 1. Taxonomic distribution of the microbial communities at the phylum, genus, and species level across three broiler flocks (**a, b,** and **c**). The 'Others' category includes phyla with a relative abundance of less than 1%. Data represent pooled samples from each flock

Table 2. *Summary of alpha-diversity indices to determine the Shannon, Simpson, and Chao1 of microbial genera and ARGs*

Parameter	Flocks	Shannon	Chao1	Simpson
Microbiome	Flock A	3.18	1021	0.92
	Flock B	1.44	756	0.5
	Flock C	3.71	969	0.95
ARG	Flock A	0.97	1055	5.06
	Flock B	0.99	1078	5.51
	Flock C	0.96	673	4.59

ARG: antimicrobial resistance genes

B had low relative abundance *(Fig. 4)*. Similarly, flock A had a notably larger proportion of phenicol AMR than flock B and C. In addition, while oxazolidinone resistance was only observed in flock A, mupirocin resistance was observed in flock B *(Fig. 4)*.

The overall structure and composition of the resistome and AMR genes are presented in *Fig. 4*. A total of 137 different antimicrobial resistance genes were detected across all flocks. Most of them were associated with resistance to macrolides in all flocks. *MLS23S* were more abundant and ubiquitous in all flocks *(Fig. 4)*.

In flock C, A16S and *tet*16S were more common AMR genes following *MLS23S* gene. Among beta-lactam AMR genes, bla_{CTX} and bla_{TEM} were relatively higher in flock B, which is beta-lactam resistance higher than other flocks. Among several phenicol AMR genes, *cmx* and *fexB* were much more abundant in flock A than in the other flocks. Of the resistant genes related to the last resort antibiotics (colistin, carbapenem, linezolid), *optrA* and *poxtA* were only detected in one flock (flock A). *mcr* gene variants and carbapenemase genes (eg, KPC, IMP, VIM, NDM, OXA-48-like) were not detected in flocks. The relative abundances of other AMR genes varied across flocks *(Fig. 4)*. Among beta-lactam resistance genes, bla_{CTX} and bla_{TEM} were relatively more abundant in Flock B, which exhibited higher overall beta-lactam resistance than the other flocks. Regarding phenicol resistance genes, *cmx* and *fexB* were significantly more abundant in Flock A. Notably, resistance genes associated with last-resort antibiotics (e.g., colistin, carbapenems, linezolid), specifically *optrA* and *poxtA*, were only detected in Flock A. Conversely, *mcr* gene variants and carbapenemase genes (e.g., bla_{KPC}, bla_{IMP}, bla_{VIM}, bla_{NDM}, $bla_{OXA-48-like}$) were not detected in any of the flocks.

The relative abundances of other AMR genes varied across flocks *(Fig. 4)*. A Venn diagram illustrated the number of common and unique genes among the groups *(Fig. 5-a)*. Furthermore, network diagrams based on the co-occurrence of bacterial genera and ARGs were presented to visualize statistical associations and identify potential resistance carriers *(Fig. 5-b)*. The majority of ARGs

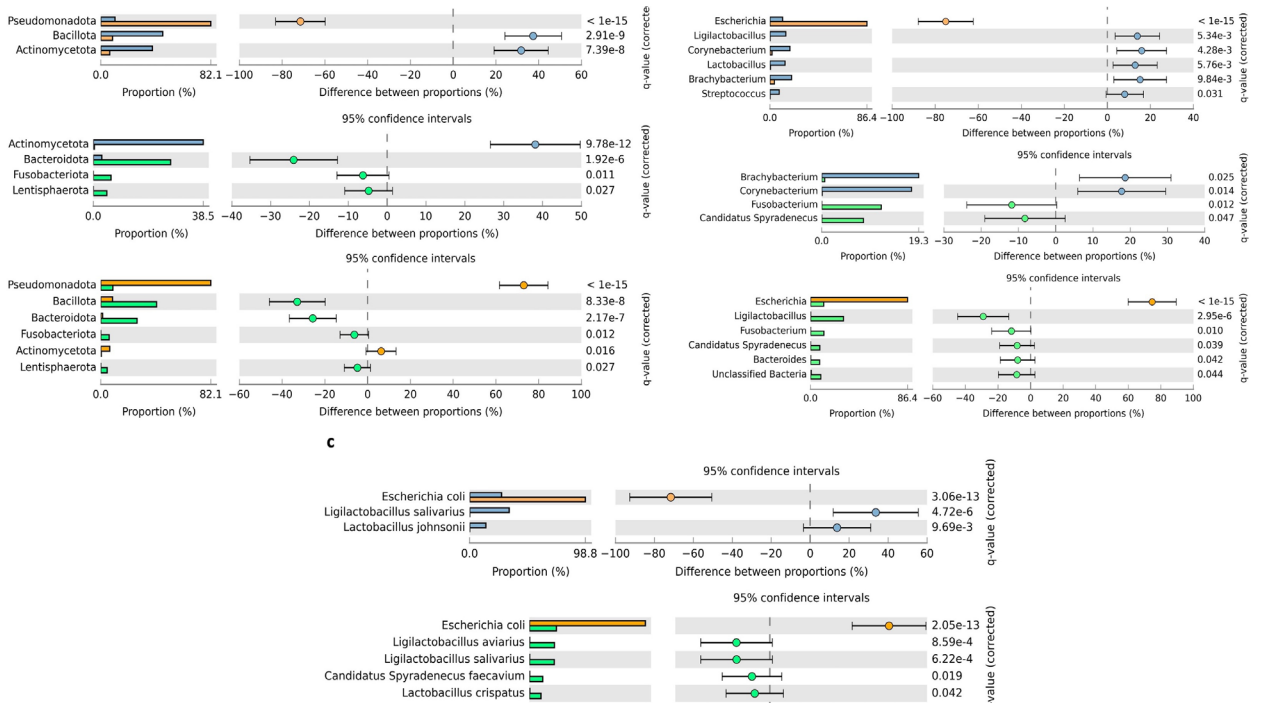

Fig 2. Extended error bar plots comparing microbial composition across the three flocks at different taxonomic levels: **a)** phylum, **b)** genus, and **c)** species. Each bar represents the proportion of taxa within each flock, with error bars indicating variability (e.g., standard error or confidence interval, if applicable). Colors denote flocks as follows: Flock A *(blue)*, Flock B *(orange)*, and Flock C *(green)*. Statistical differences between flocks were assessed using two-tailed Fisher's exact test with false discovery rate (FDR) correction (q-values <0.05)

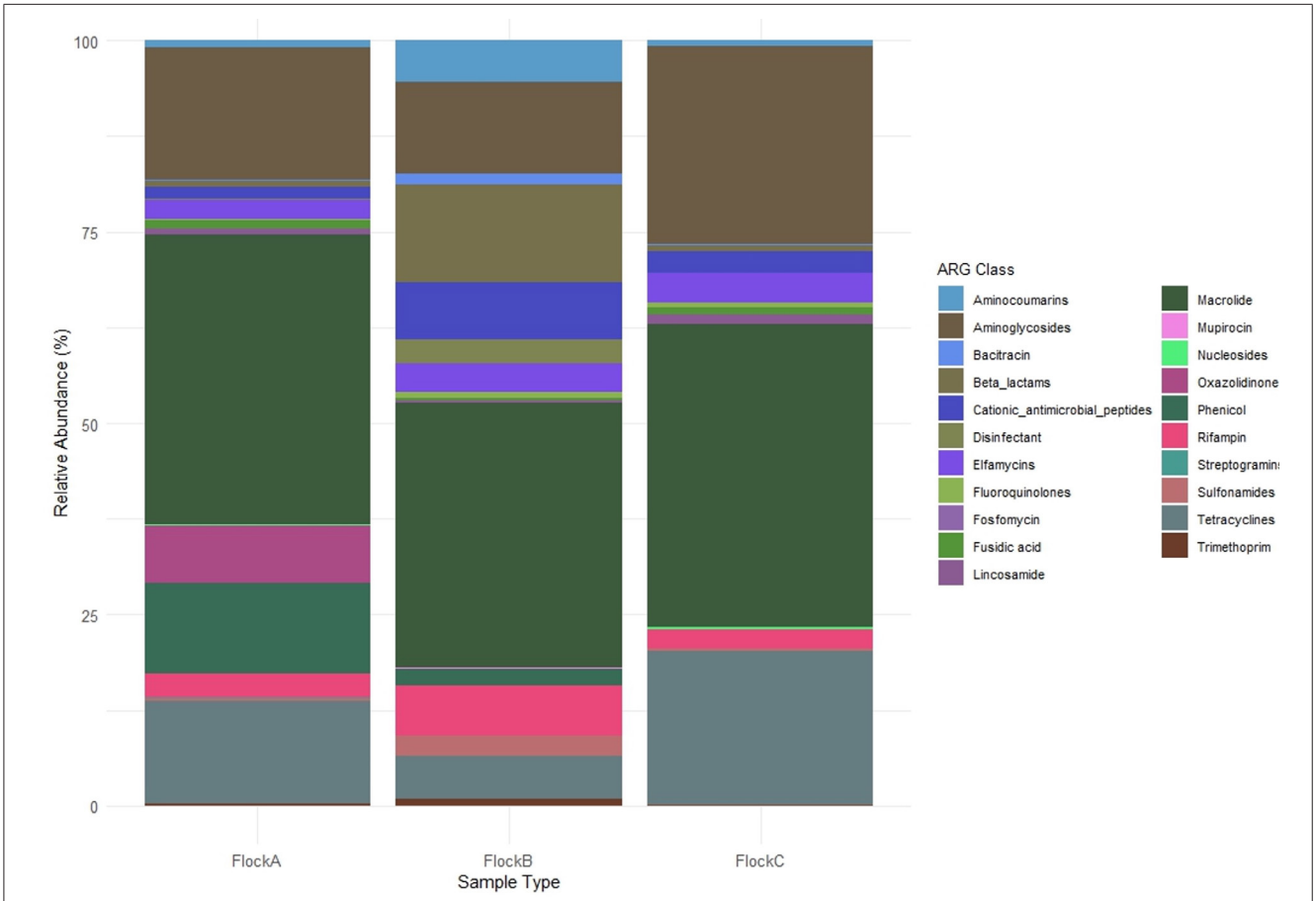

Fig 3. Stacked bar plots illustrating the relative abundance of antimicrobial resistance associated with different drug classes across the three flocks. Each bar represents an individual flock, and each segment within the bar corresponds to the proportion of resistance attributed to a specific drug class. Colors indicate distinct drug classes, as defined in the legend. The total height of each bar reflects the overall normalized abundance, enabling comparison of resistance profiles between flocks

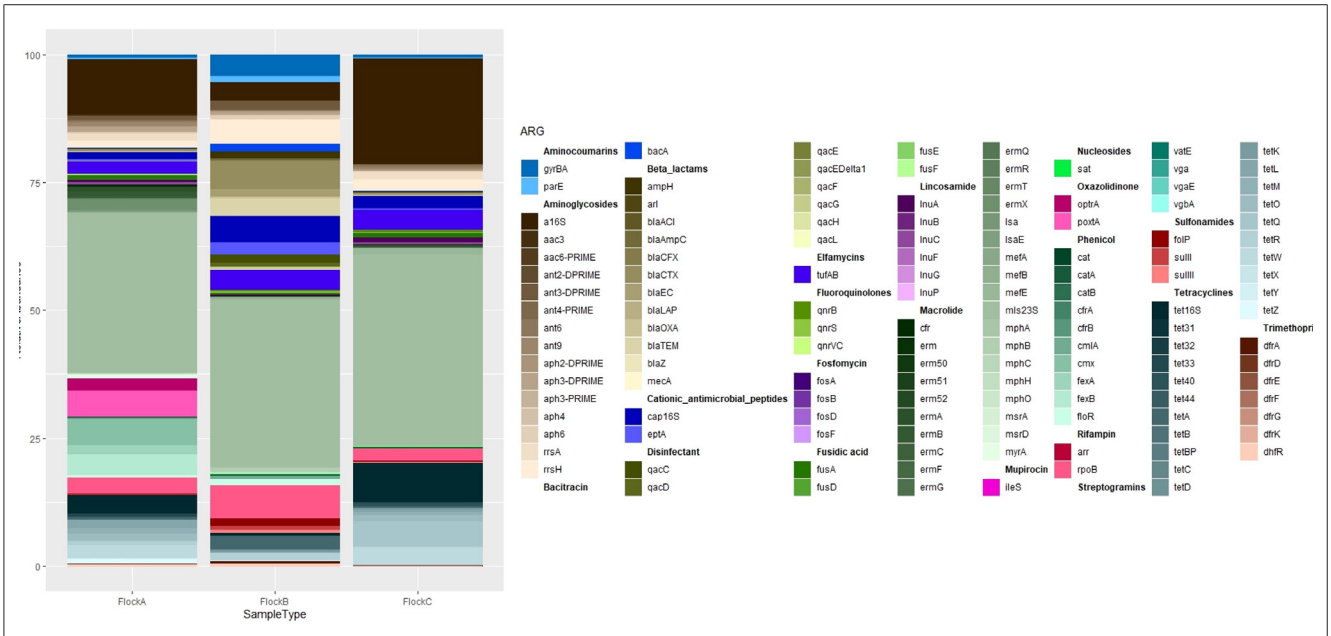

Fig 4. Stacked bar plots illustrating the relative abundance of antimicrobial resistance genes (ARGs) within each flock. Each bar represents a single flock, and each segment within the bar corresponds to the proportion of a specific ARG or ARG class. Colors indicate different ARGs (or ARG classes) as defined in the legend. The total height of each bar reflects the normalized relative abundance, allowing comparison of resistome composition across flocks

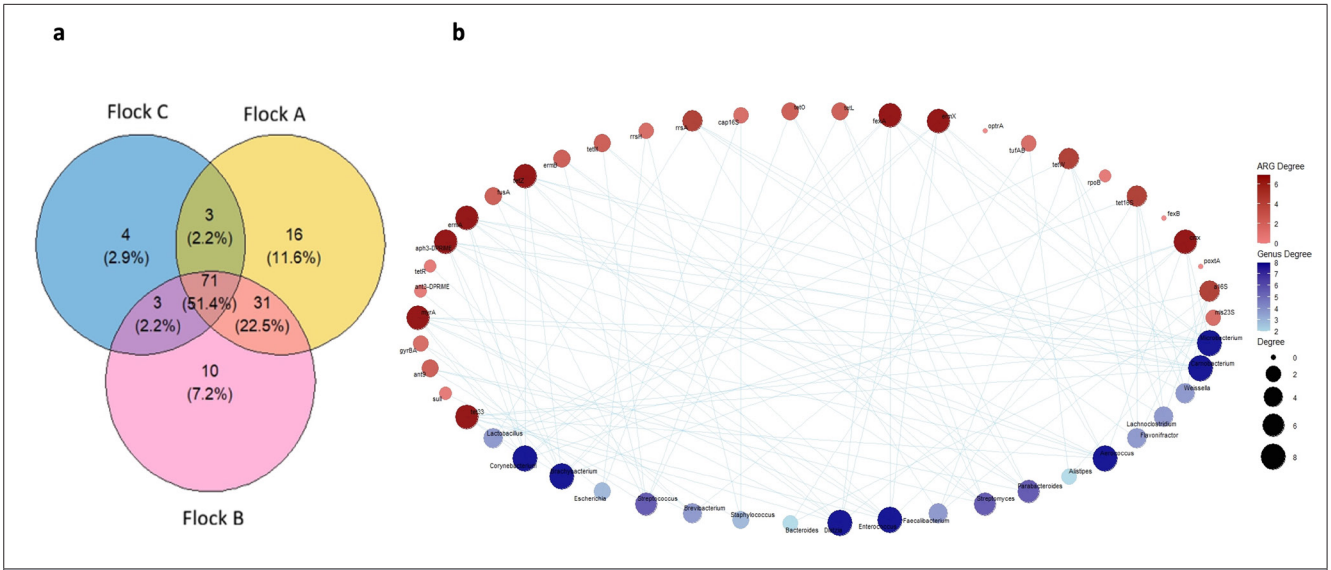

Fig 5. (a) Venn diagram showing the number of shared and unique ARGs among the flocks, **(b)** Co-occurrence network analysis identifying putative associations between bacterial genera *(red)* and ARGs *(red)*. Edges represent strong and statistically significant Spearman's correlations (rho >0.8, P<0.01). Node size is proportional to the relative abundance of each feature

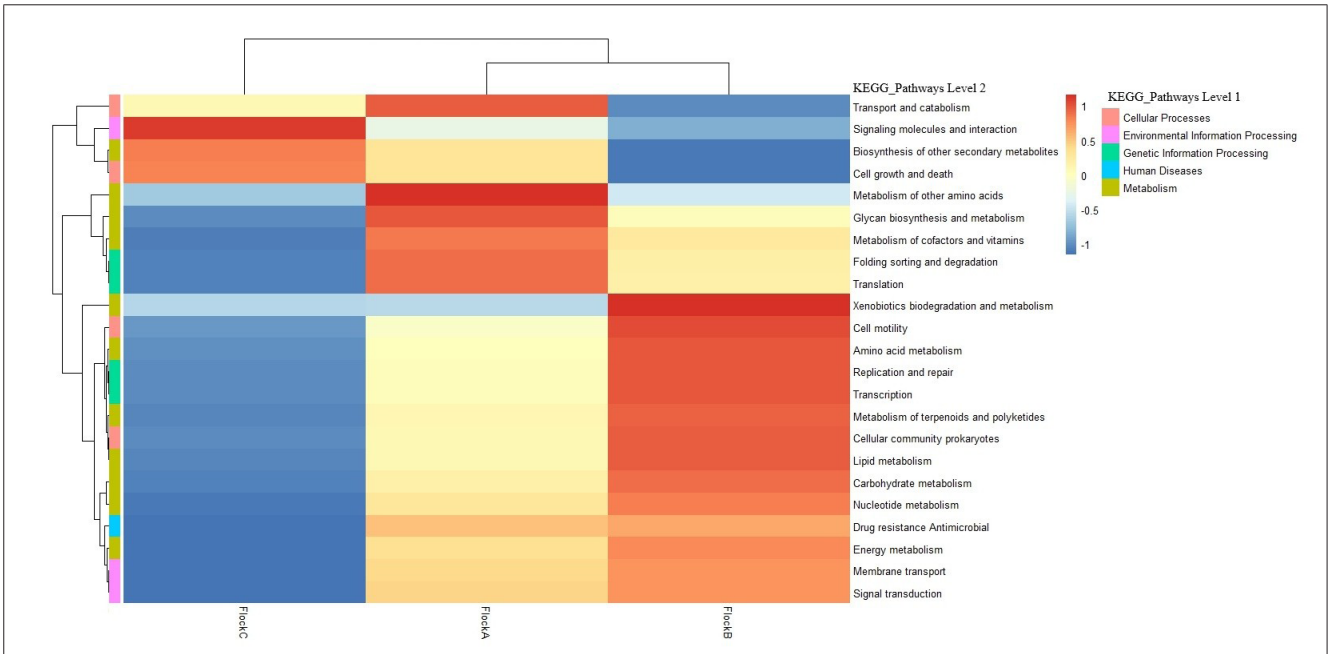

Fig 6. Heatmap illustrating the distribution of KEGG pathway abundances across the three flocks, organized according to hierarchical Levels 1 and 2. Rows represent individual KEGG pathways, while columns correspond to the different flocks. Color intensity indicates the normalized relative abundance of each pathway, with gradients reflecting lower to higher abundance levels. Pathways are grouped based on their functional hierarchy, enabling comparison of broad (Level 1) and more specific (Level 2) functional categories across flocks

were predicted to be associated with *Corynebacterium, Microbacterium, Dietzia, Enterococcus, Aerococcus, Carnobacterium,* and *Streptococcus*, suggesting their putative roles as resistance gene hosts. Specifically, the *tetZ* gene showed significant correlations with *Corynebacterium, Brachybacterium, Enterococcus, Dietzia,* and *Microbacterium*. Additionally, one of the most abundant genes, *MLS23S*, exhibited co-occurrence with *Alistipes* and *Bacteroides*. Moreover, *fexA* and *ermX* were associated with *Enterococcus, Dietzia, Carnobacterium,* and *Microbacterium (Fig. 5-b).*

Significant variations in ARG abundance and diversity were observed across the three flocks, particularly in Flock B, which showed a distinct profile characterized by a higher abundance of beta-lactam resistance genes. While these differences highlight the variability of the broiler gut resistome under different commercial conditions,

explicit records regarding on-farm management and antimicrobial usage (AMU) could not be retrieved for the sampled facilities.

The KEGG pathway analysis revealed that the most abundant pathways belonged to metabolism including carbohydrate, energy metabolism, biosynthesis of other secondary metabolites, amino acid, nucleotide, glycan biosynthesis and metabolism of cofactors and vitamins, replication and repair and genetic information processing which are folding, sorting and degradation, transcription, and translation *(Fig. 4)*. Drug resistance and antimicrobial pathway were more abundant in Flock A and B than Flock C. Xenobiotics biodegradation and metabolism pathway was the most abundant in Flock B than Flock A and C *(Fig. 6)*.

Discussion

This study aimed to comprehensively characterize the gut microbiome and resistome of broiler flocks using a shotgun metagenomics approach. The gut microbiota plays a central role in broiler health and productivity by maintaining intestinal homeostasis, inhibiting pathogen colonization, supporting intestinal development, and modulating host immune responses [26].

Previous studies have reported variable dominance patterns of major bacterial phyla, particularly Bacillota, Pseudomonadota, and Actinomycetota, in broiler gut microbiota [27,28]. In line with these findings, we observed marked compositional differences among flocks, with Bacillota predominating in Flocks A and C, while Pseudomonadota dominated Flock B. Such variation is likely driven by a complex interplay of host-related factors (e.g., age, genetics, immune status) and environmental conditions, including management practices, diet, and housing systems [29].

At the genus level, *Escherichia, Ligilactobacillus, Brachybacterium,* and *Corynebacterium* were among the most abundant taxa, consistent with previous reports [28,30]. *Ligilactobacillus salivarius,* in particular, has been associated with improved gut health and growth performance in broilers [31]. However, shifts in microbial composition may also arise under antimicrobial pressure, as antibiotic exposure has been shown to alter gut communities and increase the relative abundance of certain taxa, including *Ligilactobacillus* spp. and *Enterobacteriaceae* [32].

The increased abundance of xenobiotics biodegradation and metabolism pathways observed in Flock B may reflect greater exposure to exogenous compounds, such as pharmaceuticals or agrochemicals. These compounds can impose selective pressures on microbial communities, potentially contributing to shifts in community structure and the persistence of antimicrobial resistance [33,34]. In agreement with this observation, Flock B also exhibited higher ARG diversity. Nevertheless, due to the absence of detailed antimicrobial usage (AMU) and farm-level management data, these findings should be interpreted cautiously as indicative patterns rather than evidence of direct causal relationships.

The broiler gut microbiota constitutes an important reservoir of antimicrobial resistance genes. The widespread use of antimicrobials in poultry production has been associated with increased ARG abundance and diversity [35]. In the present study, ARGs conferring resistance to macrolides, aminoglycosides, and tetracyclines were predominant, which is consistent with previous studies [35,36]. In contrast, β-lactam resistance genes were generally less abundant, although a relatively higher proportion was observed in Flock B. These differences may reflect variations in selective pressures across farms; however, in the absence of AMU data, they should be regarded as baseline resistome characteristics rather than direct consequences of antimicrobial exposure.

Notably, resistance genes associated with critically important antimicrobials, such as *mcr,* bla_{NDM}, and bla_{KPC}, were not detected. However, the detection of linezolid resistance-associated genes *(optrA* and *poxtA)* in one flock highlights the potential emergence of resistance to last-resort antibiotics [36]. Similarly, plasmid-mediated quinolone resistance *(qnr)* genes were present at low abundance, which may not fully capture the extent of quinolone resistance, as high-level resistance is often mediated by chromosomal mutations or alternative mechanisms.

Network analysis revealed co-occurrence patterns between bacterial genera and ARGs, suggesting potential ecological associations between taxa and resistance determinants. However, these relationships should be interpreted with caution. Correlation-based analyses do not provide evidence of direct genetic linkage or host attribution. Rather, they identify statistical associations that may reflect shared ecological niches or selective pressures. High-resolution approaches, such as proximity ligation (Hi-C) sequencing or functional metagenomics, would be required to confirm host-gene relationships and horizontal gene transfer Dynamics.

In addition, the compositional nature of metagenomic data introduces inherent limitations. Because sequencing

data are relative, an apparent increase in one taxon may lead to a proportional decrease in others, potentially generating spurious correlations. Therefore, the associations identified in this study should be considered hypothesis-generating rather than definitive.

A pooling strategy was employed to characterize the resistome at the flock level. Although individual sampling can provide insights into within-flock variation, pooled samples offer a cost-effective and representative overview of dominant microbial and resistance profiles across the production unit. This approach is widely used in large-scale surveillance programs, such as DANMAP [36].

Several limitations should be acknowledged. First, the study was limited to three flocks, which may not fully capture the diversity of broiler production systems. Second, the absence of detailed antimicrobial usage and management data restricts the ability to establish causal relationships. Finally, the pooling strategy does not account for individual bird-level variation within flocks.

In conclusion, this study provides a high-resolution snapshot of the broiler gut microbiome and resistome in Türkiye. The observed differences among flocks highlight the variability of microbial and resistance profiles under commercial production conditions. However, these findings should be interpreted as baseline observations rather than evidence of causality. Future longitudinal and multi-center studies incorporating detailed antimicrobial usage and management data will be essential to better understand the drivers of antimicrobial resistance in poultry production systems.

Declarations

Availability of Data and Materials: Data are available via NCBI BioProject PRJNA1401269.

Funding Support: The study received no funding.

Conflict of Interest: The authors have no conflicts of interest to disclose.

Ethical Statement: This study was approved by Hatay Mustafa Kemal University Animal Experiments Local Ethics Committee (Decision number: 2025/07-11)

Generative Artificial Intelligence (AI): The authors declare that the article and/or tables and figures were not written/created by AI and AI-assisted technologies.

Further Considerations: We declare that the project and the information in the article are compatible and no other publications have been produced from the project, order of the researchers in the project proposal are compatible with those in the article.

Author Contributions: ÖA conceptualization, supervision, writing-review & editing, SŞD bioinformatic analysis, writing-review & editing

References

1. **WHO:** Antimicrobial resistance. https://www.who.int/health-topics/antimicrobial-resistance; *Accessed:* 24.10.2025.
2. **Singh S, Kriti M, Anamika KS, Sharma P, Pal N, Sarma DK, Tiwari R, Kumar M:** A one health approach addressing poultry-associated antimicrobial resistance: Human, animal and environmental perspectives. *The Microbe*, 7:100309, 2025. DOI: 10.1016/j.microb.2025.100309
3. **Hedman HD, Vasco KA, Zhang L:** A review of antimicrobial resistance in poultry farming within low-resource settings. Animals (Basel), 10 (8):1264, 2020. DOI: 10.3390/ani10081264
4. **Collignon P, Voss A:** China, what antibiotics and what volumes are used in food production animals? *Antimicrob Resist Infect Control,* 4, 1-4, 2015. DOI: 10.1186/s13756-015-0056-5
5. **Aarestrup FM, Bager F, Jensen NE, Madsen M, Meyling A, Wegener HC:** Resistance to antimicrobial agents used for animal therapy in pathogenic-, zoonotic- and indicator bacteria isolated from different food animals in Denmark: A baseline study for the Danish Integrated Antimicrobial Resistance Monitoring Programme (DANMAP). *APMIS,* 106, 745-770, 1998. DOI: 10.1111/j.1699-0463.1998.tb00222.x
6. **Gilbert JM, White DG, McDermott PF:** The US national antimicrobial resistance monitoring system. *Future Microbiol,* 2 (5): 493-500, 2007. DOI: 10.2217/17460913.2.5.493
7. **Schwarz S, Alesík E, Grobbel M, Lübke-Becker A, Wallmann J, Werckenthin C, Wieler LH:** The BfT-GermVet monitoring program - Aims and basics. *Berl Münch Tierärztl Wochenschr,* 120 (9-10): 357-362, 2007. DOI: 10.2376/0005-9366-120-357
8. **Aslantaş Ö:** High occurrence of CMY-2-type beta-lactamase-producing *Escherichia coli* among broiler flocks in Turkey. *Trop Anim Health Prod,* 52 (4): 1681-1689, 2020. DOI: 10.1007/s11250-019-02167-8
9. **Aslantaş Ö, Küçükaltay K:** Investigation and molecular characterization of colistin resistance in commensal *Escherichia coli* strains isolated from broiler flocks. *Isr J Vet Med,* 78 (3): 25-35, 2023.
10. **Aslantaş Ö:** Molecular and phenotypic characterization of enterococci isolated from broiler flocks in Turkey. *Trop Anim Health Prod,* 51 (5):1073-1082, 2019. DOI: 10.1007/s11250-018-01784-z
11. **Aslantaş Ö:** Antimicrobial resistance among commensal *Escherichia coli* from broilers in Turkey. *Isr J Vet Med,* 73 (3): 19-25, 2018.
12. **Yılmaz EŞ, Aslantaş Ö, Pehlivanlar Önen S, Türkyılmaz S, Kürekci C:** Prevalence, antimicrobial resistance and virulence traits in enterococci from food of animal origin in Turkey. *LWT - Food Sci Technol,* 66, 20-26, 2016. DOI: 10.1016/j.lwt.2015.10.009
13. **Pehlivanlar Önen S, Aslantaş Ö, Şebnem Yılmaz E, Kürekci C:** Prevalence of β-lactamase producing *Escherichia coli* from retail meat in Turkey. *J Food Sci,* 80 (9): M2023-M2029, 2015. DOI: 10.1111/1750-3841.12984
14. **Cason C, D'Accolti M, Soffritti I, Mazzacane S, Comar M, Caselli E:** Next-generation sequencing and PCR technologies in monitoring the hospital microbiome and its drug resistance. *Front Microbiol,* 13:969863, 2022. DOI: 10.3389/fmicb.2022.969863
15. **Szoke Z, Fauszt P, Mikolas M, David P, Szilagyi-Tolnai E, Pesti-Asboth G, Homoki JR, Kovacs-Forgacs I, Gal F, Stundl L, Czegledi L, Stagel A, Biro S, Remenyik J, Paholcsek M:** Comprehensive analysis of antimicrobial resistance dynamics among broiler and duck intensive production systems. *Sci Rep,* 15 (1):4673, 2025. DOI: 10.1038/s41598-025-89432-z
16. **Wingett SW, Andrews S:** FastQ screen: A tool for multigenome mapping and quality control. *F1000Res,* 7:1338, 2018. DOI: 10.12688/f1000research.15931.2
17. **Bolger AM, Lohse M, Usadel B:** Trimmomatic: A flexible trimmer for Illumina sequence data. *Bioinformatics,* 30, 2114-2120, 2014. DOI: 10.1093/bioinformatics/btu170

18. **Langmead B, Salzberg SL:** Fast gapped-read alignment with Bowtie2. *Nat Methods,* 9, 357-359, 2012. DOI: 10.1038/nmeth.1923

19. **Tamames J Puente-Sánchez F:** SqueezeMeta, a highly portable, fully automatic metagenomic analysis pipeline. *Front Microbiol,* 9:3349. DOI: 10.3389/fmicb.2018.03349

20. **Bonin N, Doster E, Worley H, Pinnell LJ, Bravo JE, Ferm P, Marini S, Prosperi M, Noyes N, Morley PS, Boucher C:** MEGARes and AMR++, v3.0: An updated comprehensive database of antimicrobial resistance determinants and an improved software pipeline for classification using high-throughput sequencing. *Nucleic Acids Res,* 51, D744-D752, 2023. DOI: 10.1093/nar/gkac1047

21. **Parks DH, Tyson GW, Hugenholtz P, Beiko RG:** STAMP: Statistical analysis of taxonomic and functional profiles. *Bioinformatics,* 30, 3123-3124, 2014. DOI: 10.1093/bioinformatics/btu494

22. **Harrell FE Jr, Dupont C:** Hmisc: Harrell Miscellaneous. R Package Version 4.2-0, 2019. https://CRAN.R-project.org/package=Hmisc23; *Accessed:* October 12, 2025.

23. **Csardi G, Nepusz T:** The Igraph Software Package for Complex Network Research. InterJournal, Complex Systems, 1695, 1-9, 2006. http://igraph.org; *Accessed:* October 12, 2025.

24. **Wickham H, Chang W, Henry L, Pedersen TL, Takahashi K, Wilke C, Woo K, Yutani H, Dunnington D:** *ggplot2:* Create elegant data visualisations using the grammar of graphics (R package version 3.4.0) [Computer software]. Comprehensive R Archive Network (CRAN), 2007. https://CRAN.R-project.org/package=ggplot2; *Accessed:* October 12, 2025.

25. **Yan L:** *ggvenn:* Draw Venn diagram by *"ggplot2"* (Version 0.1.9) [R package]. Comprehensive R Archive Network (CRAN), 2021. https://CRAN.R-project.org/package=ggvenn; *Accessed:* October 12, 2025.

26. **Jia M, Lei J, Dong Y, Liu X, Zhang H, Wang Q:** The interactive effects of nutrient density and breed on growth performance and gut microbiota in broilers. *Animals,* 14 (23):3528, 2024. DOI: 10.3390/ani14233528

27. **Zhou Q, Lan F, Li X, Chen Y, Zhang T, Wang H:** The spatial and temporal characterization of gut microbiota in broilers. *Front Vet Sci,* 8:712226, 2021. DOI: 10.3389/fvets.2021.712226

28. **Khan MM, Mushtaq MA, Suleman M, Ahmad A, Iqbal Z:** Fecal microbiota landscape of commercial poultry farms in Faisalabad, Pakistan: A 16S rRNA gene-based metagenomics study. *Poult Sci,* 104:105089, 2025. DOI: 10.1016/j.psj.2025.105089

29. **Diaz Carrasco JM, Casanova NA, Fernández Miyakawa ME:** Microbiota, gut health and chicken productivity: What is the connection? *Microorganisms*, 7 (10):374, 2019. DOI: 10.3390/microorganisms7100374

30. **Alvarenga BO, Paiva JB, Souza AIS, Rodrigues DR, Tizioto PC, Ferreira AJP:** Metagenomics analysis of the morphological aspects and bacterial composition of broiler feces. *Poult Sci,* 102 (2):102401, 2023. DOI: 10.1016/j.psj.2022.102401

31. **Yang J, Wang J, Liu Z, Chen J, Jiang J, Zhao M, Gong D:** *Ligilactobacillus salivarius* improve body growth and anti-oxidation capacity of broiler chickens via regulation of the microbiota-gut-brain axis. *BMC Microbiol,* 23 (1):395, 2023. DOI: 10.1186/s12866-023-03135-x

32. **Mancabelli L, Ferrario C, Milani C, Mangifesta M, Turroni F, Duranti S, Lugli GA, Viappiani A, Ossiprandi MC, van Sinderen D, Ventura M:** Insights into the biodiversity of the gut microbiota of broiler chickens. *Environ Microbiol,* 18, 4727-4738, 2016. DOI: 10.1111/1462-2920.13363

33. **Das A, Srinivasan M, Ghosh TS, Mande SS:** Xenobiotic metabolism and gut microbiomes. *PLoS One,* 11:e0163099, 2016. DOI: 10.1371/journal.pone.0163099

34. **Gonçalves M, Vale N, Martins da Costa P, Silva P:** Xenobiotics and broiler microbiota: Molecular insights into bacterial antimicrobial resistance and food-safety implications for human health. *J Xenobiotics,* 15:129, 2025. DOI: 10.3390/jox15040129

35. **Liang C, Wei Y, Wang X, Gao J, Cui H, Zhang C, Liu J:** Analysis of resistance gene diversity in the intestinal microbiome of broilers from two types of broiler farms in Hebei Province, China. *Antibiotics,* 12 (12):1664, 2023. DOI: 10.3390/antibiotics12121664

36. **Munk P, Knudsen BE, Lukjancenko O, Duarte ASR, Van Gompel L, Luiken REC, Smit LAM, Schmitt H, Garcia AD, Hansen RB, Petersen TN, Bossers A, Ruppé E; EFFORT Group; Lund O, Hald T, Pamp SJ, Vigre H, Heederik D, Wagenaar JA, Mevius D, Aarestrup FM:** Abundance and diversity of the faecal resistome in slaughter pigs and broilers in nine European countries. *Nat Microbiol,* 3 (8): 898-908, 2018. DOI: 10.1038/s41564-018-0192-9

Kafkas Universitesi Veteriner Fakultesi Dergisi
Journal Home-Page: http://vetdergikafkas.org
E-ISSN: 1309-2251

Kafkas Univ Vet Fak Derg
32 (2): 239-246, 2026
DOI: 10.9775/kvfd.2025.35579

Research Article

Dexmedetomidine Up-Regulates UCP2 via Modulation of the AMPK Pathway Is Associated with Reduced ROS and Neuroprotection in Neonatal Mice with Hypoxic-Ischemic Brain Damage

Bin NIE [1,†], Min ZHU [2,†], Songquan HU [3], Lei TAN [1], Jintao WANG [1]

[†] *The two authors contributed equally to this study*

[1] Hubei Key Laboratory of Geriatric Anesthesia and Perioperative Brain Health, and Wuhan Clinical Research Center for Geriatric Anesthesia, Tongji Hospital, Tongji Medical College, Huazhong University of Science and Technology, Department of Anesthesiology and Pain Medicine, 430030 Wuhan, CHINA

[2] The Third Affiliated Hospital of Xinjiang Medical University, Department of Anesthesiology, 830000 Urumqi, CHINA

[3] Jiangxi Maternal and Child Health Hospital, Department of Anesthesiology, 330003 Nanchang, CHINA

[*] **Corresponding author:**
Jintao Wang
Phone: +86-018564202361
E-mail: wangjtthtmc@uic-edu.cn

How to cite this article?

Nie B, Zhu M, Hu S, Tan L, Wang J: Dexmedetomidine Up-Regulates UCP2 via Modulation of the AMPK Pathway is Associated with Reduced ROS and Neuroprotection in Neonatal Mice with Hypoxic-Ischemic Brain Damage. *Kafkas Univ Vet Fak Derg*, 32 (2): 239-246, 2026
DOI: 10.9775/kvfd.2025.35579

Article ID: KVFD-2025-35579
Received: 05.11.2025
Accepted: 25.02.2026
Published Online: 05.03.2026

Abstract

We aimed to investigate whether dexmedetomidine (Dex) alleviates hypoxic-ischemic brain damage (HIBD) in neonatal mice and to explore the potential involvement of AMPK-related mechanisms. C57BL/6 neonatal mice were randomly assigned into a sham group, an HIBD group, an HIBD + Dex group, and an HIBD + Dex + Compound C (CC) group. Neurological deficits were scored, brain water content was detected and cerebral infarction areas were determined via 2,3,5-triphenyltetrazolium chloride staining. Hematoxylin-eosin staining was performed to detect the pathological changes in brain tissues. Compared with the sham group, HIBD mice showed markedly increased neurological deficit scores, brain water content, infarct area, ROS, and MDA levels, accompanied by reduced GSH-Px, SOD activity, a lower p-AMPK/AMPK ratio, and decreased UCP2 expression ($P<0.05$). Dex treatment significantly improved neurological function, reduced cerebral edema and infarction, decreased oxidative stress markers, and enhanced antioxidant enzyme activity, together with increased AMPK phosphorylation and UCP2 expression compared with HIBD ($P<0.05$). Notably, co-administration of Compound C partially attenuated the neuroprotective and antioxidative effects of Dex, supporting the involvement of AMPK-dependent mechanisms. Although UCP2 expression was altered in parallel with AMPK activity, the present data do not directly establish UCP2 as a causal mediator. Overall, these findings suggest that Dex mitigates oxidative stress and neuronal injury in neonatal HIBD, potentially through AMPK-associated pathways, with UCP2 representing a putative downstream component.

Keywords: AMPK, Brain damage, Dexmedetomidine, Neonate, Oxidative stress

Introduction

Hypoxic-ischemic brain damage (HIBD), a common brain lesion in neonates in the perinatal period, is mainly characterized by deficiency in oxygen supply or reduction in blood perfusion to brain tissues. The clinical manifestations of HIBD include a series of neurological dysfunction, and some child patients may experience sequelae including mental retardation, motor dysfunction and even cerebral palsy, posing substantial impacts on the long-term quality of life of these patients. Such a serious nervous system injury not only brings lifelong health risks to the child patients, but also imposes a heavy care burden and economic pressure on the family and society [1]. Neuronal damage serves as the kernel mechanism of HIBD development and progression, which directly affects the process and outcome of diseases. Hence, the protection of neurons has become a key strategy for HIBD treatment [2].

As a crucial pathological feature of HIBD, oxidative stress stimulates the excessive accumulation of reactive oxygen species (ROS) to attack neurons and destroy the structure and function of brain tissues [3]. Although oxidative stress has been widely recognized as a central contributor to neuronal injury in HIBD, the upstream regulatory pathways that coordinate mitochondrial redox homeostasis under hypoxic-ischemic conditions remain incompletely understood. Based on this pathological mechanism, seeking drugs that can effectively intervene in HIBD from the perspective of anti-oxidative stress has emerged as an important direction of clinical research at present.

Dexmedetomidine (Dex) is a highly specific α2 adrenergic receptor agonist, which is frequently applied to sedation and analgesia in perioperative period [4]. It possesses anti-oxidant, anti-inflammatory, anti-apoptotic and many other neuroprotective effects [5]. Previous evidence has linked Dex to the regulation of oxidative stress and energy-sensing pathways, including AMPK signaling, in different neurological injury contexts [6]. In neonatal rat model of HIBD, Dex has been shown to mitigate neuronal injury and improve neurological outcomes by relieving pathological damage, modulating inflammatory responses, and suppressing neuronal cell death [7,8]. However, how Dex integrates mitochondrial oxidative stress control with cellular energy-sensing mechanisms in neonatal HIBD remains largely unexplored.

Uncoupling protein 2 (UCP2) is a protein localized in the inner mitochondrial membrane, which can reduce ROS production by lowering the mitochondrial membrane potential, thereby exerting an anti-oxidant effect [9]. Adenosine 5'-monophosphate-activated protein kinase (AMPK) is a key metabolic sensor that responds to cellular energy stress and has been reported to influence mitochondrial function and oxidative balance [10]. Recent study suggests that AMPK may modulate UCP2 expression or activity as part of a coordinated response to metabolic and oxidative stress [11]; however, the relevance of this regulatory relationship in neonatal hypoxic-ischemic brain injury has not been established. Notably, whether AMPK-associated regulation of UCP2 contributes to Dex-mediated neuroprotection under hypoxic-ischemic conditions remains unknown.

Therefore, the present study was designed to explore the involvement of AMPK-dependent mechanisms, with a particular focus on the AMPK-UCP2 axis, in the antioxidative and neuroprotective effects of Dex in neonatal mice with HIBD.

Material and Methods

Ethical Approval

This study has been approved by the ethic committee of Tongji Hospital (Approval No. TJH-202111026), and great efforts have been made to minimize the animals' suffering.

Experimental Animals

SPF-grade C57BL/6 neonatal mice (n=40, 7 days old, no restriction in sex) were purchased from Hainan Pharmaceutical Research Institute Co., Ltd. [Animal License No. SCXK (Hainan) 2020-0007]. All mice weighing 4-5 g were uniformly raised in a sterile animal room with a temperature of 22-25°C, relative humidity of 60%, and a 12 h/12 h light/dark cycle. They were fed adaptively for 7 d before experiments, without deprivation of water and food. Sex was not treated as an independent biological variable due to the limited sample size.

Reagents and Apparatus

Dex was supplied by Beijing Kaishiyuan Biotechnology Co., Ltd. ROS detection kit was purchased from US Everbright Inc. Compound C (CC), an AMPK inhibitor, was offered by MCE (USA). Enzyme-linked immunosorbent assay (ELISA) kit sourced from Shanghai ZCi Biotech Co., Ltd. RIPA lysis buffer, bicinchoninic acid (BCA) protein assay kit, and ECL solution were provided by Beijing Solarbio Science & Technology Co., Ltd. Antibodies against phosphorylated (p)-AMPK, AMPK, and UCP2 were procured from CST (USA). A microscope (model: DM2000LED) was supplied by Leica (Germany). A microplate reader (model: Infinite M200) was bought from BioTek.

Grouping and Modeling Methods

Forty mice were allocated to a sham operation group (sham group, n=10) and a model group (n=30) in a random manner. After all mice were anesthetized with 3% pentobarbital sodium (100 μL in volume) through intraperitoneal injection. The same anesthetic protocol was applied across all experimental groups to minimize potential confounding effects. Pentobarbital was used solely for surgical anesthesia and was not considered an experimental variable in this study. After anesthesia, the neck was routinely disinfected and a median incision was made to expose the left common carotid artery. In the model group, the left common carotid artery was double ligated using surgical sutures, and the incision was sutured layer by layer. A thermostatic (37°C) pad was employed to maintain body temperature throughout the operation. After surgery, mice in the model group were placed in a customized hypoxic chamber, and exposed to a gas mixture of 8% O_2 and 92% N_2 at a flow rate of 2.5-3.5 L/min for 2 h once oxygen concentration stabilized below 10%. In the sham group, only vessel exposure was performed without arterial ligation or hypoxia intervention. The neonatal mouse model of HIBD was successfully prepared when the mice manifested toddling, limb paralysis, and other phenomena.

Totally 2 mice died during modeling, and 1 mouse failed. Thus, 27 successfully modeled mice were randomly assigned to the HIBD group (n=9), an HIBD + Dex group (n=9), and HIBD + Dex + CC group (n=9). The sample size was determined based on previous HIBD studies using similar experimental designs and outcome measures [12]. Given the exploratory nature of this study and ethical considerations regarding animal use, a formal a priori power analysis was not performed. The mice in the HIBD + Dex group were intraperitoneally injected with 50 μg/kg Dex for intervention immediately after modeling [13]. The

mice in the HIBD + Dex + CC group were intraperitoneally injected with 50 μg/kg Dex immediately after modeling, followed by intraperitoneal injection of CC (10 mg/kg) [14]. The intraperitoneal injection of 0.9% sodium chloride solution in the same volume was conducted in the sham and HIBD groups. All subsequent assessments were performed at a predefined early time point to evaluate acute pathological and biochemical changes following hypoxic-ischemic injury.

Scoring of Severity of Neurological Deficits

After the completion of drug intervention, the neurological function of neonatal mice in all experimental groups was evaluated using the neurological deficit score (NDS) system [15], with the specific scoring criteria listed in *Table 1*. All behavioral assessments were conducted by investigators blinded to group allocation. Neurological deficit scoring was conducted 24 h after hypoxic-ischemic injury and pharmacological intervention.

Sample Collection

After the NDS evaluation, 6 mice randomly selected from each group were decapitated, and craniotomy was performed rapidly to remove the brain tissues on the left side and isolate the hippocampus. Following rinsing with precooled PBS buffer, the tissue samples were immediately stored at -80°C for later use. The remaining 3 mice were fixed in the supine position, perfused with 0.9% normal saline followed by 4% paraformaldehyde, and whole brains were collected for histological examination. All tissue collection procedures for biochemical assays, Western blotting, and histological analyses were performed at the same time point.

Measurement of Brain Water Content

The whole brain tissues were immediately measured as wet weight, and the brain tissue was baked in a 100°C oven for 72 h to obtain the dry weight. The ratio of the difference between wet weight and dry weight to wet weight was determined as brain water content (%).

2,3,5-Triphenyltetrazolium Chloride (TTC) Staining

The brain tissues frozen in -20°C refrigerator were sliced to uniform sections (2 mm-thick) along the coronal plane using a microtome, followed by 30 min of incubation with ice-cold 2% TTC solution. Thereafter, the sections were taken out and immersed in 4% paraformaldehyde solution for 24 h, and the images were captured to measure and calculate the cerebral infarction area in each group of mice through ImageJ v1.8.0.

Table 1. *Neurological function scoring criteria*

Score	Symptom
0 point	No nerve damage
1 point	Inability of the left forelimb to bend inward
2 points	Rotation of the left forelimb to the left or walking toward the left side
3 points	Rotation of the mouse to the left side like chasing the tail

Hematoxylin-Eosin (HE) Staining

The 4% paraformaldehyde-fixed brain tissues were embedded in paraffin, dehydrated in a gradient of ethanol (70-100%), and transparentized using xylene solution. Later, the treated tissue blocks were prepared into 5 μm-thick serial sections *via* the microtome. After double staining with hematoxylin and eosin, the sections were mounted with drops of neutral balsam. Finally, the sections were observed under a light microscope and analyzed for pathological-morphological changes in the brain tissues.

ELISA for Levels of Oxidative Stress Indicators in Brain Tissues

The brain tissues were obtained from the mice in each group, cut into pieces (1 mm in size) with ophthalmic scissors, and transferred to a centrifuge tube on ice. Then the supernatant was discarded after the tissues were precipitated, which were digested into tissue homogenates using 0.25% trypsin. Afterward, the suspension was centrifuged at 3.000 rpm for 10 min in a centrifuge, so as to harvest the supernatant. The levels of ROS, glutathione peroxidase (GSH-Px), malondialdehyde (MDA), and superoxide dismutase (SOD) in the supernatant were measured by means of ELISA.

Determination of Protein Expressions Through Western Blotting

The hippocampal tissues homogenized and lysed using RIPA lysis buffer supplemented with protease and phosphatase inhibitors on ice for 30 min. After centrifugation at 10.000 rpm for 10 min at 4°C, the supernatant was collected as total protein extract. Protein concentration was determined using the BCA kit. Equal amounts of protein (30 μg per lane) were subjected to SDS-PAGE gel and transferred to polyvinylidene fluoride (PVDF) membranes. After blocking with 5% non-fat milk for 1 h, the membranes were incubated with primary antibodies against p-AMPK, AMPK, UCP2, and GAPDH (1:500) overnight at 4°C. ON the next day, the membranes were incubated with HRP-labeled secondary antibodies (1:1000) for 3 h at room temperature. Protein band intensities were quantified using ImageJ software. p-AMPK levels were normalized to total AMPK, and UCP2 expression was normalized to GAPDH.

Statistical Analysis

GraphPad Prism 8.0 software was employed to conduct

the statistical analysis of experimental data. Data were expressed by mean ± standard deviation (Mean ± SD). One-way ANOVA was used for comparisons among multiple groups. Post hoc multiple comparisons were performed using Tukey's test to reduce the risk of type I error. P<0.05 suggested a difference of statistical significance.

Results

The NDS of mice in the HIBD group was significantly higher than that in the sham group (P<0.05). The mice in the HIBD + Dex group had reduced NDS compared to those in the HIBD group (P<0.05) and the HIBD + Dex + CC group (P<0.05) *(Fig. 1)*.

When contrasted with the sham group, the HIBD group presented significantly raised brain water content (P<0.05). The brain water content in mice was significantly lower in the HIBD + Dex group than in the HIBD group (P<0.05) and the HIBD + Dex + CC group (p<0.05) *(Fig. 2)*.

Compared with the sham group, the cerebral infarction area was significantly increased in the HIBD group (P<0.05). In contrast, the cerebral infarction area was significantly reduced in the HIBD + Dex group compared with the HIBD group (p<0.05) and the HIBD + Dex + CC group (P<0.05) *(Fig. 3)*.

In the sham group, the hippocampal neurons were tightly and orderly arranged, with complete and regular cell morphology. The HIBD group manifested remarkable pathological changes such as obvious neuron swelling, evident reduction in cell density, and widespread neuronal damage. The density of neurons was notably elevated, the

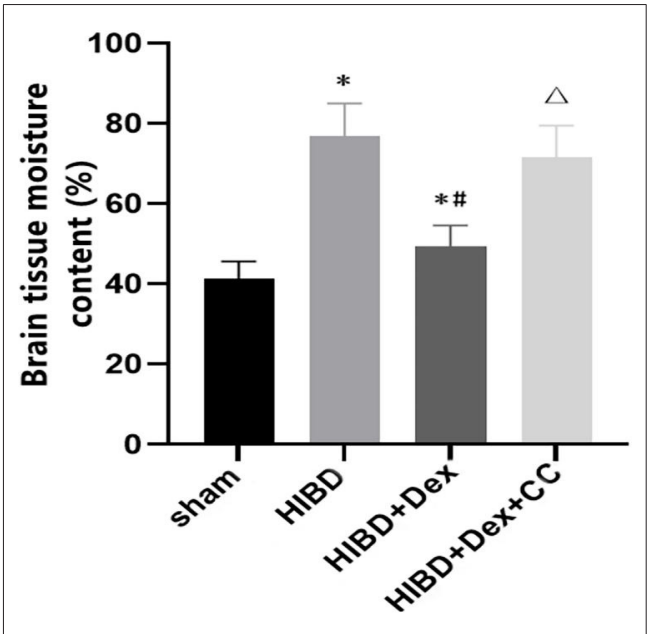

Fig 1. NDS of mice. *P<0.05 vs. Sham Group, #P<0.05 vs. HIBD Group, and *P<0.05 vs. HIBD + Dex Group

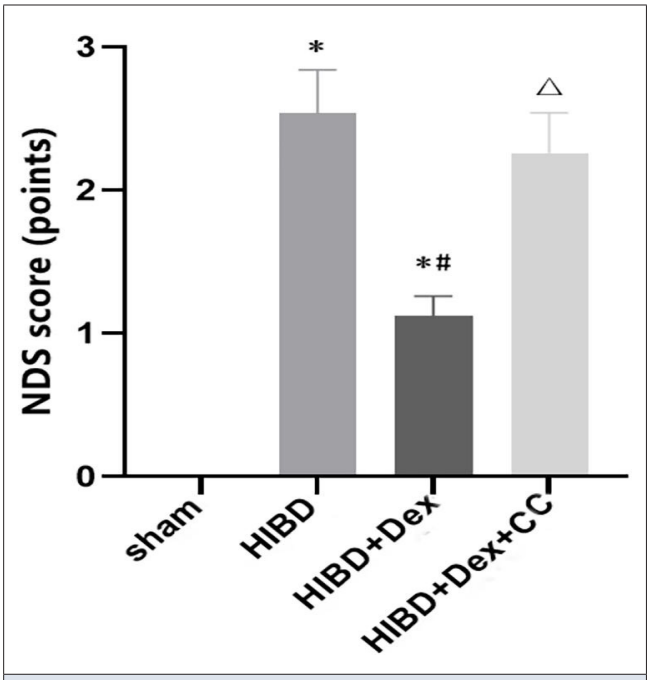

Fig 2. Brain water content in different groups of mice. *p<0.05 vs. Sham Group, #p<0.05 vs. HIBD Group, and p<0.05 vs. HIBD + Dex Group

cell arrangement tended to be regular, and the swelling was apparently improved in the HIBD + Dex group by comparison to those in the HIBD group. In contrast, the HIBD + Dex + CC group showed similar severity of neuronal damage to the HIBD group, without significant protective effect *(Fig. 4)*.

Compared with those in the sham group, the relative ROS level and MDA content in murine brain tissues rose significantly, whereas the GSH-Px content and SOD activity dropped significantly in the HIBD group (P<0.05). The HIBD + Dex group, when contrasted with the HIBD group, presented significant decreases in relative ROS level and MDA content, together with significant increases in GSH-Px content and SOD activity in the brain tissues of mice (P<0.05). The relative ROS level and MDA content in the brain tissues of mice in the HIBD + Dex + CC group were significantly higher, but the GSH-Px content and SOD activity were significantly lower than those in the HIBD + Dex group (P<0.05) *(Fig. 5)*.

The p-AMPK/AMPK ratio and UCP2 protein expression were significantly decreased in the brain tissues of mice in the HIBD group compared with the sham group (P<0.05). Dex treatment was associated with a significant increase in the p-AMPK/AMPK ratio and UCP2 protein expression compared with the HIBD group (P<0.05). These increases were attenuated in the presence of Compound C, indicating that the observed changes in UCP2 expression occurred in parallel with alterations in AMPK phosphorylation (p<0.05) *(Fig. 6)*.

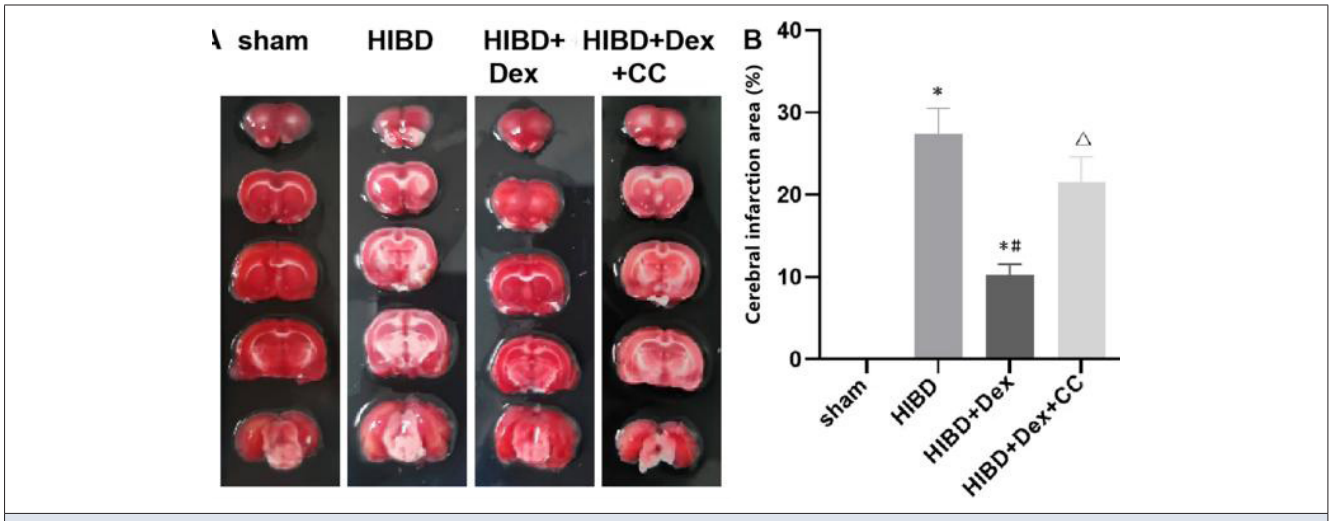

Fig 3. Cerebral infarction area in various groups of mice. A: Cerebral infarction area detected via TTC staining, B: Cerebral infarction area in diverse groups of mice. *p<0.05 vs. Sham Group, #p<0.05 vs. HIBD Group, and p<0.05 vs. HIBD + Dex Group

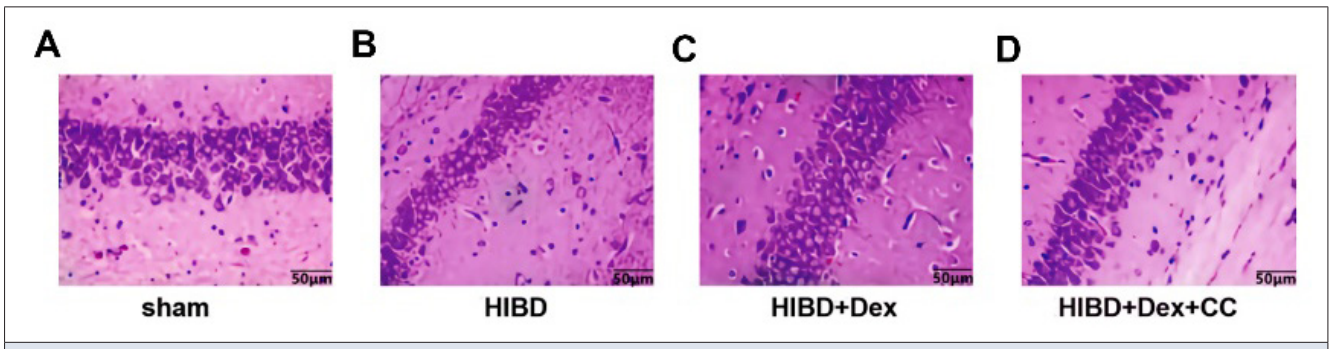

Fig 4. HE staining results of mouse brain tissues (×200). A- Sham, B- HIBD, C- HIBD + Dex, D- HIBD + Dex + CC. Neuronal injury was evident in the HIBD group, alleviated by Dex treatment, and partially reversed by CC

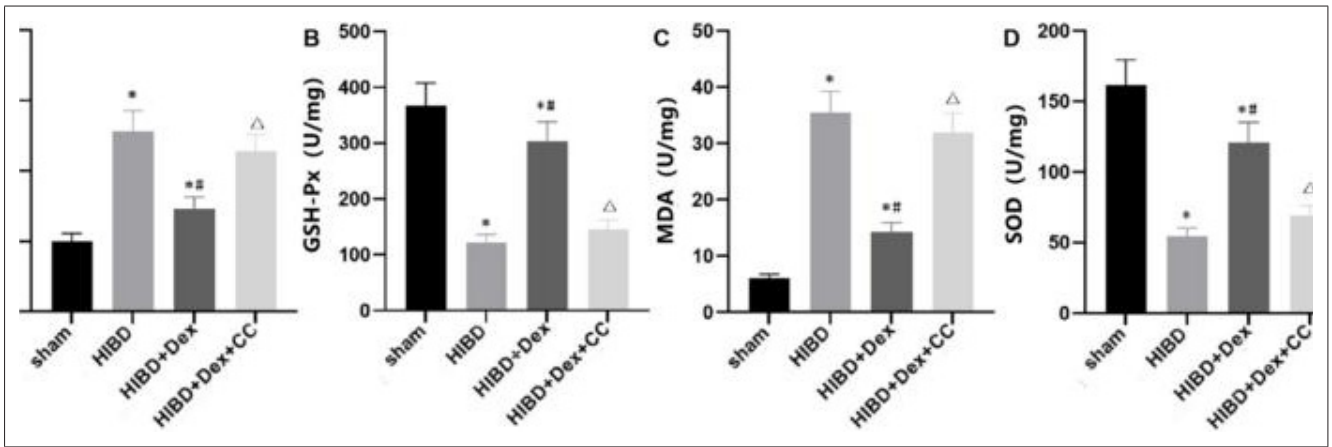

Fig 5. Oxidative stress indicators in murine brain tissues from different groups. A: Relative ROS level in brain tissues, B: GSH-Px content in brain tissues, C: MDA content in brain tissues, D: SOD activity in brain tissues. *P<0.05 vs. Sham Group, #P<0.05 vs. HIBD Group, and *P<0.05 vs. HIBD + Dex Group

Discussion

Pathologically, HIBD is typically featured with brain tissue edema, selective neuronal necrosis, marble-like pathology in the basal ganglia, neuronal damage in the parasagittal region of the brain, periventricular leukomalacia, *etc* [16]. The clinical manifestations of HIBD mainly include sudden hyperthermia, chills, and severe headache accompanied by projectile vomiting. Infants and young children suffering from this disease may present alternating dysphoria and lethargy, bilateral gaze, abnormal crying, food refusal, irritability, and other symptoms, and they may rapidly

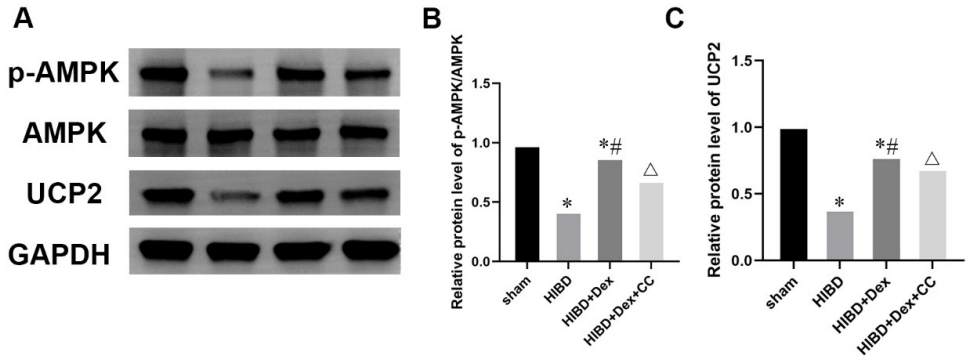

Fig 6. Protein expressions of p-AMPK, AMPK, and UCP2 in murine brain tissues from various groups. A: Protein bands of p-AMPK, AMPK, and UCP2 in murine brain tissues from diversified groups, B: p-AMPK/AMPK ratio in brain tissues of mice in each group, C: UCP2 protein expression in murine brain tissues from different groups. *P<0.05 vs. Sham Group, #P<0.05 vs. HIBD Group, and *P<0.05 vs. HIBD + Dex Group

progress to a coma state in severe cases [17]. At present, there is a lack of targeted therapeutic drugs capable of effectively relieving brain damage and preventing and treating neurological sequelae in neonates. Dex is a potent and highly specific α2 adrenergic receptor agonist, which performs the major neuroprotective mechanisms like the modulation of glutamatergic neurotransmitter release, the attenuation of inflammatory cascades, the blockade of neuronal apoptosis pathways, the scavenging of oxygen free radicals, and the enhancement of synaptic plasticity. These action mechanisms are jointly implicated in mitigating secondary damage to brain tissues and prominently improving neurological function score, and thus exerting significant neuroprotective effects [18]. As reported in the study of Hu et al.[19], Dex could markedly enhance the cognitive function in rat models of traumatic brain damage, effectively inhibit programmed nerve cell death, and substantially relieve structural damage in neurons, demonstrating distinct neuroprotective efficacy. Chen et al.[20] corroborated that Dex could lower NOX4 expression to reduce ROS generation in brain tissues, thus ameliorating neurological damage after cerebral hemorrhage in mice by alleviating oxidative stress. Through controlling the PPARγ/STAT3 signaling pathway, Dex pretreatment can efficiently relieve oxidative stress injury and interrupt the process of cell apoptosis, thereby producing a significant neuroprotective effect against HIBD [21]. Obvious decreases were detected in the NDS, brain water content, and cerebral infarction area in the HIBD + Dex group of the present study, suggesting that Dex can mitigate brain damage and exert a neuroprotective effect on HIBD mice, which is consistent with the results of the aforementioned studies.

Under physiological conditions, the ROS generated in brain tissues activates the anti-oxidant defense system in the body, in which SOD and catalase (CAT) are pivotal components of the enzymatic anti-oxidant system in nerve cells, capable of effectively removing ROS and maintaining GSH at a high level [22]. In the context of HIBD, however, excessive ROS rapidly overwhelms the anti-oxidant and scavenging capacities of nerve cells, disrupting the oxidant-anti-oxidant balance in brain tissues and leading to apparent oxidative stress in nerve cells. When HIBD induces persistent chronic oxidative stress, the activities of SOD and CAT decrease significantly in brain tissues, and large amount of GSH is consumed [23]. Meanwhile, the intensified lipid peroxidation in brain tissues causes the production of massive MDA, triggers abnormal aggregation of proteins, nucleic acids, and other macromolecules in nerve cells, and arouses neurotoxicity, further exacerbating mitochondrial dysfunction and ultimately resulting in nerve cell injury and apoptosis [24]. It was discovered in this study that the HIBD + Dex group had overtly reduced ROS level and MDA content and notably incremented SOD activity and GSH-Px content, implying that Dex can alleviate oxidative stress in HIBD mice and thus protect the neurological function, but the specific action mechanism needs in-depth research.

In the pathological process of HIBD, the activation of the AMPK-UCP2 signaling pathway is a crucial link for regulating ROS generation and maintaining mitochondrial function [25]. Once hypoxia and ischemia occur in brain tissues, the elevated intracellular AMP/ATP ratio can activate the AMPK signaling pathway. Such an energy metabolism regulatory hub not only promotes fatty acid β-oxidation to maintain energy supply, but also up-regulates UCP2 expression to improve mitochondrial function [26]. With the help of the induced mild uncoupling of the inner mitochondrial membrane, UCP2 can effectively decrease the overproduction of superoxide anions in the process of electron transport chain, thus significantly reducing the ROS accumulation. In the meantime, the activated AMPK also strengthens the activities of anti-oxidant enzymes, such as SOD and CAT, and coordinates with UCP2 in maintaining the oxidant-anti-oxidant balance in cells. This neuroprotective mechanism of the AMPK/UCP2

axis is particularly important in HIBD because it can attenuate oxidative stress injury of nerve cells, hinder the deterioration of mitochondrial dysfunction, and finally reduce neuronal apoptosis. Zeng et al.[27] proved that pterostilbene had a protective effect on neonatal rats with HIBD through the mechanism possibly highly associated with the up-regulated expression of the LKB1/AMPK/Nrf2 signaling pathway and the repressed oxidative stress responses. According to the results of the present study, the p-AMPK/AMPK ratio and UCP2 protein expression were markedly increased in the brain tissues of the HIBD + Dex group. These findings indicate that Dex treatment is associated with concurrent activation of AMPK signaling and upregulation of UCP2 expression under hypoxic-ischemic conditions. Furthermore, co-administration of the AMPK inhibitor Compound C attenuated the antioxidative and neuroprotective effects of Dex, supporting the involvement of AMPK-dependent mechanisms in Dex-mediated protection.

Several limitations should be noted. First, although changes in AMPK phosphorylation and UCP2 expression were observed after Dex treatment, direct evidence for a causal role of UCP2 is lacking, as UCP2-specific interventions were not performed. Second, sex-specific analyses were not conducted due to the limited sample size, despite potential sex differences in HIBD outcomes and AMPK-related signaling. Third, all assessments were performed at a single early time point after hypoxic-ischemic injury, which may not fully reflect the dynamic progression of HIBD. Future studies incorporating genetic approaches, sex stratification, and multiple time points are warranted.

In conclusion, Dex alleviates oxidative stress and improves neurological outcomes in neonatal mice with HIBD. These protective effects are likely associated with activation of AMPK signaling and downstream mitochondrial redox regulation, including altered UCP2 expression.

Declarations

Availability of Data and Materials: The datasets used and/or analyzed during the current study are available from the corresponding author (JW) on reasonable request.

Acknowledgments: None.

Financial Support: This study was financially supported by the Hubei Natural Science Foundation (No. No. 2023ABF707).

Conflict of Interest: The authors declared that there is no conflict of interest.

Declaration of Generative Artificial Intelligence (AI): The authors declare that the article, tables and figures were not written/ created by AI and AI-assisted Technologies

Authors Contributions: B.N. and M.Z. conceived and designed the study. S.H. performed the animal experiments and data collection. L.T. conducted the statistical analysis and prepared the figures. J.W. supervised the study, interpreted the data, and revised the manuscript.

References

1. **Wang XX, Li M, Xu XW, Zhao WB, Jin YM, Li LL, Qin ZH, Sheng R, Ni H:** BNIP3-mediated mitophagy attenuates hypoxic-ischemic brain damage in neonatal rats by inhibiting ferroptosis through P62-KEAP1-NRF2 pathway activation to maintain iron and redox homeostasis. *Acta Pharmacol Sin,* 46 (1): 33-51, 2025. DOI: 10.1038/s41401-024-01365-x
2. **Chen L, Xiong S, Zhou X, Fu Q:** Aloesin ameliorates hypoxic-ischemic brain damage in neonatal mice by suppressing TLR4-mediated neuroinflammation. *Immun Inflamm Dis,* 12 (6):e1320, 2024. DOI: 10.1002/iid3.1320
3. **Jin N, Sha S, Ruan Y, Ouyang Y:** Identification and analysis of oxidative stress-related genes in hypoxic-ischemic brain damage using bioinformatics and experimental verification. *Immun Inflamm Dis,* 12 (8):e70000, 2024. DOI: 10.1002/iid3.70000
4. **Naaz S, Ozair E:** Dexmedetomidine in current anaesthesia practice - A review. *Clin Diagn Res,* 8 (10):GE01-4, 2014. DOI: 10.7860/JCDR/2014/9624.4946
5. **Liaquat Z, Xu X, Zilundu PLM, Fu R, Zhou L:** The current role of dexmedetomidine as neuroprotective agent: An updated review. *Brain Sci,* 11 (7):846, 2021. DOI: 10.3390/brainsci11070846
6. **Mu Y, Mei Y, Chen Y, Li Y, Zhu D, Cui J, Yu L:** Perisciatic nerve dexmedetomidine alleviates spinal oxidative stress and improves peripheral mitochondrial dynamic equilibrium in a neuropathic pain mouse model in an AMPK-dependent manner. *Dis Markers,* 2022:6889676, 2022. DOI: 10.1155/2022/6889676
7. **He H, Sun M, Chen Y, Zhou Y, Qie W, Tu W:** Dexmedetomidine alleviates the hypoxic-ischemic brain damage via miR-20a-5p/methionine adenosyltransferase 2B axis in rat pups. *Neuroreport,* 33 (5): 205-214, 2022. DOI: 10.1097/WNR.0000000000001750
8. **Chen X, Chen A, Wei J, Huang Y, Deng J, Chen P, Yan Y, Lin M, Chen L, Zhang J, Huang Z, Zeng X, Gong C, Zheng X:** Dexmedetomidine alleviates cognitive impairment by promoting hippocampal neurogenesis via BDNF/TrkB/CREB signaling pathway in hypoxic-ischemic neonatal rats. *CNS Neurosci Ther,* 30 (1):e14486, 2024. DOI: 10.1111/cns.14486
9. **Luby A, Alves-Guerra MC:** UCP2 as a cancer target through energy metabolism and oxidative stress control. *Int J Mol Sci,* 23 (23):15077, 2022. DOI: 10.3390/ijms232315077
10. **Hardie DG:** AMP-activated protein kinase: An energy sensor that regulates all aspects of cell function. *Genes Dev,* 25 (18): 1895-908, 2011. DOI: 10.1101/gad.17420111
11. **Tian XY, Ma S, Tse G, Wong WT, Huang Y:** Uncoupling protein 2 in cardiovascular health and disease. *Front Physiol,* 9:1060, 2018. DOI: 10.3389/fphys.2018.01060
12. **Liu L, Yang Y, Wu T, Du J, Long F:** NKG2D knockdown improves hypoxic-ischemic brain damage by inhibiting neuroinflammation in neonatal mice. *Sci Rep,* 14 (1):2326, 2024. DOI: 10.1038/s41598-024-52780-3
13. **Mei B, Li J, Zuo Z:** Dexmedetomidine attenuates sepsis-associated inflammation and encephalopathy via central α2A adrenoceptor. *Brain Behav Immun,* 91, 296-314, 2021. DOI: 10.1016/j.bbi.2020.10.008
14. **He H, Liu P, Li P:** Dexmedetomidine ameliorates cardiac ischemia/reperfusion injury by enhancing autophagy through activation of the AMPK/SIRT3 pathway. *Drug Des Devel Ther,* 17, 3205-3218, 2023. DOI: 10.2147/DDDT.S428024
15. **Li X, Zhang Y, Chang J, Zhang C, Li L, Dai Y, Yang H, Wang Y:** Mfsd2a attenuated hypoxic-ischemic brain damage via protection of the blood-brain barrier in mfat-1 transgenic mice. *Cell Mol Life Sci,* 80 (3):71, 2023. DOI: 10.1007/s00018-023-04716-9

16. **Zhang M, Liu Z, Zhou W, Shen M, Mao N, Xu H, Wang Y, Xu Z, Li M, Jiang H, Chen Y, Zhu J, Lin W, Yuan J, Lin Z:** Ferrostatin-1 attenuates hypoxic-ischemic brain damage in neonatal rats by inhibiting ferroptosis. *Transl Pediatr,* 12 (11): 1944-1970, 2023. DOI: 10.21037/tp-23-189
17. **Sun M, An Z, Wei H, Li T, Qin M, Liu Y, Jiang H:** Xenon attenuates hypoxic-ischemic brain damage by inhibiting autophagy in neonatal rats. *Neuroreport,* 34 (5): 273-279, 2023. DOI: 10.1097/WNR.0000000000001888
18. **Xue H, Ding Z, Chen X, Yang X, Jia Y, Zhao P, Wu Z:** Dexmedetomidine improves long-term neurological outcomes by promoting oligodendrocyte genesis and myelination in neonatal rats following hypoxic-ischemic brain injury. *Mol Neurobiol,* 62 (4): 4866-4880, 2025. DOI: 10.1007/s12035-024-04564-z
19. **Hu Y, Zhou H, Zhang H, Sui Y, Zhang Z, Zou Y, Li K, Zhao Y, Xie J, Zhang L:** The neuroprotective effect of dexmedetomidine and its mechanism. *Front Pharmacol,* 13:965661, 2022. DOI: 10.3389/fphar.2022.965661
20. **Chen X, Chen D, Chen P, Chen A, Deng J, Wei J, Zeng W, Zheng X:** Dexmedetomidine attenuates apoptosis and neurological deficits by modulating neuronal NADPH oxidase 2-derived oxidative stress in neonates following hypoxic brain injury. *Antioxidants (Basel),* 11 (11):2199, 2022. DOI: 10.3390/antiox11112199
21. **Zhong Y, Wang S, Yin Y, Yu J, Liu Y, Gao H:** Dexmedetomidine suppresses hippocampal astrocyte pyroptosis in cerebral hypoxic-ischemic neonatal rats by up-regulating microRNA-148a-3p to inactivate the STAT/JMJD3 axis. *Int Immunopharmacol,* 121:110440, 2023. DOI: 10.1016/j.intimp.2023.110440
22. **Hu Y, Nan Y, Lin H, Zhao Q, Chen T, Tao X, Ding B, Lu L, Chen S, Zhu J, Guo X, Lin Z:** Celastrol ameliorates hypoxic-ischemic brain injury in neonatal rats by reducing oxidative stress and inflammation. *Pediatr Res,* 96 (7): 1681-1692, 2024. DOI: 10.1038/s41390-024-03246-9
23. **Geng J, Feng J, Ke F, Fang F, Jing X, Tang J, Fang C, Zhang B:** MicroRNA-124 negatively regulates STAT3 to alleviate hypoxic-ischemic brain damage by inhibiting oxidative stress. *Aging (Albany NY),* 16 (3): 2828-2847, 2024. DOI: 10.18632/aging.205513
24. **Li H, Sun H, Li S, Huang L, Zhang M, Wang S, Liu Q, Ying J, Zhao F, Su X, Mu D, Qu Y:** Hydrogen alleviates hypoxic-ischaemic brain damage in neonatal rats by inhibiting injury of brain pericytes. *J Cell Mol Med,* 28 (13):e18505, 2024. DOI: 10.1111/jcmm.18505
25. **Yang K, Xu X, Nie L, Xiao T, Guan X, He T, Yu Y, Liu L, Huang Y, Zhang J, Zhao J:** Indoxyl sulfate induces oxidative stress and hypertrophy in cardiomyocytes by inhibiting the AMPK/UCP2 signaling pathway. *Toxicol Lett,* 234 (2): 110-119, 2015. DOI: 10.1016/j.toxlet.2015.01.021
26. **Azizian H, Farhadi Z, Bader M, Alizadeh Ghalenoei J, Ghafari MA, Mahmoodzadeh S:** GPER activation attenuates cardiac dysfunction by upregulating the SIRT1/3-AMPK-UCP2 pathway in postmenopausal diabetic rats. *PLoS One,* 18 (12):e0293630, 2023. DOI: 10.1371/journal.pone.0293630
27. **Zeng Q, Lian W, Wang G, Qiu M, Lin L, Zeng R:** Pterostilbene induces Nrf2/HO-1 and potentially regulates NF-κB and JNK-Akt/mTOR signaling in ischemic brain injury in neonatal rats. *Biotech,* 10 (5):192, 2020. DOI: 10.1007/s13205-020-02167-8

Kafkas Universitesi Veteriner Fakultesi Dergisi
Journal Home-Page: http://vetdergikafkas.org
E-ISSN: 1309-2251

Kafkas Univ Vet Fak Derg
32 (2): 247-259, 2026
DOI: 10.9775/kvfd.2025.35867

Research Article

Thematic Mapping and Sustainability-Oriented Analysis of Veterinary Science Research in Türkiye: A Text Mining and Hybrid Hierarchical Clustering Approach (1980-2024)

Harun YONAR [1(*)], Furkan Çağrı BEŞOLUK [1], Aynur YONAR [2]

[1] Selcuk University, Faculty of Veterinary Medicine, Biostatistics Department, TR-42130 Konya - TÜRKİYE
[2] Selcuk University, Faculty of Science, Statistics Department, TR-42130 Konya - TÜRKİYE

(*) **Corresponding author:**
Harun Yonar
Phone: +90 332 223 3550
Cellular phone: +90 545 311 2080
E-mail: hyonar@selcuk.edu.tr

How to cite this article?

Yonar H, Beşoluk FÇ, Yonar A: Thematic Mapping and Sustainability-Oriented Analysis of Veterinary Science Research in Türkiye: A Text Mining and Hybrid Hierarchical Clustering Approach (1980-2024). *Kafkas Univ Vet Fak Derg*, 32 (2): 247-259, 2026.
DOI: 10.9775/kvfd.2025.35867

Article ID: KVFD-2025-35867
Received: 05.12.2025
Accepted: 11.04.2026
Published Online: 21.04.2026

Abstract

This study examines 45,769 veterinary medicine publication titles from Türkiye (1980–2024) using large-scale text mining, hybrid clustering, and Sustainable Development Goals (SDG) mapping. It aims to identify long-term thematic trends and assess alignment with global sustainability priorities. A two-stage hybrid clustering approach (k-means + hierarchical) revealed 11 thematic groups. SDG alignment was evaluated using a hybrid Aurora-Elsevier dictionary model enhanced with n-gram-based weighting and validation. Findings indicate a clear shift from traditional species- and production-focused research toward molecular, experimental, and data-driven domains. SDG mapping shows strong associations with Zero Hunger (SDG 2), Good Health and Well-being (SDG 3), Responsible Consumption and Production (SDG 12), and Life Below Water (SDG 14). In contrast, Climate Action (SDG 13) and Life on Land (SDG 15) remain underrepresented, highlighting critical gaps in environmental sustainability. Overall, veterinary research in Türkiye aligns with global production- and health-oriented trends but exhibits partial thematic divergence, particularly in aquatic systems. The comparatively lower emphasis on climate change, biodiversity, and ecosystem health suggests areas that could be further strengthened within the national research agenda. These results offer a data-driven basis for strengthening interdisciplinary research, advancing the environmental dimension of One Health, and improving alignment with global sustainability priorities.

Keywords: Hybrid clustering, One health, Sustainable development goals, Text mining, Türkiye, Veterinary medicine

Introduction

Veterinary medicine plays a critical role at the intersection of animal health, public health, food safety, environmental sustainability, and global health security. Beyond clinical practice, the discipline contributes significantly to the prevention of zoonotic diseases, the fight against antimicrobial resistance, sustainable livestock production systems, the conservation of biological diversity, and the support of ecosystem health within the One Health approach [1-3]. In this context, veterinary science is directly related to the Sustainable Development Goals (SDGs), particularly SDG 2 (Zero Hunger), SDG 3 (Good Health and Well-being), SDG 12 (Responsible Consumption and Production), SDG 13 (Climate Action), and SDG 15 (Life on Land). The strategic position of veterinary medicine in contributing to these global sustainability goals makes it important to understand the alignment of national research orientations with global priorities [4-6].

Türkiye is a strategic country in regional and global veterinary management due to its geopolitical position, animal production capacity, biological diversity, and wildlife corridors. This position makes veterinary research critical for both national animal husbandry and public health, as well as global disease surveillance, control of zoonotic risks, and sustainable food systems. Strengthening veterinary research capacity in Türkiye directly supports regional biosecurity and international collaborations such as FAO, WOAH, and WHO, in line with One Health initiatives [7-9].

In recent years, veterinary education and research infrastructure in Türkiye have developed significantly, accelerating international collaborations and integration with digital epidemiology, genomics, precision livestock farming, and sustainable agriculture policies [10,11].

Despite the growing use of text-based approaches in medicine, agriculture, and environmental sciences, the application of these methods in veterinary research within an SDG framework remains an emerging area.

This study examines 45,769 veterinary science publication titles from Türkiye (1980–2024) using text mining, hybrid hierarchical clustering, and SDG-based classification to reveal (i) the transformation of Turkish veterinary research trends over time, (ii) thematic clustering structures among departments, and (iii) the alignment of publication content with the SDGs – contributing to sustainability-focused scientific mapping in the international literature.

Material and Method

Ethical Statement

This study did not requiring ethical approval.

Material

The data used in this study includes the title, year, and division/department information of scientific articles published in the field of veterinary science in Türkiye between 1980 and 2024 [12]. The analyses were performed on article titles; the total data set consists of 45,769 unique titles obtained after cleaning.

Method

To ensure methodological transparency and reproducibility, the analysis was structured into four stages: (i) data preprocessing, (ii) TF-IDF-based text representation with SVD-based dimensionality reduction and scaling, (iii) hybrid clustering (k-means + hierarchical), and (iv) SDG mapping and validation using a hybrid dictionary approach with ranking-based evaluation. This workflow ensures a coherent and reproducible analytical process.

Data Preprocessing and Text Standardization

The texts were first subjected to a comprehensive preprocessing process. In the first stage, all titles were run through a language filter to identify those in Turkish and were translated into English to ensure linguistic consistency. Subsequently, the texts underwent cleaning, noise filtering, and tokenization processes.

Text Representation and Dimension Reduction

In the first stage, article titles were converted into high-dimensional feature vectors based on TF-IDF using a text mining approach. TF-IDF representations derived from text data typically have a high-dimensional and sparse feature space. This situation can negatively affect the performance and computational cost of clustering algorithms. Therefore, to reduce the dimensionality problem and preserve the fundamental variation components in the data structure, a dimension reduction process was applied using the Singular Value Decomposition (SVD) method. To ensure comparability among variables in the clustering analysis, the resulting vectors were subsequently scaled.

Hybrid Clustering (k-means + hierarchical)

Cluster analysis is an unsupervised learning approach for identifying homogeneous groups based on similarity patterns. In text mining, clustering reveals latent thematic structures; performance depends on appropriate feature representation, dimensionality reduction, and distance metric selection.

Due to the large-scale nature of the dataset in this study, a two-stage hybrid clustering (k-means + hierarchical) was chosen for the clustering analysis. Hybrid clustering strategies are widely recommended in the literature, particularly for large datasets, both to reduce computational costs and to enhance the interpretability of the resulting cluster structure. This approach combines the computational efficiency of the k-means algorithm with the structural interpretability provided by hierarchical clustering, offering an effective solution for revealing the thematic structures of large-scale datasets [13–18].

Pre-Clustering and Determination of Representative Centers

Given the complexity of hierarchical clustering, applying it directly to 45,769 observations would require approximately 2.1 billion pairwise distance calculations, which is computationally infeasible. By reducing the dataset to M=500 representative centroids via k-means pre-clustering, this number decreases to about 250,000. Thus, M=500 was selected as a balance between computational feasibility and preserving the global structure of the data.

Hierarchical Clustering Analysis

In the second stage, hierarchical clustering analysis was performed on the representative centers obtained using the Ward.D2 linkage method. The Ward method is an agglomerative approach aimed at minimizing intra-cluster variance and is widely used, particularly in text-based datasets. Similarities were calculated using the Euclidean distance during the clustering process.

Euclidean distance was selected as the similarity measure given the continuous, standardized feature space. Feature scaling ensured equal contribution of all dimensions. SVD-based dimensionality reduction addressed the high-dimensional, sparse nature of TF–IDF representations, reducing noise and preserving informative latent structures.

Determination of the Optimal Number of Clusters

Candidate cluster numbers were evaluated in the range k = 2-30 using four internal validation indices: Silhouette (higher = better intra-cluster cohesion [19]), Calinski-Harabasz (higher = stronger separation), Dunn (higher = better structure), and Davies-Bouldin (lower = better performance). As different indices may suggest varying optimal k values [20,21], a consensus across multiple

indices was applied [22-24], supplemented by cluster size distribution and inter-cluster variance ratio to assess over-fragmentation.

While validation indices serve as an important guide in determining the final number of clusters, the thematic consistency and interpretability of the clusters played a decisive role in the decision-making process. This approach is of critical importance in ensuring that the resulting clusters provide not only statistically valid but also meaningful and interpretable thematic structures [25-27].

SDG Mapping Using the Hybrid Dictionary Approach

A hybrid dictionary content and text mining approach was applied to determine the relationship between the articles in the study and the United Nations' 17 Sustainable Development Goals (SDGs). The analysis process was built on a two-stage design by combining the conceptual structures obtained from the Aurora [28] and Elsevier [29] SDG dictionaries [30-32]. The analysis was conducted in two consecutive design steps. In Design 1, the XML-based SDG query files of the Aurora platform were parsed, and the terms derived from this were converted into a systematic lexicon structure under the name "Aurora SDG Lexicon." In Design 2, the "Elsevier SDG Lexicon" was created using terms extracted from Elsevier's 2025 Sustainable Development Goals (SDGs) Mapping query files; then, it was integrated with the Aurora lexicon to develop a hybrid SDG assignment model based on source-based weighting. In Elsevier queries, expressions in double quotation marks were parsed as "phrases," while single words were parsed as "unigrams", and each was matched with the relevant SDG number. These terms were compared with article titles tokenized at the unigram, bigram, and trigram levels. Matching scores were calculated considering n-gram length (tri > bi > uni) and term type (phrase > unigram) weights. This hybrid structure enabled multi-source information integration at both the conceptual and linguistic levels; the most probable SDG label was identified for ranking and validation purposes based on the total score, number of matches, and maximum n-gram level, while multiple SDG matches were retained under the multi-label classification framework. Thus, a hybrid text-matching approach that integrates the strengths of dictionary-based approaches and n-gram matching techniques was developed [33,34].

Validation of the SDG Model

To assess the reliability of the SDG assignment model, a manual validation procedure was conducted using a stratified sample of article titles based on the highest detected n-gram level. This sampling strategy was adopted to separately evaluate the performance of the n-gram-based matching mechanism, which represents a fundamental component of the proposed hybrid system. In this context, 100 article titles were randomly selected from each n-gram category (trigram, bigram, and unigram) to ensure a representative evaluation. As a result, SDG labels were manually assigned to a total of 300 article titles, and these labels were compared with the SDG candidates generated by the model.

Manual verification was performed independently by two authors, and disagreements were resolved through discussion until consensus was reached. In the verification analysis, the manually assigned SDG labels were compared with the ranked SDG candidates generated by the model. Model performance was evaluated using ranking-based metrics, including coverage and Top-k accuracy (Top-1, Top-3, and Top-5). Coverage indicates the proportion of cases where the manually assigned SDG is present among the candidate SDGs generated by the model, while Top-k accuracy indicates whether the correct SDG is among the top k ranked positions. These evaluation metrics are widely used in SDG mapping and classification studies because such systems typically generate ranked lists of candidate SDGs rather than single-label predictions [35,36].

Multi-label Approach

SDG assignment was performed using a multi-label matching approach. A single article title may contain expressions related to multiple SDGs and can therefore be associated with more than one SDG. Consequently, the values derived from this process represent association counts, defined as the number of article titles matched with each SDG, rather than mutually exclusive category assignments. Percentages reported in the results are calculated based on these association counts; therefore, the total percentage may exceed 100%, which is expected in multi-label classification analyses.

Analysis of Cluster-SDG Relationships (Heatmap)

A heatmap visualization was created to examine the relationships between the identified thematic clusters and the Sustainable Development Goals (SDGs) more clearly. First, using the hybrid SDG lexicon approach, it was determined which SDGs each article title matched. Then, the SDG match frequencies were calculated for each cluster. To determine the relative weight of each SDG within a cluster, the number of SDG matches for that SDG was divided by the total number of SDG matches within the same cluster to obtain percentage values. These percentage values were visualized on the heatmap. In the heatmap, rows represent clusters, while columns represent the SDGs (SDG01–SDG17). Color intensity indicates the relative density of SDG matches within the respective cluster.

Software and Packages

All analyses were conducted in R (v4.5.1). Data handling used readxl, readr, dplyr, tidyr, stringr, and tidyverse;

tokenization and n-gram generation used tidytext; lemmatization used textstem; TF–IDF construction used text2vec; stop-word filtering used stopwords and tokenizers. Dimensionality reduction used irlba; clustering used fastcluster, proxy, and RANN; validation used cluster and igraph. Visualization used dendextend, factoextra, ggplot2, gridExtra, and forcats.

Results

Publication Trends by Year (1980-2024)

Annual publication output in veterinary medicine from Türkiye increased steadily from the 1980s, accelerating after 2000 and exceeding 1,000 per year; output first exceeded 3,000 in 2015, followed by a slight decline in 2019 and 2024 *(Fig. 1)*.

Publication Distribution by Division and Department

Fig. 2 shows the publication volume in the veterinary field in Türkiye by division and department between 1980 and 2024.

Preclinical Sciences accounted for the highest publication share (29.9%), followed by Clinical Sciences (29.0%), Basic Sciences (19.3%), Zootechnics and Animal Nutrition (15.8%), and Food Hygiene and Technology (6.1%) *(Fig. 2)*.

Division and Department Collaboration Network

Fig. 3 shows the network structure of joint publication relationships at the division and department levels in the field of veterinary science. Each node represents a department, the edge thickness represents the frequency of joint publications between two departments, and the coloring represents the divisions.

The strongest inter-departmental connections occur between Preclinical and Clinical Sciences, with Basic Sciences (Biochemistry, Physiology, Histology) bridging both divisions. Zootechnics and Animal Nutrition has multiple connections, while Food Hygiene and Technology shows more limited network links *(Fig. 3)*.

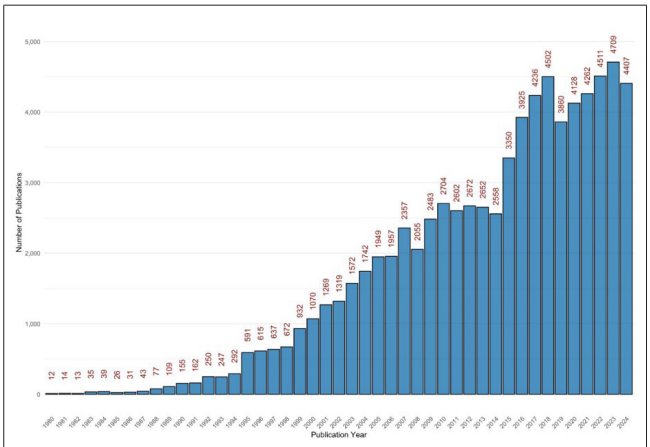

Fig 1. Annual publication numbers in the field of veterinary medicine between 1980 and 2024

Unigram and Bigram Frequency Analyses

Fig. 4 shows the distribution of the 20 most frequently occurring single words (unigrams) and two-word expressions (bigrams) in the titles of veterinary research in Türkiye.

The most frequently occurring terms in the unigram analysis were dog, rat, turkey, sheep, cattle, cow, and goat. Among methodological terms, investigation, parameter, evaluation, treatment, and performance showed high frequency. The most frequently used bigram in the bigram analysis was oxidative stress. This was followed by dairy cows, biochemical parameters, blood parameters, escherichia coli, rainbow trout, and broiler chickens.

Trend Topics Diagram

Fig. 5 and *Fig. 6* display, for the 30 most frequent unigrams and bigrams respectively, the first appearance, peak usage, and last appearance year as horizontal trend lines.

Species-based terms (dog, sheep, cattle, goat, turkey) dominated the 1980-2000 period. After 2000, molecular-focused terms such as oxidative, stress, biochemical, and antioxidant increased rapidly, reaching peak frequencies between 2020–2024 alongside production-related terms (broiler, dairy, meat) *(Fig. 5)*.

Production-related bigrams (broiler chickens, dairy cows, rainbow trout) appeared consistently from the 1980s. Post-2000, mechanistic bigrams (oxidative stress, biochemical parameters, lipid peroxidation, heat stress) became increasingly frequent, with marked increases in oxidative stress and biochemical parameters after 2020 *(Fig. 6)*.

Examining SDG Associations Using a Hybrid Dictionary-Based Approach

Fig. 7 shows the pattern of SDG associations obtained by applying a hybrid dictionary-based approach to all article titles published between 1980 and 2024.

The results indicate that academic publications are most strongly associated with SDG 2 (36.3%), followed by SDG 14 (19.0%), SDG 3 (18.1%), and SDG 12 (15.8%). Goals with moderate association levels include SDG 4 (12.3%), SDG 6 (10.6%), SDG 8 (11.6%), SDG 11 (11.9%), and SDG 17 (9.3%). Lower association levels are observed for SDG 1 (8.6%), SDG 5 (7.6%), SDG 7 (8.5%), SDG 9 (5.7%), SDG 10 (7.0%), SDG 13 (6.4%), SDG 15 (8.0%), and SDG 16 (5.2%).

Validation of the SDG Classification Model

Comparative validation results for the Aurora, Elsevier,

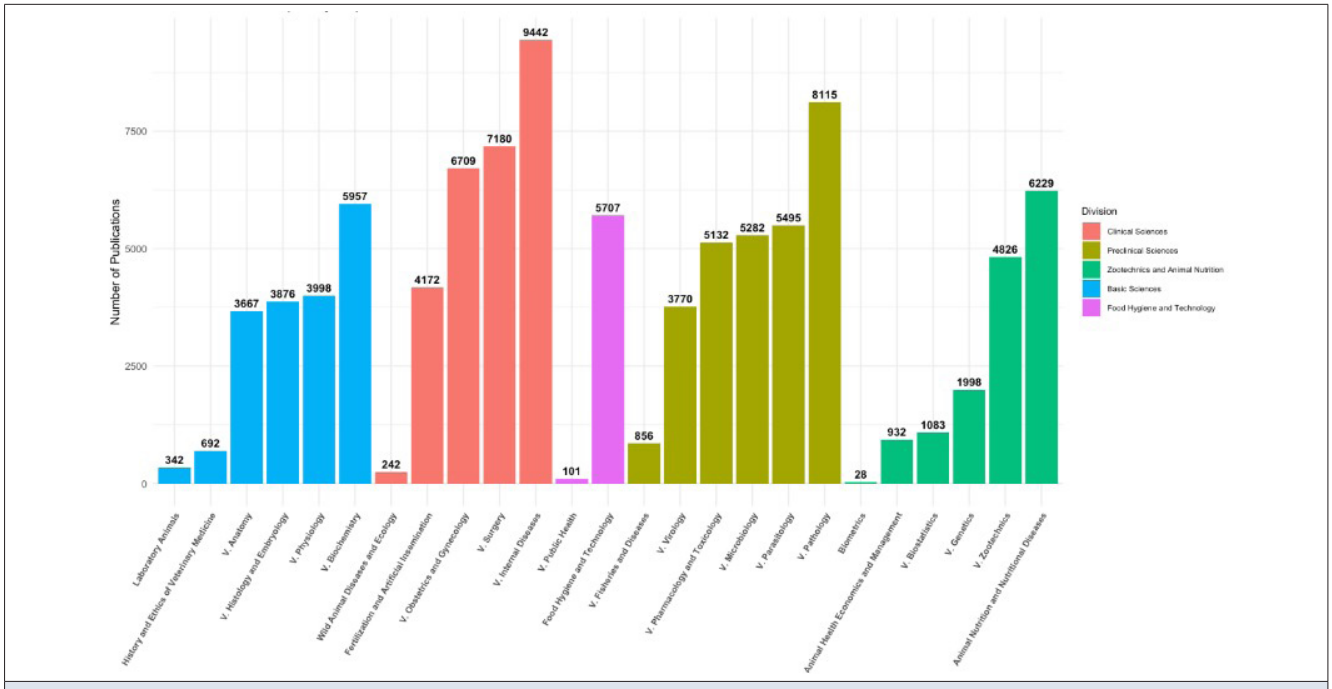

Fig 2. Distribution of publications by veterinary departments according to divisions

and Hybrid SDG models across different n-gram levels and for the overall validation dataset are presented in *Table 1*.

The hybrid model outperformed both Aurora and Elsevier models across all n-gram levels *(Table 1)*. For the overall validation set (n = 300), hybrid coverage was 0.755 vs. Aurora 0.631 and Elsevier 0.359; Top-3 accuracy was 0.645 vs. 0.510 and 0.355, respectively, confirming that the hybrid approach provides more reliable identification of SDG-related themes.

These results indicate that the hybrid SDG assignment approach provides a more reliable identification of SDG-related themes in article titles compared with the single-dictionary approaches.

SDG and Division Relationship

Fig. 8 shows the top 5 veterinary divisions contributing most to each SDG, revealing the distribution of research production in these divisions from a sustainability perspective.

Clinical Sciences and Preclinical Sciences lead across the majority of SDGs. Basic Sciences ranks among the top three for nearly all SDGs, while Zootechnics and Animal Nutrition stands out particularly in SDG 2, 8, and 17. Overall, the findings suggest that interdisciplinary contributions within veterinary sciences exhibit a thematically differentiated yet balanced distribution across the SDG portfolio.

Cluster Validation and Dendrogram

Cluster validation indices for k=2-30 indicated the Silhouette maximum at k=9 (0.288), with k=10–12 forming a stable region (0.186-0.220). Calinski-Harabasz increased gradually through this range (10: 12.30; 11: 12.56; 12: 12.94) while Davies-Bouldin reached its minimum at k = 11 (2.17). The Dunn index peaked locally

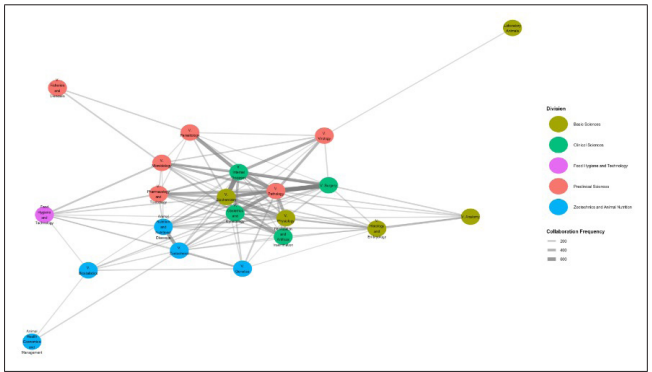

Fig 3. Collaborative publication network among veterinary departments

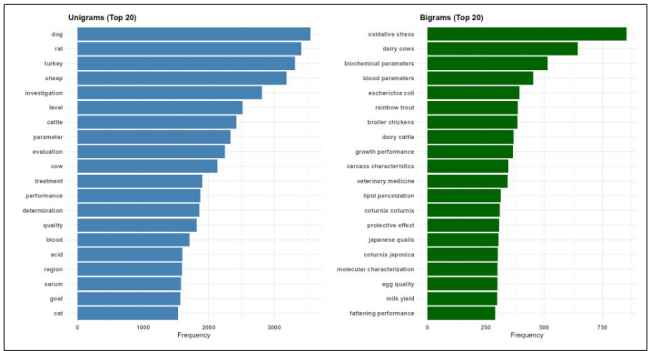

Fig 4. Top 20 unigrams and bigrams from article titles

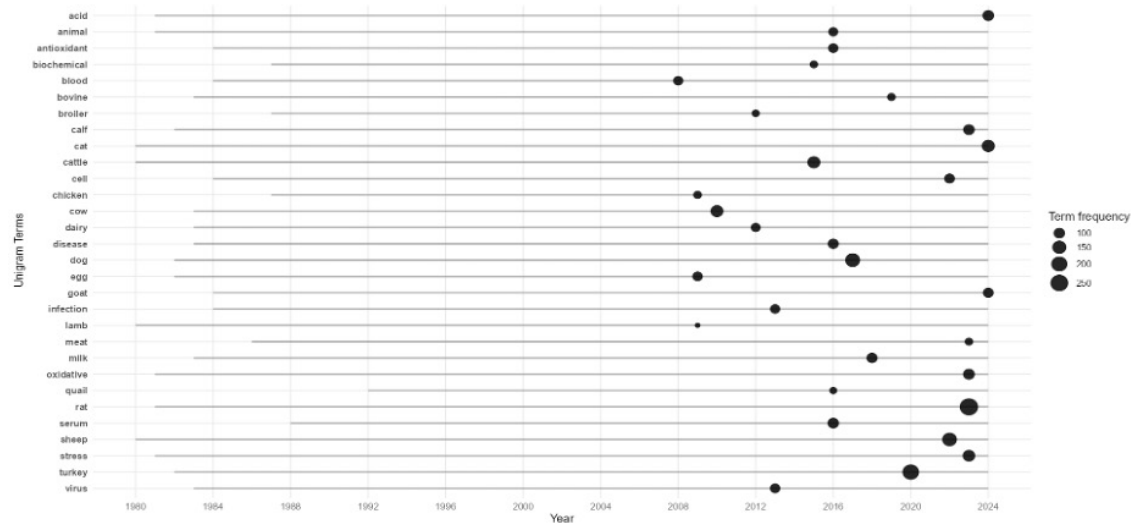

Fig 5. Trend analysis of unigram terms by year

at k = 12 (0.145) and k = 15 (0.150), but increases at higher k were attributed to fragmentation effects. At k ≥12, minimum cluster size dropped substantially; the k = 11 solution yielded a minimum size of 7 and a between-cluster variance ratio of 0.197, representing the optimal balance of separation, interpretability, and balance.

When all validation indices were considered together, the range of k = 10-12 emerged as an appropriate solution region in terms of clustering quality. Within this range, the k = 11 solution was selected as the optimal cluster structure, as it (i) ensured a balanced distribution of cluster sizes, (ii) provided adequate cluster separation, and (iii) prevented over-fragmentation. Therefore, k = 11 was determined as the final number of clusters that best represents the thematic structure of the dataset from both statistical and interpretability perspectives.

Eleven thematic clusters were obtained as a result of two-stage hybrid clustering. The dendrogram generated using the hybrid structure (k-means & Ward) shows distinct clustering between clusters.

Fig. 9 shows the final dendrogram resulting from the Ward. D2 hierarchical clustering applied to the 500 centroids obtained in the k-means preprocessing stage.

The dendrogram *(Fig. 9)* shows five main groupings: Cluster 3 as a dominant independent block; Clusters 2-6-9 on a shared main branch; Clusters 5-8 in the same region; Clusters 7-10 under a common branch; and Clusters 1-4-11 within the same large block. Long top-level branches indicate high semantic distances, while Clusters 7, 10, 9, and 6 form compact, closely related structures.

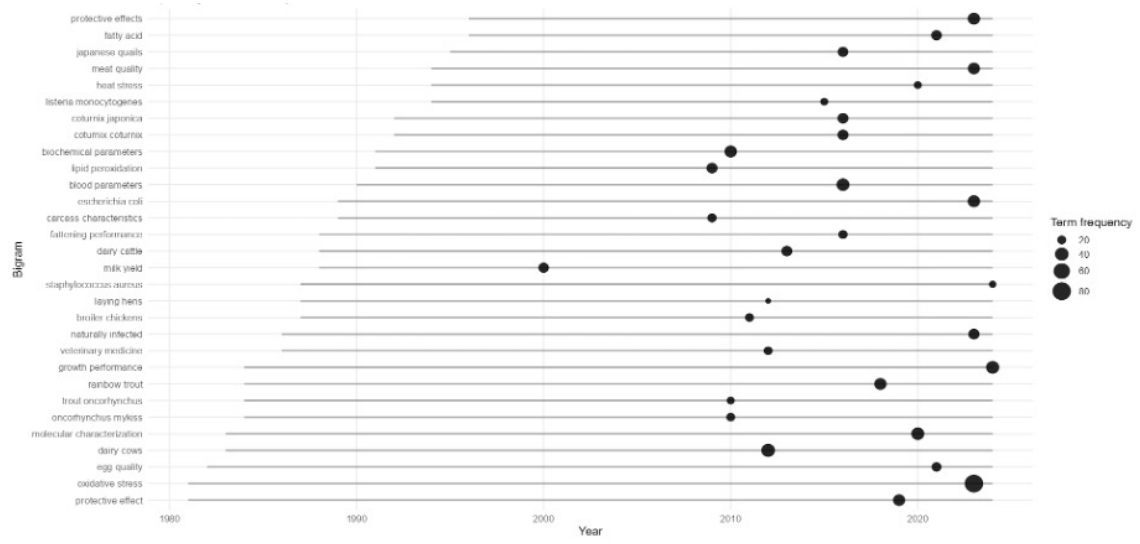

Fig 6. Trend analysis of bigram terms by year

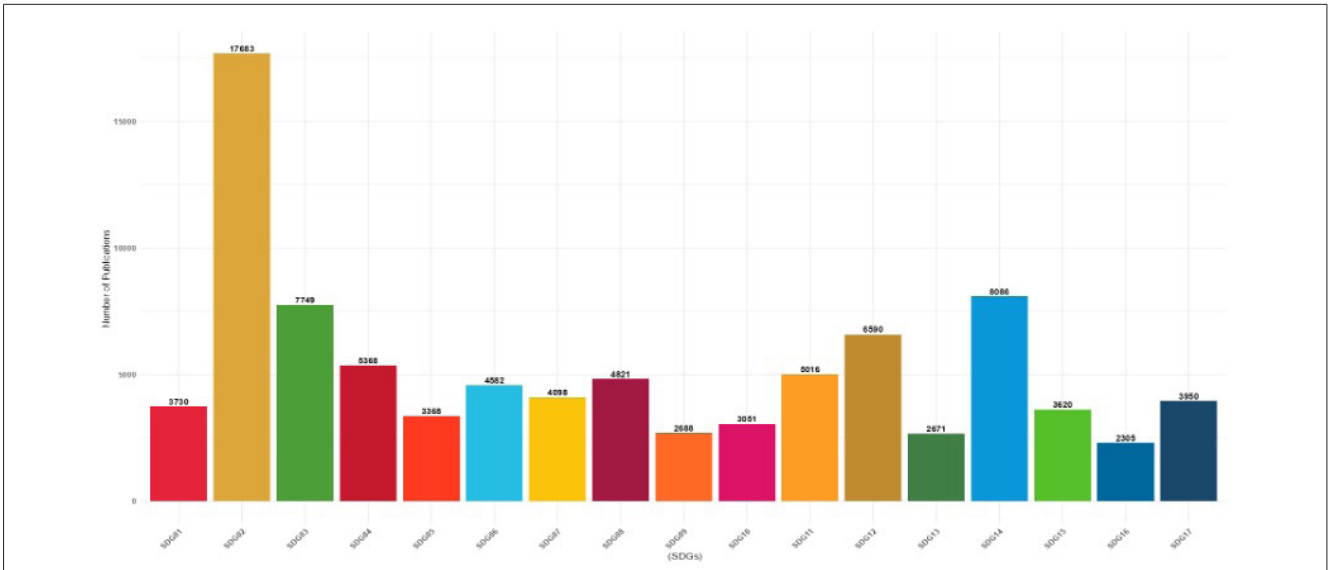

Fig 7. Article-SDG associations identified using a hybrid dictionary-based multi-label matching approach (1980-2024). A single article title may be associated with more than one SDG because the SDG assignment follows a multi-label matching approach. Therefore, the total counts across SDGs may exceed the total number of articles. The values shown in the figure represent the number of article titles matched with each SDG, while percentages reported in the text are calculated based on these counts

Content Characteristics of Clusters

Table 2 shows the terms with the highest TF-IDF weight and cluster sizes for each of the 11 thematic clusters obtained using the hybrid clustering method.

Cluster 3 (n=27,081) is the largest and most heterogeneous structure, dominated by species terms. Clusters 2, 6, and 9 form a production-biochemical-molecular branch; Clusters 5 and 8 a pathogen-dairy branch; Clusters 7 and 10 represent aquaculture and poultry-egg specializations; Clusters 1, 4, and 11 form a clinical-institutional-public health block *(Table 2, Fig. 9)*.

The Evolution of Clusters Over the Years

Fig. 10 shows the annual number of articles in the thematic cluster for the period 1980-2024. In each panel, the black line represents the number of publications in the relevant cluster in the relevant year.

Cluster 3 shows the largest and most steadily increasing trend from the 1980s; Cluster 2 rose markedly after 2000; Clusters 5 and 6 show steady growth. Smaller clusters (1, 4, 7, 8, 9, 10, 11) show lower publication volumes and no discernible trend *(Fig. 10)*.

Table 1. *Comparative validation performance of Aurora, Elsevier, and Hybrid SDG models across different n-gram levels*

N-gram Level	Model	n	Coverage	Top-1	Top-3	Top-5
Trigram	Hybrid	100	**0.833**	**0.456**	**0.711**	**0.744**
	Aurora	100	0.689	0.311	0.556	0.611
	Elsevier	100	0.511	0.467	0.511	0.511
Bigram	Hybrid	100	**0.780**	**0.420**	**0.650**	**0.750**
	Aurora	100	0.590	0.330	0.430	0.540
	Elsevier	100	0.490	0.390	0.480	0.490
Unigram	Hybrid	100	**0.660**	**0.300**	**0.580**	**0.620**
	Aurora	100	0.620	0.280	0.550	0.590
	Elsevier	100	0.090	0.080	0.090	0.090
Overall	Hybrid	300	**0.755**	**0.390**	**0.645**	**0.703**
	Aurora	300	0.631	0.307	0.510	0.579
	Elsevier	300	0.359	0.307	0.355	0.359

Coverage and Top-k accuracy values represent proportions of correct matches. Top-k accuracy indicates the proportion of cases in which the manually assigned SDG appears within the first k ranked SDG candidates generated by the model

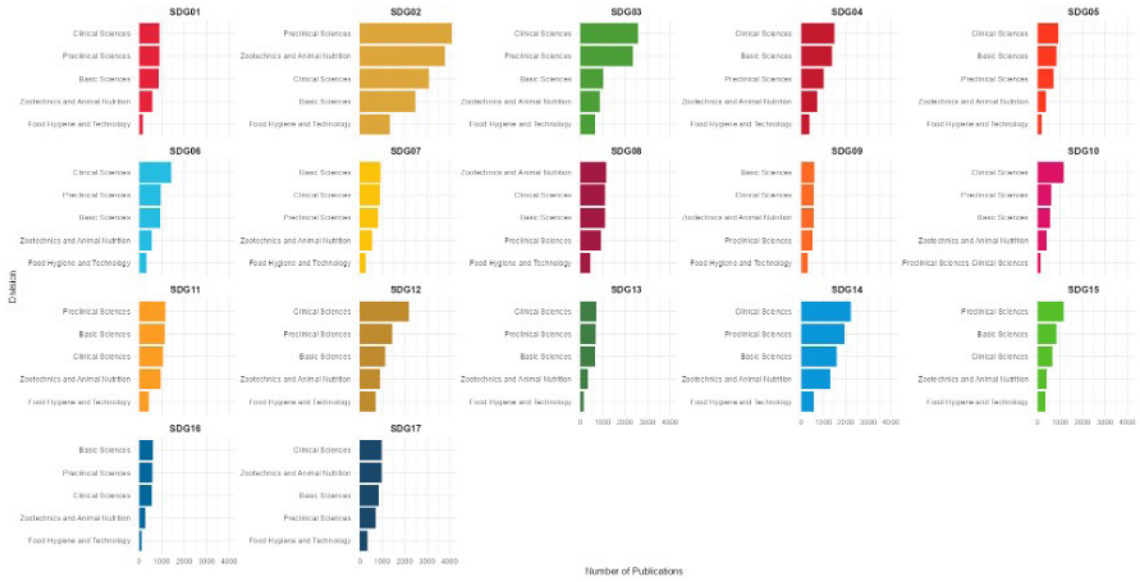

Fig 8. Comparative analysis of publication contributions by veterinary divisions according to SDGs

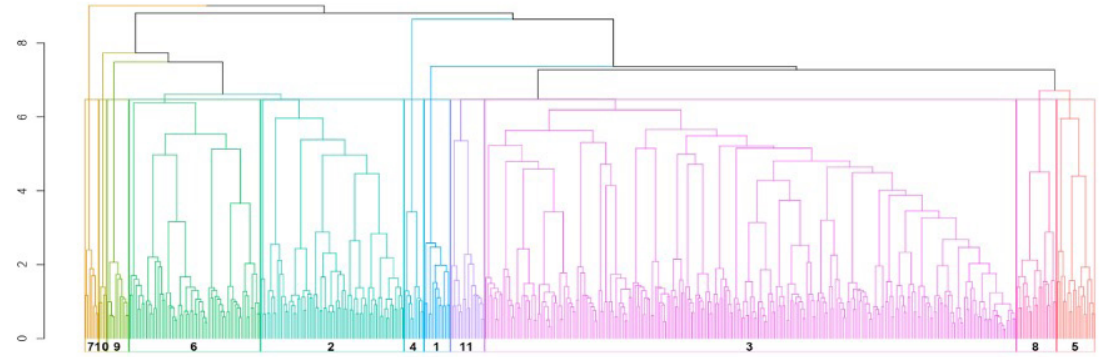

Fig 9. Dendrogram obtained using the hybrid clustering method (k=11)

The Relationship Between Thematic Clusters and the Sustainable Development Goals (Heatmap Analysis)

Fig. 11 presents a heatmap of within-cluster relative SDG association densities, with rows representing thematic clusters and columns representing SDGs (SDG01-SDG17); color intensity reflects the percentage of SDG matches within each cluster.

SDG02 exhibits relatively higher density in Clusters 2, 5, 8, 10, and 11; SDG03 is more prominent in Cluster 5; SDG14 in Cluster 7; and SDG06 in Cluster 9. Other SDGs show a more balanced distribution across clusters *(Fig. 11)*.

Discussion

This study provides a comprehensive analysis of the thematic evolution of veterinary science in Türkiye (1980–2024) based on 45,769 publications, integrating hybrid clustering and SDG alignment within a unified analytical framework [37-43]. The hybrid clustering approach reduced the computational load on the large dataset [14,44], while the n-gram-weighted combination of Aurora and Elsevier SDG dictionaries substantially reduced the risk of context-disconnected matching inherent in single-dictionary approaches [32,45].

International scientometric research indicates that sustainability research is unevenly distributed across SDGs, with environmental goals relatively underrepresented [46], a pattern reflected in veterinary and animal sciences where production, health, and clinical fields dominate over environmental topics [42].

Global veterinary research capacity remains geographically skewed toward Western Europe and North America, while emerging countries like Türkiye have concentrated thematically on specific areas [4]. Methodological variability across SDG-based analyses limits direct quantitative comparisons; findings are therefore evaluated at the contextual and conceptual level.

Table 2. Dominant terms and publication count of the cluster		
Cluster	**Representative Terms (Top-TF-IDF)**	**n**
1	case, case_report, report, dog, calf, cat, dog_case, congenital, cause, two, myiasis, atresia, treatment, case_congenital, calf_case	1122
2	effect, performance, parameter, egg, broiler, different, lamb, characteristic, biochemical, blood, hen, in vitro, diet, quail, carcass	5642
3	dog, turkey, sheep, effect, study, cattle, treatment, investigation, use, cat, evaluation, disease, region, goat, infection	27081
4	veterinary, medicine, veterinary_medicine, faculty, university, faculty_veterinary, university_faculty, journal, clinic, veterinary_faculty, education, animal, student, turkish_veterinary, history	690
5	isolate, resistance, coli, escherichia, escherichia coli, antibiotic, staphylococcus, listeria, monocytogenes, listeria monocytogenes, o, aureus, staphylococcus aureus, antibiotic resistance, strain	1582
6	rat, effect, acid, activity, sperm, protective, antioxidant, vitamin, protective_effect, ram, damage, model, injury, lipid, e	5347
7	trout, rainbow, rainbow_trout, mykiss, oncorhynchus, oncorhynchus_mykiss, trout_oncorhynchus, walbaum, mykiss_walbaum, effect, isolate_rainbow, isolate, w, mykiss_w, farm	389
8	milk, cow, dairy_cow, dairy, milk_yield, yield, mastitis, subclinical, subclinical_mastitis, effect, lactation, somatic_cell, somatic, relationship, holstein	1480
9	oxidative stress, oxidative, stress, rat, effect, apoptosis, inflammation, stress inflammation, stress parameter, stress rat, parameter, damage, protective, inflammation apoptosis, antioxidant	755
10	Coturnix, Coturnix coturnix, japonica, Coturnix japonica, quail coturnix, quail, Japanese, Japanese quail, egg, effect, performance, weight, hatch, egg weight, egg quality	319
11	animal, food, health, importance, public_health, public, nutrition, use, safety, domestic_animal, welfare, food_safety, animal_nutrition, animal_welfare, human	1362

The dominance of SDG 2 (Zero Hunger) and SDG 3 (Good Health and Well-being) reflects veterinary science's long-standing focus on animal production, food safety, and zoonotic disease control - a structure aligned with global veterinary orientation rather than a national deviation [11,47-49].

The cluster evolution data corroborate the global shift toward molecular and data-driven veterinary research [41,50-53]: species- and production-focused studies dominated before 2000, after which molecular-biochemical terms (oxidative stress, antioxidant activity, lipid peroxidation) rapidly gained prominence, consistent with methodological diversification in the global literature [4,54,55].

The relatively high representation of SDG 14 (19%) is notable, as this goal is predominantly associated with marine sciences globally [46]. Türkiye's prominence likely reflects its aquaculture production capacity and geographical advantages, evidenced by the concentration of rainbow trout and aquaculture terms in Cluster 7, suggesting a distinct national specialization partially diverging from the global veterinary literature [2].

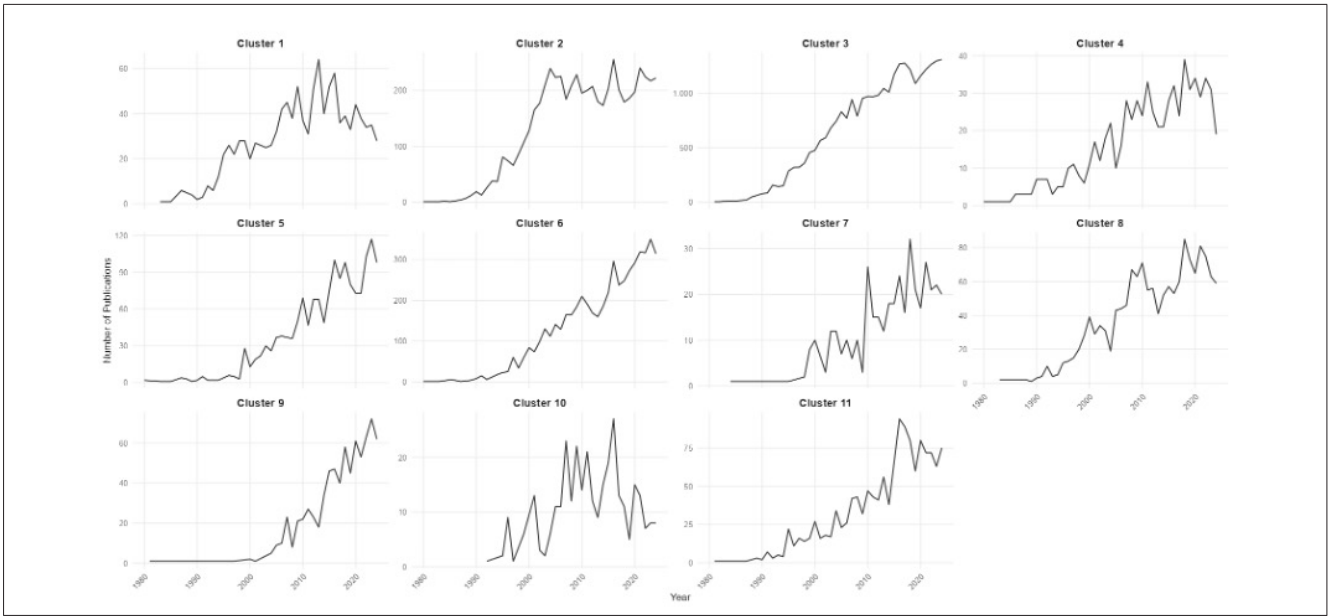

Fig 10. Development profiles of thematic clusters by year

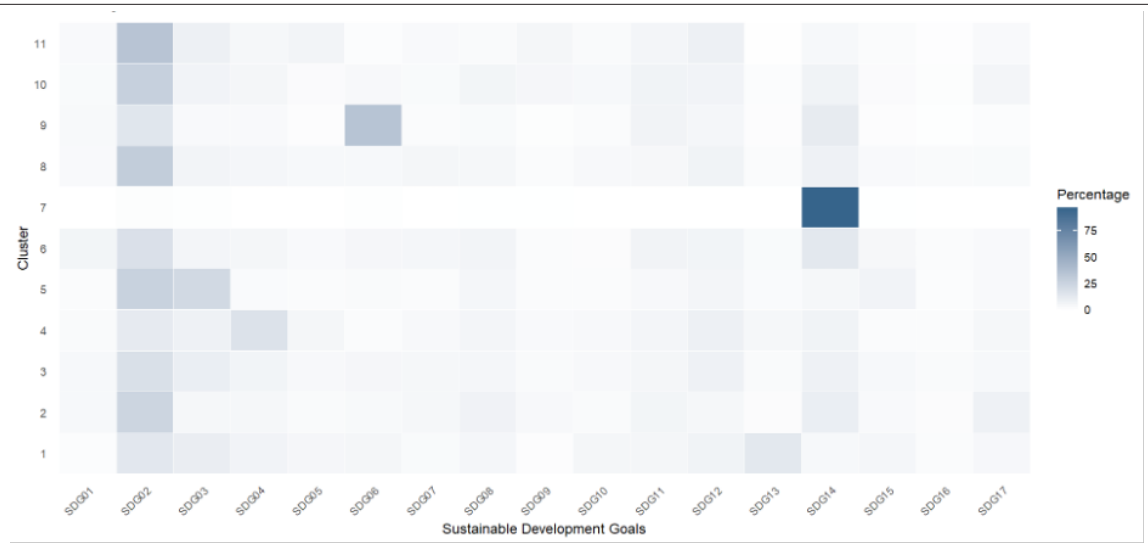

Fig 11. Heatmap showing the within-cluster relative associations between thematic clusters and the Sustainable Development Goals (SDGs)

The comparatively lower representation of SDG 13 (Climate Action) and SDG 15 (Life on Land) represents an area warranting further attention. Global veterinary and livestock literature increasingly emphasizes climate change, heat stress, methane emissions, vector dynamics, and biodiversity loss [2,11,52,56-59], indicating a partial misalignment between national veterinary research priorities and these emerging global trends.

Several structural factors may explain this pattern: veterinary curricula have historically centered on clinical sciences and production efficiency; research funding has favored directly observable outcomes such as disease control and production gains; and climate/biodiversity topics inherently require interdisciplinary integration with ecology, environmental sciences, and public health that remains underdeveloped [2,11].

From a One Health perspective, the strong associations with SDG 2, 3, 12, and 14 confirm that veterinary research robustly addresses human-animal-production system linkages [2,6,58]. However, weaker representation of SDG 13 and SDG 15 indicates that the environmental dimension of One Health has not been sufficiently addressed; a stronger research focus on climate change, ecosystem degradation, and biodiversity is needed [6,59].

The low publication volume in Food Hygiene and Technology highlights the need for strengthening research in food safety surveillance and sustainable food chains. The literature indicates that the relationship between meat inspection, surveillance, food safety, and animal welfare is multifaceted; however, data gaps and insufficient systematic utilization are reported in many areas [47]. Whether this reflects a Türkiye-specific pattern or a broader global trend warrants comparative investigation.

Academic output in Türkiye is primarily concentrated in animal health and production, consistent with existing bibliometric analyses [11,56]. Emerging global priorities -climate change, ecosystem health, and biodiversity- have not yet been fully integrated into the national veterinary research agenda.

The spread of zoonotic diseases emerging due to climate change, changes in vector distributions, habitat transformation, and the impacts of extreme weather events on animal health and production systems are risks that are difficult to manage without adequate scientific infrastructure [6,59]. Furthermore, the strengthening of relationships between ecosystem degradation, pathogen circulation, interactions between wild and domestic animals, and agroecological vulnerabilities makes the environmental dimension of veterinary research even more critical [2]. In this context, comparatively lower levels of knowledge production in relevant fields may influence Türkiye's preparedness for multidimensional environmental and biological challenges. Global scientific trends increasingly shift toward climate change, environmental adaptation, and ecosystem-based research, comparatively lower academic output in these areas may influence Türkiye's international scientific competitiveness [11].

This study has certain limitations. Since analyses rely solely on publication titles, context-sensitive themes -particularly those associated with SDG 13 and SDG 15- that tend to be elaborated in abstracts or full texts may not be fully captured. Manual entry inconsistencies in the YÖK Academic dataset and the English-based nature of the SDG dictionaries may have led to partial underrepresentation of Turkish-titled studies. While the cluster number k was determined through multiple validation criteria, the final selection inevitably involves a degree of interpretive judgment. Additionally, the multi-label SDG approach

may have contributed to a relative overrepresentation of structurally overlapping goals (e.g., SDG 2 and SDG 14 in aquaculture-related studies), though this is an inherent feature of multi-label classification frameworks rather than a methodological flaw.

In conclusion, the field of veterinary sciences in Türkiye demonstrates a strong thematic concentration, particularly within the context of SDG 2 (Zero Hunger) and SDG 3 (Good Health and Well-being), and in this regard, aligns significantly with global trends. Conversely, the relatively high representation of SDG 14 suggests that Türkiye may have developed a distinct specialization in aquatic systems and aquaculture, whereas the comparatively lower representation of SDG 13 and SDG 15 indicates areas that may benefit from further research attention in climate change, biodiversity, and ecosystem health.

Strengthening interdisciplinary collaborations and directing funding toward environmental sustainability, food security, and ecosystem health -and expanding the One Health framework to encompass its environmental dimension- will enhance Türkiye's sustainability-focused scientific output and global alignment [58]. In this context, the findings reveal that veterinary sciences are not merely a discipline focused on production and health, but a strategic field that must be re-examined and repositioned within the context of global environmental crises.

Declarations

Availability of Data and Materials: The datasets generated and analyzed during the current study are available from the corresponding author upon reasonable request. Due to the inclusion of publication records obtained from the YÖK Academic platform, data sharing is restricted to aggregated or anonymized formats to comply with platform usage policies.

Acknowledgements: The authors would like to thank the institutions and researchers whose publicly available publication records contributed to the construction of the dataset analyzed in this study.

Financial Support: This research received no specific grant from any funding agency, commercial organization or not-for-profit body.

Competing Interests: The authors declared that there is no competing of interests.

Declaration of Generative Artificial Intelligence (AI): The authors declare that the article, tables and figures were not written/created by AI and AI-assisted Technologies. All analyses, visualizations, and textual content were produced solely by the authors using only R (v4.5.1) and its associated packages, with no other software or tools employed.

Author Contributions: H.Y. designed the study, developed the text-mining workflow, performed the hybrid clustering and SDG-matching analyses, and interpreted the results. F.Ç.B. contributed to the literature review, data collection and curation, and assisted in the implementation and validation of analytical procedures. A.Y. supported the analytical evaluation and contributed to the review and critical revision of the manuscript. All authors read and approved the final manuscript.

References

1. **Akello W:** Climate change and veterinary medicine: A call to action for a healthier planet. *F1000Research,* 13:1360, 2024. DOI: 10.12688/f1000research.158307.1
2. **Destoumieux-Garzón D, Bonnet P, Teplitsky C, Criscuolo F, Henry PY, Mazurais D, Prunet P, Salvat G, Usseglio-Polatera P, Verrier E, Friggens NC:** Animal board invited review: OneARK: Strengthening the links between animal production science and animal ecology. *Animal,* 15 (1):100053, 2020. DOI: 10.1016/j.animal.2020.100053
3. **Kiran D, Sander W, Duncan C:** Empowering veterinarians to be planetary health stewards through policy and practice. *Front Vet Sci,* 9:775411, 2022. DOI: 10.3389/fvets.2022.775411
4. **Christopher MM:** A new decade of veterinary research: societal relevance, global collaboration, and translational medicine. *Front Vet Sci,* 2:1, 2015. DOI: 10.3389/fvets.2015.00001
5. **Olmos G, Tunón H, de Oliveira D, Jones M, Wallenbeck A, Swanson J, Blokhuis H, Keeling L:** Animal welfare and the United Nations' sustainable development goals - Broadening students' perspectives. *Sustainability*, 13 (6):3328, 2021. DOI: 10.3390/su13063328
6. **Pappaioanou M, Kane TR:** Addressing the urgent health challenges of climate change and ecosystem degradation from a One Health perspective: What can veterinarians contribute? *J Am Vet Med Assoc,* 261 (1): 49-55, 2022. DOI: 10.2460/javma.22.07.0315
7. **Küçükaslan Ö, Küçükaslan İ:** Bibliometric profile of postgraduate theses in veterinary obstetrics and gynecology in Turkey. *J Turk Vet Med Assoc,* 93 (1): 52-64, 2021. DOI: 10.33188/vetheder.1016877
8. **Sacchini S, Castro-Alonso A:** Veterinary Medical Education: Challenges and Perspectives. MDPI Books, Basel, 2024.
9. **Yıldırım Ö, Yaralı C, Danyer E:** The importance of veterinary medicine in the provision of sufficient and healthy food and the role of Veterinary Control Research Institutes. *Etlik Vet Microbiol J,* 31 (1): 101-109, 2020. DOI: 10.35864/evmd.746011
10. **Baker D, Jackson E, Cook SJ:** Perspectives of digital agriculture in diverse types of livestock supply chain systems. Making sense of uses and benefits. *Front Vet Sci,* 9:992882, 2022. DOI: 10.3389/fvets.2022.992882
11. **Manyike JZ, Taruvinga A, Akinyemi BE:** Mapping the research landscape of livestock adaptation to climate change: A bibliometric review using Scopus database (1994-2023). *Front Clim,* 7:1567674, 2025. DOI: 10.3389/fclim.2025.1567674
12. **Yüksek Öğretim Kurulu:** YÖK Akademik. Academic Search System. https://akademik.yok.gov.tr; *Accessed:* 05.02.2025.
13. **Akoğul S, Erişoğlu M:** An approach for determining the number of clusters in a model-based cluster analysis. *Entropy,* 19 (9): 452, 2017. DOI: 10.3390/e19090452
14. **Alasali T, Ortakcı Y:** Clustering techniques in data mining: A survey of methods, challenges, and applications. *Computer Sci,* 9 (1): 32-50, 2024. DOI: 10.53070/bbd.1421527
15. **Hennig C:** Clustering strategy and method selection. **In**, Hennig C, Meila M, Murtagh F, Rocci R: Handbook of Cluster Analysis, 724, Chapman and Hall/CRC eBooks, Informa, London, 2015.
16. **Lizenberger A, Pfeifer F, Polewka B:** Rethinking Recommender Systems: Cluster-based Algorithm Selection. *arXiv,* 2024:1-16, 2024. DOI: 10.48550/arxiv.2405.18011
17. **Sangam RS, Om H:** Hybrid data labeling algorithm for clustering large mixed type data. *J Intell Inf Syst,* 45 (2): 273-294, 2014. DOI: 10.1007/s10844-014-0348-x
18. **Yang Y, Nan F, Yang P:** Effective multilayer hybrid classification approach for automatic bridge health assessment on large-scale

uncertain data. *J Ind Inf Integr,* 24, 100234, 2021. DOI: 10.1016/j.jii.2021.100234

19. **Rousseeuw PJ:** Silhouettes: A graphical aid to the interpretation and validation of cluster analysis. *J Comput Appl Math,* 20, 53-65, 1987. DOI: 10.1016/0377-0427(87)90125-7
20. **Milligan GW, Cooper MC:** An examination of procedures for determining the number of clusters in a data set. *Psychometrika,* 50 (2): 159-179, 1985. DOI: 10.1007/BF02294245
21. **Halkidi M, Batistakis Y, Vazirgiannis M:** On clustering validation techniques. *J Intell Inf Syst,* 17 (2-3): 107-145, 2001. DOI: 10.1023/A:1012801612483
22. **Kaufman L, Rousseeuw PJ:** Finding Groups in Data: An Introduction to Cluster Analysis. Wiley, New York, 1990.
23. **Han J, Kamber M, Pei J:** Data Mining: Concepts and Techniques. 3rd ed., Morgan Kaufmann, Waltham, 2012.
24. **Tan PN, Steinbach M, Kumar V:** Introduction to Data Mining. 2nd ed., Pearson, New York, 2019.
25. **Chen C:** CiteSpace II: Detecting and visualizing emerging trends and transient patterns in scientific literature. *J Am Soc Inf Sci Technol,* 57 (3): 359-377, 2006. DOI: 10.1002/asi.20317
26. **Waltman L, Van Eck NJ:** A smart local moving algorithm for large-scale modularity-based community detection. *Eur Phys J B,* 86 (11):471, 2013. DOI: 10.1140/epjb/e2013-40829-0
27. **Šubelj L, Van Eck NJ, Waltman L:** Clustering scientific publications based on citation relations. *J Informetr,* 10 (4): 1020-1032, 2016. DOI: 10.1371/journal.pone.0154404
28. **Vanderfeesten M, Otten R, Spielberg E:** Search Queries for Mapping Research Output to the Sustainable Development Goals (SDGs) v5.0.2 (5.0.2). Zenodo, 2020.
29. **Roberge G, James C:** Elsevier 2025 Sustainable Development Goals (SDGs) Mapping (V1). Elsevier Data Repository, 2025.
30. **Bordignon F:** Dataset of search queries to map scientific publications to the UN sustainable development goals. *Data Brief,* 34:106731, 2021. DOI: 10.1016/j.dib.2021.106731
31. **Salazar MA, Loaiza MEB, Gómez M:** Natural language processing to analyze textual information from the SDGs. *International Meeting on Engineering Education,* 1-8, 2024. DOI: 10.26507/paper.3759
32. **Wulff DU, Meier DS, Mata R:** Using novel data and ensemble models to improve automated labeling of sustainable development goals. *Sustain Sci,* 19 (5): 1773-1786, 2024. DOI: 10.1007/s11625-024-01516-3
33. **Meier D, Mata R, Wulff DU:** text2sdg: An open-source solution for monitoring sustainable development goals from text. arXiv, Cornell University, 2021. http://arxiv.org/abs/2110.05856; *Accessed:* 08.09.2025.
34. **Pukelis L, Bautista-Puig N, Skrynik M, Stančiauskas V:** OSDG -- Open-source approach to classify text data by UN sustainable development goals (SDGs). *arXiv,* 2020:1-10, 2020. DOI: 10.48550/arxiv.2005.14569
35. **Tsoumakas G, Katakis I:** Multi-label classification: An overview. *Int J Data Warehous Min,* 3 (3): 1-13, 2007. DOI: 10.4018/jdwm.2007070101
36. **Schmidt F, Vanderfeesten M:** Evaluation of the accuracy of mapping science to the United Nations' Sustainable Development Goals (SDGs) using Aurora SDG queries. *Zenodo,* 2021.
37. **Adamakopoulou C, Benedetti B, Zappaterra M, Felici M, Masebo ND, Previti A, Passantino A, Paladino B:** Cats' and dogs' welfare: Text mining and topics modeling analysis of the scientific literature. *Front Vet Sci,* 10:1268821, 2023. DOI: 10.3389/fvets.2023.1268821
38. **Benedetti B, Felici M, Costa LN, Padalino B:** A review of horse welfare literature from 1980 to 2023 with a text mining and topic analysis approach. *Ital J Anim Sci,* 22 (1): 1095-1109, 2023. DOI: 10.1080/1828051x.2023.2271038
39. **Davies H, Nenadić G, Alfattni G, Castelerio AM, Moubayed NA, Farrell SO, Radford AD, Noble PM:** Text mining for disease surveillance in veterinary clinical data. Part one: The language of veterinary clinical records and searching for words. *Front Vet Sci,* 11:1352239, 2024. DOI: 10.3389/fvets.2024.1352239
40. **İstek Ö:** Bibliometric analysis of postgraduate theses on eye and their diseases in animals in Turkey. *Kocatepe Vet J,* 18 (3): 329-336, 2025.
41. **Ouyang Z, Sargeant JM, Thomas A, Wycherley K, Ma R, Esmaeilbeigi R, Versluis A, Deborah S, Stone E, Poljak Z, Bernardo TM:** A scoping review of 'big data', 'informatics', and 'bioinformatics' in the animal health and veterinary medical literature. *Anim Health Res Rev,* 20 (1): 1-16, 2019. DOI: 10.1017/s1466252319000136
42. **Vaitsi GA, Bourganou MV, Lianou DT, Kiouvrekis Y, Michael CC, Gougoulis DA, Fthenakis GC:** Scientometric analysis: An emerging tool in veterinary and animal scientific research. *Animals,* 14 (21): 3132, 2024. DOI: 10.3390/ani14213132
43. **Taçbaş E, Çakır Ş, Özkan S, Demir D:** Bibliometric analysis of articles produced from research projects supported by TAGEM according to scientific disciplines. *Etlik Vet Microbiol J,* 35 (2): 179-180, 2025. DOI: 10.35864/evmd.1248719
44. **Dörterler S, Dumlu H, Özdemir D, Temurtaş H:** Hybridization of meta-heuristic algorithms with K-means for clustering analysis: Case of medical datasets. *Gazi J Eng Sci,* 10 (1): 1-15, 2024. DOI: 10.30855/gmbd.0705n01
45. **Lemarchand P, MacMahon C, McKeever M, Owende P:** An evaluation of a computational technique for measuring the embeddedness of sustainability in the curriculum aligned to AASHE-STARS and the United Nations Sustainable Development Goals. *Front Sustain,* 4:997509, 2023. DOI: 10.3389/frsus.2023.997509
46. **Asatani K, Takeda H, Yamano H, Sakata I:** Scientific attention to sustainability and SDGs: Meta-analysis of academic papers. *Energies,* 13 (4):975, 2020. DOI: 10.3390/en13040975
47. **Stärk KDC, Alonso S, Dadios N, Dupuy C, Ellerbroek L, Georgiev M, Hardstaff J, Huneau-Salaün A, Laugier C, Mateus A, Nigsch A, Afonso A, Lindberg A:** Strengths and weaknesses of meat inspection as a contribution to animal health and welfare surveillance. *Food Control,* 39, 154-162, 2013. DOI: 10.1016/j.foodcont.2013.11.009
48. **Christopher MM, Marusic A:** Geographic trends in research output and citations in veterinary medicine: Insight into global research capacity, species specialization, and interdisciplinary relationships. *BMC Vet Res,* 9, 115, 2013. DOI: 10.1186/1746-6148-9-115
49. **Uzabacı E:** Evaluation of the 100 most-cited articles published in veterinary journals. *Vet Med Sci,* 11 (5):e70545, 2025. DOI: 10.1002/vms3.70545
50. **Topuz D, Tekgöz S:** Hybrid ensemble model for lactation milk yield prediction of Holstein cows. *Kafkas Univ Vet Fak Derg,* 31 (5): 603-611, 2025. DOI: 10.9775/kvfd.2025.34031
51. **Bağlıoğlu M, Özen A:** Veteriner Hekimliği Açısından İnformatik Devrimi. *Lokman Hekim Dergisi,* 48-48, 2014.
52. **Yardibi F, Fırat MZ, Teke EÇ:** Trend topics in animal science: A bibliometric analysis using CiteSpace. *Turk J Vet Anim Sci,* 45 (5): 833-841, 2021. DOI: 10.3906/vet-2001-103
53. **Savaş T, Yurtman İY:** Hayvan davranış bilimi ve zootekni: Tanım ve izlem. *Hay Üretim Derg,* 49 (2): 36-42, 2008.
54. **Yıldız Bİ:** Comparative performance of convolutional neural network models in wing morphometric classification of honey bee populations across Europe. *Kafkas Univ Vet Fak Derg,* 31 (5): 653-659, 2025. DOI: 10.9775/kvfd.2025.34544
55. **Akıllı A, Kezer G, Kul E:** Evaluation of microbiological properties in kefir production with fuzzy logic-based decision support system. *Kafkas Univ Vet Fak Derg,* 31 (5): 679-688, 2025. DOI: 10.9775/kvfd.2025.34643
56. **Diop S, İnci A, Kızgın AD, Düzlü Ö:** Understanding one health and zoonosis: A systematic review with a bibliometric analysis of Turkish research and global perspectives (1974-2023). *Kafkas Univ Vet Fak Derg,* 2025. DOI: 10.9775/kvfd.2025.34009
57. **Ramírez-Durán JA, Niebles W, Stojanovich-Morente Z, Gallego G, Guerra-Cogollo JA:** Use of technology for sustainable livestock processes: A bibliometric review. *Afr J Food Agric Nutr Dev,* 24 (7): 23934-23953, 2024. DOI: 10.18697/ajfand.132.23515

58. **Abbasi K, Ali P, Barbour V, Benfield T, Bibbins-Domingo K, Hancocks S, Horton R, Laybourn-Langton L, Mash R, Sahni P, Mohammad Sharief W, Yonga P, Zielinski C:** Time to treat the climate and nature crisis as one indivisible global health emergency. *Kafkas Univ Vet Fak Derg,* 30 (1): 1-3, 2024. DOI: 10.9775/kvfd.2023.editorial

59. **Alkheraije KA:** Climate change, vector-borne animal diseases: Impacts on livestock health: A narrative review. *Kafkas Univ Vet Fak Derg,* 2025. DOI: 10.9775/kvfd.2025.35482

Kafkas Universitesi Veteriner Fakultesi Dergisi
Journal Home-Page: http://vetdergikafkas.org
E-ISSN: 1309-2251

Kafkas Univ Vet Fak Derg
32 (2): 261-273, 2026
DOI: 10.9775/kvfd.2025.36016

RESEARCH ARTICLE

Comparative Analysis of Gut Microbiota Between Healthy and Diarrheic Tibetan Pigs Using 16S rRNA Sequencing

Xinxin YU [1], Yan LUO [1], Chengyu GENG [1], Yurong HUANG [1], Kai LIU [1], Zhenyu CHANG [2], Khalid MEHMOOD [3], Hui ZHANG [1,2(*)], Ying LI [1 (*)]

[1] College of Veterinary Medicine, South China Agricultural University, Guangzhou, 510642, CHINA
[2] College of Animal Science, Xizang University of Agriculture and Animal Husbandry, Linzhi, 860000, CHINA
[3] Department of Pathology, Faculty of Veterinary and Animal Sciences, the Islamia University of Bahawalpur 63100, PAKISTAN

(*) **Corresponding author:**
Hui Zhang & Ying Li
Phone: +86 02085280234
Cellular phone: +86 16676734751
Fax: +86 02085280234
E-mail: hz236@scau.edu.cn (ZH), lying@scau.edu.cn (LY)

How to cite this article?

Yu X, Luo Y, Geng C, Huang Y, Liu K, Chang Z, Mehmood K, Zhang H, Li Y: Comparative Analysis of Gut Microbiota Between Healthy and Diarrheic Tibetan Pigs Using 16S rRNA Sequencing. *Kafkas Univ Vet Fak Derg*, 32 (2): 261-273, 2026.
DOI: 10.9775/kvfd.2025.36016

Article ID: KVFD-2025-36016
Received: 29.12.2025
Accepted: 10.04.2026
Published Online: 21.04.2026

Abstract

Diarrhea is a common gastrointestinal symptom in Tibetan pigs, generally considered to be related to gut microbiota imbalance. However, studies comparing the gut microbiota of healthy and diarrheal Tibetan pigs are relatively few. This study used high-throughput 16S rRNA gene sequencing to analyze the fecal microbiota of diarrheal Tibetan pigs. Diversity analysis and functional prediction results showed that the microbiota richness of healthy Tibetan pigs was significantly higher than that of diarrheal Tibetan pigs, and the clustering of gut microbiota between the two groups was more obvious. The gut microbiota of healthy Tibetan pigs was mainly composed of *Firmicutes* and *Lactobacillus*, while the abundance of *Proteobacteria* and *Eubacterium* increased in diarrheal Tibetan pigs. In particular, the abundance of *Lactobacillus* was significantly different between the two groups in the Tibetan pig gut, demonstrating the role of probiotics in gut health. In addition, the complexity of the gut microbiota of diarrheal Tibetan pigs was reduced, and the stability of the gut microbiota was disrupted. Metabolic analysis showed significant differences between the different groups: the intestinal fermentation and nitrate reduction pathways were increased in diarrheal Tibetan pigs, while healthy Tibetan pigs showed enhanced amino acid metabolism and a more pronounced anaerobic phenotype. These findings elucidate the structural and functional alterations in the gut microbiota associated with diarrhea in Tibetan pigs, offering new insights for potential interventions.

Keywords: Diarrhea, Gut microbiota, Tibetan pigs, 16S rRNA sequencing

INTRODUCTION

Tibetan pigs are a unique domesticated animal breed native to the Qinghai-Tibet Plateau region of China. They possess a strong adaptability to harsh, cold environments and can survive even in conditions of extreme cold, hypoxia, and feed scarcity [1-3]. Previously, Tibetan pigs were raised through grazing, freely foraging on grasslands. However, increasing research indicates that this method makes them more susceptible to various pathogens (such as bacteria, viruses, and parasites) [4-6]. These pathogens pose a threat to the health of the herd, preventing large-scale farming of Tibetan pigs.

Diarrhea is one of the most common and harmful clinical syndromes in Tibetan pig farming, particularly affecting weaned piglets [7-9]. Its etiology involves multiple interacting factors, including pathogen infection, nutritional imbalance, environmental stress, and host immune status [10,11]. Studies have confirmed that the gut microbiota plays a crucial role in nutrient metabolism, barrier protection, and immune regulation [12-14]. In healthy pigs, dominant beneficial bacteria, such as *Lactobacillus* and *Bifidobacterium*, maintain intestinal homeostasis by producing short-chain fatty acids (SCFAs), enhancing the mucosal barrier, and competitively inhibiting pathogen colonization [15-18]. However, factors such as weaning stress, dietary changes, or environmental stress can easily disrupt the balance of the gut microbiota [19]. This dysbiosis typically manifests as a reduction in symbiotic beneficial bacteria and an overgrowth of opportunistic or pathogenic bacteria (e.g., *Escherichia coli, Clostridium* spp., and *Fusobacterium* spp.), leading to diarrhea in animals [20,21]. Bacterial pathogens, the primary causative agents of diarrhea in Tibetan pigs, include enterotoxigenic *Escherichia coli* (ETEC), *Salmonella* spp., and *Shigella* spp. ETEC frequently causes

watery diarrhea and severe dehydration in newborn piglets [22], while *Salmonella* infection can lead to acute enteritis and systemic disease with a high mortality rate [23].

Studies have found that changes in gut microbiota structure are closely related to the occurrence of diarrhea in hosts [24,25]. For example, diarrheal piglets typically exhibit reduced microbial diversity and loss of functional groups associated with carbohydrate fermentation and short-chain fatty acid production. Furthermore, early stressors such as group housing, low temperatures, and sudden changes in diet exacerbate these microbiota alterations, impairing intestinal barrier function and triggering inflammatory responses. With advancements in high-throughput sequencing technology, microbial community analysis using 16S rRNA gene sequencing has become an important method for exploring gut microbiota and its disease-related microbial changes. Despite progress in related research, studies on local pig breeds raised under unique ecological conditions (such as Tibetan pigs endemic to the Qinghai-Tibet Plateau) remain limited. Tibetan pigs are frequently subjected to factors such as cold stress, hypoxia, and dietary changes, which may affect the composition and resilience of their gut microbiota. Elucidating the differences in gut microbiota between diarrheal and healthy Tibetan pigs is crucial for revealing the microbial mechanisms of diarrhea in this unique genetic and environmental context.

This study analyzed the composition and diversity of the gut microbiota in diarrheal Tibetan pigs using high-throughput 16S rRNA gene sequencing technology. By comparing the gut microbiota of individuals with diarrhea and healthy individuals, we can identify key bacterial communities that may be associated with the occurrence of diarrhea, as well as the dominant bacterial species in the gut environment of healthy individuals. This reveals the microbial mechanisms of diarrhea in Tibetan pigs and the protective role of the microbial community in the gut environment, thus providing a basis for developing effective diagnostic and preventive strategies.

Material and Methods

Ethical Approval

All animal experiments were reviewed and approved by the Animal Ethics Committee of South China Agricultural University (approval number: 2024A637), and conducted in accordance with the institutional guidelines for the care and use of laboratory animals.

Animal Management and Clinical History

All Tibetan pigs were housed under standard commercial farming conditions. The animals were kept in naturally ventilated pens with a relatively constant temperature (20-25°C) and natural light cycles. All pigs had ad libitum access to a standard commercial basal diet and clean drinking water throughout the study period. Crucially, regarding their clinical history and medication, none of the selected Tibetan pigs (both healthy and diarrheal groups) had received any antibiotic therapies, probiotic supplements, or vaccinations for at least one month prior to fecal sample collection. This strict selection criterion was implemented to ensure that the baseline gut microbiota composition was not artificially perturbed by external pharmacological or immunological interventions.

Experimental Animals and Sample Collection

This study collected fecal samples from six healthy Tibetan pigs (healthy group, C: C1-C6) and six clinically diagnosed Tibetan pigs exhibiting diarrhea symptoms (diarrhea group, F: F1-F6) at a commercial Tibetan pig farm in Linzhi, Xizang, Tibet, China. All samples were immediately frozen and transported to the laboratory under cold chain conditions to prevent degradation.

To minimize environmental contamination and maintain the integrity of microbial DNA, all sample processing was performed under sterile conditions. The core portion of each fecal sample was aseptically collected using sterile swabs to avoid contact with potentially oxidized or contaminated surface materials. Approximately 0.5-2 g of material from each sample was transferred to sterile cryopreservation tubes and aliquoted into 2-3 equal portions for later use. Processed samples were immediately flash-frozen in liquid nitrogen and subsequently transported via cold chain logistics to a commercial sequencing provider for further analysis.

DNA Extraction, 16S rRNA Gene Sequencing, and Bioinformatics Analysis

Microbial DNA extraction, PCR amplification of the V3-V4 hypervariable region of the bacterial 16S rRNA gene, library preparation, high-throughput sequencing, and downstream data analysis were performed by Beijing Tsingke Biotechnology Co., Ltd. (Guangzhou, China). Sequencing utilized the Illumina NovaSeq 6000 platform with a paired-end strategy (2 × 250 bp).

Raw reads underwent demultiplexing, quality filtering, merging, and denoising using the DADA2 algorithm integrated in QIIME2 version 2020.6 to generate high-quality amplicon sequence variants (ASVs). Chimeric sequences were removed during this process. Representative sequences were classified and annotated using a pre-trained classifier trained against the SILVA database.

Diversity analysis was conducted as follows: α-diversity metrics (Chao1, Shannon, Simpson, etc.) were compared using biological t-tests. β-diversity (Bray-Curtis dissimilarity) was assessed via principal coordinate analysis (PCoA),

non-metric multidimensional scaling (NMDS), and UPGMA clustering, with statistical testing performed using PERMANOVA and ANOSIM.

Additionally, LEfSe, STAMP, and Metastats were employed to identify differentially abundant taxa. PICRUSt2, BugBase, and FAPROTAX were utilized to infer microbial metabolic functions, phenotypes, and ecological roles. In all comparative analyses, P-values <0.05 were considered statistically significant.

Results

Sequencing Quality and ASV Statistics

16S rRNA gene sequencing was performed using the Illumina NovaSeq platform with a paired-end sequencing strategy. In total, 930.725 raw reads were generated across the 12 samples. After quality filtering, noise reduction, chimera removal, and sequence merging using the DADA2 plugin in QIIME2 (version 2020.6), a total of 871.049 clean reads were retained, ranging from 47.685 to 75.511 reads per sample. The final results showed that 4.683 non-chimeric amplicon sequence variants (ASVs) were identified in the samples *(Fig. 1-a)*. The number of ASVs per sample ranged from 352 to 938, and the average number of ASVs in diarrheal samples was noticeably lower than in healthy samples.

Prior to the calculation of alpha and beta diversity metrics, the ASV table was rarefied to an even depth of 47.685 reads per sample (based on the sample with the minimum number of clean sequences) to correct for differences in sequencing depth. Furthermore, the dilution curves at both the sample and population levels eventually approached saturation after a certain fold of dilution, indicating that the sequencing depth was sufficient for assessing microbial diversity *(Fig. 1-c, d)*. Venn diagram analysis showed that the healthy group (C) and the diarrheal group (F) shared 480 ASVs, while the healthy group and the diarrheal group had 2.700 and 1.503 unique ASVs, respectively *(Fig. 1-b)*. This indicates that diarrhea strongly alters the gut microbiota composition, resulting in a pronounced reduction in the gut microbiota of diarrheal Tibetan pigs. Simultaneously, similar to the previous results, the species richness in the diarrhea group was consistently lower than that in the healthy group, suggesting that the gut microbiota of diarrheal Tibetan pigs was more impoverished and unstable.

Alpha Diversity Analysis

Based on the ASV abundance matrix, we calculated four indices for α-diversity: ACE, Chao1, Shannon, and Simpson. The results showed that the ACE and Chao1 indices of the gut microbiota in diarrheal pigs were significantly lower than those in healthy pigs *(Fig. 2-a, b)*. The Shannon and Simpson indices also showed a decreasing trend in diversity in the diarrheal group *(Fig. 2-c, d)*, indicating that after diarrhea symptoms appeared in Tibetan pigs, community complexity and evenness decreased, and the abundance of related microorganisms significantly declined. The Shannon abundance curve further supported these findings, showing a lower abundance level in the diarrheal group compared to the healthy group *(Fig. 2-e)*, clearly demonstrating the reduced gut microbiota diversity under diarrheal conditions. The

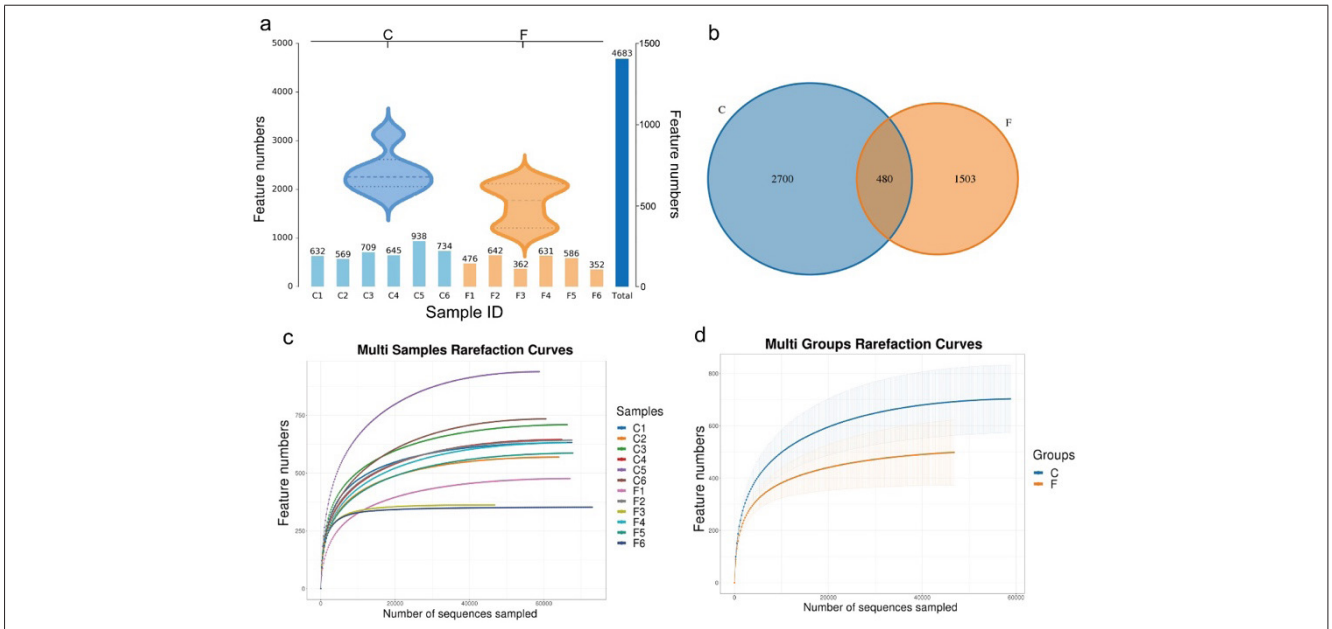

Fig 1. Sequence data quality assessment and diversity saturation analysis. **a)** Bar charts display the number of observed features (ASVs) per sample, with violin plots illustrating distributions across both datasets, **b)** Venn diagram. **c)** Dilution curves for individual samples. **d)** Sparsity curves for group samples

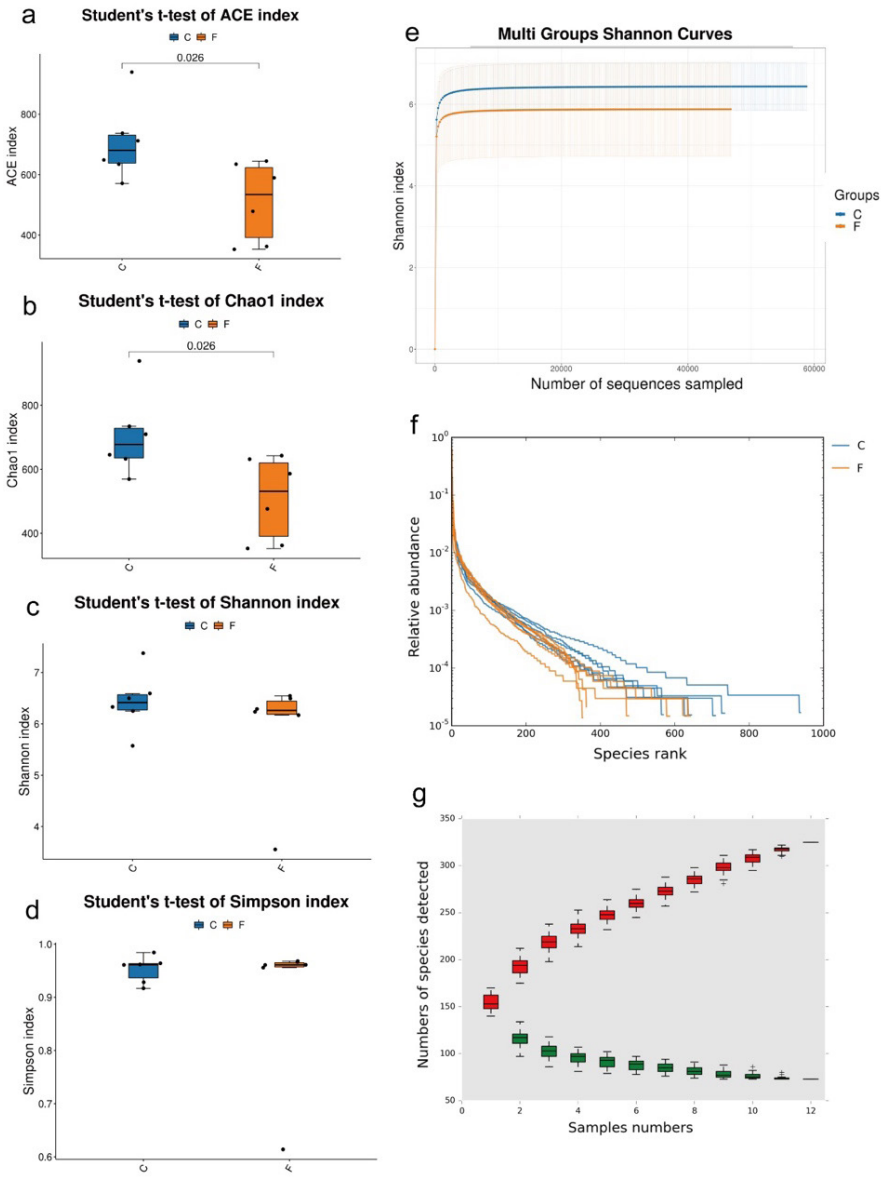

Fig 2. Analysis of gut microbiota α diversity. **a, b, c, d**) Box plots of α diversity indices between groups, including: ACE index, Chao1 index, Shannon index, Simpson index, **e)** Shannon rarity curve, **f)** Abundance-richness curve. **g)** Shared species accumulation curve

abundance ranking curves also illustrate this: the curve for the healthy group was wider and flatter, indicating higher species richness and more even distribution; while the curve for the diarrheal group was steeper, reflecting the absence of some species *(Fig. 2-f)*.

Furthermore, the shared species accumulation curve *(Fig. 2-g)* showed a rapid upward trend, indicating that the current sample size was sufficiently large and that most microbial taxa were successfully detected.

Beta Diversity Analysis

Beta diversity analysis was performed based on Bray-Curtis similarity. The results of principal component analysis (PCA), principal coordinate analysis (PCoA), and non-metric multidimensional scaling (NMDS) are shown in *Fig. 3-a, b, c*. The first two principal coordinates of PCA explained 72.60% and 10.71% of the variance, respectively, while PCoA explained 25.75% and 23.08% of the variance, respectively. A clear separation trend was observed between the healthy and diarrheal groups in the ordination plots, indicating a distinct structural shift in the gut microbiota composition associated with diarrhea. To rigorously evaluate this divergence, PERMANOVA and ANOSIM were conducted. PERMANOVA indicated that the disease status explained 17.5% of the variation in microbiota composition (R^2=0.175, P=0.023]). Consistent with the visual separation, the ANOSIM test supported a strong trend of community divergence (R=0.152, P=0.069). These results further suggest a strong correlation between diarrheal status and altered gut microbiota composition

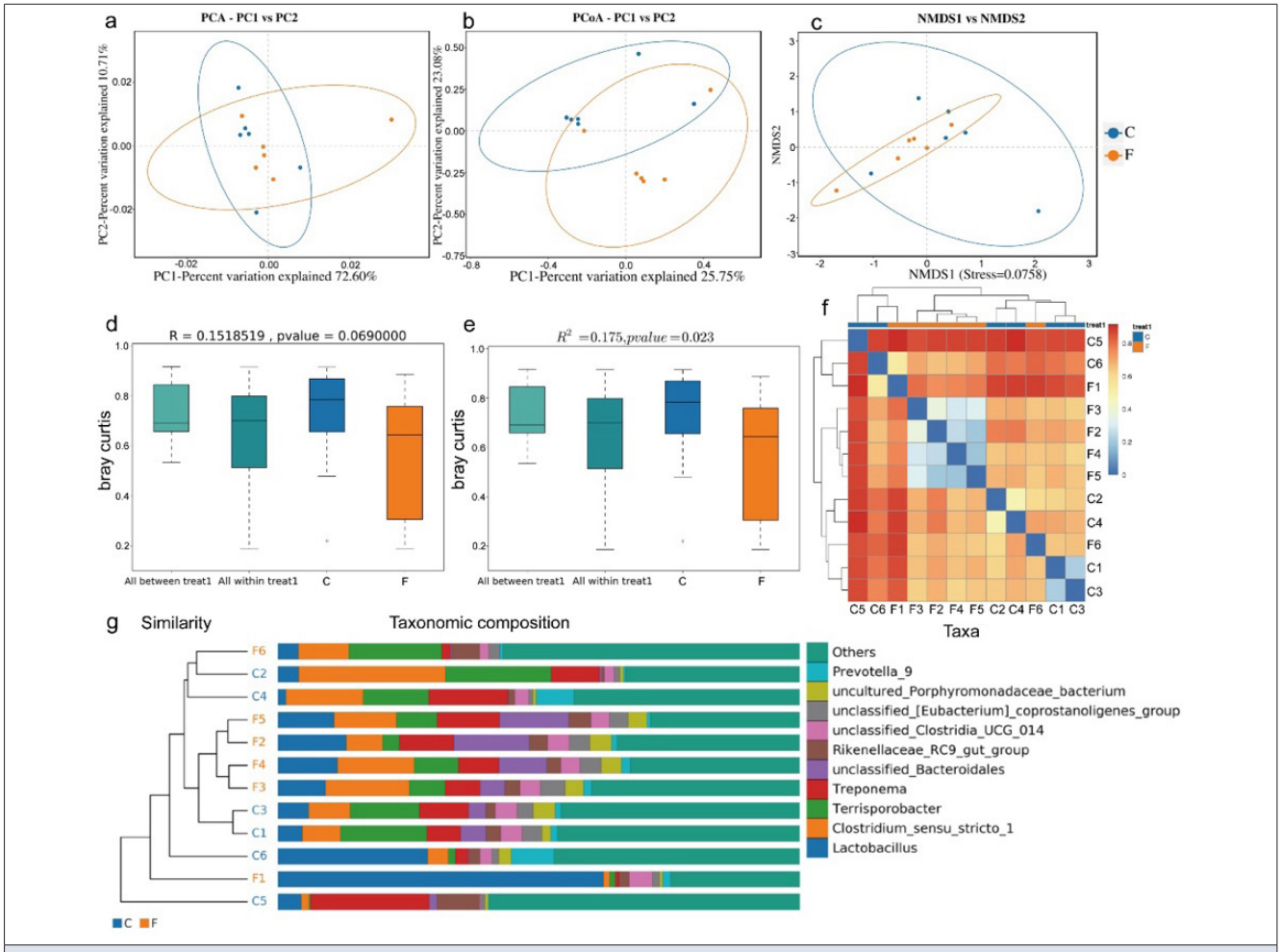

Fig 3. β-diversity analysis of the gut microbiota. **a, b, c)** Ordination plots of Bray-Curtis distances. Including: Principal Component Analysis (PCA), Principal Coordinate Analysis (PCoA), Non-metric Multidimensional Scaling (NMDS), **d)** ANOSIM results, **e)** PERMANOVA analysis, **f)** Heatmap of Bray-Curtis distances among all samples, **g)** UPGMA clustering tree and genus-level bar chart

in Tibetan pigs, albeit with some inter-individual variations.

A heatmap based on Bray-Curtis distance further confirmed this difference in microbiota composition, with most samples clustering according to group *(Fig. 3-f)*. Genus-level UPGMA clustering analysis also revealed different microbiota patterns within specific groups, with samples from the same cohort tending to cluster together *(Fig. 3-g)*. This indicates that the changes in the gut microbiota caused by diarrhea are quite similar, with a more significant impact on specific bacterial groups.

Taxonomic Composition and Relative Abundance Analysis

Further hierarchical clustering analysis based on the heatmap of the top 50 genera *(Fig. 4-a)* revealed significant differences in the gut microbiota between healthy and diarrheal pigs. Samples from the healthy group clustered together, rich in various beneficial or symbiotic bacteria, such as *Lactobacillus, Bacteroides,* and the [*Eubacterium*] *eligens* group; while samples from the diarrheal group clustered together, rich in the *NK4A214* group, *Colidextribacter,* and other unclassified bacteria that may be associated with dysbiosis or inflammation.

To further investigate the taxonomic composition of the Tibetan pig gut microbiota, we performed visualization analysis of the microbial community structure at the phylum and genus levels for both the healthy and diarrheal groups. At the phylum level *(Fig. 4-b)*, the dominant phyla in all samples were *Firmicutes, Bacteroidota,* and *Spirochaetota*. Notably, *Firmicutes* were dominant in the healthy group, while the relative abundance of *Spirochaetota* decreased in the diarrheal group, suggesting that diarrhea symptoms may be related to changes in the gut microbiota structure.

At the genus level *(Fig. 4-c)*, the composition of the gut microbiota became more diverse. The healthy group showed a relatively even distribution of microbial species, with *Terrisporobacter mayombei* and *Clostridium disporicum* being particularly abundant. In contrast, the diarrheal group showed an increased proportion of *Lactobacillus*

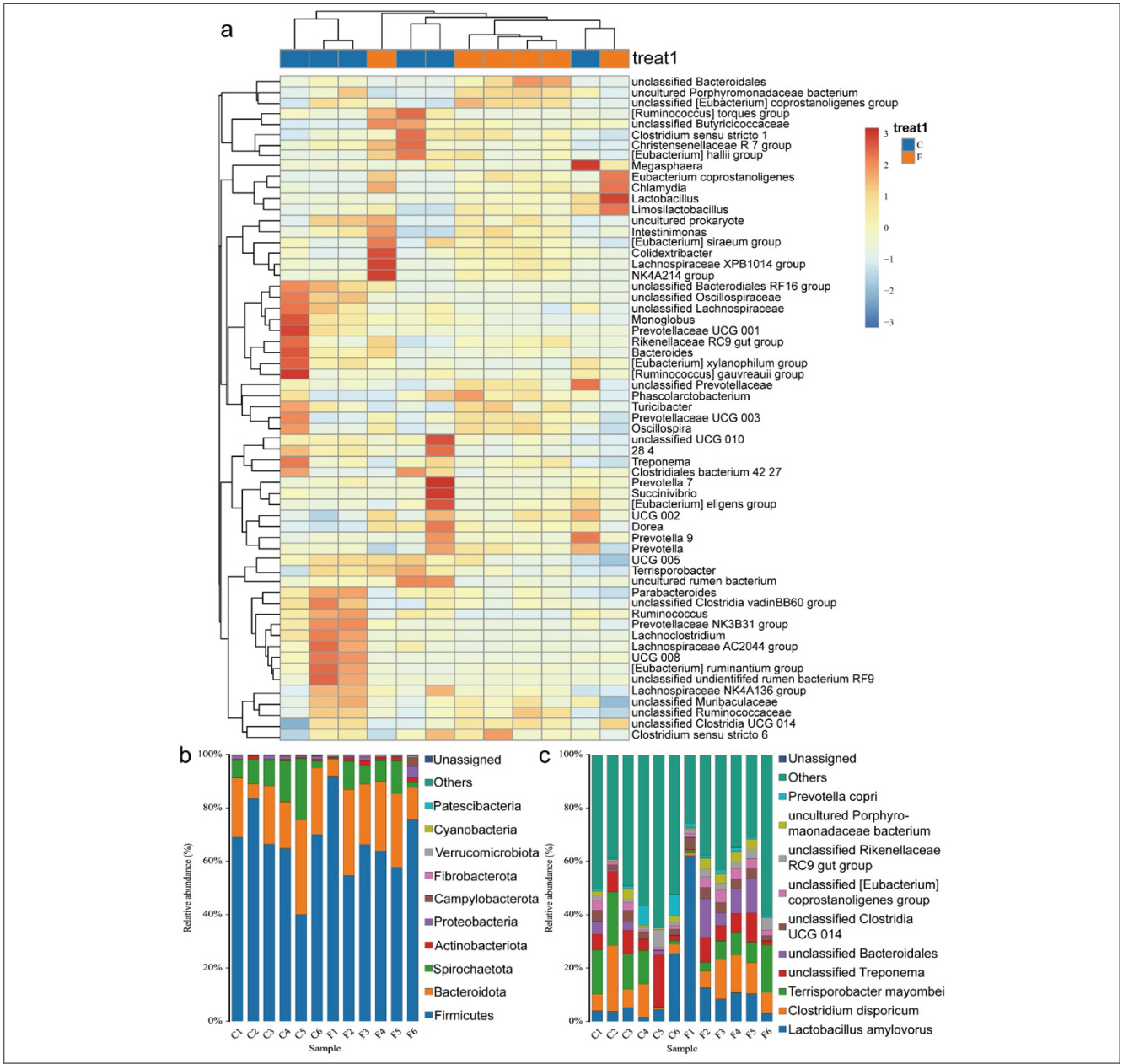

Fig 4. Taxonomic composition and heatmap analysis of the gut microbiota. **a)** Hierarchical clustering heatmap of genus-level abundance based on Z-score standardization, **b)** Relative abundance composition at the bacterial phylum level, **c)** Relative abundance composition at the bacterial genus level

amylovorus, uncultured *Porphyromonadaceae,* unclassified *Eubacterium coprostanoligenes* group, and unclassified *Bacteroidales*. These changes in the microbiota may reflect changes in the dominant bacterial species and their resistance to pathogenicity during diarrhea in Tibetan pigs.

Furthermore, a circular phylogenetic tree was constructed to explore the phylogenetic relationships of the dominant groups in the Tibetan pig gut microbiota *(Fig. 5)*. The results showed different clustering patterns between the healthy and diarrheal groups, with significant segregation of dominant bacterial groups. In the healthy group, members of the phylum *Firmicutes* (yellow portion), especially *Lactobacillus* and *Clostridium*, were significantly enriched and showed close phylogenetic relationships. Conversely, the abundance of *Bacteroides* was significantly increased in the diarrhea group, including *Treponema* and the *NK4A214* group. These bacteria are located on different branches and are phylogenetically distant from the core symbiotic flora of the healthy group.

These results indicate that the composition of the gut microbiota in Tibetan pigs undergoes significant changes after diarrhea occurs. These changes suggest that the cause of diarrhea in Tibetan pigs is a reduction or disappearance of beneficial microorganisms and an increase or appearance of potentially pathogenic or opportunistic taxa.

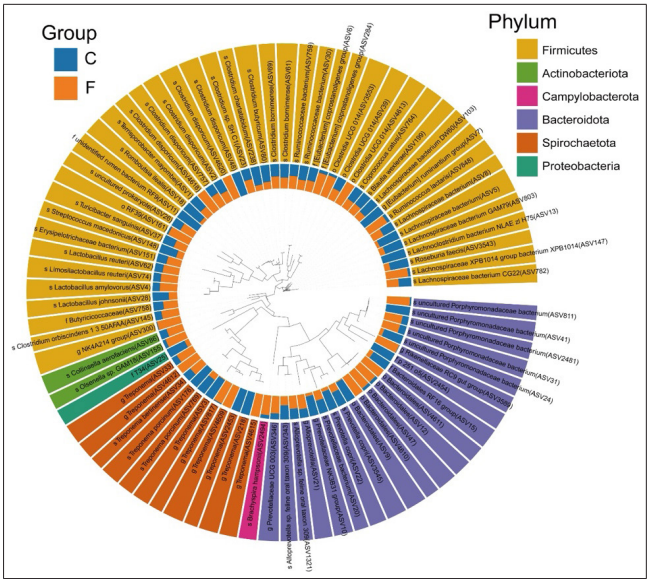

Fig 5. Phylogenetic tree and taxonomic distribution of dominant bacterial communities. The inner circle indicates the relative abundance of corresponding genera across samples. The outer circle displays phylum-level taxonomy, with branches colour-coded. Blue and orange distributions within each segment of the inner circle represent Groups C and F respectively

Abundance Difference Analysis Between Healthy and Diarrhea Groups

To further identify the key taxa that differentiate between diarrheal and healthy Tibetan pigs, species-level abundance difference analyses were performed using LEfSe, Metastats, and univariate statistical methods *(Fig. 6)*. LEfSe analysis *(Fig. 6-a, b)* showed that members of the *Lachnospiraceae* and *Lactobacillus* families were significantly enriched in the healthy group. Conversely, the *Eubacterium coprostanoligenes* group was significantly enriched in the diarrheal group, with a linear discriminant analysis (LDA) score exceeding 4.0, indicating a greater degree of difference. Relative abundance histograms further illustrated these differences. *Lactobacillus* consistently showed high abundance in healthy samples, with significantly increased proportions of *Lachnoclostridium* and *Ruminococcus,* suggesting a potential role in preventing diarrhea-related dysbiosis. In contrast, unclassified *RF39* and *Eubacterium coprostanoligenes* were significantly increased in diarrheal samples *(Fig. 6-c, d, e)*, and the occurrence of intestinal inflammation is likely related to this dysbiosis.

Transposon analysis *(Fig. 6-f)* confirmed the above results, revealing statistically significant differences in the bacterial communities of multiple genera between the two groups (P<0.05). Box plots *(Fig. 6-g)* further illustrated the different distribution patterns of key taxa. Notably, in the healthy group, several species, including *Terrisporobacter*, *Treponema*, and *Lachnoclostridium,* showed significant increases, suggesting that these bacteria play an important role in maintaining the health of Tibetan pigs. In contrast, the increased taxa such as *Subdoligranulum* in the diarrhea group may indicate inflammatory damage to the intestines, leading to diarrhea symptoms in Tibetan pigs.

Co-occurrence Network and Microbial Interaction Analysis

To investigate the ecological interactions among the gut microbiota of Tibetan pigs, co-occurrence network analysis was performed based on Spearman's rank correlation coefficient, yielding the network diagram *(Fig. 7-a)*: a complex interaction network with 46 nodes and multiple edges was constructed, indicating the complexity and diversity of the microbial structure in the gut micro-ecosystem. Most correlations were positive (red lines), suggesting synergistic effects among most bacterial groups; while a few negative correlations (green lines) indicated potential competition. Bacteria belonging to the phyla *Firmicutes* and *Bacteroidota* were located in the central region of the network and had high node degrees, indicating their important role in stabilizing the gut micro-ecological environment as major gut microbes. Clearly, *Lactobacillus* (node 33), *Terrisporobacter* (node 35), and unclassified *Bacteroidales* (node 36) had the highest connectivity, suggesting they may be key species in the gut micro-ecological environment of Tibetan pigs.

Further ecological analysis using Zi-Pi topology analysis confirmed the ecological roles of these groups *(Fig. 7-b)*. The results showed that most groups were classified as marginal groups, i.e., Zi <2.4 and Pi <0.62, indicating that the role of most gut microbiota communities was limited to their respective low-connectivity groups. However, a node located in the peripheral region, with Pi >0.62, was marked in red, indicating that this group played a unique role in the connectivity network.

Functional Prediction of Microbial Communities

Metagenomic maps were inferred from 16S rRNA data using PICRUSt2, and pathway annotation was performed using the KEGG, BugBase, and FAPROTAX databases to investigate the functional potential of the gut microbiota. The results are shown in *Fig. 8*. KEGG pathway prediction results showed a significant difference in microbial metabolic capacity between the healthy and diarrheal groups *(Fig. 8-a)*. Specifically, the healthy group showed significant enrichment in pathways such as global and overview maps, amino acid metabolism, and metabolism of cofactors and vitamins, indicating that their gut microbiota is better suited to regulating overall metabolism and nutrient transformation. In contrast, the diarrheal group showed upregulated expression in pathways such as membrane transport, translation, nucleotide metabolism, and replication and repair. This result demonstrates the adaptive response of the Tibetan

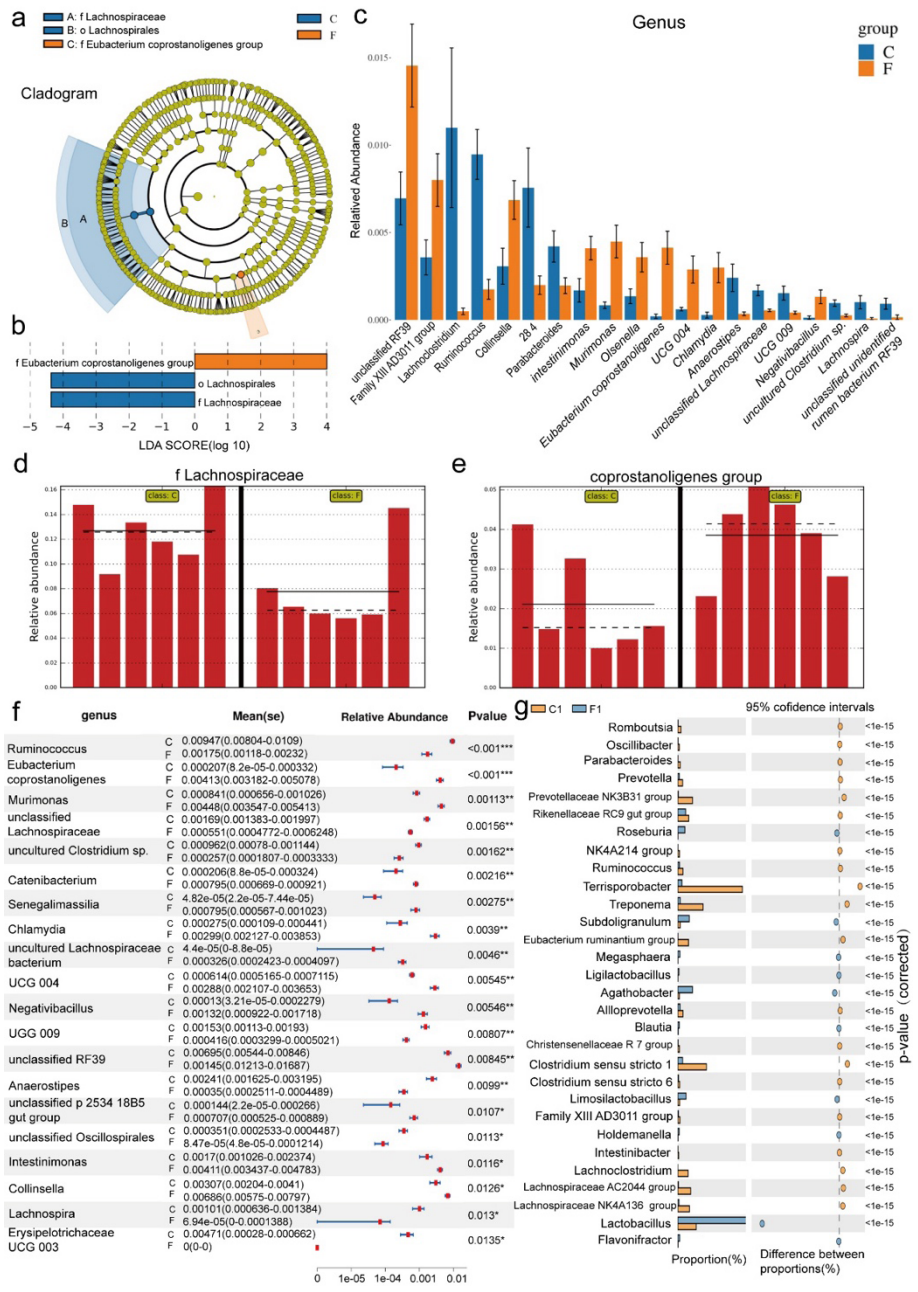

Fig 6. Analysis of differential bacterial genus abundance. **a)** LEfSe analysis results and corresponding phylogenetic tree, **b)** Histogram of LDA scores (log10) for taxonomic units with significant intergroup abundance differences, **c)** Relative abundance bar chart of the top 20 genera with significant differences between groups C and F, **d, e)** Inter-group relative abundance comparisons for *Lactobacillus* (d) and *Coprosterolus* (e), **f)** Metastats analysis results, **g)** STAMP analysis

pig's gut microbiota to intestinal environmental dysbiosis and inflammation after the onset of diarrheal symptoms. Furthermore, the diarrheal group showed upregulated abundance of functional genes related to carbohydrate metabolism, suggesting significant changes in the intestinal environment and that the microbiota influenced changes in carbohydrate metabolism. Compositional and functional analysis of the dominant phyla indicated that these changes primarily originated from *Acidobaceriota*, *Actinobacteriota*, and *Bacteroidota* (*Fig. 8-b*).

FAPROTAX functional annotation further confirmed these findings. Fermentation and chemoheterophy-related processes were significantly enhanced in the diarrhea group. In contrast, the healthy group exhibited more stable functions, but showed stronger expression in xylanolysis-related processes (*Fig. 8-c*). BugBase phenotypic prediction revealed an increase in aerobic and gram-negative bacteria in the diarrhea group, particularly potentially pathogenic bacteria, indicating a significant increase. This suggests that the hypoxic environment of the gut alters after diarrhea, affecting gut microbiota

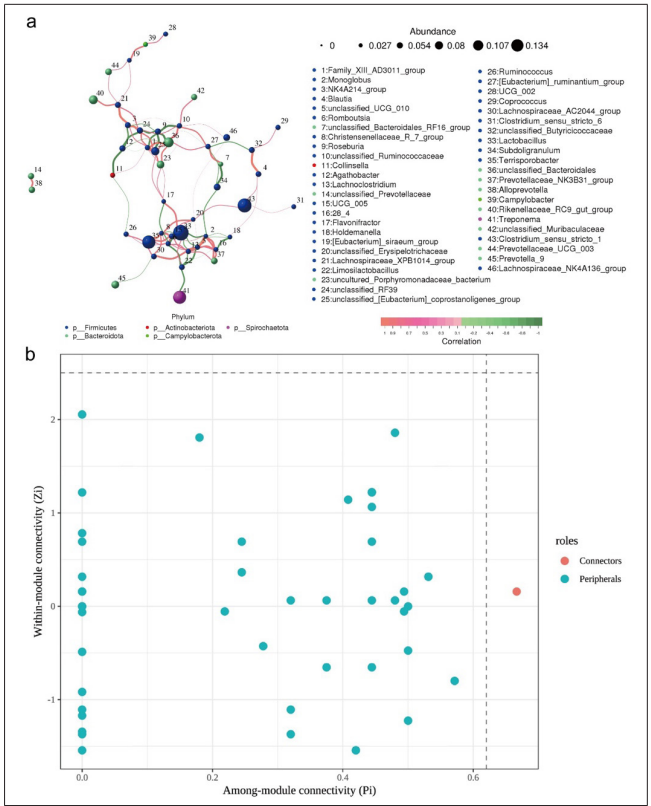

Fig 7. Co-occurrence network analysis and topological role classification of gut microbial species. **a)** Microbial co-occurrence network derived from Spearman's correlation analysis. Nodes represent microbial genera, with size indicating average abundance. Edges denote significant correlations ($|\rho| > 0.6$, $P < 0.05$), **b)** Z-P plot classifying topological roles based on intra-module connectivity (Zi) and inter-module connectivity (Pi). Nodes are categorised as connectors (high Pi, red) and peripheral nodes (low Pi, blue)

metabolism. Conversely, the healthy group showed a higher abundance of anaerobic bacteria, which can indicate the homeostatic balance of the gut microbiota *(Fig. 8-d, e)*.

Discussion

This study used 16S rRNA gene sequencing technology to comprehensively characterize the changes in the gut microbiota of healthy and diarrheal Tibetan pigs. The results showed significant differences in the composition, diversity, and functional potential of the gut microbiota between the two groups, indicating that diarrhea significantly remodels the gut microbiota. These findings are consistent with previous reports on the association between intestinal diseases and dysbiosis in pigs and other mammals [26-30].

Analysis of α- and β-diversity of the gut microbiota in Tibetan pigs revealed a significant decrease in the number of gut microbiota communities and a decreasing trend in community complexity, which were significantly different from healthy pigs. Decreased α-diversity is typically associated with gut ecosystem dysbiosis, decreased resistance to beneficial bacteria colonization, and increased susceptibility to pathogens [26,31]. While previous studies suggest external factors may perturb the microenvironment and trigger dysbiosis [32], it is highly plausible that this relationship is bidirectional. The rapid intestinal transit and excessive fluid secretion during diarrheal episodes can mechanically flush out commensal bacteria, further driving the loss of diversity. Compared to the diarrhea group, the healthy group exhibited a richer and more homogeneous gut microbiota composition, likely due to its larger and more stable population, stronger resilience to external factors, and greater capacity to repair the effects of external factors on the gut [33].

Taxonomic analysis showed that both groups were dominated by *Firmicutes* and *Bacteroidetes,* consistent with previous findings on porcine gut microbiota [34-36]. However, *Firmicutes* abundance was higher in the healthy group, while *Spirochetes* abundance was lower in the diarrhea group. At the genus level, *Terrisporobacter mayombei* and other bacteria were dominant in the healthy group, while *Porphyromonadaceae* and *Bacteroidales* showed significant aggregation in the gut of diarrheal pigs. Interestingly, *Lactobacillus amylovorus* also showed an unexpected increasing trend in diarrheal pigs. Rather than a simple "compensatory increase", this proliferation can be explained by its strong amylolytic capacity. During diarrhea, the impaired absorptive function of the small intestine often allows undigested carbohydrates, such as starches, to reach the hindgut. This nutrient influx provides an ideal substrate for *L. amylovorus*, driving its opportunistic overgrowth. Consequently, excessive fermentation by this species can lead to the accumulation of lactic acid, potentially causing hindgut acidosis and exacerbating osmotic diarrhea [37,38]. These changes in gut microbiota may suggest that diarrhea is related to the proliferation of harmful bacteria that cause inflammation or the reduction of beneficial bacteria such as *Lactobacillus* that can maintain gut microbiota balance. This may lead to damage to intestinal epithelial tissue and immune system dysregulation [39,40], resulting in the invasion and colonization of opportunistic pathogens. Therefore, specific gut microbiota, especially *Lactobacillus* and related bacteria, can serve as biomarkers of gut health in Tibetan pigs, and the increase of *Subdoligranulum* and related bacteria may indicate the occurrence of inflammation, possibly reflecting gut microbiota dysregulation associated with diarrhea [41]. Co-occurrence network analysis supports this explanation. Some important nodes appeared in the microbial network, with closer connections and more obvious interactions with other microbiota. Among them, *Lactobacillus*, as mentioned above, had the highest connectivity in the shared network, indicating that it is a key species in the gut of Tibetan pigs. This species may serve as an indicator of gut health and homeostasis in Tibetan pigs, and it may also exchange metabolites with other

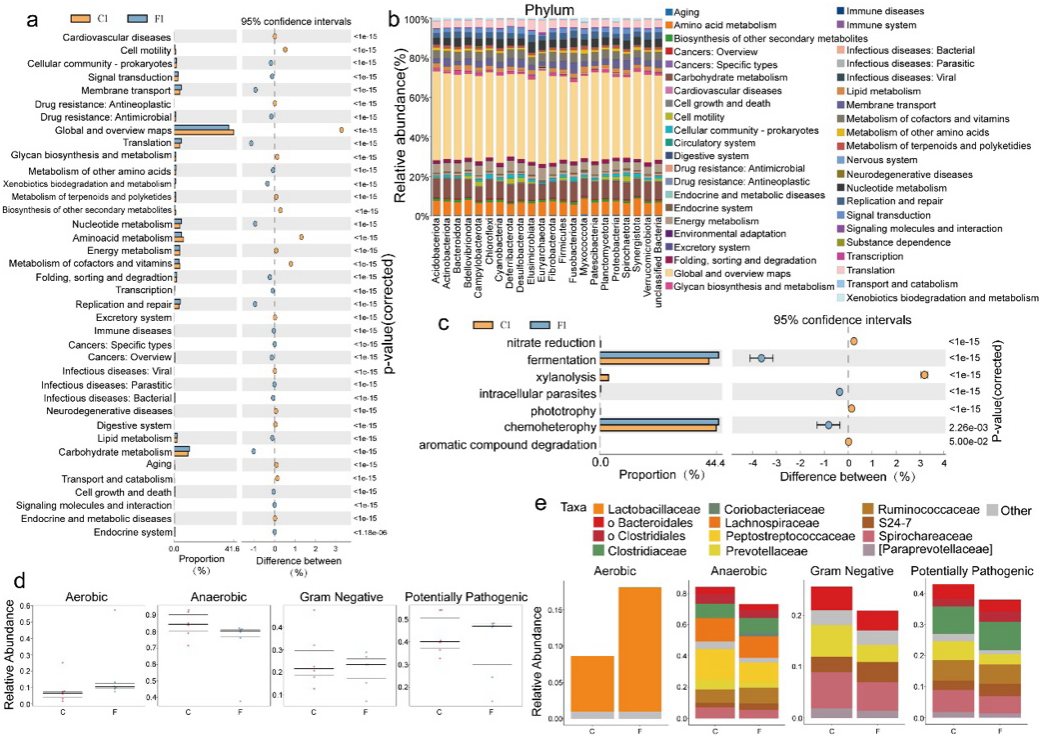

Fig 8. Gut microbiota functional prediction by PICRUSt2 and FAPROTAX. **a)** Differences in abundance of PICRUSt2-predicted KEGG level-2 functional pathways, **b)** PICRUSt2 KEGG level-2 functional composition profile, **c)** FAPROTAX-predicted functional features, **d)** BugBase predictions, **e)** Comparison of BugBase-predicted microbial phenotypes across samples using bar charts and differential plots

microbial communities in the gut, potentially reflecting the synergistic effect of *Lactobacillus* in the Tibetan pig gut and its resistance to external interference[26].

Differential abundance analysis using LEfSe and Metastats further identified several key taxa associated with specific groups. We found that the enrichment of *Lachnospiracea, Lactobacillus,* and *Ruminococcus* in healthy pigs indicated a functional protective role of the microbiome [42-44], while the significantly increased *Eubacterium coprostanoligenes* in the gut of diarrheal Tibetan pigs suggested a close relationship with diarrhea. Notably, *Eubacterium coprostanoligenes* has been found to be associated with lipid metabolism and pro-inflammatory states [45,46], and other elevated proportions of certain microbial communities in the gut of diarrheal Tibetan pigs have also been associated with intestinal barrier dysfunction and intestinal inflammation [47]. These results suggest that key taxa, such as *Lactobacillus,* may serve as microbial biomarkers for the intestinal health or disease progression of Tibetan pigs in future research.

Functional predictions further confirmed the biological significance of these taxonomic changes. Pathway enrichment in diarrheal Tibetan pigs was associated with membrane transport, translation, nucleotide metabolism, and replication and repair processes, indicating that Tibetan pigs have begun to develop repair mechanisms to combat the disordered intestinal environment under diarrheal conditions [48,49]. Furthermore, the fermentation potential in the intestines of diarrheal Tibetan pigs was also increased, possibly related to a significant increase in fermentative microbiota. This enhanced fermentation capacity may lead to excessive production of organic acids or gases, thereby exacerbating diarrhea symptoms [50]. In contrast, healthy Tibetan pigs exhibited enhanced pathways related to amino acid and vitamin metabolism, suggesting that the gut microbiota of healthy Tibetan pigs plays an indispensable role in maintaining intestinal microecological homeostasis [40]. BugBase predictions highlighted an increase in Gram-negative bacteria and potentially pathogenic bacterial phenotypes in diarrheal pigs, which may exacerbate fluctuations in the intestinal microbiota, potentially exacerbating intestinal inflammation and promoting diarrhea [51]. In summary, these results indicate that diarrhea in Tibetan pigs is characterized not only by altered gut microbiota composition but also by significant metabolic and phenotypic changes. These alterations suggest an intricate interplay where dysbiosis and inflammation may mutually exacerbate diarrheal symptoms. Identified functional pathways, particularly those involved in membrane transport, fermentation, and processes related to potential pathogens, may serve as key indicators or therapeutic targets for managing gut microbiota dysbiosis in high-altitude local pig breeds.

In summary, the findings indicate multifaceted dysbiosis in the gut microbiota of diarrhea-prone Tibetan pigs, characterized by reduced ecological diversity and stability, decreased probiotic counts, increased potential pathogenic bacteria, and a shift towards intestinal barrier disruption and inflammatory damage. While such changes have been observed in other species [52,53], Tibetan pigs living at high altitudes require further investigation due to their unique environmental adaptability and disease resistance. Importantly, given the cross-sectional design of this study, we cannot definitively establish a causal direction between gut dysbiosis and diarrhea. It is highly likely that the observed microbial alterations are, at least in part, a consequence of the diarrheal environment (e.g., increased gut motility and luminal wash-out) rather than the sole primary cause. Therefore, longitudinal studies or fecal microbiota transplantation (FMT) models are needed to track microbial succession and determine causality. Additionally, the specific duration and severity of diarrhea prior to sampling were not incorporated as continuous variables in the current evaluation criteria, which limits our understanding of the temporal dynamics of dysbiosis during disease progression. Furthermore, the lack of measurement of host physiological parameters limits our ability to investigate the mechanisms of host-microbiota interactions. Finally, the limited capabilities of 16S rRNA sequencing suggest that functional inferences may require further validation through metabolomics analysis. Despite these limitations, this study comprehensively explores the associations between gut microbiota changes and diarrhea in Tibetan pigs, focusing on candidate biomarkers and therapeutic targets. These findings lay the foundation for future microbial therapies such as probiotic supplementation or fecal microbiota transplantation, which could help reduce the incidence of digestive diseases in high-altitude livestock farming and thus improve animal health.

This study employed 16S rRNA gene sequencing to comprehensively characterize the gut microbiota of healthy and diarrheal Tibetan pigs. Diarrhea was associated with significantly reduced microbial richness and diversity, altered community structure, and an increased abundance of potentially pathogenic and pro-inflammatory bacteria, particularly *Eubacterium coprostanoligenes*. In contrast, healthy pigs harbored a higher proportion of beneficial genera such as *Lactobacillus*, which contribute to gut microbiota balance and intestinal barrier integrity. Functionally, the diarrheal microbiota exhibited enhanced fermentation capacity and elevated pathogenicity potential. These findings demonstrate that gut microbiota dysbiosis plays a critical role in the pathogenesis of diarrhea in Tibetan pigs and identify potential microbial biomarkers for diagnosis and intervention. This study provides a foundation for developing microbiome-based strategies to improve gut health in Tibetan pigs, particularly in high-altitude pastoral environments.

Declarations

Availability of Data and Materials: The datasets used and/or analyzed during the current study are available from the corresponding authors (ZH, LY) on reasonable request.

Financial Support: This research was supported by the Science and Technology Projects of Xizang Autonomous Region (XZ202401YD0005), Science and Technology Projects of Xizang Autonomous Region (XZ202501ZY0143; XZ202501ZY0147), National Key R&D Program (2022YFD1600904), and Science and Technology Program of Linzhi (XDHZ-2025-02).

Ethical Approval: All animal experiments were reviewed and approved by the Animal Ethics Committee of South China Agricultural University (approval number: 2024A637), and conducted in accordance with the institutional guidelines for the care and use of laboratory animals.

Conflict of Interest: The authors have no relevant financial or non-financial interests to disclose.

Declaration of Generative Artificial Intelligence (AI): The authors declare that the article, tables and figures were not written/created by AI and AI-assisted Technologies.

Author Contributions: Y: Writing-reviewing and editing; writing-drafting; methodology; conception. L, G, H , M and L: methodology; investigation. L: writing-reviewing-editing; supervision. Z and C: supervision; funding acquisition; conceptualization; funding acquisition; conceptualization.

References

1. **Shang P, Li W, Tan Z, Zhang J, Dong S, Wang K, Chamba Y:** Population genetic analysis of ten geographically isolated Tibetan pig populations. *Animals (Basel),* 10 (8):1297, 2020. DOI: 10.3390/ani10081297
2. **Zhang B, Chamba Y, Shang P, Wang Z, Ma J, Wang L, Zhang H:** Comparative transcriptomic and proteomic analyses provide insights into the key genes involved in high-altitude adaptation in the Tibetan pig. *Sci Rep,* 7 (1):3654, 2017. DOI: 10.1038/s41598-017-03976-3
3. **Li M, Tian S, Jin L, Zhou G, Li Y, Zhang Y, Wang T, Yeung CKL, Chen L, Ma J, Zhang J, Jiang A, Li J, Zhou C, Zhang J, Liu Y, Sun X, Zhao H, Niu Z, Lou P, Xian L, Shen X, Liu S, Zhang S, Zhang M, Zhu L, Shuai S, Bai L, Tang G, Liu H, Jiang Y, Mai M, Xiao J, Wang X, Zhou Q, Wang Z, Stothard P, Xue M, Gao X, Luo Z, Gu Y, Zhu H, Hu X, Zhao Y, Plastow GS, Wang J, Jiang Z, Li K, Li N, Li X, Li R:** Genomic analyses identify distinct patterns of selection in domesticated pigs and Tibetan wild boars. *Nat Genet,* 45 (12): 1431-1438, 2013. DOI: 10.1038/ng.2811
4. **Chen X:** Molecular epidemiological investigation of *Cryptosporidium* sp., *Giardia duodenalis, Enterocytozoon bieneusi* and *Blastocystis* sp. infection in free-ranged yaks and Tibetan pigs on the plateau. *The Pak Vet J,* 42 (4): 533-539, 2022. DOI: 10.29261/pakvetj/2022.060
5. **Qin S, Hu C, Yang D, Wu J, Yue H, Tang C, Zhang B:** Emergence of porcine epidemic diarrhea viruses with the novel S genes in Tibetan pigs in the Qinghai-Tibetan plateau in China. *Virus Res,* 270:197652, 2019. DOI: 10.1016/j.virusres.2019.197652
6. **Wu Q, Zhang H, Dong H, Mehmood K, Chang Z, Li K, Liu S, Rehman MU, Nabi F, Javed MT, Zhu H, Li J:** Seroprevalence and risk factors associated with *Pseudorabies* virus infection in Tibetan pigs in Tibet. *BMC Vet Res,* 14 (1):347, 2018. DOI: 10.1186/s12917-018-1347-x

7. **Li M, Pan Y, Xi Y, Wang M, Zeng Q:** Insights and progress on epidemic characteristics, genotyping, and preventive measures of PEDV in China: A review. *Microb Pathog,* 181:106185, 2023. DOI: 10.1016/j.micpath.2023.106185
8. **Tao S, Zou H, Li J, Wei H:** Landscapes of enteric virome signatures in early-weaned piglets. *Microbiol Spectr,* 10 (4):e01698-22, 2022. DOI: 10.1128/spectrum.01698-22
9. **Kongsted H, Pedersen K, Hjulsager CK, Larsen LE, Pedersen KS, Jorsal SE, Kbo PB:** Diarrhoea in neonatal piglets: A case control study on microbiological findings. *Porcine Health Manag,* 4 (1):17, 2018. DOI: 10.1186/s40813-018-0094-5
10. **Xu J, Andrani M, Rup RBDK, Dalgaard TSR, Eriksen C, Laustsen AH, Brix S, Thrane SW, Canibe N:** In-feed provision of binding proteins sustains piglet gut health and mitigates ETEC-induced post-weaning diarrhea. *J Anim Sci Biotechnol,* 16 (1):18, 2025. DOI: 10.1186/s40104-025-01209-6
11. **Tang Q, Lan T, Zhou C, Gao J, Wu L, Wei H, Li W, Tang Z, Tang W, Diao H, Xu Y, Peng X, Pang J, Zhao X, Sun Z:** Nutrition strategies to control post-weaning diarrhea of piglets: From the perspective of feeds. *Anim Nutr,* 17 (2): 297-311, 2024. DOI: 10.1016/j.aninu.2024.03.006
12. **Duarte ME, Kim SW:** Intestinal microbiota and its interaction to intestinal health in nursery pigs. *Anim Nutr,* 8, 169-184, 2022. DOI: 10.1016/j.aninu.2021.05.001
13. **Shi N, Li N, Duan X, Niu H:** Interaction between the gut microbiome and mucosal immune system. *Mil Medl Res,* 4 (1):14, 2017. DOI: 10.1186/s40779-017-0122-9
14. **Li Q, de Oliveira Formiga R, Puchois V, Creusot L, Ahmad AH, Amouyal S, Campos-Ribeiro MA, Zhao Y, Harris DMM, Lasserre F, Ellero-Simatos S, Guillou H, Huang Z, Brot L, Hu Y, Chollet L, Danne C, Scandola C, Ledent T, Chevreux G, Arguello RJ, De Carvalho Bittencourt M, Bettinger J, D'Aveni-Piney M, Moulin D, Schreiber S, Aden K, Rolhion N, Michel M-L, Wai T, Sokol H:** Microbial metabolite indole-3-propionic acid drives mitochondrial respiration in CD4(+) T cells to confer protection against intestinal inflammation. *Nat Metab,* 7 (12): 2510-2530 2025. DOI: 10.1038/s42255-025-01396-6
15. **Li N, Wang H, Zhao H, Wang M, Cai J, Hao Y, Yu J, Jiang Y, Lu X, Liu B:** Cooperative interactions between *Veillonella ratti* and *Lactobacillus acidophilus* ameliorate DSS-induced ulcerative colitis in mice. *Food Funct,* 14 (23): 10475-10492, 2023. DOI: 10.1039/d3fo03898j
16. **Wang D, Zeng J, Wujin C, Ullah Q, Su Z:** Lactobacillus reuteri derived from horse alleviates Escherichia coli-induced diarrhea by modulating gut microbiota. *Microb Pathog,* 188:106541, 2024. DOI: 10.1016/j.micpath.2024.106541
17. **Lv J, Lang G, Wang Q, Zhao W, Shi D, Zhou Z, Shen Y, Xia H, Han S, Li L:** *Lactobacillus helveticus* attenuates alcoholic liver injury via regulation of gut microecology in mice. *Microb Biotechnol,* 17 (10):e70016, 2024. DOI: 10.1111/1751-7915.70016
18. **Cheng J, Laitila A, Ouwehand AC:** *Bifidobacterium animalis* subsp. *lactis* HN019 Effects on gut health: A review. *Front Nutr,* 8:790561, 2021. DOI: 10.3389/fnut.2021.790561
19. **Moeser AJ, Pohl CS, Rajput M:** Weaning stress and gastrointestinal barrier development: Implications for lifelong gut health in pigs. *Anim Nutr,* 3 (4): 313-321, 2017. DOI: 10.1016/j.aninu.2017.06.003
20. **Ali M, Xu C, Hina Q, Li A, Li K:** Interrelations between probiotics, gut microbiota, intestinal barrier, and immune response: Focusing on diarrhea in dairy calves. *J Integr Agric,* 25 (1): 16-29, 2026. DOI: 10.1016/j.jia.2024.05.022
21. **Rodríguez C, Romero E, Garrido-Sanchez L, Alcaín-Martínez G, Andrade R, Taminiau B, Daube G, García-Fuentes E:** Microbiota insights in clostridium difficile infection and inflammatory bowel disease. *Gut Microbes,* 12 (1):1725220, 2020. DOI: 10.1080/19490976.2020.1725220
22. **Bin P, Tang Z, Liu S, Chen S, Xia Y, Liu J, Wu H, Zhu G:** Intestinal microbiota mediates enterotoxigenic *Escherichia coli*-induced diarrhea in piglets. *BMC Vet Res,* 14 (1):385, 2018. DOI: 10.1186/s12917-018-1704-9
23. **Soliani L, Rugna G, Prosperi A, Chiapponi C, Luppi A:** *Salmonella* infection in pigs: Disease, prevalence, and a link between swine and human health. *Pathogens,* 12 (10):1267, 2023. DOI: 10.3390/pathogens12101267
24. **Han D, Gao P, Li R, Tan P, Xie J, Zhang R, Li J:** Multicenter assessment of microbial community profiling using 16S rRNA gene sequencing and shotgun metagenomic sequencing. *J Adv Res,* 26, 111-121, 2020. DOI: 10.1016/j.jare.2020.07.010
25. **Maheshwari K, Musyuni P, Moulick A, Mishra H, Ekielski A, Mishra PK, Aggarwal G:** Unveiling the microbial symphony: Next-gen sequencing and bioinformatics insights into the human gut microbiome. *Health Sci Rev,* 11:100173, 2024. DOI: 10.1016/j.hsr.2024.100173
26. **Wu Z, Li X, Wang Y, Zhang J, Ji L, Gan L:** Microbiome analysis reveals gut bacterial alterations in adult Tibetan pigs with diarrhea. *Front Microbiol,* 16:1524727, 2025. DOI: 10.3389/fmicb.2025.1524727
27. **Zhong W, Liu R, Lan R, Chen J, Tian J-B, Wang R, Wang D, Yin C:** Potential Negative Impact of *Actinobacteria* Phylum on Middle-Aged Equines Based on 16s rDNA Analysis.*Pak Vet J*, 44(4):1215-1222, 2024.
28. **Wang M, Gao Y, Li Y, Peng K, Sun X, Xu X, Li R and Wang Z:** A Resistome Profiling and Microbiome Analysis in Zoo Animals: Uncovering Hidden Threatsto Public Health. *Pak Vet J*, 45 (2):880-886, 2025. DOI: 10.29261/pakvetj/2025.175
29. **Bai H, Liu T, Wang S, Gong W, Shen L, Zhang S, Wang Z:** Identification of gut microbiome and metabolites associated with acute diarrhea in cats. *Microbiol Spectr,* 11 (4):e0059023, 2023. DOI: 10.1128/spectrum.00590-23
30. **Yan Z, Zhang K, Zhang K, Wang G, Wang L, Zhang J, Qiu Z, Guo Z, Song X, Li J:** Integrated 16S rDNA gene sequencing and untargeted metabolomics analyses to investigate the gut microbial composition and plasma metabolic phenotype in calves with dampness-heat diarrhea. *Front Vet Sci,* 9:703051, 2022. DOI: 10.3389/fvets.2022.703051
31. **Li A, Liu B, Li F, He Y, Wang L, Fakhar-E-Alam Kulyar M, Li H, Fu Y, Zhu H, Wang Y, Jiang X:** Integrated bacterial and fungal diversity analysis reveals the gut microbial alterations in diarrheic giraffes. *Front Microbiol,* 12:712092, 2021. DOI: 10.3389/fmicb.2021.712092
32. **Li Y, Xia S, Jiang X, Feng C, Gong S, Ma J, Fang Z, Yin J, Yin Y:** Gut microbiota and diarrhea: An updated review. *Front Cell Infect Microbiol,* 11:625210, 2021. DOI: 10.3389/fcimb.2021.625210
33. **Pires L, Gonzalez-Paramás AM, Heleno SA, Calhelha RC:** Gut microbiota as an endocrine organ: Unveiling its role in human physiology and health. *Appl Sci,* 14 (20):9383, 2024. DOI: 10.3390/app14209383
34. **Ren W, Yu B, Yu J, Zheng P, Huang Z, Luo J, Mao X, He J, Yan H, Wu J, Chen D, Luo Y:** Lower abundance of *Bacteroides* and metabolic dysfunction are highly associated with the post-weaning diarrhea in piglets. *Sci China Life Sci,* 65 (10): 2062-2075, 2022. DOI: 10.1007/s11427-021-2068-6
35. **Wang M, Zheng H, Wang S, Luo H, Li Z, Song X, Xu H, Li P, Sun S, Wang Y, Yuan Z:** Comparative analysis of changes in diarrhea and gut microbiota in Beigang pigs. *Microb Pathog,* 185:106441, 2023. DOI: 10.1016/j.micpath.2023.106441
36. **Zheng X, Xu L, Tang Q, Shi K, Wang Z, Shi L, Ding Y, Yin Z, Zhang X:** Integrated metagenomic and metabolomics profiling reveals key gut microbiota and metabolites associated with weaning stress in piglets. *Genes,* 15 (8):970, 2024. DOI: 10.3390/genes15080970
37. **Jing Y, Mu C, Wang H, Shen J, Zoetendal EG, Zhu W:** Amino acid utilization allows intestinal dominance of Lactobacillus amylovorus. *ISME J,* 16 (11): 2491-2502, 2022. DOI: 10.1038/s41396-022-01287-8
38. **Fassarella M, Blaak EE, Penders J, Nauta A, Smidt H, Zoetendal EG:** Gut microbiome stability and resilience: Elucidating the response to perturbations in order to modulate gut health. *Gut,* 70 (3): 595-605, 2021. DOI: 10.1136/gutjnl-2020-321747
39. **Panah FM, Lauridsen C, Jberg OH, Jensen HE, Nielsen TS:** Composition of mucus- and digesta-associated bacteria in growing pigs with and without diarrhea differed according to the presence of colonic inflammation. *BMC Microbiol,* 23 (1):287, 2023. DOI: 10.1186/s12866-023-02874-1

40. **Venegas DP, De la Fuente MK, Landskron G, González MJ, Quera R, Dijkstra G, Harmsen HJM, Faber KN, Hermoso MA:** Short chain fatty acids (SCFAs)-mediated gut epithelial and immune regulation and its relevance for inflammatory bowel diseases. *Front Immunol,* 10:277, 2019. DOI: 10.3389/fimmu.2019.00277

41. **Niu H, Feng XZ, Shi CW, Zhang D, Chen HL, Huang HB, Jiang YL, Wang JZ, Cao X, Wang N, Zeng Y, Yang GL, Yang WT, Wang CF:** Gut bacterial composition and functional potential of tibetan pigs under semi-grazing. *Front Microbiol,* 13:850687, 2022. DOI: 10.3389/fmicb.2022.850687

42. **Zaplana T, Miele S, Tolonen AC:** *Lachnospiraceae* are emerging industrial biocatalysts and biotherapeutics. *Front Bioeng Biotechnol,* 11:1324396, 2024. DOI: 10.3389/fbioe.2023.1324396

43. **Crost EH, Tailford LE, Monestier M, Swarbreck D, Henrissat B, Crossman LC, Juge N:** The mucin-degradation strategy of *Ruminococcus gnavus*: The importance of intramolecular *trans*-sialidases. *Gut Microbes,* 7 (4): 302-312, 2016. DOI: 10.1080/19490976.2016.1186334

44. **Ring KK, Just S, Lagkouvardos I, Hanske L, Haller D, Blaut M, Wenning M, Clavel T:** Murimonas intestini gen. nov., sp. nov., an acetate-producing bacterium of the family *Lachnospiraceae* isolated from the mouse gut. *Int J Syst Evol Microbiol,* 65 (3): 870-878, 2015. DOI: 10.1099/ijs.0.000030

45. **Bai D, Zhao J, Wang R, Du J, Zhou C, Gu C, Wang Y, Zhang L, Zhao Y, Lu N:** Eubacterium coprostanoligenes alleviates chemotherapy-induced intestinal mucositis by enhancing intestinal mucus barrier. *Acta Pharm Sin B,* 14 (4): 1677-1692, 2024. DOI: 10.1016/j.apsb.2023.12.015

46. **Wei W, Jiang W, Tian Z, Wu H, Ning H, Yan G, Zhang Z, Li Z, Dong F, Sun Y, Li Y, Han T, Wang M, Sun C:** Fecal *g. Streptococcus and g. Eubacterium_coprostanoligenes_group* combined with sphingosine to modulate the serum dyslipidemia in high-fat diet mice. *Clin Nutr,* 40 (6): 4234-4245, 2021. DOI: 10.1016/j.clnu.2021.01.031

47. **Chen C, Fang S, Wei H, He M, Fu H, Xiong X, Zhou Y, Wu J, Gao J, Yang H, Huang L:** Prevotella copri increases fat accumulation in pigs fed with formula diets. *Microbiome,* 9 (1):110, 2021. DOI: 10.1186/s40168-021-01110-0

48. **Hoque KM, Chakraborty S, Sheikh IA, Woodward OM:** New advances in the pathophysiology of intestinal ion transport and barrier function in diarrhea and the impact on therapy. *Expert Rev Anti Infect Ther,* 10 (6): 687-699, 2012. DOI: 10.1586/eri.12.47

49. **Hodges K, Gill R:** Infectious diarrhea: Cellular and molecular mechanisms. *Gut Microbes,* 1 (1): 4-21, 2010. DOI: 10.4161/gmic.1.1.11036

50. **Mortensen PB, Clausen MR:** Short-chain fatty acids in the human colon: Relation to gastrointestinal health and disease. *Scand J Gastroenterol,* 216, 132-148, 1996. DOI: 10.3109/00365529609094568

51. **Zhang Y, Ma Y, Qi Y:** Potential relationship between gut microbiota and animal diarrhea: A systematic review. *Front Microbiol,* 16:1637331, 2025. DOI: 10.3389/fmicb.2025.1637331

52. **Camilleri M:** Human intestinal barrier: Effects of stressors, diet, prebiotics, and probiotics. *Clin Transl Gastroenterol,* 12 (1):e00308, 2021. DOI: 10.14309/ctg.0000000000000308

53. **Serek P, Oleksy-Wawrzyniak M:** The effect of bacterial infections, probiotics and zonulin on intestinal barrier integrity. *Int J Mol Sci,* 22 (21):11359, 2021. DOI: 10.3390/ijms222111359

Kafkas Universitesi Veteriner Fakultesi Dergisi
Journal Home-Page: http://vetdergikafkas.org
E-ISSN: 1309-2251

Kafkas Univ Vet Fak Derg
32 (2): 275-280, 2026
DOI: 10.9775/kvfd.2026.36026

RESEARCH ARTICLE

Red Blood Cell Distribution Width in Cats with Chronic Kidney Disease: A Retrospective Study

Şahin AKYÜZ [1 (*)], Mustafa KABU [1]

[1] Afyon Kocatepe University, Faculty of Veterinary Medicine, Department of Internal Medicine, TR-03200 Afyonkarahisar - TÜRKİYE

[(*)] **Corresponding author:**
Şahin Akyüz
Phone: +90 541 272 08 30
E-mail: vetnephrology@gmail.com

How to cite this article?

Akyüz Ş, Kabu M: Red Blood Cell Distribution Width in Cats with Chronic Kidney Disease: A Retrospective Study. *Kafkas Univ Vet Fak Derg*, 32 (2): 275-280, 2026.
DOI: 10.9775/kvfd.2025.36026

Article ID: KVFD-2026-36026
Received: 05.01.2026
Accepted: 17.03.2026
Published Online: 02.04.2026

Abstract

Chronic kidney disease (CKD) is one of the commonly observed progressive diseases in cats. Red blood cell distribution width (RDW) is a parameter that reflects variability in erythrocyte size. Recently, RDW has been shown to have potential value as a biomarker for disease severity and progression in various conditions in both human and veterinary medicine; however, information regarding its clinical significance in feline CKD remains limited. The aim of this study was to compare RDW values among cats with CKD, acute-on-chronic kidney disease, and healthy cats and to evaluate the relationship between RDW and hematological and biochemical parameters. In this study, cats with CKD, AOC, and healthy cats presented to our clinic between 2022 and 2025 were retrospectively evaluated. Cats with any concurrent endocrine, neoplastic, or infectious diseases were excluded from the study. Cats with CKD were divided into three groups: early-stage kidney disease (IRIS stages 1 and 2), advanced-stage kidney disease (IRIS stages 3 and 4), and acute on chronic kidney disease (AOC). Hematological, biochemical, and ultrasonographic findings were evaluated. One-way analysis of variance (ANOVA) and Pearson correlation analysis were performed. No significant relationships were detected between RDW and SDMA, UPC, BUN, or phosphorus (PHOS) among the study groups. Only a borderline negative correlation was identified between RDW and serum creatinine concentration (r=−0.216; P=0.050). In conclusion, although RDW may be used in other diseases or in human medicine, it does not appear to be a reliable marker for determining disease progression in feline CKD.

Keywords: Cat, Chronic kidney disease, Acute-on-chronic kidney disease, RDW

Introduction

Chronic kidney disease (CKD) is one of the most common diseases in cats. CKD is defined as the presence of structural and functional abnormalities in one or both kidneys persisting for more than three months. The International Renal Interest Society (IRIS) has established classification criteria based on creatinine and SDMA values in stable kidney patients. These classification criteria are used both therapeutically and prognostically [1]. CKD can be observed at any age; however, its prevalence is generally higher in older cats compared to younger ones. A previous study reported that approximately 63% of cats with kidney disease were over 10 years of age, while 37% were under 10 years of age [2]. CKD is a progressive disorder characterized by ongoing nephron loss over time [3]. Proteinuria, anemia, hypertension, hyperphosphatemia, and acute on chronic kidney disease (AOC) are considered to be associated with the progression of chronic kidney damage [4].

Acute on chronic kidney disease (AOC) can be defined as an episodic decrease in glomerular filtration rate (GFR) resulting from renal injury (prerenal, renal, or postrenal) in a cat with pre-existing chronic kidney damage. It is frequently characterized by acute renal parenchymal injury and a decline in renal function. The prognosis of acute kidney injury is influenced by multiple factors, including etiology, severity of injury, availability of treatment options (e.g., hemodialysis), and owner compliance [5].

An increase in red blood cell distribution width (RDW), expressed as a percentage, is a common indicator of heterogeneity in red blood cell (RBC) size and is reported as part of a complete blood count. RDW is calculated by dividing the standard deviation of mean cell volume by the mean corpuscular volume (MCV) [6,7]. An increase in RDW generally occurs due to a decrease in MCV or an increase in RBC size [8].

The association between high RDW and renal impairment

is multifactorial. According to studies in human cohorts, chronic inflammation suppresses erythropoiesis, while oxidative stress leads to premature erythrocyte destruction [9-11]. Furthermore, inflammation induced hepcidin elevation in CKD patients disrupts iron metabolism, a process that inherently increases RDW values [12].

Recently, increased RDW has been used as a prognostic factor [13,14]. One study demonstrated that an increased RDW value was associated with higher mortality in hospitalized dogs [15]. Another study conducted in humans showed that increased RDW was independently associated with the progression of CKD. These findings suggest that RDW has prognostic value and may be an indicator of CKD progression [16].

The aim of this study was to compare RDW values among cats with CKD, acute on chronic kidney disease, and healthy controls and to evaluate the relationship between RDW and hematological and biochemical parameters.

We hypothesized that RDW values would be higher in cats with CKD and acute on chronic kidney disease and that RDW would be associated with selected hematological and biochemical parameters.

Material and Methods

Ethical Statement

The Afyon Kocatepe University Local Ethics Committee for Animal Experiments determined that ethical committee approval was not required, as this was a retrospective study. (Approval no: 49533702/354).

A total of 95 medical records of cats presented to the clinic between 2022 and 2025 were screened for eligibility. Following application of the predefined exclusion criteria, 12 cats were excluded from the study, including 7 with heart disease, 4 with infectious disease, and 1 that had received a blood transfusion within the previous three months. Ultimately, 83 cats were included in the final analysis: 12 healthy controls, 20 cats with early stage CKD (IRIS stages 1-2), 24 cats with advanced stage CKD (IRIS stages 3-4), and 27 cats with acute on chronic kidney disease (AOC).

For inclusion of cats with CKD, CKD diagnosis was established based on persistent azotemia (elevated serum creatinine concentration for at least three months) together with clinical and laboratory findings compatible with chronic kidney disease. These included decreased urine specific gravity (USG <1.035), increased SDMA concentration, and/or characteristic ultrasonographic changes such as increased renal cortical echogenicity and loss of corticomedullary differentiation. CKD staging was performed according to IRIS guidelines based primarily on serum creatinine concentrations obtained from clinically stable patients [17]. Urinalysis and ultrasonographic examination were performed as part of the diagnostic process in included cats. Cats with a positive urine culture, urinary tract obstruction, liver disease, heart disease, or infectious disease within the previous month were excluded from the study.

For the acute on chronic kidney disease (AOC) group, cats were considered eligible if they exhibited clinical signs consistent with acute kidney injury (anorexia, lethargy, vomiting), a >20% increase in creatinine concentration compared to previously classified values according to IRIS criteria, the presence of certain urinalysis markers (glycosuria with normoglycemia, cylindruria), and more than two characteristic findings on abdominal ultrasonography, such as increased renal cortical echogenicity and loss of corticomedullary differentiation [18].

Because RDW may be affected by concurrent conditions, cats with simultaneous systemic or endocrine diseases, neoplasia, or infectious diseases were excluded. Additionally, cats that had received a blood transfusion within the previous three months, had blood loss due to trauma, or had undergone recent surgical intervention were excluded from the study. These conditions were diagnosed through physical examination and laboratory and radiological methods [19].

Cats with CKD were divided into three groups: early stage kidney disease (IRIS stages 1 and 2), advanced stage kidney disease (IRIS stages 3 and 4), and acute on chronic kidney disease (AOC). For the control group, 12 healthy cats that presented for annual check-ups or had blood samples collected prior to neutering procedures were included. Hematological and biochemical analyses, urinalysis, and ultrasonographic evaluations were performed. Cats included in the control group were assessed for health parameters and confirmed to be within reference ranges, and only cats without evidence of infection were selected.

Hematological analysis results (complete blood count with leukocyte differential), biochemical profiles (serum urea, creatinine, total protein, albumin, total calcium, total phosphorus, alanine aminotransferase and alkaline phosphatase activities), and urinalysis results (dipstick analysis, microscopic examination of urinary sediment, urine specific gravity [USG], and urine protein to creatinine ratio [UPC]) were evaluated. However, only red blood cell count (RBC), hemoglobin concentration (HGB), hematocrit (HCT), urea, creatinine, USG, and UPC were reported and included in the statistical analysis for this study.

Blood parameters of cats in the CKD and control groups were measured using a hematology analyzer (IDEXX

ProCyte Dx), a biochemical analyzer and urine protein/creatinine ratio (UPC) using a biochemical analyzer (IDEXX Catalyst ONE), and urinalysis using a urine analyzer (IDEXX UA). Ultrasonographic examinations were performed using an ultrasound device (Philips Affiniti 70).

Statistical Analysis

Statistical analyses of the data obtained in this study were performed using IBM SPSS Statistics 26.0 software. Descriptive statistics included frequency (n) and percentage (%) for qualitative variables, and mean, standard deviation, minimum, and maximum values for quantitative variables. Data distribution was assessed using the Shapiro-Wilk test and homogeneity of variance was evaluated using Levene's test. Since the data followed a normal distribution, parametric tests (One-Way ANOVA and Pearson correlation) were employed. One-way analysis of variance (One-Way ANOVA) was used to evaluate differences among the groups (Control, AOC, IRIS 1-2, and IRIS 3-4). For variables showing statistically significant differences in ANOVA, the Duncan post hoc test was applied to determine intergroup differences. In addition, Pearson correlation analysis was performed to assess relationships between certain hematological and biochemical variables and SDMA, RDW, and creatinine levels. A P-value <0.05 was considered statistically significant in all analyses. Because this was a retrospective study, the sample size was determined by the number of eligible cases available in the medical records during the study period. Therefore, a priori sample size calculation was not performed.

Results

Demographic characteristics of cats, including sex distribution, age, and body weight, are summarized in *Table 1*.

No statistically significant differences were detected in RDW values among the study groups (P>0.05). When hematological and biochemical parameters evaluated among the control, AOC, IRIS 1-2, and IRIS 3-4 groups were examined, statistically significant differences were detected in HCT (%), LYM (%), MONO (%), MONO (K/uL), SDMA, creatinine (CREA), BUN, BUN/CREA ratio, phosphorus (PHOS), and UPC values (P<0.05). Significant differences were observed for HCT, LYM, MONO, SDMA, creatinine, BUN, phosphorus, and UPC values among the groups (P<0.05) *(Table 2)*. In contrast, no statistically significant differences were found for RBC, HGB, MCV, MCH, MCHC, RDW, RETIC, WBC, Neu, EOS, BAS, PLT, MPV, PDW, or PCT parameters (P>0.05). All results are presented in *Table 2*.

Table 1. *Distribution of sex, age and weight according to control, aoc and IRIS stages*

Variable		Groups			
Control		AOC	IRIS 1- 2	IRIS 3- 4	
Sex	Female	6 (50.0)	15 (55.6)	14 (70.0)	15 (62.5)
	Male	6(50.0)	12 (44.4)	6 (30.0)	9 (37.5)
Age (Year)		5.67±4.81 (1-15)	10.37±2.86 (5-16)	10.05±4.18 (3-18)	11.75±2.86 (6-16)
Weight (kg)		4.27±0.56 (3.5-5.2)	4.26±0.94 (2.65-6.1)	3.89±0.7 (2.35-5.5)	3.83±0.7 (2.5-5.5)

AOC: Acute on chronic kidney disease; IRIS: International renal interest society

According to correlation analysis, relationships between RDW values and hematological and biochemical parameters were evaluated. The analysis revealed a significant positive correlation only between RDW and red blood cell count (RBC) (R=0.439; P=0.000), indicating that increases in RDW were associated with increases in RBC count. A weak and borderline negative correlation was observed between RDW and creatinine (CREA) (R=−0.216; P=0.050), suggesting a slight tendency for creatinine levels to decrease as RDW increased; however, this relationship should be interpreted cautiously due to its borderline statistical significance. No significant correlations were found between RDW and SDMA, HCT, HGB, BUN, PHOS, or urine protein/creatinine ratio (UPC) (P>0.05). All data and results of the correlation analysis are presented in *Table 3*.

Discussion

In this retrospective study, RDW values were evaluated in cats diagnosed with chronic kidney disease at different stages and acute on chronic kidney disease and compared with healthy cats. RDW values did not show a statistically significant difference among the groups. RDW was found to have a positive correlation with erythrocyte count and a weak, borderline significant negative correlation with creatinine. However, RDW primarily reflects variability in erythrocyte size rather than erythrocyte number. Therefore, the biological significance of this correlation remains unclear and should be interpreted cautiously. Additionally, the weak negative correlation detected between RDW and creatinine indicates that RDW is not directly associated with loss of renal function but is more influenced by hematological changes.

In the veterinary literature, RDW has been suggested to have prognostic importance in feline cardiovascular diseases, such as hypertrophic cardiomyopathy [19]. Similar findings have been reported in human studies, where RDW showed a negative correlation with glomerular filtration rate and a positive association with serum creatinine levels [20]. Although a statistically significant correlation was observed, its strength was weak and may

Table 2. *Comparative descriptive statistics of hematological and biochemical parameters according to control. Aoc and IRIS stages*

Parameters	Groups				F	P
	Control	AOC	IRIS 1- 2	IRIS 3- 4		
RDW%	24.53±1.91 (21.8-27.3)	24.61±4.46 (19.1-36.1)	26.29±5.34 (18.9-35.4)	24.46±6.34 (19.1-47.1)	0.606	0.613
RBC M/uL	9.68±1.24 (7.12-11.48)	8.71±1.5 (6.29-11.69)	8.8±1.79 (4.91-11.39)	8.31±1.81 (5.54-13.73)	1.860	0.143
HCT%	43.05±6.09a (29.6-53.1)	36.21±7.7b (26.9-56)	38.35±7.44ab (23.9-51.7)	34.87±7.08b (23.3-46.5)	3.757	0.014*
HGB g/dL	14.02±1.79 (10-16.3)	11.75±1.82 (9.3-15.3)	12.17±2.18 (7.7-16.4)	15.68±19.59 (8-107)	0.677	0.569
MCV fL	44.54±3.54 (38.4-49.6)	41.78±6.00 (31.4-54.6)	44.19±6.58 (33-56.2)	42.24±4.83 (32.7-52.2)	1.193	0.318
MCH pg	14.50±1.04 (12.9-16.4)	13.66±1.91 (10.1-19.8)	14.02±1.82 (11.7-19.6)	14.19±1.98 (10.7-19.8)	0.709	0.550
MCHC pg/dL	32.63±1.39 (30.7-34.3)	31.68±4.73 (14-37.9)	31.94±2.81 (27.4-37.5)	33.38±2.67 (28-38.5)	1.202	0.315
RETIC%	0.30±0.17 (0.1- 0.7)	0.60±0.39 (0.1-1.3)	0.39±0.24 (0.1-1)	0.48±0.41 (0-1.5)	2.584	0.059
RETIC K/uL	28.63±15.86 (5.8-66.5)	46.02±35.85 (5.7-113)	33.95±22.35 (7.2-82.7)	38.78±34.42 (4-121.4)	1.124	0.345
WBC	8.58±2.95 (3.52-12.79)	17.62±14.78 (4.04-63.8)	11.03±4.91 (4.56-26.35)	11.11±13.26 (2.66-70.6)	2.493	0.066
Neu%	49.83±11.1 (32.8-66.4)	57.79±19.15 (21.2-89.3)	61.8±18.22 (23.7-83.6)	56.78±18.57 (16.8-87.6)	1.139	0.338
Lym%	38.29±11.44a (22.3-57.9)	22.06±13.51b (4.8-45.7)	26.95±15.92b (4.8-65)	25.78±15.6b (4.8-60.1)	3.514	0.019*
Mono%	2.78±0.88b (1.5-4.2)	6.53±2.95a (2.1-16.2)	4.83±2.56a (2.1-13.1)	5.74±2.61a (1.9-13.4)	6.435	0.001*
EOS%	8.04±3.73 (2.4-15.8)	6.46±6.1 (0.4-29.7)	5.76±4.41 (0.9-19.3)	5.97±3.72 (0.4-13.7)	0.656	0.582
BAS%	1.06±0.71 (0.3-2.7)	0.98±1.24 (0.1-4.6)	0.58±0.29 (0.01-1.1)	1.20±1.97 (0.3-9.91)	0.856	0.467
Neu K/uL	4.15±1.31 (1.4-6.91)	12.86±20.28 (1.52-106)	6.74±3.69 (2.06-14)	5.2±3.54 (1.33-12.89)	2.418	0.072
Lym K/uL	3.44±2 (1.38-7.41)	2.72±2 (0.32-7.29)	2.74±1.97 (0.71-9.38)	2.1±1.36 (0.32-4.77)	1.507	0.219
Mono K/uL	0.25±0.13c (0.07-0.51)	0.89±0.63a (0.13-2.33)	0.57±0.44b (0.15-2.03)	0.51±0.3bc (0.14-1.41)	6.477	0.001*
EOS K/uL	0.64±0.3 (0.27-1.26)	0.67±0.53 (0.03-2.07)	0.56±0.39 (0.09-1.8)	0.43±0.26 (0.03-1.05)	1.615	0.193
BAS K/uL	0.09±0.07 (0.02-0.23)	0.06±0.05 (0.01-0.16)	0.06±0.03 (0.01-0.1)	0.06±0.03 (0.01-0.11)	2.142	0.102
PLT K/uL	246.58±97.77 (72-411)	298.78±132.59 (112-561)	282.95±117.19 (106-515)	315.04±91.94 (171-488)	1.045	0.378
SDMA	10.00±1.81c (7-13)	41.00±18.84a (18-82)	19.90±5.96b (14-41)	34.38±11.6a (25-67)	21.314	0.000*
CREA	1.20±0.2d (0.8-1.5)	8.96±2.24a (5.8-13.6)	4.68±2.7c (1.4-8.8)	6.94±1.34b (2.9-9.8)	47.864	0.000*
BUN	23.00±5.03d (15-32)	126.11±19.99a (81-175)	65.95±30.08c (21-114)	88.50±18.94b (44-125)	72.384	0.000*
BUN/CREA Ratio	19.58±5.85a (11-30)	14.97±3.28b (9.26-24)	15.33±4.17b (10-25)	13.08±2.80b (8-19)	7.686	0.000*
PHOS	4.48±0.51c (3.4-5.4)	11.47±3.47a (4.5-20)	7.50±2.74b (2.8-12)	7.51±2.41b (3.4-12)	21.096	0.000*

* P<0.05; *Different superscript letters (a, b, c) within a row indicate statistically significant differences between groups according to duncan post hoc test (P<0.05). RDW: Red blood cell distribution width; RBC: Red blood cell count; HCT: Hematocrit; HGB: Hemoglobin; MCV: Mean corpuscular volume; MCH: Mean corpuscular hemoglobin; MCHC: Mean corpuscular hemoglobin concentration; RETIC: Reticulocyte; WBC: White blood cell; Neu: Neutrophil; Lym: Lymphocyte; Mono: Monocyte; EOS: Eosinophil; BAS: Basophil; PLT: Platelet count; SDMA: Symmetric dimethylarginine; CREA: Creatinine; BUN: Blood urea nitrogen; BUN/CREA ratio: Blood urea nitrogen to creatinine ratio; PHOS: Phosphorus*

Table 3. Correlation analysis between rdw values and hematological and biochemical parameters

Parameters		RDW%
SDMA	R	0.020
	P	0.855
CREA	R	-0.216
	P	0.050
RBC M/uL	R	0.439
	P	0.000*
HCT%	R	0.069
	P	0.537
HGB g/dL	R	-0.038
	P	0.733
BUN	R	-0.096
	P	0.390
PHOS	R	-0.097
	P	0.382
UPC	R	-0.062
	P	0.608

** P<0.05; R: Correlation coefficient; SDMA: Symmetric dimethylarginine; CREA: Creatinine; RBC: Red blood cell count; HCT: Hematocrit; HGB: Hemoglobin; BUN: Blood urea nitrogen; PHOS: Phosphorus; UPC: Urine protein/creatinine ratio*

not have strong clinical relevance. However, in the present study, RDW did not demonstrate similar value in the context of CKD and AOC. Therefore, RDW may exhibit different prognostic behavior across different disease groups in cats. RDW alone does not appear to be a reliable or clinically useful indicator for identifying the presence or progression of CKD or AOC in cats.

In chronic kidney disease, inflammation, decreased erythropoietin production, bone marrow dysfunction due to uremic toxins, and disturbances in iron metabolism can significantly affect red blood cell distribution width [21]. Studies conducted in human and veterinary medicine have shown that increased RDW values may be associated with mortality, inflammation, and prognosis of chronic diseases [6,15,16,19,22]. Although RDW has been shown to be prognostically associated with many chronic diseases in the literature, it remains unclear whether RDW increases with CKD progression in cats. Therefore, this study was designed to investigate the relationship between RDW and CKD and to determine whether RDW could be used as a parameter to predict disease progression.

The main reasons for differences among study results may include interspecies hematological differences, the fact that normocytic normochromic anemia is commonly observed in cats with CKD, and that RDW yields more meaningful results particularly in conditions where erythrocyte morphology changes markedly, such as regenerative anemia [22].

Limitations of this study include the relatively small sample size, the retrospective nature of data collection, potential differences in age distribution between groups, and the lack of inclusion of inflammatory markers that may influence RDW values. The heterogeneity between CKD and AOC groups may have influenced the variability of RDW values. Future studies with larger populations and prospective designs may be useful in elucidating the true prognostic significance of RDW in CKD and AOC.

In conclusion, RDW values did not differ significantly among cats with chronic kidney disease, acute on chronic kidney disease, and healthy controls. Furthermore, RDW showed no clinically relevant associations with most hematological and biochemical parameters, except for a weak and borderline negative correlation with creatinine concentration. These findings suggest that RDW is not a reliable biomarker for assessing disease progression in feline renal disease. The discrepancy between the present results and previous studies conducted in humans may be attributed to species specific differences in erythrocyte physiology. Future prospective studies with larger sample sizes and inclusion of inflammatory markers are warranted to better elucidate the potential role of RDW in feline renal diseases.

Declarations

Availability of Data and Materials: The datasets generated and/or analyzed during this study are available from the corresponding author (ŞA) upon reasonable request.

Acknowledgements: The authors would like to thank the staff of Terapist Veterinary Clinic for their assistance with data collection

Funding Support: This study did not receive any specific grants from any funding organization in the public, commercial, or non-profit sectors.

Competing Interests: The authors declare that they have no competing interests.

Declaration of Generative Artificial Intelligence (AI): The authors declare that no generative artificial intelligence tools were used to generate the scientific content of this manuscript. AI-assisted technologies were used only for language editing and readability improvement.

Author Contributions: SA: Study design, data collection, drafting of the manuscript. MK: Statistical analysis, interpretation of data, critical revision of the manuscript.

References

1. **Bartges JW:** Chronic kidney disease in dogs and cats. *Vet Clin North Am Small Anim Pract*, 42 (4): 669-692, 2012. DOI: 10.1016/j.cvsm . 2012.04.008

2. **Marino CL, Lascelles BDX, Vaden SL, Gruen ME, Marks SL:** Prevalence and classification of chronic kidney disease in cats randomly selected from four age groups and in cats recruited for degenerative joint disease studies. *J Feline Med Surg,* 16 (6): 465-472, 2014. DOI: 10.1177/1098612X13511446
3. **Polzin DJ:** Chronic kidney disease. **In,** Ettinger SJ, Feldman EC (Eds): Textbook of Veterinary Internal Medicine. 7th ed., 1955-2115, Saunders, Philadelphia, 2010.
4. **Cowgill LD, Polzin DJ, Elliott J, Nabity MB, Segev G, Grauer GF, Brown S, Langston C, van Dongen AM:** Is progressive chronic kidney disease a slow acute kidney injury? *Vet Clin North Am Small Anim Pract,* 46 (6): 995-1013, 2016. DOI: 10.1016/j.cvsm.2016.06.001
5. **Langston CE:** Acute uremia. In, Ettinger SJ, Feldman EC (Eds): Textbook of Veterinary Internal Medicine. 7th ed., 1955-2115, Saunders, Philadelphia, 2010.
6. **Salvagno GL, Sanchis-Gomar F, Picanza A, Lippi G:** Red blood cell distribution width: A simple parameter with multiple clinical applications. *Crit Rev Clin Lab Sci,* 52 (2): 86-105, 2015. DOI: 10.3109/10408363.2014.992064
7. **Buttarello M:** Laboratory diagnosis of anemia: Are the old and new red cell parameters useful in classification and treatment, how? *Int J Lab Hematol,* 38 (Suppl. 1): 123-132, 2016. DOI: 10.1111/ijlh.12500
8. **Lushbaugh CC, Maddy JA, Basmann NJ:** Electronic measurement of cellular volumes. I. Calibration of the apparatus. *Blood,* 20 (2): 233-240, 1962. DOI: 10.1182/blood.V20.2.233.233
9. **Lippi G, Targher G, Montagnana M, Salvagno GL, Zoppini G, Guidi GC:** Relationship between red blood cell distribution width and kidney function tests in a large cohort of unselected outpatients. *Scand J Clin Lab Invest,* 68 (8): 745-748, 2008. DOI: 10.1080/00365510802213550
10. **Chen T, Wang X, Bi Q:** Blood cell distribution width is associated with glomerulonephritis in diabetic patients with albuminuria. *Med Sci Monit,* 26:e924923. 2020. DOI: 10.12659/MSM.924923
11. **Lippi G, Henry BM, Sanchis-Gomar F:** Red blood cell distribution is a significant predictor of severe illness in coronavirus disease. *Acta Haematol,* 144 (4): 360-364, 2023. DOI: 10.1159/000510914
12. **Yang Y, Wang Q, Gao L, Liu S, Zhao J, Liu G, Zhang S:** Promising applications of red cell distribution width in diagnosis and prognosis of diseases with or without disordered iron metabolism. *Cell Biol Int,* 47, 1161-1169, 2023. DOI: 10.1002/cbin.12029
13. **Vashistha T, Streja E, Molnar MZ, Rhee CM, Moradi H, Soohoo M, Kovesdy CP, Kalantar-Zadeh K:** Red cell distribution width and mortality in hemodialysis patients. *Am J Kidney Dis,* 68 (1): 110-121, 2016. DOI: 10.1053/j.ajkd.2015.11.020
14. **Lu X, Huang X, Xue M, Zhong Z, Wang R, Zhang W, Wang L, Qiao Y, Ling F, Zhang Q, Zhang Y:** Prognostic significance of increased preoperative red cell distribution width (RDW) and changes in RDW for colorectal cancer. *Cancer Med,* 12, 13361-13373, 2023. DOI: 10.1002/cam4.6036
15. **Ludwik TM, Heinrich DA, Rendahl A, Friedenberg SG:** Red cell distribution width is a predictor of all-cause mortality in hospitalized dogs. *J Vet Emerg Crit Care,* 31 (5): 1-9, 2021. DOI: 10.1111/vec.13093
16. **Deng XW, Gao BX, Wang F, Zhao MH, Wang JW, Zhang LX:** Red blood cell distribution width is associated with adverse kidney outcomes in patients with chronic kidney disease. *Front Med,* 9:877220, 2022. DOI: 10.3389/fmed.2022.877220
17. **International Renal Interest Society (IRIS):** IRIS staging of chronic kidney disease. www.iris-kidney.com; *Accessed:* 15.01.2025.
18. **Chen H, Dunaevich A, Apfelbaum N, Aroch I, Segev G:** Acute on chronic kidney disease in cats: Etiology, clinical and clinicopathologic findings, prognostic markers, and outcome. *J Vet Intern Med,* 34 (4): 1496-1506, 2020. DOI: 10.1111/jvim.15820
19. **Stanzani G, Cowlam R, English K, Connolly DJ:** Evaluation of red blood cell distribution width in cats with hypertrophic cardiomyopathy. *J Vet Cardiol,* 17 (Suppl. 1): S233-S243, 2015. DOI: 10.1016/j.jvc.2015.09.001
20. **Barker E:** Approach to diagnosing and managing anaemia in cats. *In Pract,* 46, 508-521, 2024. DOI: 10.1002/inpr.493
21. **Matsuoka T, Abe M, Kobayashi H:** Iron metabolism and ınflammatory mediators in patients with renal dysfunction. *Int J Mol Sci,* 25 (7):3745, 2024. DOI: 10.3390/ijms25073745
22. **Limijadi EKS, Rachma DE, Hastuti AT:** Correlation between red cell distribution width (RDW) and chronic kidney disease patients in Semarang Indonesia. *Modern Med,* 31 (4): 345-352, 2024. DOI: 10.31689/rmm.2024.31.4.345

Kafkas Universitesi Veteriner Fakultesi Dergisi
Journal Home-Page: http://vetdergikafkas.org
E-ISSN: 1309-2251

Kafkas Univ Vet Fak Derg
32 (2): 281-290, 2026
DOI: 10.9775/kvfd.2026.36051

Research Article

Early Outcomes of Image-Guided Hypofractionated Volumetric Modulated Arc Radiotherapy (IG-HyVMAT) in Dogs with Non-Lymphomatous Nasal Tumors (NLNT)

Onur ÜLGENALP [1], Emine Esma ÇERKEZ [1], Vildan ALPAN [1], Ezgi OYMAK [2], Fatma Eser ÖZGENCİL [1], Özgecan KULEYİNOĞLU [1 (*)], Alper DEMİRUTKU [3], Adeviye Perran GÖKÇE [1], Yasemin ATAGUN [2,4], Uğur SELEK [2,4]

[1] VetAmerikan Animal Hospital, TR-34406 İstanbul-TÜRKİYE
[2] VKV American Hospital, Department of Radiation Oncology, TR-34365 İstanbul - TÜRKİYE
[3] Faculty of Veterinary Medicine, University of Istanbul Cerrahpaşa, Department of Surgery, TR-34320 İstanbul - TÜRKİYE
[4] School of Medicine, Koç University, Department of Radiation Oncology, TR-34450 İstanbul - TÜRKİYE

[(*)] **Corresponding author:**
Özgecan Kuleyinoğlu
Phone: +90 534 411 1386
E-mail: ozgecank@vetamerikan.org

How to cite this article?

Ülgenalp O, Çerkez EE, Alpan V, Oymak E, Özgencil FE, Kuleyinoğlu Ö, Demirutku A, Gökçe AP, Atagun Y, Selek U: Early Outcomes of Image-Guided Hypofractionated Volumetric Modulated Arc Radiotherapy (IG-HyVMAT) in Dogs with Non-Lymphomatous Nasal Tumors (NLNT). *Kafkas Univ Vet Fak Derg*, 32 (2): 281-290, 2026.
DOI: 10.9775/kvfd.2026.36051

Article ID: KVFD-2026-36051
Received: 06.01.2026
Accepted: 20.04.2026
Published Online: 26.04.2026

Abstract

Radiotherapy is a cornerstone in the management of canine non-lymphomatous nasal tumors (NLNT), providing both palliative benefit and local tumor control. Image-Guided Hypofractionated Volumetric Modulated Arc Radiotherapy (IG-HyVMAT) has recently emerged as a promising treatment modality for canine sinonasal tumors; however, data regarding tumor control, radiation-associated morbidity, and treatment outcomes across specific tumor histotypes remain limited. This retrospective study evaluated treatment response as well as early and late toxicities in 12 dogs with NLNT treated using IG-HyVMAT or IG-HyVMAT with a simultaneous integrated boost (SIB) protocol. Tumors were staged using a modified veterinary radiotherapy staging system, and treatment-related toxicities were assessed according to the Veterinary Radiation Therapy Oncology Group (VRTOG) criteria. IG-HyVMAT, most commonly delivered in combination with SIB, was prescribed at doses ranging from 25 to 40 Gy. The treatment protocols were well tolerated and associated with minimal acute toxicity. Clinical signs such as dyspnea and nasal congestion were identified as important prognostic indicators for survival in dogs with NLNT. The observed overall survival time (OST) and progression-free survival time (PFST), together with the low incidence of acute adverse effects, suggest that the SIB approach may offer potential clinical benefits, particularly in cases requiring palliative treatment. Overall, the findings of this study indicate that IG-HyVMAT, frequently applied with SIB, may provide meaningful survival advantages in dogs with NLNT while maintaining an acceptable toxicity profile. Nevertheless, further studies incorporating more advanced dose-optimization strategies for adjacent critical organs are warranted.

Keywords: Dog, IG-HyVMAT, IMRT, Non-lymphomatous nasal tumor, Radiotherapy, Toxicity, VMAT

Introduction

Non-lymphomatous sinonasal tumors (NLNTs) in dogs are predominantly of epithelial or mesenchymal origin and are characterized by aggressive local invasion. These tumors typically extend from the rostral nasal cavity toward the frontal sinuses and may progress intracranially, including invasion of adjacent bony structures such as the cribriform plate [1]. Due to their locally invasive behavior and anatomically complex location, the treatment of NLNTs remains challenging. Previous studies have demonstrated that chemotherapy, either alone or in combination with surgery, does not provide superior outcomes compared with radiotherapy (RT) in dogs with NLNT. Consequently, RT has become the primary treatment modality for these tumors and is used with either palliative or curative intent [2].

Reported survival times following treatment vary considerably. Median survival in untreated dogs is approximately 3.1 months (93 days), while dogs receiving chemotherapy alone may achieve survival times of up to 7.8 months (234 days). In contrast, dogs treated with RT have reported median survival times ranging from 10 to 19 months (300-540 days) [3,4].

Conventional two-dimensional radiotherapy is associated with limited conformity, often resulting in inadequate dose delivery to the tumor target while exposing adjacent

normal tissues to substantial radiation. In addition to increased toxicity, this limitation frequently prevents the delivery of an adequate dose to the tumor target volume. In contrast, three-dimensional conformal radiotherapy (3D-CRT), although still relatively limited in veterinary medicine, enables improved target delineation through advanced imaging and allows radiation delivery from multiple beam angles. Within this framework, target volumes are defined as the Gross Tumor Volume (GTV), representing macroscopic disease; the Clinical Target Volume (CTV), encompassing potential microscopic tumor extension; and the Planning Target Volume (PTV), which accounts for patient positioning uncertainties and internal motion. Surrounding normal tissues are contoured as Organs at Risk (OARs) to facilitate dose optimization and reduce treatment-related toxicity.

Further advances in conformal radiotherapy have led to the development of intensity-modulated radiotherapy (IMRT) and volumetric modulated arc therapy (VMAT). These techniques represent an evolution in conformal radiotherapy, using inverse planning algorithms to generate complex dose distributions that conform to predefined dose constraints for both target volumes and organs at risk. Within this context, the simultaneous integrated boost (SIB) technique improves dose conformity by enabling the delivery of different dose levels to multiple target volumes within the same treatment course, potentially enhancing local tumor control. In human head and neck oncology, the application of IMRT with SIB has been associated with reduced acute toxicity and improved clinical outcomes compared with earlier radiotherapy techniques [2].

Advances in imaging, immobilization, and image-guided verification systems have further improved treatment accuracy, enabling the adoption of hypofractionated RT protocols that deliver biologically effective doses comparable to or greater than conventional fractionation schedules (typically 1.8-2 Gy per fraction delivered over 25-40 fractions). Hypofractionated regimens used in canine NLNT typically involve higher doses per fraction (5-8 Gy) administered over 5-15 fractions, providing logistical advantages such as shorter treatment duration and fewer anesthetic events [1]. Considering the need for repeated general anesthesia and the associated financial burden in canine RT treatments, hypofractionated protocols are increasingly accepted in appropriately equipped veterinary oncology centers.

Despite these technical advances, the prognosis of dogs with NLNT remains variable. Tumor stage, histologic type, radiation dose, and fractionation schedule play critical roles in determining clinical outcomes. Because studies reporting radiotherapy planning approaches in dogs with NLNT are relatively scarce, recent research has focused on optimizing dose and fractionation strategies to improve treatment efficacy while minimizing radiation-induced toxicity [1,4-11].

Therefore, the aim of the present study was to evaluate early and late adverse effects in dogs with NLNT treated at our institution using an image-guided hypofractionated VMAT protocol with simultaneous integrated boost (IG-HyVMAT-SIB), and to provide additional data regarding treatment protocol distribution and clinical outcomes in veterinary radiation oncology.

Material and Methods

Ethical Statement

This study protocol was reviewed by the Koç Üniversity Local Animal Experiments Ethics Committee (Approval No: 2025. HADYEK.031). An informed consent form was obtained from each animal owner.

Case Selection

A total of twelve dogs diagnosed with non-lymphomatous nasal tumors (NLNT) at the time of presentation were included in the study. Diagnosis was established based on histopathological evaluation and/or computed tomography (CT) findings, and only cases without regional lymph node involvement or distant metastasis were enrolled. The follow-up period, including both surviving and deceased cases, was defined as 15 months (450 days). Previous surgical interventions were not considered as exclusion criteria.

All cases were staged using the modified Adams staging system. According to this system, tumors confined to a single nasal passage, paranasal sinus, or frontal sinus without bone involvement beyond the turbinates were classified as T1. Tumors with bone involvement extending beyond the turbinates but without orbital, subcutaneous, or submucosal mass formation were classified as T2. Tumors showing orbital, nasopharyngeal, subcutaneous, or submucosal involvement were classified as T3. Tumors associated with cribriform plate lysis were classified as T4, whereas tumors demonstrating intracranial extension into brain tissue were classified as T4a [4].

Clinical signs observed at presentation for each dog were recorded *(Table 1)*. Radiation-associated toxicities were assessed according to the Veterinary Radiation Therapy Oncology Group (VRTOG) scoring system. Toxic effects observed within the first three months following radiotherapy were classified as acute, whereas those developing later were considered late toxicities [12]. Tumor regrowth following an initial regression or progression of residual disease based on post-treatment imaging findings was defined as disease recurrence.

Table 1. *Breed-age distribution, common clinical distribution, tumor type, tumor stage, disease-free survival conditions (PFST), survival conditions (ST), acute and chronic side effects of RT, and G-HyVMAT and SIB with IG-HyVMAT administration doses (total dose Gy/fr) were reported in 12 dogs with NLNT*

Case	Breed/Age	CCS	T	PFST day	ST day	MAS	ASE /Grade	CSE/Grade	IG-HyVMAT Gy/fr	IG-HyVMAT SIB Gy/fr
N1	GR/12	E, DY, EP, NC	MC	132	150	4	Sk/G3, MM/G0, E/G2	-	30/5	
N2	GR/14	DY, NC	SCC	91	105	1	Sk/G1, MM/G3, E/G1		-	15-25/5
N3	T/8	EP, SN	HMC	440	450 survival	2	Sk/G2, MM/G0, E/G1	Sk/G1, E/G0		30-35/5
N4	GR/13	EP, DY, NC	AC	403	440	2	Sk/G2, MM/G0, E/G2	Sk/G2, E/G2		30-35/5
N5	GR/9	EP, NC	AC	17	40	3	-	-		30-35/5
N6	T/8	DE, EP	SCC	304	450 survival	3	Sk/G2, MM/G2, E/G2	Sk/G1, E/G2		25-35/5
N7	GR/8	DE, EP, NC	SCC	266	450 survival	3	Sk/G3, MM/G0, E/G2	Sk/G1, E/G2		30-35/5
N8	St/11	EP, NC, SN	SCC	207	450 survival	2	Sk/G2, MM/G0, E/G0	Sk/G1, E/G0		35-40/5
N9	T/2	DE	MH	443	450 survival	3	Sk/G1, MM/G0, E/G0	Sk/G0, E/G0	30/5	
N10	LR/13	EP, EX, DE	TCC	320	450 survival	4a	Sk/G1, MM/G0, E/G0	Sk/G2, E/G0	30/10	
N11	T/14	DE, EX	NA	208	450 survival	4	Sk/G0, MM/G0, E/G0	Sk/G0, E/G0	30/5	
N12	GR/14	NC	NA	87	100	3	-	-	18/3	

GR: *Golden retriever,* ***T:*** *Terrier,* ***LR:*** *Labrador retriever,* ***ST:*** *Setter,* ***MCCS:*** *Most Common Clinical Symptoms,* ***DE:*** *Deformity,* ***DY:*** *Dyspnea,* ***EP:*** *Epistaxis,* ***NC:*** *Nasal Congestion,* ***SN:*** *Sneeze,* ***EX:*** *Exoftalmus,* ***TT:*** *Tumor Type,* ***HMC:*** *Hemanjiosarcom,* ***SCC:*** *Squamos Cell Carcinoma,* ***AC:*** *Adenocarcinoma,* ***MH:*** *Malignant Histiocytoma,* ***TCC:*** *Transitional Cell Carcinoma,* ***NA:*** *Undifferentiated Adenocarcinoma,* ***PFST:*** *Progression-Free Survival Time/Disease-Free Survival,* ***ST:*** *Survival time,* ***MAS:*** *Modified Adams Stages,* ***ASE:*** *Acute Side Effects,* ***CSE:*** *Chronic Side Effects,* ***G:*** *Grade,* ***Sk:*** *Skin,* ***MM:*** *Mucous membrane,* ***E:*** *Eye,* ***IG-HyVMAT D:*** *Image guided hypofractionated volumetric modulated arc radiotherapy dose,* ***IG-HyVMAT SIB D:*** *Image guided hypofractionated volumetric modulated arc radiotherapy with simultaneous integrated boost dose,* ***Gy:*** *Total radiation dose,* ***fr:*** *Fraction*

Treatment Protocol

In the treatment approach, IG-HyVMAT was primarily preferred for more localized lesions and in situations where proximity to critical organs was a concern. The IG-HyVMAT with simultaneous integrated boost (SIB) protocol was applied in cases with substantial gross tumor volume (GTV) where the treatment objective was to achieve improved local palliative control. Doses administered to animals were determined based on the tumor's Adam's staging and proximity to critical organs. Controls were generally provided at 8-10 week intervals.

All simulation and treatment procedures were performed under general anesthesia. Anesthesia was induced with propofol (4-8 mg/kg; Polifarma, Türkiye), followed by endotracheal intubation and maintenance with sevoflurane in 80% oxygen under controlled mechanical ventilation. Patients were continuously monitored via camera throughout the anesthetic period.

For each treatment session, dogs were positioned and immobilized to ensure reproducible head and body alignment. Immobilization was achieved on the CT simulation table with the patient in sternal recumbency, using a patient-specific molded foam head support, thermoplastic mask, and vacuum cushion (Civco) *(Fig. 1)*. The forelimbs were aligned parallel to the body, the shoulders were positioned symmetrically, and the hind limbs were extended to improve stability. To further reduce variability in head and neck positioning and control the mandibular angle, a patient-specific tongue depressor and maxillary dental bite block were incorporated during thermoplastic mask fabrication.

CT images were acquired from the vertex to the level of

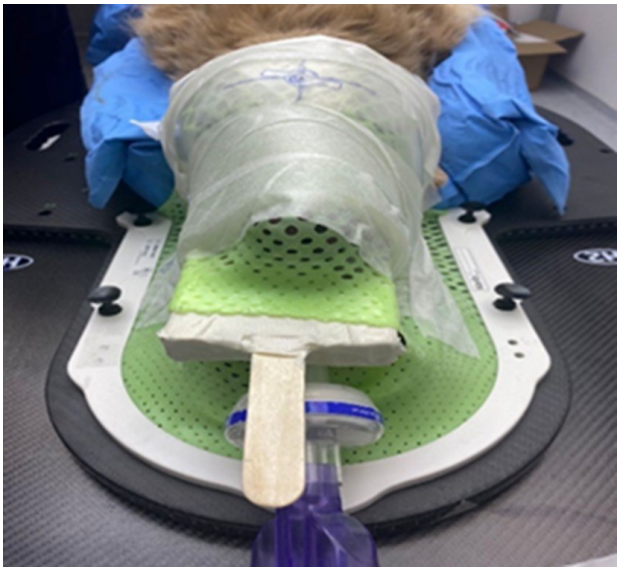

Fig 1. Head mask that prevents head movement during radiation therapy

the C3 vertebra with a slice thickness of 1 mm. To assist with accurate target delineation, magnetic resonance imaging (MRI) scans were co-registered with the planning CT images.

The GTV, CTV, and OARs were contoured by a veterinarian in collaboration with a radiation oncology specialist. The GTV was defined based on CT and MRI findings combined with physical examination results. The CTV was generated by applying a 5 mm expansion to the GTV and subsequently cropped at uninvolved anatomical barriers; the entire nasal cavity and sinuses were included within the CTV.

Treatment planning was performed using the Eclipse™ v16.1 treatment planning system (Varian Medical Systems, Palo Alto, CA) with the Analytical Anisotropic Algorithm (AAA) v16.1.2. In this study, the Planning Target Volume (PTV) was defined as a uniform 3 mm expansion of the CTV in all directions *(Fig. 2)*. All treatment plans utilized VMAT.

Each treatment fraction was delivered under general anesthesia. Prior to irradiation, two-dimensional setup verification was performed in the anteroposterior and right lateral planes, followed by three-dimensional verification using onboard cone-beam computed tomography (CBCT). Treatment delivery was initiated only after setup confirmation by both a veterinary specialist and a medical physicist. Patient-specific quality assurance was performed using Siemens Varian portal dosimetry.

The decision to apply IG-HyVMAT alone or in combination with SIB was made jointly by the radiation oncology specialist and the veterinarian, considering tumor size, location, proximity to critical structures, and the overall condition of the patient. To avoid prolonging treatment schedules, SIB planning typically involved assigning two different dose levels to the GTV and CTV within the same number of fractions. In cases where SIB was not applied, a single prescription dose was delivered to both target volumes *(Fig. 3)*.

Based on evaluation of imaging findings in cases treated with IG-HyVMAT, the following fractionation schemes were applied: Cases N1, N9, and N11 received a total dose of 30 Gy (30 Gy/5 fractions) delivered over five consecutive treatments; case N10 received 30 Gy (30 Gy/10 fractions) over ten consecutive treatments; and case N12 received 18 Gy (18 Gy/3 fractions) delivered over three consecutive treatments.

In cases treated with IG-HyVMAT with SIB, case N2 received 15 Gy to the CTV and 25 Gy to the GTV in five consecutive fractions. Cases N3, N4, N5, and N7 received 30 Gy to the CTV and 35 Gy to the GTV over five consecutive fractions, whereas case N6 received 25 Gy to the CTV and 35 Gy to the GTV over five consecutive fractions. Case N8 received 35 Gy to the CTV and 40 Gy to the GTV in five consecutive fractions.

Since the eye is the most affected organ during nasal tumor irradiation, the dose delivered to the right lacrimal gland ranged from 4.4 to 29 Gy (mean: 19.78 Gy), while the dose delivered to the left lacrimal gland ranged from 5.3 to 28.6 Gy (mean: 19.15 Gy).

Statistical Analysis

Descriptive statistics were calculated and are presented

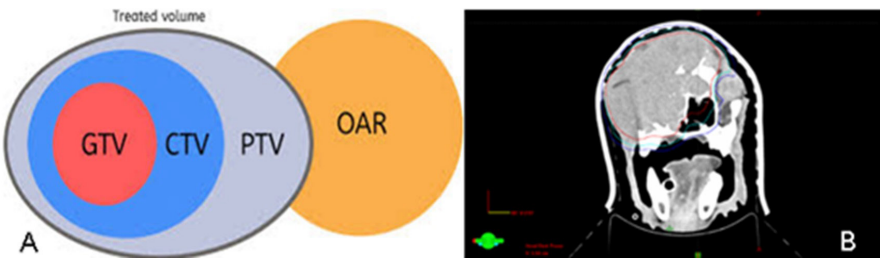

Fig 2. A- Schematic visualization of GTV, CTV, PTV, and QAR determination, B- Planning of GTV (*red line*), CTV (*turquoise line*) created with GTV + 5 mm, and PTV (*dark blue line*) created with CTV + 3 mm in the transverse view

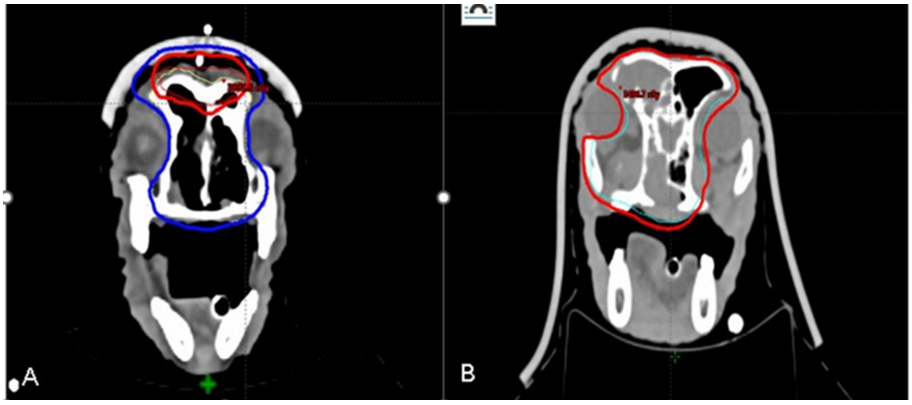

Fig 3. A) Dose of 35Gy/5Fr is given to GTV (*red isodose line*), while the dose prescribed to PTV created with CTV + 3 mm is 30Gy/5Fr (SIB) (*dark blue isodose line*), **B)** Dose prescribed to PTV volume created with CTV + 3 mm: 30 Gy/5Fr (*red isodose line*)

as mean, standard deviation (SD), median, interquartile range (25^{th}-75^{th} percentiles), and frequency (number and percentage), as appropriate. The Fisher-Freeman-Halton exact test was used to evaluate associations between categorical variables. The relationship between age and survival was assessed using Spearman's rank correlation analysis.

Survival outcomes, including progression-free survival time (PFST), were compared between breeds and radiotherapy protocols using the log-rank (Mantel-Cox) test and Kaplan-Meier survival curves were generated. The likelihood ratio chi-square test was used to compare acute and chronic side effects between two groups. A two-sided P value <0.05 was considered statistically significant. All statistical analyses were performed using SPSS software (version 29.0).

Results

A total of 12 dogs were included in the study. Breed distribution consisted of 6 Golden Retrievers, 3 Terriers, 1 Labrador Retriever, 1 Jack Russell Terrier, and 1 Setter. The mean age of the dogs was 9 years (range: 2-14 years), and the population included 6 males and 6 females. The primary tumor was located in the right nasal cavity in 5 dogs, the left nasal cavity in 6 dogs, and bilaterally in 1 dog. Common clinical signs included facial deformity (DE), dyspnea (DY), epistaxis (EP), nasal congestion (NC), sneezing (SN), and exophthalmos (EX).

Based on histopathological examination and CT evaluation, tumor types were identified as follows: 4 squamous cell carcinomas (SCC), 2 adenocarcinomas (ACA), 2 hemangiosarcomas (HSA), 1 transitional cell carcinoma (TCC), 1 malignant fibrous histiocytoma (MFH), and 2 undifferentiated neoplasms (UN). According to the modified Adams staging system, 1 case was classified as T1, 3 as T2, 5 as T3, 2 as T4, and 1 as T4a *(Table 1; Fig. 4)*.

During the 450-day study period, 5 of the 12 dogs died: case N1 on day 150, N2 on day 105, N4 on day 440, N5 on day 40, and N12 on day 100. Cases N1 and N4 died due to multiple organ failure, whereas cases N2, N5, and N12 died as a result of respiratory failure.

During the planned follow-up period, the overall survival time (OST) and progression-free survival time (PFST) were 346 days and 238 days, respectively, for dogs treated with IG-HyVMAT. In dogs treated with the IG-HyVMAT SIB protocol, OST was 340 days and PFST was 238 days.

Case N6 exhibited a PFST of 304 days, whereas case N9 showed a PFST of 443 days, after which recurrence was detected on day 450, marking the end of the study. The owners of both dogs declined further treatment and could not be contacted for continued follow-up.

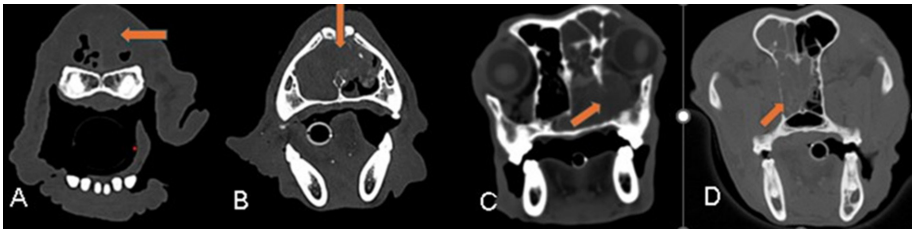

Fig 4. A) Stage 1, rostral mass involvement at N2 (*arrow*), **B)** Stage 2, nasal septum involvement at N3 (*arrow*), **C)** Stage 3, orbital involvement at N9 (arrow), **D)** Stage 4a, cribriform plate invasion at N10 (*arrow*)

Seven dogs remained alive at the end of the follow-up period. Among these, three dogs (N9, N10, N11) had been treated with the IG-HyVMAT protocol, while four dogs (N3, N6, N7, N8) had received IG-HyVMAT SIB. The mean PFST among the seven surviving dogs was 312 days *(Table 1)*.

Although a moderate negative correlation was observed between age and PFST, this relationship was not statistically significant (r=−0.508, P=0.092). Mortality rates were found to be significantly higher in Golden Retrievers and in dogs presenting with dyspnea (DY) and nasal congestion (NC). No significant association was detected between recurrence rates and the other evaluated variables.

Acute Toxicity

Early toxicity evaluations were performed in 10 cases. Regarding cutaneous toxicity, no findings were observed in one patient (G0), whereas three patients developed dry desquamation and alopecia (G1). Moist desquamation (G2) was observed in four patients, and edematous desquamation (G3) occurred in two patients. With respect to mucosal membranes, no early side effects were observed in eight patients (G0), while one patient developed G2 toxicity and another developed G3 toxicity *(Fig. 5)*. According to VRTOG criteria, early ocular toxicities are defined as moderate conjunctivitis and scleral congestion (G1); keratoconjunctivitis sicca (KCS) requiring artificial tears, moderate conjunctivitis, and iridocyclitis requiring treatment (G2); and ulcerative keratitis with or without vision loss and glaucoma (G3). In this study, evaluation of early ocular side effects revealed no toxicity in four patients, moderate conjunctivitis (G1) in two patients, and KCS requiring artificial tears (G2) in four patients. These early side effects appeared during the second week following radiotherapy and resolved within approximately 1-1.5 months *(Table 1)*.

Late Toxicity

Late toxicity evaluation was performed in 8 cases. All late adverse effects that developed after the third month following radiotherapy were considered permanent. Regarding cutaneous findings, no abnormalities were observed in two cases. Four dogs exhibited G1 toxicity (alopecia, hyperpigmentation, and leukotrichia), while two dogs developed G2 toxicity characterized by symptomatic induration and fibrosis *(Fig. 6)*. According to VRTOG parameters, late ocular toxicities in sinonasal tumor irradiation include asymptomatic cataracts or KCS (G1); symptomatic cataracts, keratitis, corneal ulceration, minor retinopathy, or moderate glaucoma (G2); and panophthalmitis, blindness, severe glaucoma, or retinal detachment (G3). In this study, five dogs showed no late ocular toxicity, while three dogs developed G2 toxicities. Ophthalmologic examinations revealed no G3-level adverse effects. Among the three dogs exhibiting G2 toxicity (N4, N6, N7), all had persistent KCS requiring ongoing supportive therapy, which had initially developed during the acute phase. In addition, cases N6 and N7 developed symptomatic right-sided cataracts with visual impairment, accompanied by bilateral keratitis, corneal ulceration, and descemetocele formation. None of the more severe ocular lesions that may occur at the G2 level, such as minor retinopathy or glaucoma, were observed. In case N7, bilateral limbal stem cell deficiency developed alongside cataract formation. Although this finding is not included in the VRTOG late toxicity scoring system, it was considered clinically significant. In the same patient, vision in the right eye was restored following extracapsular lens extraction (ECLE) using phacoemulsification, performed at the owner's request *(Fig. 7)*.

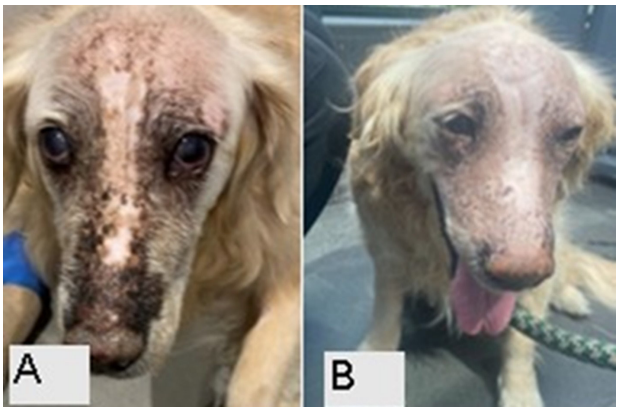

Fig 6. Late-stage skin toxicity. **A)** Alopecia, hyperpigmentation, leucotricha (Grade 1), **B)** Asymptomatic induration/fibrosis (Grade 2)

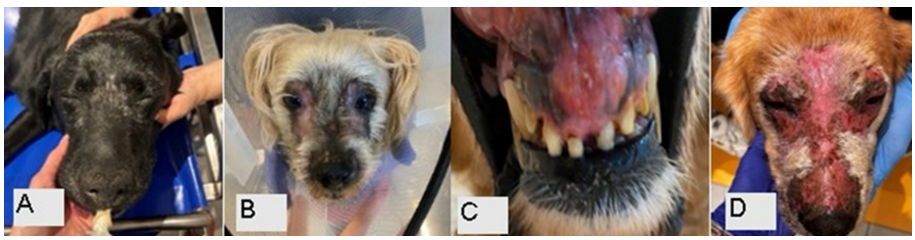

Fig 5. Early skin and mucous membrane toxicity. **A)** Erythema, dry desquamation, alopecia (Grade 1), **B)** Moist desquamation (Grade 2), **C)** Pachy mucositis (Grade 2), **D)** Conflient desquamation with edema (Grade 3)

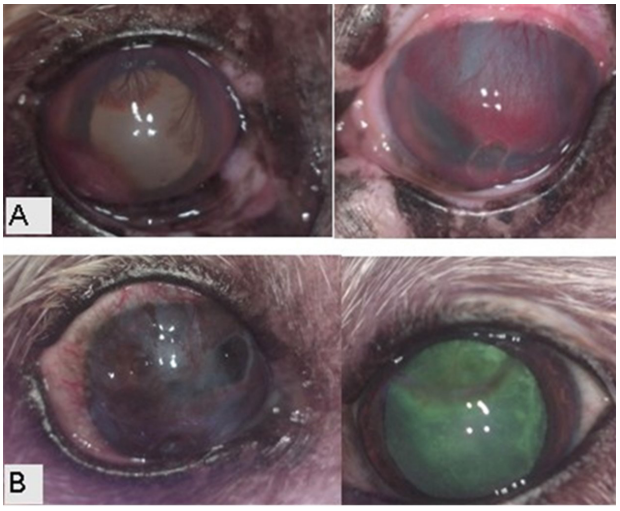

Fig 7. Late-stage ocular toxicity. **A)** Keratitis due to KCS (G1) and limbal stem cell insufficiency in both right and left eye (G2), **B)** Descematocele in the right eye, limbal stem cell insufficiency in both eyes (G2) and KCS (G1)

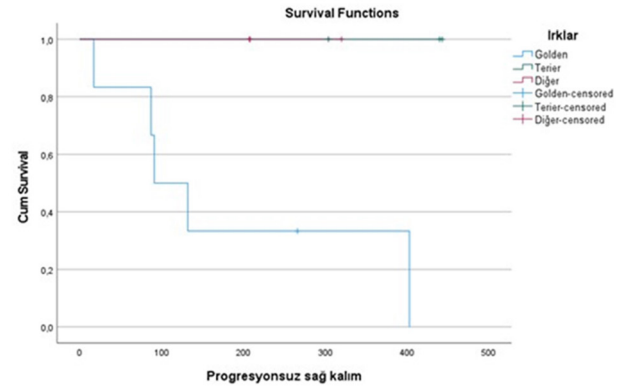

Fig 8. Kaplan-Meier curve for progression-free survival time in Golden Retrievers, Terriers, and other breeds

in terms of acute side effects. However, significant differences were detected in chronic toxicities, particularly involving the skin (P=0.020) and ocular tissues (P=0.049) in dogs treated with IG-HyVMAT SIB *(Table 1)*. Comparative analysis of PFST between breeds demonstrated a statistically significant difference (χ^2=7.51, P=0.028). Golden Retrievers exhibited significantly shorter PFST compared with Terriers and other breeds *(Fig. 8)*. No statistically significant difference in progression-free survival time (PFST) was observed between the IG-HyVMAT and IG-HyVMAT SIB groups (χ^2=0.002, P=0.964). Follow-up CT examinations performed approximately 120 days after radiotherapy in dogs treated with IG-HyVMAT SIB generally demonstrated a marked reduction in gross tumor volume (GTV) *(Fig. 9)*.

Discussion

Adenocarcinomas are generally reported to be the most common histologic subtype in canine nasal tumors, followed by squamous cell carcinomas (SCCs) and, less frequently, chondrosarcomas. Other tumor types, including fibrosarcomas, osteosarcomas, and undifferentiated or anaplastic sarcomas, have also been described [2,11]. In a study evaluating radiotherapy outcomes in 166 dogs diagnosed with NLNT, a significant difference in survival time was demonstrated between adenocarcinoma and squamous cell carcinoma [13]. In contrast to those reports, SCCs were more common than adenocarcinomas in the present cohort. Nevertheless, our findings were consistent with previous data showing the overall predominance of carcinomas over sarcomas [2,14].

Nasal carcinomas have been reported most frequently

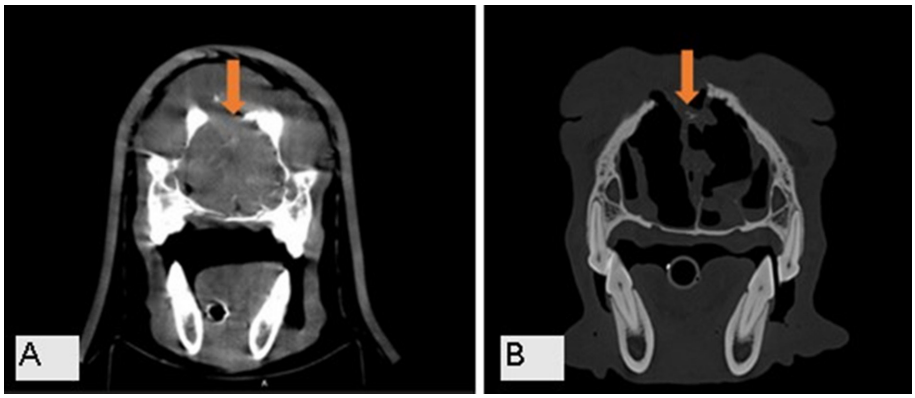

Fig 9. A) Simulation CT image taken during radiotherapy planning for N7 showing the mass covering both cavities, **B)** Near complete regression of the mass in the CT image taken at the 16th week follow-up after RT

Comparative Treatment Outcomes

No statistically significant difference was observed between the IG-HyVMAT and IG-HyVMAT SIB groups in dolichocephalic breeds such as Golden Retrievers, Labrador Retrievers, German Shepherd Dogs, and English Springer Spaniels, with a median age at diagnosis

of approximately 10 years [2,14]. In the present study, although a moderate negative correlation was observed between age and PFST, mortality was significantly higher in Golden Retrievers than in Terriers and other breeds. This finding suggests that breed-related differences may influence disease behavior or treatment response in ways not fully explained by current staging systems. Evaluation of tumor laterality revealed 5 right-sided, 6 left-sided, and 1 bilateral lesion, with no meaningful difference identified, suggesting that either side of the nasal cavity may be affected.

In linac-based hypofractionated stereotactic radiotherapy (SRT) studies for canine nasal tumors delivering a total dose of 30 Gy, overall survival time (OST) has been reported to range from 500 to 586 days, with minimal acute adverse effects [7,15]. Similarly, a study using SRT at a dose of 10 Gy × 3 fractions in dogs with NLNT reported an OST of 745 days [9]. In another report including 182 dogs with NLNT treated with 10 Gy × 3 fractions, OST was 441 days and acute morbidity was minimal [1]. In dogs with NLNT treated with either 3 consecutive fractions of 9-10 Gy or a single fraction of 20 Gy SRT, OST was reported as 388 days [8]. Another study in 129 dogs with NLNT treated with 10 Gy × 3 fractions reported clinical improvement with minimal acute toxicity and an OST of 542 days [10].

In cases diagnosed with stage 4 nasal carcinoma, characterized by cribriform plate lysis and adjacent bone lysis extending into the intracranial region, SRT was delivered at a total dose of 30-35 Gy in 3-5 sessions (7-10 Gy per fraction), and recurrence was observed 3 to 5 months later, with an OST of 170 days [11]. In another study, 88% of dogs with NLNT treated with SRT derived clinical benefit, with a PFST of 359 days and an OST of 563 days [15].

Considering the small number of cases included in our study, the limited follow-up period for evaluating early findings, and the fact that 7 of 12 dogs were still alive on day 450, our overall apparent success rate was 58%. We considered the mean PFST of the 7 dogs that remained alive throughout the 450-day follow-up period (312 days) to be clinically relevant, and this finding was consistent with the PFST of 359 days reported by Fox-Alvarez et al.[15].

The SIB technique is considered important because it combines the advantages of dose escalation and fractionation by delivering different dose levels to different target volumes within the same treatment course. In a study of 49 dogs with NLNT, 27 dogs received conventional SRT (10 × 4.2 Gy), whereas 22 dogs were treated with an SIB protocol (10 × 4.83 Gy to the gross tumor). The mean PFST was 274 days for the conventional protocol and 300 days for the SIB protocol. Although the SIB protocol was reported to be positively associated with prognosis, the difference between groups was not statistically significant [16].

In the present study, IG-HyVMAT, predominantly applied with SIB, was prescribed at doses ranging from 25 to 40 Gy. In dogs treated with IG-HyVMAT, OST and PFST were 346 and 238 days, respectively, and 60% survived today 450. In dogs treated with IG-HyVMAT SIB, OST and PFST were 340 and 238 days, respectively, and 57% survived today 450. These treatment regimens were well tolerated and associated with minimal acute toxicity. Although the small sample size and presence of censored cases limit definitive conclusions, the achievement of meaningful survival times with minimal acute toxicity in dogs treated with SIB supports further investigation of this approach. On the other hand, tumor size and location also appeared to be major factors influencing the clinician's decision regarding dose escalation and the extent of organ-at-risk sparing.

An et al.[11] reported three dogs presented with epistaxis and facial deformity in which CT demonstrated soft tissue-attenuating, contrast-enhancing masses involving both nasal cavities, together with cribriform plate lysis and adjacent bone lysis extending intracranially. These cases were diagnosed as stage 4 nasal carcinoma and treated with radiotherapy at a total dose of 30-35 Gy over 3-5 sessions (7-10 Gy per fraction). Monthly follow-up CT examinations showed tumor shrinkage after treatment, although recurrence was observed 3 to 5 months later, and the mean OST was 170 days. The authors concluded that SRT provided treatment precision even in dogs with nasal carcinoma and cribriform plate lysis without causing severe radiation toxicity. They recommended follow-up CT evaluations at 1, 3, and 6 months after SRT for prognostic assessment and recurrence monitoring. Clinical signs initially observed in dogs with nasal tumors include epistaxis, mucopurulent nasal discharge, facial deformity, sneezing, stertorous breathing, dyspnea, ocular discharge, and, in advanced cases, neurologic signs associated with cribriform plate invasion.

In the present study, one case with T4-stage cribriform plate destruction died on day 150, whereas another case with T4a-stage brain invasion was still alive at the end of follow-up; therefore, no clear conclusion could be drawn regarding the prognostic significance of these findings. No neurologic deficits or fistula formation were encountered, including in the dog with cribriform plate lysis, although other common clinical signs were observed. This suggests that radiologic invasion may not necessarily be associated with neurologic dysfunction. However, the significantly higher mortality observed in dogs presenting with dyspnea (DY) and nasal congestion (NC) suggests that these clinical signs may reflect more advanced

local disease and may serve as additional prognostic indicators.

It is well established that OST in dogs with NLNT treated with SRT ranges from 10 to 19 months (300-540 days) [3,4]. In the present study, OST was 346 days in dogs treated with IG-HyVMAT and 340 days in those treated with IG-HyVMAT SIB, further supporting the clinical effectiveness of radiotherapy. Comparative analysis of PFST between breeds revealed a statistically significant difference, with Golden Retrievers demonstrating significantly shorter PFST than Terriers and other breeds. This may be associated with the shorter survival observed in this breed. Earlier mortality in Golden Retrievers may also have limited the observation period during which recurrence could be detected, suggesting the possibility of survival-related bias in breed-based comparisons of recurrence.

Although no significant difference in PFST was observed between the IG-HyVMAT and IG-HyVMAT SIB groups, follow-up CT examinations performed on day 120 after radiotherapy in the IG-HyVMAT SIB group generally demonstrated a marked reduction in gross tumor volume (GTV). This finding supports further investigation of this protocol, particularly in cases where GTV is substantial and the primary aim is to achieve improved local palliation.

In the present study, acute side effects resolved within 1 to 1.5 months, while chronic adverse effects included permanent alopecia and hyperpigmentation (G1) in four cases and asymptomatic induration/fibrosis (G2) in one case, none of which appeared to negatively affect patient quality of life. In addition, permanent KCS of G1 severity was observed in four dogs, and G2 symptomatic cataract and keratitis were observed in three dogs, whereas other adverse effects such as retinopathy, glaucoma, and permanent blindness were not encountered. Furthermore, restoration of vision in the right eye of one dog with cataract following extracapsular lens extraction suggested that these adverse effects did not severely compromise patient comfort and also contributed to owner satisfaction. In contrast, limbal stem cell deficiency observed in two cases, although not included in the VRTOG toxicity scoring system, suggests that this entity should also be considered in ophthalmologic assessments of late morbidity. These findings support the importance of lacrimal gland and corneal dose constraints as reported by Poirier et al.[17]. Our observations regarding early and late radiotherapy-related morbidity were also consistent with the toxicities described by Mortier and Blackwood [2].

Although no significant difference in acute adverse effects was observed between dogs treated with IG-HyVMAT and those treated with IG-HyVMAT SIB, significant differences in chronic skin and ocular toxicities were observed in the SIB-treated group. This finding may be attributable to the higher doses delivered within the planned target volume (PTV) in dogs receiving SIB.

Radiation-induced visual impairment has been shown to be dose-dependent; mean ocular doses of approximately 39 Gy have been associated with vision loss, whereas doses below 30 Gy are generally reported to preserve visual function [18]. In hypofractionated IMRT protocols, radiation-induced KCS represents a clinically important late complication, and a retrospective case-control study identified a corneal dose threshold of 14.9 Gy predictive of KCS development in dogs treated with large fraction sizes [19].

In the present study, the mean lacrimal gland dose in cases that developed cataract and KCS approached 29 Gy, which was consistent with previous reports. Notably, the mean lacrimal gland doses in this study were approximately 19 Gy on both sides, and permanent KCS occurred only in dogs receiving doses near the upper end of the reported range. This observation supports the concept that tumor proximity to ocular structures, and the resulting unavoidable dose escalation, plays a critical role in the development of late ocular toxicity. Consistent with previous IMRT planning studies, these findings reinforce the importance of lacrimal gland contouring and the application of conservative dose constraints, particularly when hypofractionated SRT protocols are used. Vision-threatening complications involving the lens, retina, or optic nerve were rare in our study, with only three dogs developing G2 ocular toxicity. These findings emphasize the importance of careful dose planning for ocular structures, particularly the corneal limbus and lacrimal gland, in order to minimize the risk of permanent KCS and stem cell deficiency. Although symptomatic treatment provided clinical improvement, these complications underscore the need for stricter dose constraints in hypofractionated SRT protocols.

Because there is no standardized radiotherapy protocol for canine nasal tumors, further studies with larger case numbers, longer follow-up periods, and more detailed reporting of early and late toxicities are needed. The results of the present study, conducted in a veterinary hospital setting in Türkiye using an officially authorized and legally established certified radiotherapy device and a multidisciplinary team including a veterinary oncology specialist and a medical physicist from the same institution, support the use of IG-HyVMAT as an effective treatment modality capable of providing meaningful survival benefits with an acceptable toxicity profile.

In conclusion, our findings were consistent with previously published studies in terms of OST, PFST, toxicity, and dose parameters. Radiotherapy appeared to increase PFST and OST with minimal adverse effects. Future research

should focus not only on PFST, OST, and toxicity grading according to VRTOG criteria, but also on SIB-based treatment planning strategies in which dose constraints for adjacent functionally critical organs, particularly the lacrimal gland and corneal structures, are carefully evaluated.

Declarations

Availability of Data and Materials: All data generated or analyzed during this study are available from the corresponding author (Ö. K.) upon reasonable request.

Acknowledgements: The authors would like to thank all staff members of the VetAmerikan Animal Hospital Radiotherapy Unit for their support during the study.

Financial Support: This research received no specific grant from any funding agency.

Conflict of Interest: The authors declare no conflicts of interest.

Declaration of Generative Artificial Intelligence (AI): This manuscript (including tables and figures) was not written using generative artificial intelligence or AI-assisted technologies.

Author Contributions: Data collection, study execution, and analysis: OÜ, EEÇ, VA, EO, US, YB, AD; manuscript preparation: FEÖ, EEÇ, ÖK, VA, YB; critical review: OÜ, YB, US, EO, FEÖ, APG. All authors have read and approved the final manuscript and agree to take responsibility for all aspects of the work. This statement complies with the journal's "Ethical Principles and Publication Policy/Authorship and Author Rights" guidelines.

References

1. **Yoshikawa H, Lafferty MH, Griffin LR, LaRue SM:** A retrospective study of sinonasal tumors in 182 dogs treated with stereotactic radiotherapy (3 × 10 Gy) (2010–2015). *J Vet Intern Med,* 37, 2356-2367, 2023. DOI: 10.1111/jvim.16838
2. **Mortier JR, Blackwood L:** Treatment of nasal tumours in dogs: A review. *J Small Anim Pract,* 61, 404-415, 2020. DOI: 10.1111/jsap.13173
3. **Woodruff MJ, Heading KL, Bennett P:** Canine intranasal tumours treated with alternating carboplatin and doxorubicin in conjunction with oral piroxicam: 29 cases. *Vet Comp Oncol,* 17 (1): 42-48, 2019. DOI: 10.1111/vco.12443
4. **Stevens A, Turek M, Vail D, Christensen N, Forrest L:** Definitive-intent intensity-modulated radiotherapy for modified-Adams stage 4 canine sinonasal cancer: A retrospective study of 29 cases (2011-2017). *Vet Radiol Ultrasound,* 61, 718-725, 2020. DOI: 10.1111/vru.12899
5. **Fujiwara A, Kobayashi T, Kazato Y, Yayoshi N, Fujita M:** Efficacy of hypofractionated radiotherapy for nasal tumours in 38 dogs (2005-2008). *J Small Anim Pract,* 54, 80-86, 2013. DOI: 10.1111/jsap.12024
6. **Tollett MA, Duda L, Brown DC, Krick EL:** Palliative radiation therapy for solid tumors in dogs: 103 cases (2007-2011). *J Am Vet Med Assoc,* 248, 72-82, 2016. DOI: 10.2460/javma.248.1.72
7. **Gieger TL, Nolan MW:** Linac-based stereotactic radiation therapy for canine non-lymphomatous nasal tumours: 29 cases (2013-2016). *Vet Comp Oncol,* 16, E68-E75, 2017. DOI: 10.1111/vco.12334
8. **Mayer MN, DeWalt JO, Sidhu N, Mauldin GN, Waldner CL:** Outcomes and adverse effects associated with stereotactic body radiation therapy in dogs with nasal tumors: 28 cases (2011-2016). *J Am Vet Med Assoc,* 254 (5): 602-609, 2019. DOI: 10.2460/javma.254.5.602
9. **Gieger TL, Haney SM, Nolan MW:** Re-irradiation of canine non-lymphomatous nasal tumours using stereotactic radiation therapy (10 Gy × 3) for both courses: 11 dogs. *Vet Comp Oncol,* 20, 502-508, 2022. DOI: 10.1111/vco.12801
10. **Nolan MW, Berman AR, Watson-Skaggs ML, Quinn CN, Marcus KL, Russell K, Yoshikawa H, Olby NJ, Gieger TL:** Stereotactic radiotherapy (10 Gy × 3) for canine nonlymphomatous intranasal tumors is associated with prolonged survival and minimal risk of severe radiotoxicity. *J Am Vet Med Assoc,* 260 (12): 1496-1506, 2022. DOI: 10.2460/javma.22.03.0141
11. **An SY, Hwang GH, Choi MY, Huh C, Yoon YM, Lee HC, Hwang TS:** Stereotactic radiation therapy for nasal carcinoma with cribriform plate destruction in three dogs: A Serial CT study. *J Vet Clin,* 40 (2): 139-146, 2023. DOI: 10.17555/jvc.2023.40.2.139
12. **Vanhaezebrouck IF, Scarpelli ML:** Companion animals as a key to success for translating radiation therapy research into the clinic. *Cancers,* 15:3377, 2023. DOI: 10.3390/cancers15133377
13. **Mizuno R:** Prognostic factors and survival following radiation therapy for canine nasal tumors: A single-institution retrospective study of 166 cases. *Open Vet J,* 14 (7): 1538-1552, 2024. DOI: 10.5455/OVJ.2024.v14.i7.3
14. **Sones E, Smith A, Schleis S, Brawner W, Almond G, Taylor K, Haney S, Wypij J, Keyerleber M, Arthur J, Hamilton T, Lawrence J, Gieger T, Sellon R, Wright Z:** Survival times for canine intranasal sarcomas treated with radiation therapy: 86 cases (1996-2011). *Vet Radiol Ultrasound,* 54 (2): 194-201, 2013. DOI: 10.1111/vru.120062
15. **Fox-Alvarez S, Shiomitsu K, Lejeune AT, Szivek A, Kubicek L:** Outcome of intensity-modulated radiation therapy-based stereotactic radiation therapy for treatment of canine nasal carcinomas. *Vet Radiol Ultrasound,* 61, 370-378, 2020. DOI: 10.1111/vru.12854
16. **Meier V, Staudinger C, Körner M, Soukup A, Rohrer Bley C:** Dose-escalated simultaneously integrated boost radiation protocol fails to result in a survival advantage for sinonasal tumors in dogs. *Vet Radiol Ultrasound,* 63, 633-648, 2022. DOI: 10.1111/vru.13086
17. **Poirier VJ, Matsuyama A, Kim C, Darko J, Fleck A:** Clinical-dosimetric relationship between lacrimal gland dose and keratoconjunctivitis sicca in dogs with sinonasal tumors treated with radiation therapy. *J Vet Intern Med,* 34 (2): 867-872, 2020. DOI: 10.1111/jvim.15744
18. **Wolf F, Meier VS, Pot SA, Rohrer Bley C:** Ocular and periocular radiation toxicity in dogs treated for sinonasal tumors: A critical review. *Vet Ophthalmol,* 23 (4): 596-610, 2020. DOI: 10.1111/vop.12761
19. **Ohnishi A, Takeda S, Okada Y, Tokoro M, Kageyama S, Itoh Y, Asanuma T:** Risk factors for radiation-induced keratoconjunctivitis sicca in dogs treated with hypofractionated IMRT for intranasal tumors. *Animals (Basel),* 15 (15):2258, 2025. DOI: 10.3390/ani15152258

Kafkas Universitesi Veteriner Fakultesi Dergisi
Journal Home-Page: http://vetdergikafkas.org
E-ISSN: 1309-2251

Kafkas Univ Vet Fak Derg
32 (2): 291-298, 2026
DOI: 10.9775/kvfd.2026.36166

RESEARCH ARTICLE

Diagnosis of Postpartum Endometritis in Dairy Cows Using a Portable Endovideo-Vaginoscope with PCR Confirmation

Dauletbek MURATBAYEV [1], Yernur SAKHARIYEV [1], Shynar TASTEMIROVA [1], Isatai JAKUPOV [2], Ainur AKHMADIYEVA [1], Cihan KACAR [3], Yavuz OZTURKLER [4 (*)]

[1] Department of Veterinary Medicine, Faculty of Veterinary and Agricultural Sciences, Shakarim University, Semey, Abai Region, KAZAKHSTAN
[2] Department of Veterinary Medicine, Faculty of Veterinary Medicine and Animal Husbandry Technology, S. Seifullin Kazakh Agrotechnical Research University, Astana, KAZAKHSTAN
[3] Department of Obstetrics and Gynelogy, Faculty of Veterinary Medicine, Kafkas University, TR-36100 Kars - TÜRKIYE
[4] Department of Reproduction and Artificial Insemination, Faculty of Veterinary Medicine, Kafkas University, TR-36100 Kars - TÜRKIYE

(*) **Corresponding author:**
Yavuz Öztürkler
Phone: +90 474 242 6836/5232
Mobile: +90 533 611 5799
E-mail: yavuzozturkler@gmail.com

How to cite this article?

Muratbayev D, Sakhariyev Y, Tastemirova S, Jakupov I, Akhmadiyeva A, Kacar C, Ozturkler Y: Diagnosis of Postpartum Endometritis in Dairy Cows Using a Portable Endovideo-Vaginoscope with PCR Confirmation. *Kafkas Univ Vet Fak Derg*, 32 (2): 291-298, 2026.
DOI: 10.9775/kvfd.2026.36166

Article ID: KVFD-2026-36166
Received: 24.01.2026
Accepted: 23.04.2026
Published Online: 26.04.2026

Abstract

Endometritis remains a major cause of reduced reproductive efficiency in dairy cattle, necessitating practical methods for clinical detection and identification of bacterial etiology under farm conditions. The aim of this exploratory field study was to evaluate the practical applicability of a complex diagnostic protocol utilizing a novel portable endovideo-vaginoscope custom-designed for farm use. The device features autonomous heating (to prevent lens fogging), Wi-Fi data transmission, and smartphone integration and was used alongside laboratory verification. In the Abai region of Kazakhstan, 100 Holstein-Friesian cows were screened on days 20-30 postpartum. Clinical signs of endometritis were detected in 21 animals (21%) by video-vaginoscopy, after which uterine contents from affected cows were aseptically collected for bacteriological culture and PCR analysis. Under the aerobic culture conditions used, laboratory findings most frequently identified *Escherichia coli* and/or *Staphylococcus aureus*, including in mixed bacterial infections. PCR analysis identified the *fimH* gene in *E. coli*-positive material and the *nuc* gene in *S. aureus*-positive material, supporting the bacterial etiology of the inflammation visualized instrumentally. Antimicrobial susceptibility testing revealed a high prevalence of resistance to ampicillin and oxytetracycline among the isolates, whereas gentamicin and cephalosporins demonstrated high in vitro activity. The novelty of this study lies in the field validation of a portable device with thermostabilization and wireless archiving capabilities. Overall, the results indicate that this protocol, combined with molecular verification, provides a practical field-adapted approach for the diagnosis and monitoring of postpartum uterine health in remote farm settings.

Keywords: Abai region, Bovine endometritis, Diagnostics, *Escherichia coli*, *fimH, nuc*, PCR, Portable endovideo-vaginoscope, *Staphylococcus aureus*

Introduction

Postpartum endometritis, clinically characterized primarily by mucopurulent or purulent vaginal discharge after 21 days in milk (DIM), remains a major cause of reduced reproductive efficiency in dairy cattle, as it is associated with impaired conception rates, increased days open, and significant economic losses [1-4]. Beyond the direct economic burden, postpartum uterine disease has important sanitary implications at the herd level, because persistent uterine infection contributes to increased antimicrobial use, higher treatment costs, and management challenges related to animal welfare and biosecurity [3,4]. In modern dairy herds, the risk of clinical postpartum uterine disease remains substantial; therefore, the practical value of any diagnostic strategy depends on its on-farm reproducibility, rapid turnaround time, and the ability to document findings for monitoring and decision-making [3,4].

The pathogenesis of endometritis is viewed as the result of an interaction between bacterial contamination in the early postpartum period, trauma or contamination of the reproductive tract, and the endometrial immune response. However, colonization does not invariably lead to clinical inflammation. Mechanisms of "resilience" -specifically pathogen avoidance, tolerance, and resistance (elimination)- are critical in determining whether

contamination progresses to established disease, and recent reviews emphasize that the endometrium functions as an active organ of innate immunity shaping the severity and consequences of postpartum uterine disease [5-7].

Etiologically, clinical endometritis in cattle is polymicrobial and dynamic over time. In addition to *Escherichia coli*, *Trueperella pyogenes* and anaerobic taxa (e.g., *Fusobacterium, Porphyromonas/Prevotella, Bacteroides)* are frequently associated with postpartum uterine disease. A crucial pathogenetic feature may be not only the presence of bacteria but also their localization and tissue invasion. The application of fluorescence in situ hybridization (FISH) to endometrial biopsies has demonstrated that specific anaerobes can be detected intracellularly within the epithelium and in the lamina propria, supporting the concept of tissue invasiveness as a factor in the persistence of inflammation [8]. In parallel, increased attention has been given to antimicrobial resistance (AMR) in uterine isolates and to rational antibiotic stewardship, because empirical treatment without pathogen verification or susceptibility testing increases the risk of failure and selection for resistance [9,10].

From a practical perspective, the "bottleneck" often lies in clinical diagnosis under field conditions. Traditionally, clinical endometritis is identified via visual assessment of vaginal contents (speculum/vaginoscopy, Metricheck device, gloved hand) based on discharge scoring systems. While these methods may show comparable predictive value for reproductive outcomes, they can yield different diagnostic frequencies for the same animals, indicating a risk of variability and misclassification [11]. Given the lack of a single "gold standard," modern studies increasingly refine diagnostic criteria and evaluate test performance using probabilistic approaches and Bayesian latent class models to estimate sensitivity and specificity under field conditions [12-16]. This has supported interest in instrumental visualization that allows standardization, image storage, and subsequent audit of findings-particularly relevant for geographically dispersed farms and remote production settings, where specialist access and quality control of reproductive examinations may be limited [17-20].

In this context, portable video/electronic solutions facilitate vaginoscopy by providing stable visualization with digital archiving for longitudinal monitoring and consultation [17-20]. At the same time, laboratory verification remains critical: culture confirms viable pathogens and enables AMR profiling, while molecular methods (PCR/RT-PCR) offer greater speed and specificity, especially in mixed infections. For *E. coli*, the *fimH* adhesin has been reported among virulence factors associated with clinical endometritis, supporting its use as a marker for potentially more pathogenic strains in the postpartum period [21]. For *Staphylococcus aureus,* the *nuc* gene is a widely accepted species-specific PCR marker used for rapid identification [22]. Contemporary experimental and field data continue to clarify how *S. aureus* and other microbial components influence endometrial inflammation and the uterine microbial community [23], and studies of genital *E. coli* populations suggest that reservoirs and virulence determinants may differ between healthy animals and cows with postpartum uterine disease, which is important for interpreting PCR results clinically [24,25].

Overall, modern approaches to the field diagnosis of clinical endometritis are increasingly viewed as a multi-stage reproducible protocol comprising: (i) standardized visual assessment of vaginal discharge (with a trend toward digital capture for comparability); (ii) aseptic sampling from the uterine cavity/cervical canal; (iii) culture confirmation with AMR profiling; and (iv) targeted molecular verification of key pathogens and/or virulence markers to confirm etiology and improve comparability between herds [3,11,15,19]. In this framework, a protocol combining portable video-vaginoscopy adapted for farm conditions (including optics thermostabilization/anti-fogging, wireless transmission, and image archiving) with bacteriology and PCR detection of *fimH (E. coli)* and *nuc (S. aureus)* markers appears logically sound and addresses both diagnostic subjectivity and etiological verification [24].

Accordingly, the aim of this exploratory field study was to assess the practical applicability of a portable endovideo-vaginoscope, used in combination with bacteriological culture and PCR, for the detection of clinical endometritis and for descriptive characterization of associated bacterial findings in Holstein herds.

Material and Methods

Ethical Statement

The study was conducted with written consent from the farm owner and approved by the Institutional Ethics Committee of Shakarim University (Protocol No. 16, dated September 10, 2025).

Study Design

This study was conducted on the commercial dairy farm "Kalihanuly" in the Abai region of Kazakhstan. A total of 100 Holstein-Friesian cows, producing approximately 25 L of milk per day, aged between 3 and 8 years, were screened during the early postpartum period (20-30 days in milk, DIM). The herd was managed under routine commercial farm conditions in the study region, and all examinations were performed on-farm. The laboratory analyses were carried out at the "Agrotechnopark" Research Laboratory of Shakarim University. The study

was designed as an exploratory field-validation study; uterine samples were collected only from cows meeting the clinical definition of endometritis, and no clinically healthy control group was included.

Feeding and Body Condition

The cows were fed a Total Mixed Ration (TMR) consisting of alfalfa hay, corn silage, and concentrates, formulated to meet the nutritional requirements of lactating dairy cattle. Water was provided ad libitum. At the time of enrollment (20-30 DIM), the average body condition score (BCS) of the animals was within the optimal range (approximately 3.0-3.5 on a 5-point scale) [26].

Reproductive History

Review of the medical history revealed that the study cohort included animals with a history of dystocia and retained fetal membranes (>12 h postpartum). Additionally, cases of acute puerperal metritis treated during the early postpartum period (0-10 DIM) were recorded in the history of several cows. These conditions had either clinically resolved or transitioned into the chronic forms studied here by the time of enrollment [1].

Clinical and Instrumental Diagnosis

The diagnostic workflow included medical history review (focusing on calving and postpartum events), a general clinical examination, and endovideovaginoscopic assessment. A custom-designed portable video-vaginoscope was used for visual inspection of the vaginal and cervical mucosa *(Fig. 1)*. The instrument was constructed from medical-grade stainless steel (AISI 304), with a distal module equipped with a miniature video camera, LED illumination, and a built-in heating system to prevent condensation (anti-fogging) and to warm the metal surface.

Real-time video transmission via Wi-Fi allowed the operator to view and record intra-vaginal and cervical findings using a mobile device. To ensure hygiene and prevent cross-contamination, the device underwent thorough mechanical cleaning after each use, followed by high-level disinfection via immersion in a 7.5% hydrogen peroxide solution for 15 min, and finally double rinsing with sterile distilled water.

To clinically assess uterine health, the Vaginal Discharge Score (VDS) system was employed as follows: Score 0 - no discharge or clear mucus.

Score 1 - mucous discharge with small flecks or strands of pus.

Score 2 - mucopurulent discharge (<=50% purulent content).

Score 3 - purulent discharge (>50% pus), possibly with malodor or bloody components.

Clinical endometritis was diagnosed when cows had a VDS >= 2 between 20 and 30 days in milk (DIM) [1,27].

Sample Collection and Microbiological Analysis

Uterine samples were collected transcervically from cows that showed clinical signs of endometritis on video-vaginoscopic examination (presence of purulent or mucopurulent exudate, n=21). The procedure was performed under aseptic conditions and visual guidance using a certified sampling device (Patent No. 10148, Republic of Kazakhstan). Samples were transported to the laboratory at +4°C and processed within 2 h.

Initial inoculation was performed on MacConkey agar and Columbia blood agar supplemented with 5% defibrinated sheep blood (Oxoid Ltd., Basingstoke, UK). Plates were incubated aerobically at 37°C for 24-48 h. Preliminary species identification was based on colony morphology, Gram staining, and standard biochemical assays: catalase and coagulase tests for staphylococci; oxidase and lactose fermentation tests for Enterobacteriaceae. Because bacteriological culture in the present study was restricted to aerobic incubation, strict anaerobes were not specifically targeted. Molecular confirmation of *E.*

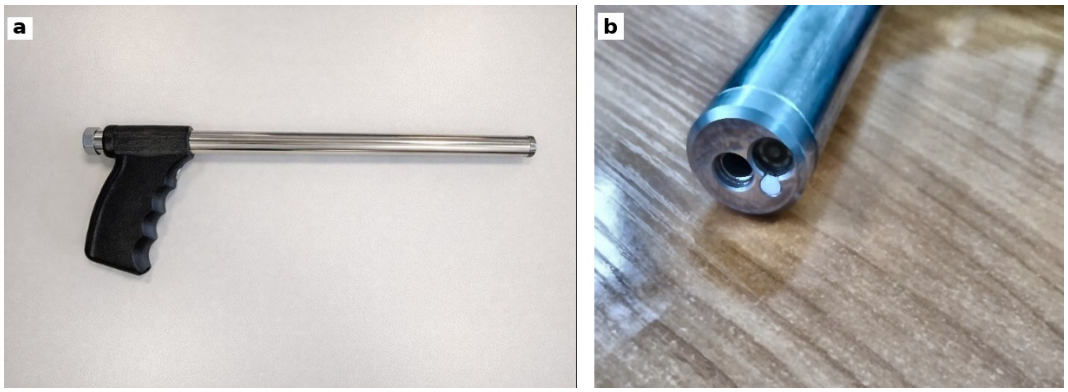

Fig 1. Portable endovideovaginoscope designed for cattle examination. **a)** General view of the portable endovideovaginoscope (handle and stainless-steel probe), **b)** Distal tip showing the built-in video camera, LED illumination, and the working/inspection channel

coli and *S. aureus* was performed using PCR targeting the *fimH* and *nuc* genes, respectively.

Antimicrobial Susceptibility Testing

Antimicrobial susceptibility of the isolates was evaluated using the disk diffusion method on Mueller-Hinton agar (Oxoid Ltd., Basingstoke, UK), following CLSI VET01-A4 (2020) guidelines. The following antibiotic disks were used: ampicillin (10 µg), oxytetracycline (30 µg), gentamicin (10 µg), cephalothin (30 µg), ceftiofur (30 µg), enrofloxacin (5 µg), florfenicol (30 µg), and trimethoprim/sulfamethoxazole (1.25/23.75 µg). Zone diameters were interpreted per CLSI criteria, and the proportion of susceptible isolates was calculated using the formula: %S = S/(S + I + R) x 100.

Molecular Genetic Analysis (PCR)

DNA extraction was performed using a phenol-chloroform protocol. PCR amplification was carried out using DreamTaq PCR Master Mix (Thermo Fisher Scientific, Waltham, MA, USA). Species-specific primers targeting virulence factors were used as previously described [22]:

- nuc gene *(S. aureus):*
  Forward: 5'-ATGAAGTCAAATAAAATCGCT-3'
  Reverse: 5'-TTTGGTGAAAATACTTCTC-3'
- fimH gene *(E. coli):*
  Forward: 5'-TGCAGAACGGATAAGCCGTGG-3'
  Reverse: 5'-GCAGTCACCTGCCCTCCGGTA-3'

Thermal cycling conditions:

- For *nuc*: initial denaturation at 95°C for 5 min; 35 cycles of 94°C for 30 sec, 55°C for 30 sec, and 72°C for 30 sec; final elongation at 72°C for 3 min.
- For *fimH*: initial denaturation at 95°C for 7 min; 35 cycles of 94°C for 30 sec, 57°C for 30 sec, and 72°C for 60 sec; final elongation at 72°C for 7 min.

Amplicons were visualized by agarose gel electrophoresis (3%) under UV illumination.

Statistical Analysis

Because this study was exploratory and based on convenience sampling under field conditions, no a priori power analysis was performed. Statistical analysis was conducted using R software v4.3.2 (packages: epiR, AMR, binom) and GraphPad Prism v10.2. The results are presented primarily as descriptive data. Categorical variables (e.g., pathogen detection and antimicrobial susceptibility categories) are reported as counts, proportions, and 95% confidence intervals (CI) calculated by the Wilson method. Where appropriate, comparisons of proportions were explored using Fisher's exact test or the chi-square test. A P value <0.05 was considered statistically significant, but all inferential results were interpreted cautiously given the limited sample size and the absence of a healthy control group.

Results

Endovideo-vaginoscopic examination of cows diagnosed with clinical endometritis *(Fig. 2)* revealed characteristic pathomorphological changes in the cervico-vaginal region. Direct visualization identified pronounced hyperemia and edema of the cervical mucosa and vaginal fornix, with the mucosal surface appearing moist and glossy. A mucopurulent exudate, distinguished by the loss of transparency and the presence of turbid, viscous mucus containing whitish-yellow flocculent purulent inclusions, was observed accumulating predominantly at the external cervical os. Based on the proportion of purulent material within the mucus (pus ≤50%), the clinical presentation was classified as VDS 2, providing direct visual confirmation of an active inflammatory process within the reproductive tract.

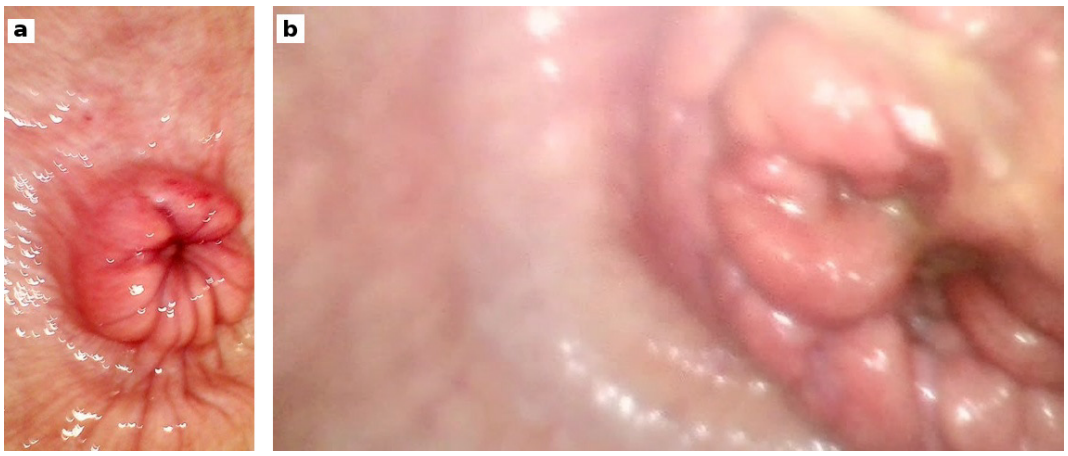

Fig 2. Cervico-vaginal images of clinical endometritis obtained via endovideovaginoscopy. **a)** External cervical os with marked hyperemia and edema, **b)** Mucopurulent exudate and swollen mucosa around the external cervical os, corresponding to a Vaginal Discharge Score (VDS) of 2

Microbiological Profile and Molecular Verification

Bacteriological analysis of 21 samples from cows with clinical endometritis showed that *S. aureus* and *E. coli* were the most frequently isolated bacteria under the aerobic culture conditions used. *S. aureus* was isolated in 11 cases (52.4%) and *E. coli* in 9 cases (42.9%). In several samples, mixed microbial associations (co-infections) were observed, consistent with the polymicrobial nature of postpartum endometritis.

Polymerase chain reaction (PCR) was used for molecular verification and further characterization of the detected bacteria. PCR was performed on a subset of samples (n=15 for *fimH* and n=14 for *nuc),* because some specimens yielded insufficient material and/or DNA of inadequate quality for reliable amplification. These PCR findings should therefore be interpreted as confirmatory results for the tested subset rather than as prevalence estimates for the full cohort.

fimH gene *(E. coli).* Among the 15 DNA samples tested, a specific 508 bp amplicon was detected in 10 cases *(Fig. 3).* The presence of the *fimH* gene, encoding type 1 fimbrial adhesin, supports the adhesion potential of these *E. coli* strains and is consistent with their possible involvement in persistence of endometrial inflammation [21].

nuc gene *(S. aureus).* Among the 14 DNA samples tested, a specific amplicon corresponding to the *nuc* gene was identified in 11 cases *(Fig. 4).* The *nuc* gene is a species-specific marker for *S. aureus,* encoding thermostable nuclease (DNase), and served here as a confirmatory molecular marker for the tested material [22].

Antimicrobial Susceptibility Testing

The results of antimicrobial susceptibility testing (AST) for the isolated pathogens are presented in *Table 1.* Interpretative categories were assigned according to veterinary-specific CLSI standards (CLSI VET01-A4, 2020).

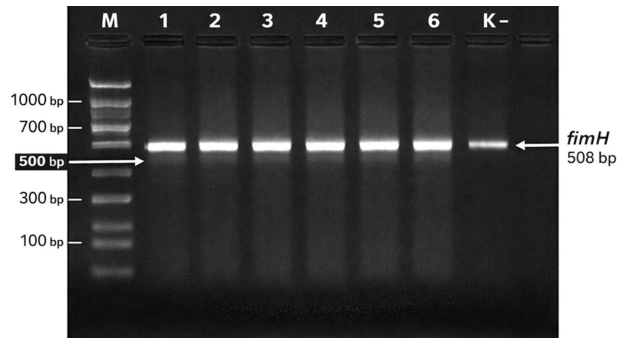

Fig 3. Gel electrophoresis of PCR products for detection of the *fimH* gene in *Escherichia coli.* M, 100 bp DNA ladder; lanes 1-15, samples from the uteri of cows with postpartum endometritis. The presence of a specific band at 508 bp indicates a positive result. No amplicons were detected in negative samples

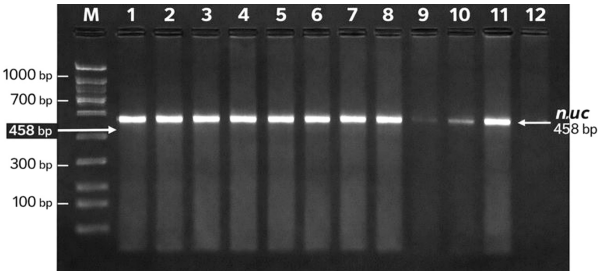

Fig 4. Gel electrophoresis of PCR products for detection of the *nuc* gene in *Staphylococcus aureus.* M, 100 bp DNA ladder; lanes 1-14, samples from the uterine cavity of cows with postpartum endometritis. The presence of a specific band at 458 bp corresponds to a positive result. No amplicons were detected in negative samples

Table 1. *Antimicrobial susceptibility profiles of E. coli and S. aureus isolates obtained from cows with clinical endometritis*

Antimicrobial Agent (Disc Content)	*Escherichia coli* (n=9)			*Staphylococcus aureus* (n=10)		
	S	I	R	S	I	R
Ampicillin (10 µg)	0	1	8	0	2	8
Oxytetracycline (30 µg)	2	1	6	2	1	7
Gentamicin (10 µg)	7	1	1	10	0	0
Cephalothin (30 µg)	6	1	2	8	1	1
Ceftiofur (30 µg)	7	1	1	8	1	1
Enrofloxacin (5 µg)	5	2	2	8	1	1
Florfenicol (30 µg)	6	2	1	8	1	1
Trimethoprim/Sulfamethoxazole (1.25/23.75 µg)	2	1	6	9	0	1

S, susceptible; I, intermediate; R, resistant

Susceptibility profiles were assessed for all *E. coli* isolates (n=9) and for available pure cultures of *S. aureus* (n=10). One *S. aureus* isolate was excluded from AST due to insufficient growth and inability to obtain a stable pure culture during subculturing.

Discussion

In this study, clinical endometritis was diagnosed in 21% of the cows examined at 20-30 DIM. This figure is within the range of prevalence reported for postpartum uterine disease in dairy cows [1,4,28]. Local studies in Kazakhstan similarly indicate a high incidence of endometritis; for example, some surveys have reported clinical endometritis rates on the order of 15-30%, and up to 40% in certain herds [29].

Endovideovaginoscopy under farm conditions facilitated the detection and documentation of clinical endometritis in postpartum cows, particularly in animals lacking overt signs of estrus, in which the condition may be underestimated during routine examination. Rather than inferring uterine status indirectly, video-assisted

vaginoscopy enables direct visualization of the cervico-vaginal mucosa and of vaginal discharge characteristics (Vaginal Discharge Score, VDS), which are widely used clinical indicators of endometritis [18]. However, because this study did not include a head-to-head comparison with conventional vaginoscopy, a speculum examination, or the Metricheck device, the present findings should be interpreted as evidence of field feasibility rather than proof of superior diagnostic performance.

The implementation of endovideovaginoscopy extends standard vaginoscopy by enabling digital imaging and documentation. Veterinary practitioners can record photo and video material directly to a smartphone, facilitating longitudinal monitoring and improving reproducibility of VDS assessment. An additional practical advantage is the integrated heating system for the metallic probe, which may improve operator workflow by reducing optical fogging and may improve animal comfort during field examinations, particularly in unheated facilities and cold climates. Rodrigues et al.[17] reported clearer visualization and greater comfort with videovaginoscopy than with a standard speculum examination in heifers. Our portable system additionally incorporates active heating and wireless data transfer, which enhance its practical field applicability; nevertheless, direct comparative validation against conventional methods remains warranted.

In our study, *T. pyogenes* and strict anaerobes were not isolated. This finding should be interpreted cautiously, because bacteriological culture was limited to aerobic methods and therefore was not designed to recover obligate anaerobic pathogens. Accordingly, the absence of these organisms in the present dataset does not demonstrate their true absence from the uterine environment. Nevertheless, the presence of purulent discharge combined with the isolation of *E. coli* and *S. aureus* supports the bacterial nature of the inflammation in affected cows. Previous studies have shown that up to 15-20% of cases with purulent vaginal discharge may yield no significant bacterial growth, which is consistent with our findings in some samples [19,20].

Analysis of the antibiograms revealed limited *in vitro* activity of several commonly used first-line antimicrobials. In the present study, ampicillin and oxytetracycline showed poor activity against both *E. coli* and *S. aureus* isolates, whereas gentamicin and cephalosporins retained comparatively higher activity. Similar concerns regarding antimicrobial resistance among postpartum uterine isolates have been reported in other settings. In southern Ethiopia, postpartum dairy cows with uterine infections yielded bacterial isolates with variable resistance profiles, highlighting the importance of local susceptibility testing [30]. In China, *S. aureus* isolates obtained from dairy cows also showed substantial resistance and diverse virulence-associated characteristics, supporting the need for cautious antimicrobial selection in bovine practice [31]. In addition, minimum inhibitory concentration data from postpartum bovine uterine isolates demonstrated considerable variability in antimicrobial susceptibility patterns among *E. coli* and *T. pyogenes*, including differences according to clinical status [32]. Likewise, genomic and susceptibility analysis of bovine intrauterine *E. coli* has shown that antimicrobial resistance profiles may differ among strains associated with postpartum uterine infections [21]. Taken together, these findings support our results and reinforce that antimicrobial susceptibility data should be interpreted as descriptive *in vitro* findings from clinically affected cows on a single farm, while treatment decisions should preferably rely on local bacteriological and susceptibility testing. Given the limited number of isolates, these antimicrobial susceptibility findings should be interpreted as descriptive *in vitro* results from clinically affected cows on a single farm.

From a practical perspective, the proposed protocol enables on-farm identification of cows with clinical endometritis based on standardized visual assessment (VDS) with digital documentation, thereby supporting monitoring and record-keeping. The combination of instrumental evaluation with bacteriological culture, antimicrobial susceptibility testing, and targeted molecular verification *(fimH* for *E. coli* and *nuc* for *S. aureus)* strengthens the interpretation of bacteriological findings in clinically affected cows and may support evidence-based antimicrobial selection when treatment is indicated [2,21,22]. The use of a portable, wireless-enabled system may improve the reproducibility of postpartum uterine health monitoring and facilitate data exchange between farms and specialists, especially in remote settings. However, the study has important limitations. Samples were collected only from cows with clinical signs of endometritis, without a contemporaneous clinically healthy control group, which limits pathogen-specific interpretation. Molecular analysis was performed only on a subset of samples because of limited sample volume and/or DNA quality. In addition, the study did not include direct comparison with conventional diagnostic methods and did not assess anaerobic pathogens. Therefore, the microbiological and antimicrobial susceptibility data should be interpreted as descriptive findings from clinically affected cows on a single farm under the conditions of this study.

In conclusion, under farm conditions, the implementation of a portable video-vaginoscopy system combined with bacteriological culture and PCR detection enabled structured on-farm identification and laboratory-supported characterization of clinical endometritis in 21% of cows in the early postpartum period. *E. coli* and *S. aureus* were the most frequently isolated bacteria under the aerobic

culture conditions applied in this cohort. This integrative protocol appears suitable as a practical field approach for reproductive health monitoring and for supporting therapeutic decision-making in remote settings. Nevertheless, further studies including matched healthy controls, anaerobic microbiology, and direct comparison with conventional diagnostic methods are required before stronger conclusions regarding diagnostic accuracy or comparative effectiveness can be made.

Declarations

Availability of Data and Materials: The datasets generated and/or analyzed during the current study are available from the corresponding author (YÖ) upon reasonable request.

Acknowledgements: The authors thank the staff of "Kalihanuly" farm and the AgroTechnopark Research Laboratory at Shakarim University for their assistance in animal handling and sample collection.

Funding Support: This research was funded by the Science Committee of the Ministry of Science and Higher Education of the Republic of Kazakhstan (Grant IRN AP22685400: Development and testing of an endovideovaginoscope for artificial insemination and diagnosis of diseases of the genital organs of cows and sheep).

Ethical Statement: The study was conducted with written consent from the farm owner and approved by the Institutional Ethics Committee of Shakarim University (Protocol No. 16, dated September 10, 2025).

Conflict of Interest: The authors declared that there is no conflict of interest.

Declaration of Generative Artificial Intelligence (AI): The authors declare that the article, tables and figures were not written/created by AI and AI-assisted Technologies.

Authors' Contributions: Conceptualization: Y.O., C.K.; Methodology and study design: D.M.M., Y.S.S., I.T.J.; Field examinations and sample collection: D.M.M., Y.S.S.; Laboratory analyses (bacteriology and PCR): D.M.M., S.A.T., A.A.; Data analysis and interpretation: D.M.M., Y.S.S., C.K., Y.O.; Writing-original draft: D.M.M.; Writing-review and editing: all authors. All authors read and approved the final manuscript.

References

1. **Sheldon IM, Lewis GS, LeBlanc SJ, Gilbert RO:** Defining postpartum uterine disease in cattle. *Theriogenology,* 65 (8): 1516-1530, 2006. DOI: 10.1016/j.theriogenology.2005.08.021
2. **LeBlanc SJ:** Postpartum uterine disease and dairy herd reproductive performance: A review. *Vet J,* 176 (1): 102-114, 2008. DOI: 10.1016/j.tvjl.2007.12.019
3. **LeBlanc SJ:** Postpartum reproductive disease and fertility in dairy cows. *Animal,* 17:100781, 2023. DOI: 10.1016/j.animal.2023.100781
4. **Várhidi Z, Csikó G, Bajcsy ÁC, Jurkovich V:** Uterine disease in dairy cows: A comprehensive review of treatment and prevention strategies. *Vet Sci,* 11 (2):66, 2024. DOI: 10.3390/vetsci11020066
5. **Sheldon IM, Cronin JG, Bromfield JJ:** Tolerance and innate immunity shape the development of postpartum uterine disease and the impact of endometritis in dairy cattle. *Annu Rev Anim Biosci,* 7, 361-384, 2019. DOI: 10.1146/annurev-animal-020518-115227
6. **Galvão KN, Bicalho RC, Jeon SJ:** Symposium review: The uterine microbiome associated with the development of uterine disease in dairy cows. *J Dairy Sci,* 102 (12): 11786-11797, 2019. DOI: 10.3168/jds.2019-17106
7. **Sheldon IM, Molinari PCC, Ormsby TJR, Bromfield JJ:** Preventing postpartum uterine disease in dairy cattle depends on avoiding, tolerating and resisting pathogenic bacteria. *Theriogenology,* 150, 158-165, 2020. DOI: 10.1016/j.theriogenology.2020.01.017
8. **Karstrup CC, Agerholm JS, Jensen TK, Swaro LRV, Schou KK, Rasmussen EL, Krogh KM, Pedersen HG:** Presence and localization of bacteria in the bovine endometrium postpartum using fluorescence in situ hybridization. *Theriogenology,* 92, 167-175, 2017. DOI: 10.1016/j.theriogenology.2017.01.026
9. **Iancu I, Popa SA, Degi J, Gligor A, Popa I, Iorgoni V, Nistor P, Imre K, Nichita I, Herman V:** Aerobic uterine pathogens in dairy cattle: Surveillance and antimicrobial resistance profiles in postpartum endometritis. *Antibiotics (Basel),* 14 (7):650, 2025. DOI: 10.3390/antibiotics14070650
10. **Shafique L, Wu S, Aqib AI, Ali MM, Ijaz M, Naseer MA, Sarwar Z, Ahmed R, Saleem A, Qudratullah, Ahmad AS, Pan H, Liu Q:** Evidence-based tracking of MDR *Escherichia coli* from bovine endometritis and its elimination using colistin in the field. *Antibiotics (Basel),* 10 (8):997, 2021. DOI: 10.3390/antibiotics10080997
11. **Pleticha S, Drillich M, Heuwieser W:** Evaluation of the Metricheck device and the gloved hand for the diagnosis of clinical endometritis in dairy cows. *J Dairy Sci,* 92 (11): 5429-5435, 2009. DOI: 10.3168/jds.2009-2117
12. **Denis-Robichaud J, Dubuc J:** Determination of optimal diagnostic criteria for purulent vaginal discharge and cytological endometritis in dairy cows. *J Dairy Sci,* 98 (10): 6848-6855, 2015. DOI: 10.3168/jds.2014-9120
13. **Denis-Robichaud J, Barbeau-Grégoire N, Gauthier ML, Dufour S, Roy JP, Buczinski S, Dubuc J:** Validity of diagnostic tests for purulent vaginal discharge and endometritis in dairy cows using Bayesian latent class analysis. *Prev Vet Med,* 239:106521, 2025. DOI: 10.1016/j.prevetmed.2025.106521
14. **Ernstberger M, Oehl H, Haessig M, Hartnack S, Bollwein H:** Predicting the probability of conception based on a combination of clinical examination results of cows with limited vaginal discharge. *Theriogenology,* 137, 121-128, 2019. DOI: 10.1016/j.theriogenology.2019.07.004
15. **Tobolski D, Krupa M, Polak Z, Pascottini OB, Opsomer G, Barański W:** Exploring the influence of endometritis diagnostic criteria on uterine involution, milk yield and reproductive performance in dairy cows. *BMC Vet Res,* 21 (1):276, 2025. DOI: 10.1186/s12917-025-04727-7
16. **Moore SG, Feehily C, Doyle RC, Buckley F, Lonergan P, Cotter PD, Butler ST:** Associations among postpartum uterine and vaginal microbiota and the development of purulent vaginal discharge in dairy cows. *J Dairy Sci,* 106 (11): 8133-8151, 2023. DOI: 10.3168/jds.2022-22720
17. **Rodrigues GJ, Monteiro BM, Viana RB, da Silva AOA, Monteiro FDO, Teixeira PPM:** New method of video-assisted vaginoscopy in Nellore heifers. *Vet Med Sci,* 9 (6): 2781-2785, 2023. DOI: 10.1002/vms3.1232
18. **Leutert C, von Krueger X, Plöntzke J, Heuwieser W:** Evaluation of vaginoscopy for the diagnosis of clinical endometritis in dairy cows. *J Dairy Sci,* 95 (1): 206-212, 2012. DOI: 10.3168/jds.2011-4603
19. **Westermann S, Drillich M, Kaufmann TB, Madoz LV, Heuwieser W:** A clinical approach to determine false-positive findings of clinical endometritis by vaginoscopy using uterine bacteriology and cytology in dairy cows. *Theriogenology,* 74 (7): 1248-1255, 2010. DOI: 10.1016/j.theriogenology.2010.05.028
20. **Runciman DJ, Anderson GA, Malmo J, Davis GM:** Use of postpartum vaginoscopic examination of dairy cows for the diagnosis of endometritis and the association of endometritis with reduced reproductive performance. *Aust Vet J,* 86 (5): 205-213, 2008. DOI: 10.1111/j.1751-0813.2008.00301.x

21. **Yang LM, Wang YH, Peng Y, Min JT, Hang SQ, Zhu WY:** Genomic characterization and antimicrobial susceptibility of bovine intrauterine *Escherichia coli* and its relationship with postpartum uterine infections. *J Integr Agric,* 15 (6): 1345-1354, 2016. DOI: 10.1016/S2095-3119(15)61170-4

22. **Brakstad OG, Aasbakk K, Maeland JA:** Detection of *Staphylococcus aureus* by polymerase chain reaction amplification of the nuc gene. *J Clin Microbiol,* 30 (7): 1654-1660, 1992. DOI: 10.1128/jcm.30.7.1654-1660.1992

23. **Li Z, Teng Y, Feng S, Hu Z, Zhao J, Ding H, Fang Y, Liu H, Ma X, Guo J, Wang J, Lv W:** Microbial responses and changes in metabolic products in bovine uteri infected with *Staphylococcus aureus*. *Int J Biol Macromol,* 262 (Pt 2):130039, 2024. DOI: 10.1016/j.ijbiomac.2024.130039

24. **Gonzalez Moreno C, Torres Luque A, Oliszewski R, Rosa RJ, Otero MC:** Characterization of native *Escherichia coli* populations from bovine vagina of healthy heifers and cows with postpartum uterine disease. *PLoS One,* 15 (2):e0228294, 2020. DOI: 10.1371/journal.pone.0228294

25. **He X, Wang J, Jiang L, Wang X, Wang Y, Liu Y, Cheng Y, Xu F, Li X:** Uterine microbiota composition in dairy cows with different vaginal discharge scores: Suggesting *Caviibacter* as a potential pathogen in mild purulent metritis. *Microorganisms,* 13 (8):1728, 2025. DOI: 10.3390/microorganisms13081728

26. **Edmonson AJ, Lean IJ, Weaver LD, Farver T, Webster G:** A body condition scoring chart for Holstein dairy cows. *J Dairy Sci,* 72 (1): 68-78, 1989. DOI: 10.3168/jds.S0022-0302(89)79081-0

27. **Okawa H, Fujikura A, Wijayagunawardane MMP, Vos PLAM, Taniguchi M, Takagi M:** Effect of diagnosis and treatment of clinical endometritis based on vaginal discharge score grading system in postpartum Holstein cows. *J Vet Med Sci,* 79 (9): 1545-1551, 2017. DOI: 10.1292/jvms.16-0593

28. **Kurt S, Salar S, Özdal Salar M:** Antibiogram and pathogen isolation from vaginal discharge in dairy cows with metritis. *Vet Hekim Der Derg,* 90 (2): 66-70, 2019. DOI: 10.33188/vetheder.509535

29. **Gabdullin DE, Julanov M, Tagayev O, Zainettinova DB, Kadraliyeva B, Zakirova F, Kozhayeva A, Sidikhov B, Zholdasbekov A, Yertleuova B, Aitpakova Z:** Evaluation of blood parameter changes on treatment efficacy in cows with purulent-catarrhal endometritis in farms of West Kazakhstan Region. *Int J Vet Sci,* 15 (1): 225-232, 2026. DOI: 10.47278/journal.ijvs/2025.113

30. **Shafique L, Wu S, Aqib AI, Ali MM, Ijaz M, Naseer MA, Sarwar Z, Ahmed R, Saleem A, Qudratullah, Ahmad AS, Pan H, Liu Q:** Evidence-based tracking of MDR *Escherichia coli* from bovine endometritis and its elimination by effective novel therapeutics. *Antibiotics (Basel),* 10 (8):997, 2021. DOI: 10.3390/antibiotics10080997

31. **Dan M, Yehui W, Qingling M, Jun Q, Xingxing Z, Shuai M, Kuojun C, Jinsheng Z, Zibing C, Zaichao Z, Xuepeng C:** Antimicrobial resistance, virulence gene profile and molecular typing of *Staphylococcus aureus* isolates from dairy cows in Xinjiang Province, northwest China. *J Glob Antimicrob Resist,* 16, 98-104, 2019. DOI: 10.1016/j.jgar.2018.08.024

32. **Basbas C, Garzon A, Silva-Del-Rio N, Byrne BA, Karle B, Aly SS, Champagne JD, Williams DR, Lima FS, Machado VS, Pereira RV:** Evaluation of antimicrobial resistance and risk factors for recovery of intrauterine *Escherichia coli* from cows with metritis on California commercial dairy farms. *Sci Rep,* 12:13937, 2022. DOI: 10.1038/s41598-022-18347-w

Kafkas Universitesi Veteriner Fakultesi Dergisi
Journal Home-Page: http://vetdergikafkas.org
E-ISSN: 1309-2251

Kafkas Univ Vet Fak Derg
32 (2): 299-300, 2026
DOI: 10.9775/kvfd.2026.36194

LETTER TO THE EDITOR

Increasing Feline Mycobacterial Infections and Diagnostic Confusion

Ebru ERAVCI YALIN [1 (*)], Mehmet Fatih BOZKURT [2]

[1] Istanbul University-Cerrahpaşa, Faculty of Veterinary Medicine, Surgery Department, TR-34320 Istanbul - TÜRKİYE
[2] Afyon Kocatepe University, Faculty of Veterinary Medicine, Pathology Department, TR-03200 Afyonkarahisar - TÜRKİYE

(*) **Corresponding author:**
Ebru Eravci Yalin
Phone: +90 212 404 0300
Cellular phone: +90 537 572 9679
E-mail: ebru.eravciyalin@iuc.edu.tr

Article ID: KVFD-2026-36194
Received: 24.01.2026
Accepted: 24.02.2026
Published Online: 24.02.2026

How to cite this article?

Eravcı Yalın E, Bozkurt MF: Increasing Feline Mycobacterial Infections and Diagnostic Confusion. *Kafkas Univ Vet Fak Derg*, 32 (2): 299-300, 2026. DOI: 10.9775/kvfd.2026.36194

Dear Editor,

Mycobacterial infections in cats are characterized by granulomatous inflammation and are considered among diseases that are infrequently reported in the literature, while being capable of involving multiple organ systems and presenting with variable clinical manifestations [1]. During the evaluation of feline patients presenting to the clinics of Istanbul University-Cerrahpaşa Veterinary Hospital and the review of imaging consultations referred to our unit, cases exhibiting findings consistent with mycobacterial infections were encountered with noteworthy frequency. In addition, consultation requests from colleagues in different cities regarding feline cases with similar clinical and radiological features suggest that this situation may indicate a broader distribution rather than merely reflecting a local case accumulation.

When feline cases diagnosed with mycobacterial infection in the clinic were examined, it was observed that mycobacterial infections may involve numerous organs and systems. Ocular involvement was identified as retinal detachment, uveitis, intraocular or retrobulbar mass-like formations, and conjunctival masses. Central nervous system involvement manifested as single or multiple mass lesions in the brain and spinal cord, as well as a meningitis pattern. Pulmonary involvement was characterized by diffuse or localized interstitial pneumonia patterns accompanied by nodular opacities. In the nasal region, space-occupying lesions involving the nasal cavity and sinuses, with associated involvement of the bone and the potential to cause soft tissue swelling or ulcerative lesions, were detected. In addition, single or multiple mass-like lesions in the skin and subcutaneous tissue, lytic lesions or cortical thickening in bone, enlargement and mineralization of lymph nodes, as well as various internal organ involvements, were identified during clinical and imaging evaluations.

One of the main problems encountered during the diagnostic process is that lesions may be interpreted as progressive histiocytoma or nonspecific histiocytic inflammation during histopathological evaluation of biopsy specimens. In lesions in which granulomatous or pyogranulomatous inflammation predominates, failure to adequately consider a mycobacterial etiology during the initial evaluation may lead to delays in diagnosis. Imaging findings also contribute significantly to diagnostic uncertainty. In cases with central nervous system involvement, contrast-enhancing lesions producing mass effect on magnetic resonance imaging are frequently interpreted in favor of neoplastic processes. Similarly, nodular or interstitial patterns detected on thoracic radiographs are often considered consistent with fungal infections. To illustrate these diagnostic challenges, representative examples of clinical appearance and imaging findings corresponding to different anatomical localizations are presented below *(Fig. 1)*.

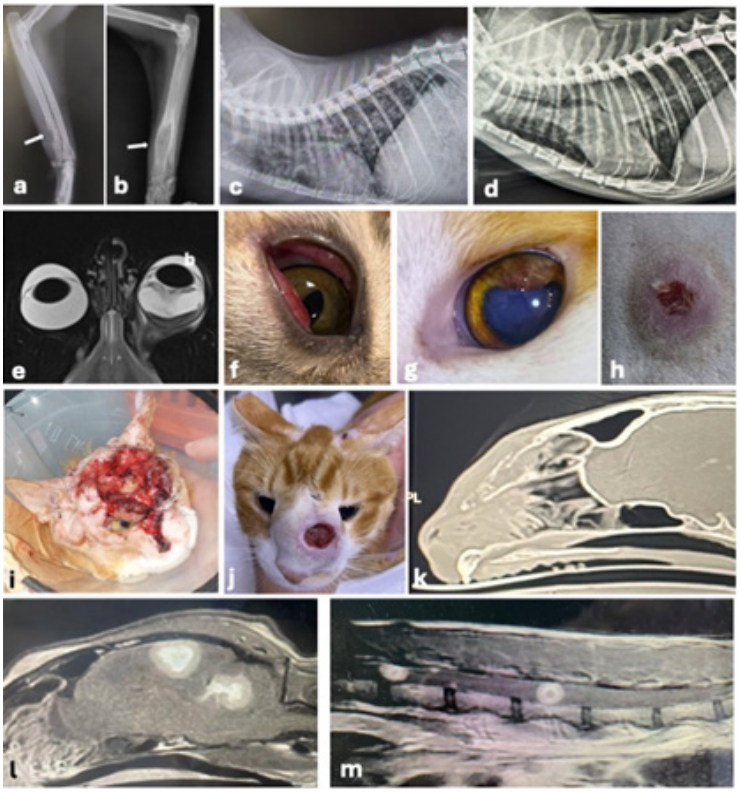

Fig 1. (a) Lateral radiograph of the ulna with osteolysis (arrow), (b) the radius with fusiform shaped, moth eaten- lysis and cortical expansion, (c) a miliary nodular pattern with multiple small soft tissue nodules, (d) marked perihilar lymphadenopathy, (e) retinal detachment with subretinal exudation and perineural mass surrounding the optic nerve, (f) upper and lower eyelid conjunctival mass, (g) dorsolateral uveal granuloma, (h) cutaneous nodular lesion with a centrally ulcerated, well-defined margin, (i) severe ulcerated cutaneous mass with raised, irregular margins, (j) nasal cutaneous lesion with central ulceration, raised margins, and expansion of the nasal bone, (k) computed tomography image of the nasal region showing soft tissue attenuation occupying the nasal cavity, and a focal lytic area involving the dorsal nasal wall, MRI images of the brain (l) and spinal cord (m), sagittal T1W post-contrast sequences shows round mass like lesions with a concentric target sign

Another important consequence of delayed or incorrect recognition of mycobacterial infections is the underestimation of the disease's potential for transmission. Members of the Mycobacterium tuberculosis complex are known to pose a zoonotic risk in cats. In particular, Mycobacterium bovis infections represent a public health concern for animal owners and veterinary professionals who are in contact with infected animals [2,3].

In feline cases presenting with granulomatous lesions involving multiple organ systems and mimicking neoplastic or fungal diseases, mycobacterial infections should be carefully considered in the differential diagnosis. Considering the presence of similar cases reported from different cities, increasing veterinary awareness of this disease is expected to contribute significantly to improving diagnostic accuracy and to a better understanding of its epidemiological characteristics.

References

1. **Lloret A, Hartmann K, Pennisi MG, Gruffydd-Jones T, Addie D, Belák S, Boucraut-Baralon C, Egberink H, Frymus T, Hosie MJ, Lutz H, Marsilio F, Möstl K, Radford AD, Thiry E, Truyen U, Horzinek MC:** Mycobacterioses in cats: ABCD guidelines on prevention and management. *J Feline Med Surg*, 15 (7): 591-597, 2013. DOI: 10.1177/1098612X13489221
2. **O'Halloran C, Tørnqvist-Johnsen C, Woods G, Mitchell J, Reed N, Burr P, Gascoyne-Binzi D, Wegg M, Beardall S, Hope J, Gunn-Moore D:** Feline tuberculosis caused by *Mycobacterium bovis* infection of domestic UK cats associated with feeding a commercial raw food diet. *Transbound Emerg Dis*, 68 (4): 2308-2320, 2021. DOI: 10.1111/tbed.13889
3. **Commandeur S, van der Most M, Koomen J, van Keulen L, Dinkla A, Luinenburg X, Escher M, Jacobs P, Keur I, Grinwis GCM, Weerts E, Broens EM, Anthony R, Kamst-van Agterveld M, Rebel K, Huisman E, Heijne M, Koets A:** *Mycobacterium bovis* infected domestic cats in an officially bovine tuberculosis free country resulting in human infection. *One Health*, 20:101048, 2025. DOI: 10.1016/j.onehlt.2025.101048

Kafkas Universitesi Veteriner Fakultesi Dergisi
Journal Home-Page: http://vetdergikafkas.org
E-ISSN: 1309-2251

Kafkas Univ Vet Fak Derg
Volume: 32, Issue: 2, Year: 2026

ETHICAL PRINCIPLES AND PUBLICATION POLICY

Kafkas Universitesi Veteriner Fakultesi Dergisi follows and implements internationally accepted ethical standards to provide the necessary support to original scientific ideas and to publish high quality, reliable scientific articles in this direction. The journal's publication policy and ethical principles include the ethical standards of conduct that should be followed by author(s), journal editor(s), associate editors, subject editors, reviewers, and publishers who are the participants of this action.

The ethical statement of Kafkas Universitesi Veteriner Fakultesi Dergisi is based on the principles indicated in the "COPE Code of Conduct and Best Practice Guidelines for Journal Editors" (http://publicationethics.org/files/Code_of_conduct_for_journal_editors_Mar11.pdf) and "COPE Best Practice Guidelines for Journal Editors" (http://publicationethics.org/files/u2/Best_Practice.pdf).

GENERAL ETHICAL PRINCIPLES

• Objectivity and Independence

Editor-in-chief, editors, associate editors, and referees conduct the evaluation process of the manuscript sent to the journal objectively and in coordination within the framework of ethical principles. Editorial decisions are independent, and internal or external factors cannot influence these decisions. In accordance with the principle of impartiality, academics working in our institution are not deemed eligible to work as a section editor in Kafkas Universitesi Veteriner Fakultesi Dergisi, in order not to be effective in the evaluation of articles due to conflict of interest.

• Privacy

The content of the articles and the personal information of the authors such as name, e-mail address, and telephone numbers that are sent to Kafkas Universitesi Veteriner Fakultesi Dergisi are used only for the scientific purposes of the journal and not for other purposes, and cannot be shared with third parties. Article evaluation processes are also carried out confidentially.

• Authorship and Authors Rights

The authors of the manuscripts sent to Kafkas Universitesi Veteriner Fakultesi Dergisi must have contributed significantly to the design, execution or interpretation of the study. For example, in view of the research and publication ethics as well as authors rights, it is not acceptable to include those as authors who do not actively contribute to the research but just only help in writing or data collection processes, which may not require any scientific knowledge. All the authors in a publication should be in agreement of the names and the orders of the authors in the manuscript.

The competence of the authors to the subject of the study is evaluated by the editor within the framework of deontological rules and the professional fields of each author.

The corresponding author of the article should declare the contributions of the authors to the work under the title of "Author contributions". The corresponding author is primarily responsible for the problems that may arise in this regard.

In multidisciplinary studies, 2 authors who are from different disciplines can be "equivalent first name authors" and up to most 3 authors who are also from different disciplines can be "equivalent second name authors".

• Generative Artificial Intelligence (AI)

This declaration outlines the acceptable uses of generative AI technology in writing or editing manuscripts submitted to Kafkas Universitesi Veteriner Fakultesi Dergisi. During the writing process, AI and AI-assisted technologies are prohibited from writing or creating the article, tables, or figures. Authors should use AI and AI-assisted technologies solely to enhance the readability and language of the article. Authors should carefully review and edit the result of assisted parts of the manuscript by AI in term of reliability of the applying technologies.

When using generative AI and AI-assisted technologies in scientific writing, authors must declare this by including a statement in the cover letter when the article is first submitted. Once the article is accepted for publication, this statement should be included in the declarations section of the manuscript's final part.

If anything other than the declared conditions is detected, the articles in the evaluation stage will be rejected, and if it is detected in the published articles, the article will be retracted.

• Originality of Research Findings

The authors should declare that the article they presented contained the original research results, that the study data were analyzed correctly, and that they were prepared for publication using adequate and appropriate references, in the "cover letter" section of the on-line system at the submission stage. Using expressions such as "it is the first study done", "there has been no previous study on this subject" and "there is a limited number of studies" to add originality and importance to the article is not acceptable and may cause prevention of the scientific evaluation of the article by the editor.

• Similarity

Articles submitted to the journal are subjected to similarity analysis using appropriate software (iThenticate by CrossCheck) at the beginning and at every required stage. If unethical similarities are detected regardless of the rate of similarity, this situation is reported to the authors and corrections are requested or articles containing excessive similarities are rejected at the first evaluation stage without being evaluated.

• Plagiarism/Self-Plagiarism, Duplicate Publication

Kafkas Universitesi Veteriner Fakültesi Dergisi applies publication ethics and verifies the originality of content submitted before publication and checks all submitted manuscripts for plagiarism/self-plagiarism, similarity and duplication. All submitted manuscripts are meticilously screened by a similarity detection software (iThenticate by CrossCheck). Papers previously presented at scientific meetings and published only as an "abstract" should be indicated in the Title Page file as stated in the "Guidance for Authors". Authors do not have the right to use entire paragraphs from their previous publications into a new submission. These actions are also considered as a plagiarism. In any case, the manuscript should be original in terms of scientific contents and writing. In the event of alleged or suspected research misconduct, the Editorial Board will follow and act in accordance with "COPE Guidelines".

• Multi-part Publication (Piecemeal Publication)

Some authors may tend to divide study data into two or more articles and publish the results in different journals also having different authors names and orders. In principal, Kafkas Universitesi Veteriner Fakultesi Dergisi is against multi-part publication. When necessary, the ethical committee approval information of the study, project information, congress presentations, etc. are checked and such situations that will create an ethical problem are identified and reported to the authors.

Authors may think that their work should be published in multi parts that complement each other. For this, each part of the article should be titled "Part-I", "Part-II" and submitted to the journal "simultaneously". This issue can be evaluated by the editor-in-chief/subject editors/referees who may suggest that the article can be published in parts or as a whole. In addition, rejection of a submission presented in parts means that all parts will be rejected.

• Animal Rights and Ethics

The authors are responsible for conducting experimental and clinical studies on animal experiments within the framework of existing international legislation on animal rights. Authors must also obtain permission from the Animal Experiment Ethics Committees and provide relevant information in the Material and Method section to experiment with animals. In clinical studies, as well as the approval of the ethics committee, an "informed consent form" should be obtained from the animal owners and the information related to it should be declared in the Material and Method section. Declaration of "informed consent form" is sufficient for the articles in the "Case report" and "Letter to the Editor" category.

Ethics committee permission taken for a study can only be used in one article. It is unacceptable to use the same ethics committee approval number in articles with different names and contents. The editor/subject editors can request from the corresponding author, if necessary, to send a copy of the ethics committee approval form to the journal (electronically or by post).

In cases of violation ethical rules, the article is not taken into consideration or if it is in the evaluation stage, the procedure is terminated and the article is rejected.

• Conflicts of Interest/Competing Interests

The editor-in-chief pays attention to whether there is a conflict of interest or union of interest between editors, reviewers and author (s) for an objective and unbiased evaluation of the article. In addition, the authors should disclose any financial interests or links or any conditions that may raise the bias issue in research and article under the above heading.

• Copyright

The authors must fill in the "Copyright Agreement Form" and sign it with a wet signature. Authors who submit articles from abroad should scan the signed form and send it to the editor via the system or by e-mail. Original forms that are wet signed for articles sent domestically should be submitted to the journal via mail or cargo. The works of the authors who do not submit the Copyright Agreement Form on time are not published.

• Withdrawal of a Submission

In case of if the authors detect a significant error or deficiency in their article under review or if this error is reported to them by the editor/subject editor/referees they can contact immediately to the editor-in-chief and ask the request to withdraw the article by stating the reason. The decision on this issue is up to the editorial board.

• Erratum

After an article has been published, the corresponding author may request the editor to publish "erratum" for any errors or inaccuracies noticed by the authors, editors or readers. In collaboration with the authors, the editor prepares and publishes the Erratum article in the first upcoming issue. These articles, like other publications, should contain the publication tag and DOI number.

• Retraction

If any ethical problem is detected about the article that cannot be compensated and cannot be eliminated with erratum after the article is published, the editor-in-chief and associate editors prepare a justification about the article and apply the retraction procedure to the article. The text file on the web page of a retracted article is blocked and the reason for retraction is added to the system as a file, ensuring that it is constantly in the archive.

• Advertising

Kafkas Universitesi Veteriner Fakultesi Dergisi do not accept advertising and sponsorships that are believed to create a potential conflict of interest. If the article sent to Kafkas Universitesi Veteriner Fakultesi Dergisi is for the promotion of a commercial product and/or the work carried out is directly supported by a company, it is rejected without consideration.

OPEN ACCESS STATEMENT

Kafkas Universitesi Veteriner Fakultesi Dergisi
Journal Home-Page: http://vetdergikafkas.org
E-ISSN: 1309-2251

Kafkas Univ Vet Fak Derg
Volume: 32, Issue: 2, Year: 2026

ARTICLE EVALUATION AND PUBLICATION PROCESS

• Initial Evaluation Process

Articles submitted to Kafkas Universitesi Veteriner Fakultesi Dergisi are primarily evaluated by the editors and associate editors. At this stage, articles not having suitable scope and aims, with low original research value, containing scientific and ethically important errors, having low potential to contribute to science and the journal, and having poor language and narration are rejected by the editor without peer-review process. Initial evaluation process takes up to most 2 weeks.

• Preliminary Evaluation Process

Articles that are deemed appropriate for editorial evaluation are sent to the subject editor related to the category of articles to be examined in terms of scientific competence and to the statistics editor for evaluation in terms of statistical methods. The suject editors examine the article in all aspects and report their decisions (rejection, revision or peer-review) to the chief editor. This stage takes about 1 month.

• Peer-review Process

Double-blind peer-review is applied to the articles that have completed preliminary evaluation process. Suggestions of subject editors are primarily considered in referee assignment. In addition, reviews can be requested from the referees registered in the journal's referee pool. At least 2 referees are assigned for peer-review. Opinion of more referees can be required depending on the evaluation process. At this stage, referees send their decision (reject, revision or accept) about the article to the editor-in-chief. If the rejection decision given by a referee reflects sufficient examination and evidence-based negativities or ethical problems about the scientific content and accuracy of the article, this decision is checked by the editor-in-chief and associate editors and submitted to the authors regardless of the other referees' decisions. The time given to referees to evaluate an article is ~4 weeks.

• Publication Process of an Article

Total evaluation period of an article, which is completed in the peer-review phase after completing the initial and preliminary evaluation process, takes 4-6 months. The articles that have completed the subject editorial and peer-review evaluation stages and accepted by the editorial are sent to the corresponding author for final checks and necessary final additions. After the acceptance, the article designed in the publication format of the journal is given an DOI number and published immediately on the Article in Press page. When it is time to publish the periodic edition of the journal, a selection is made from the articles kept on the Article in Press page, taking into account the submission date. The time it takes for the article to be published by taking the page number is 6-12 months.

NO PUBLICATION FEE

Processing and publication are free of charge with the journal. There is no article processing charges, submission fees or any other fees for any submitted or accepted articles.

RESPONSIBILITIES OF THE PUBLISHER, EDITORS AND ASSOCIATE EDITORS

The publisher (Dean of the Faculty of Veterinary Medicine of Kafkas University) contributes to the execution of the journal's routine processes such as printing, archiving, and mailing, in line with requests from the editor.

The publisher undertakes to carry out an independent and fair decision-making mechanism for its editors and assistants in the article evaluation process and decisions.

The publisher undertakes to carry out an independent and fair decision-making mechanism for its editors and associate editors in the article evaluation process and decisions.

Editor-in-chief/editors/associate editors of Kafkas Universitesi Veteriner Fakultesi Dergisi evaluate the articles submitted to the journal regardless of their race, gender, religious belief, ethnicity, citizenship or political views. In addition, it undertakes not to give any information about the article except for the authors, subject editors and referees.

Kafkas Universitesi Veteriner Fakultesi Dergisi follows internationally accepted principles and criteria and takes the necessary decisions to apply in the journal.

Editor-in-chief/editors/associate editors conduct the evaluation and decision process in the journal in coordination within the principles of confidentiality and have independent decision-making authority and responsibility without being affected by any internal or external factors.

Editor-in-chief/editors/associate editors make and implement all kinds of planning for the development of the journal and its international recognition. They also follow national and international meetings or events on the development of journals and article evaluation, and ensures that the journal is represented on these platforms.

The editor-in-chief/editors/associate editors make every effort to ensure that the journal's subject editors and referee pool have international qualifications. Likewise, it makes the necessary attempts to strengthen the author's profile.

Editor-in-chief/editors/associate editors make plans to improve the quality of the articles published in the journal and carry out the necessary process.

Editor-in-chief/editors/associate editors regularly conduct and control the initial evaluation, preliminary evaluation, peer review and acceptance-rejection decisions of articles submitted to the journal. While carrying out these procedures, features such as the suitability of the study for the aims and scope of the journal, its originality, the up-to-date and reliability of the scientific methods used, and the potential it will contribute to the development of the journal as well as its benefit to science/practice are taken into consideration.

Editor-in-chief/editors/associate editors systematically review, inspect and make decisions about the articles submitted to the journal in terms of features such as author rights, conflict of interest, observance and protection of animal rights, and compliance with research and publication ethics.

The editor-in-chief conducts the evaluation/revision process between the authors and subject editors and referees, and ensures that it is completed within the prescribed time.

Kafkas Universitesi Veteriner Fakultesi Dergisi
Journal Home-Page: http://vetdergikafkas.org
E-ISSN: 1309-2251

Kafkas Univ Vet Fak Derg
Volume: 32, Issue: 2, Year: 2026

ARCHIVE POLICY

The editorial office of the Kafkas Üniversitesi Veteriner Fakültesi Dergisi and the publisher (Dean's Office of the Faculty of Veterinary Medicine, Kafkas University) keep all the articles (electronic and printed) published in the journal in their archives. All articles and their attachment files sent to the journal are kept securely in the archive. In light of the technological developments, the editorial office of the Kafkas Üniversitesi Veteriner Fakültesi Dergisi regularly performs electronic processes for the development and updating of materials in digital environment and presents them to its readers on condition of keeping in safe the original documents and information regarding the articles.

Even if the journal ceases to be published for any reason, the publisher (Dean's Office of the Faculty of Veterinary Medicine, Kafkas University) will continue to protect the journal content in the long term and provide convenient access to users. Electronic services of Kafkas University Information Technologies Department will be used for the journal to maintain this responsibility.

RESPONSIBILITIES OF SUBJECT EDITORS

Subject editors do reviews and evaluations in accordance with the main publication goals and policies of the journal and in line with the criteria that will contribute to the development of the journal.

Author information is kept confidential in articles sent to the subject editor for preliminary evaluation by the editor.

Subject editors thoroughly examine the sections of the introduction, materials and methods, results, discussion and conclusion, in terms of journal publication policies, scope, originality and research ethics. Subject editor submits its decision (rejection, revision or peer-review) after evaluation to the chief editor in a reasoned report.

Subject editor may request additional information and documents related to the study from the authors, when necessary.

In multidisciplinary studies, the article can be submitted for the evaluation of multiple subject editors.

RESPONSIBILITIES OF REFEREES

Double-blinded peer-review procedure is applied in Kafkas Universitesi Veteriner Fakultesi Dergisi in order to evaluate the articles submitted to the journal in accordance with the principle of impartiality and in objective criteria; that is, referees and writers do not know about each other.

The referees submit their opinions and reports to the editor-in-chief to ensure the control and suitability of a submitted article, its scientific content, scientific consistency and compliance with the principles of the journal. When a referee makes a decision "reject" about an article, he/she prepares the reasons for the decision in accordance with the scientific norms and presents it to the editor.

The referee(s) also gives the authors the opportunity to improve the content of the article. Accordingly, the revisions requested from the authors should be of a quality that explains/questions specific issues rather than general statements.

Referees appointed for the evaluation of the articles agree that the articles are confidential documents and will not share any information about these documents with third parties, except for the editors participating in the evaluation.

Referees should place their criticism on scientific infrastructure and write their explanations based on scientific evidence. All comments made by the referees to improve the articles should be clear and direct, and should be written away from disturbing the feelings of the author. Insulting and derogatory statements should be avoided.

If a referee has an interest relationship with the author(s) on one or more issues, he/she must report the situation to the editor and ask his/her to withdraw from the referee position. The same is also applicable when the authors illegally obtain information about the referees of the article and try to influence them.

The editor-in-chief can share the comments and reports from the referees with the editors/associate editors and the relevant subject editor, as necessary, to ensure that the decision on the article is optimal. If necessary, the editor may share the critical decision and its grounds that a referee has sent about the article with the other referee(s) and present them to their attention.

Referee(s) may request revision many times for the article they evaluated.

The content of the referee reports is checked and evaluated by editor-in-chief/editors/associate editors. The final decision belongs to the editorial.

RESPONSIBILITIES OF AUTHOR(S)

It is not tolerable for the author (s) to send an article, which has been already sent to another journal, to Kafkas Universitesi Veteriner Fakultesi Dergisi within the scope of "which accepts" or "which publishes first" approach. If this is detected, the article is rejected at any stage of the evaluation. As a possible result of these actions, in the process following the previous acceptance of the article sent to another journal, the withdrawal request with this excuse that the authors submit for this article, the evaluation process of which is going on in our journal, is evaluated by the editors and associate editors of the journal and disciplinary action on the grounds of ethical violations about those responsible is started. This unethical action is also informed to the journal editor (if known) who accepted the article.

It is essential that the articles to be sent to Kafkas Universitesi Veteriner Fakultesi Dergisi include studies that have up-to-date, original and important clinical/practical results and prepared in accordance with the journal's writing rules.

Authors should choose the references they use during the writing of the article in accordance with the ethical principles and cite them according to the rules.

The authors are obliged to revise the article in line with the issues conveyed to them during the initial evaluation, preliminary evaluation and peer-review phases of the article and to explain the changes they made/did not make sequentially in the "response to editor" and "response to reviewer comments" sections.

If information, documents or data regarding to the study are requested during the evaluation process, the corresponding author is obliged to submit them to the editorial.

Authors should know and take into account the issues listed in the "General Ethical Principles" section regarding scientific research and authors.

The authors do not have the right to simultaneously submit multiple articles to Kafkas Universitesi Veteriner Fakultesi Dergisi. It is more appropriate to submit them with acceptable time intervals for the journal's policy.

Kafkas Universitesi Veterinar Fakultesi Dergisi
Journal Home-Page: http://vetdergikafkas.org
E-ISSN: 1309-2251

Kafkas Univ Vet Fak Derg
Volume: 32, Issue: 2, Year: 2026

INSTRUCTION FOR AUTHORS

1- Kafkas Universitesi Veteriner Fakultesi Dergisi (abbreviated title: Kafkas Univ Vet Fak Derg), published bi-monthly (E-ISSN: 1309-2251). We follow a double-blind peer-review process, and therefore the authors should remove their name and any acknowledgment from the manuscript before submission. Author names, affiliations, present/permanent address etc. should be given on the title page only.

The journal publishes full-length research papers, short communications, preliminary scientific reports, case reports, observations, letters to the editor, and reviews. The scope of the journal includes all aspects of veterinary medicine and animal science.

Kafkas Universitesi Veteriner Fakultesi Dergisi is an Open Access journal, which means that all content is freely available without charge to the user or his/her institution. Users are allowed to read, download, copy, distribute, print, search, or link to the full texts of the articles, or use them for any other lawful purpose, without asking prior permission from the publisher or the author. This is in accordance with the BOAI definition of Open Access.

2- The official language of our journal is English.

3- The manuscripts submitted for publication should be prepared in the format of Times New Roman style, font size 12, A4 paper size, 1.5 line spacing, and 2.5 cm margins of all edges. The legend or caption of all illustrations such as figure and table and their appropriate position should be indicated in the text. Refer to tables and figures in the main text by their numbers. Also figure legends explanations should be given at the end of the text.

The figures should be at least 300 dpi resolution.

The manuscript and other files (figure etc.) should be submitted by using online manuscript submission system at the address of http://vetdergi.kafkas.edu.tr/

During the submission process, the authors should upload the figures of the manuscript to the online manuscript submission system. If the manuscript is accepted for publication, the Copyright Agreement Form signed by all the authors should be sent to the editorial office.

4- The authors should indicate the name of the institute approves the necessary ethical commission report and the serial number of the approval in the material and methods section. If necessary, the editorial board may also request the official document of the ethical commission report. In case reports, a sentence stating that "informed consent" was received from the owner should be added to the main document. If an ethical problem is detected (not reporting project information, lack of ethical committee information, conflict of interest, etc.), the editorial board may reject the manuscript at any stage of the evaluation process.

5- Authors should know and take into account the "Generative Artificial Intelligence (AI)" and other matters listed in the **"Ethical Principles and Publication Policy"** section regarding scientific research and authors.

6- Types of Manuscripts

Original (full-length) manuscripts are original and proper scientific papers based on sufficient scientific investigations, observations and experiments.

Manuscripts consist of the title, abstract and keywords, introduction, material and methods, results, discussion, and references and it should not exceed 12 pages including text. The number of references should not exceed 50. The page limit does not include tables and illustrations. Abstract should contain 200±20 words.

Short communication manuscripts contain recent information and findings in the related topics; however, they are written with insufficient length to be a full-length original article. They should be prepared in the format of full-length original article but the abstract should not exceed 100 words, the reference numbers should not exceed 15 and the length of the text should be no longer than 6 pages in total. The page limit does not include tables and illustrations. Additionally, they should not contain more than 4 figures or tables.

Preliminary scientific reports are a short description of partially completed original research findings at an interpretable level. These should be prepared in the format of full-length original articles. The length of the text should be no longer than 4 pages in total.

Case reports describe rare significant findings encountered in the application, clinic, and laboratory of related fields. The title and abstract of these articles should be written in the format of full-length original articles (but the abstract should not exceed 100 words) and the remaining sections should be followed by the Introduction, Case History, Discussion and References. The reference numbers should not exceed 15 and the length of the text should be no longer than 4 pages in total. The page limit does not include tables and illustrations.

Letters to the editor are short and picture-documented presentations of subjects with scientific or practical benefits or interesting cases. The length of the text should be no longer than 3 pages in total. The page limit includes tables and illustrations.

Reviews are original manuscripts that gather the literature on the current and significant subject along with the commentary and findings of the author on a particular subject (It is essential that the author/s have international scientific publications on this subject). The title and summary of this manuscript should be prepared as described for the full-length original articles and the remaining sections should be followed by introduction, text (with appropriate titles), conclusion, and references.

"Invited review" articles requested from authors who have experience and recognition in international publishing in a particular field are primarily published in our journal.

Review articles submitted to our journal must be prepared in accordance with any of the three categories listed below.

Narrative reviews describe current published information on a scientific topic. However, it does not include a specific methodological process.

Systematic reviews include the search for original studies published in that field on a specific topic, the evaluation of validity, synthesis and interpretation within a systematic methodology.

Meta-analysis is a method of evaluating the results of many studies on a subject with the methods defined in this category and statistical analysis of the obtained findings.

7- The necessary descriptive information (thesis, projects, financial supports, etc.) scripted as an italic font style should be explained below the manuscript title after placing a superscript mark at the end of the title.

8- At least 30% of the references of any submitted manuscript (for all article categories) should include references published in the last five years.

References should be listed with numerical order as they appear in the text and the reference number should be indicated inside the parentheses at the cited text place. References should have the order of surnames and initial letters of the authors, title of the article, title of the journal (original abbreviated title), volume and issue numbers, page numbers and the year of publication and the text formatting should be performed as shown in the example below.

Example: Yang L, Liu B, Yan X, Zhang L, Gao F, Liu Z: Expression of ISG15 in bone marrow during early pregnancy in ewes. *Kafkas Univ Vet Fak Derg*, 23 (5): 767-772, 2017. DOI: 10.9775/kvfd.2017.17726

If the reference is a book, it should follow surnames and initial letters of the authors, title of the book, edition number, page numbers, name and location of publisher and year of publication. If a chapter in a book with an editor and several authors is used, names of chapter authors, name of chapter, editors, name of the book, edition number, page numbers, name and location of publisher and year of publication and the formatting should be performed as shown in the example below.

Example: Mcllwraith CW: Disease of joints, tendons, ligaments, and related structures. **In,** Stashak TS (Ed): Adam's Lameness in Horses. 4th ed., 339-447, Lea and Febiger, Philadelphia, 1988.

DOI number should be added to the end of the reference.

In the references can be reached online only, the web address and connection date should be added at the end of the reference information. The generally accepted scientific writing instructions must comply with the other references. Abbreviations, such as "et al" and "and friends" should not be used in the list of the references.

Follow the link below for EndNote Style of Kafkas Universitesi Veteriner Fakultesi Dergisi;
https://researchsoftware.com/downloads/journal-faculty-veterinary-medicine-kafkas-university

9- Latin expression such as species names of bacteria, virus, parasite, and fungus and anatomical terms should be written in italic character, keeping their original forms.

10- The editorial board has the right to perform necessary modifications and a reduction in the manuscript submitted for publication and to express recommendations to the authors. The manuscripts sent to authors for correction should be returned to the editorial office within a month. After pre-evaluation and agreement of the submitted manuscripts by the editorial board, the article can only be published after the approval of the field editor and referee/s specialized in the particular field.

11- All responsibilities from published articles merely belong to the authors. According to the ethical policy of our journal, plagiarism/self-plagiarism will not be tolerated. All manuscripts received are checking by plagiarism checker software, which compares the content of the manuscript with a broad database of academic publications.

12- The editorship may request the language editing of the manuscript submitted to the journal. If the article is accepted, it will not be published without language editing. Before publication, a declaration and/or certificate stating that proofreading is done by a registered company will be requested from the corresponding author.

13- No fee is charged at any stage in Kafkas Üniversitesi Veteriner Fakültesi Dergisi (No APC/APF)

SUBMISSION CHECKLIST

Please use below list to carry out a final check of your submission before you send it to the journal for review. Ensure that the following items are present in your submission:

- Cover Letter

• Importance and acceptability of the submitted work for the journal have been discussed (Please avoid repeating information that is already present in the abstract and introduction).

• Other information has been added that should be known by the editorial board (e.g.; the manuscript or any part of it has not been published previously or is not under consideration for publication elsewhere.

- Title Page

• Title, Running Title (should be a brief version of the title of your paper, no exceed 50 characters)

• The author's name, institutional affiliation, Open Researcher and Contributor ID (ORCID)

• Congress-symposium, project, thesis etc. information of the manuscript (if any)

• Corresponding author's address, phone, fax, and e-mail information

- Manuscript

• Title, abstract, keywords and main text

• All figures (include relevant captions)

• All tables (including titles, description, footnotes)

• Ensure all figure and table citations in the text match the files provided

- Declarations

• Availability of Data and Materials

• Acknowledgements

• Funding Support

• Competing Interests

• Generative Artificial Intelligence (AI)

• Authors' Contributions

Further Considerations

• Journal policies detailed in this guide have been reviewed

• The manuscript has been "spell checked" and "grammar checked"

• Relevant declarations of interest have been made

• Statement of Author Contributions added to the text

• Acknowledgment and conflicts of interest statement provided